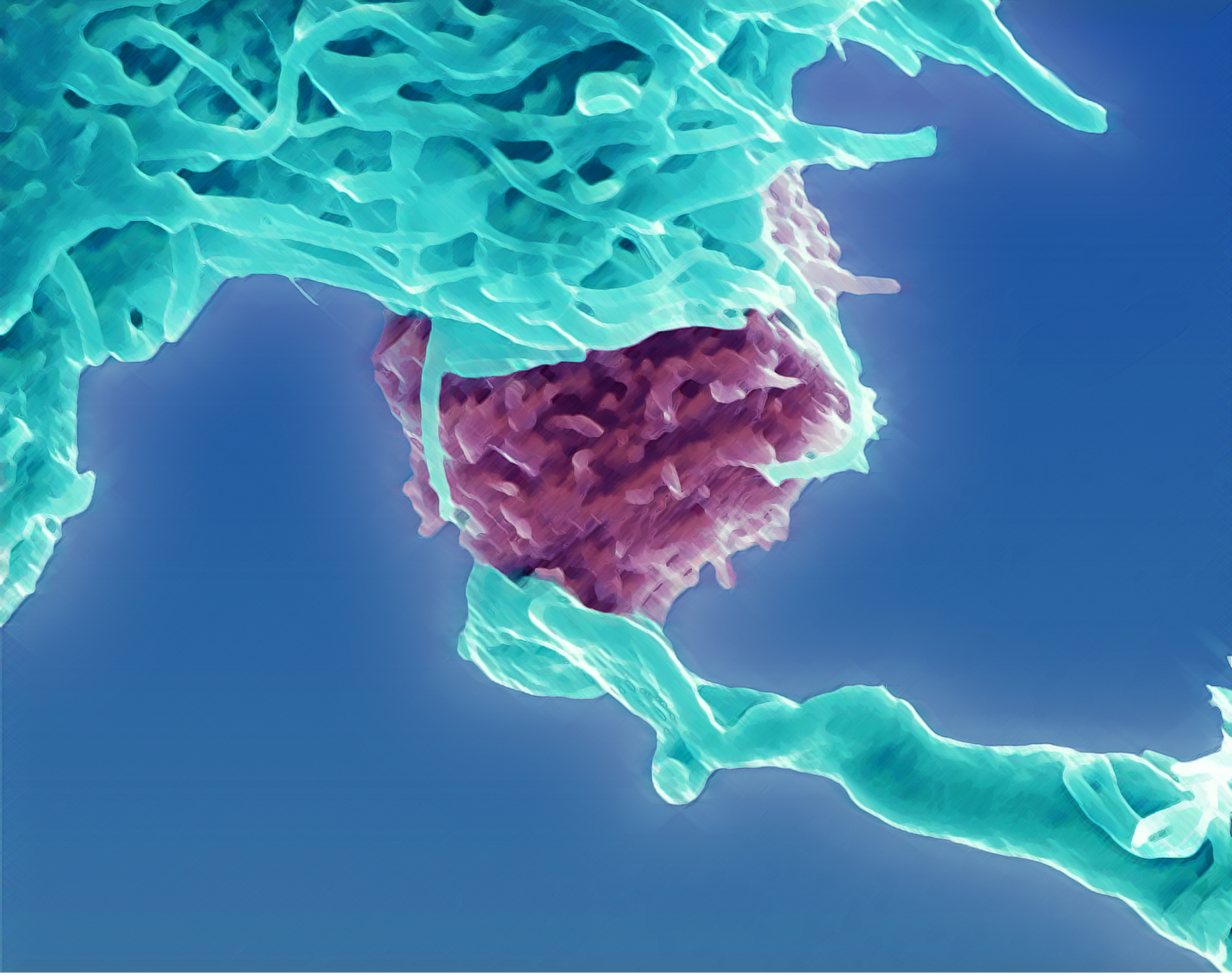


# MOLECULAR INTERACTIONS AT THE T CELL SURFACE

Marta Isabel Abreu Oliveira | Porto 2007

Instituto de Ciências Biomédicas Abel Salazar | Universidade do Porto

U.PORTO
INSTITUTO DE CIÊNCIAS BIOMÉDICAS ABEL SALAZAR
UNIVERSIDADE DO PORTO

IBMC
INSTITUTO DE BIOLOGIA MOLECULAR E CELULAR
INSTITUTE FOR MOLECULAR AND CELL BIOLOGY

University of Oxford

# Molecular Interactions at the T cell Surface

Dissertation to obtain Doctoral Degree in Biomedical Sciences, speciality in Immunology, submitted to the Institute of Biomedical Sciences Abel Salazar of the University of Porto


Supervisor: Prof. Alexandre M. Carmo

Institute for Molecular and Cell Biology,
Rua do Campo Alegre, 823, 4150-180 Porto, Portugal

Molecular Pathology and Immunology Department
Institute of Biomedical Sciences Abel Salazar
Largo Prof. Abel Salazar, 2, 4099-003 Porto, Portugal

Co-supervisor: Prof. Simon J. Davis

Nuffield Department of Clinical Medicine and Medical Research Council, Human Immunology Unit, Weatherall Institute of Molecular Medicine,
The University of Oxford, Oxford Radcliffe Hospital, Oxford, UK.

Marta Isabel Abreu Oliveira


Porto, 2007

*Ao Nuno*

*Aos meus pais*

Summary, Sumário, Sommaire

Acknowledgments/ Agradecimentos

Abbreviations

Publications

**I - General Introduction**

**Introductory notes** 2

**1. Elements of T cell recognition** 3

1.1 Important T cell surface molecules and their ligands 4
1.1.1 The T cell receptor 4
1.1.2 The coreceptors CD4 and CD8 7
1.1.3 Co-stimulation and co-inhibition: the case of CD28 and CTLA-4 8
1.1.4 The phosphatase CD45 10
1.1.5 The accessory receptor CD2 13
1.1.6 The accessory receptor CD6 14

**2. Alternative Splicing** 16

2.1 Mechanisms 16
2.2 Functional consequences 16

**3. T cell activation** 18

3.1 The triggering question 18
3.2 From the membrane to the nucleus 19
3.3 The Immunological synapse: formation and importance 22

**4. General features of interactions at the membrane** 26

4.1 Consequences of membrane tethering 27
4.2 Binding properties – an overview 28
4.3 Oligomerization 29
4.3.1 Role in triggering of single-pass (class I) membrane receptors 30
4.3.2 GPCRs – too many dimers? 30

**5. Characterization of protein-protein interactions** 32

5.1 Interactions between cells: the Biacore 33
5.2 Interactions within the membrane/ stoichiometry: BRET 34

**6. Aims of the thesis** 37

## II – Research work

1. A rigorous experimental framework for detecting protein oligomerization using bioluminescence resonance energy transfer

    1.1 Abstract 40
    1.2 Introduction 40
    1.3 Materials and Methods 42
    1.4 Results 43
    1.5 Discussion 50
    1.6 References 52

2. Analysis of T cell surface organization using BRET

    2.1 Abstract 65
    2.2 Introduction 65
    2.3 Materials and Methods 67
    2.4 Results 69
    2.5 Discussion 79
    2.6 References 81

3. Extracellular isoforms of CD6 generated by alternative splicing regulate targeting of CD6 to the immunological synapse

    3.1 Abstract 87
    3.2 Introduction 87
    3.3 Materials and Methods 89
    3.4 Results 93
    3.5 Discussion 106
    3.6 References 108

4. CD6 attenuates calcium signals on the onset of T cell activation

    4.1 Abstract 114
    4.2 Introduction 114
    4.3 Materials and Methods 115

4.4 Results 117
4.5 Discussion 122
4.6 References 124

**III –Concluding remarks**

**IV - References**

## Summary, Sumário, Sommaire

The physiological response of a naïve T cell, initiated by the engagement of its clonotypic TCR by the appropriate pMHC, requires not only the first TCR-dependent signal but also secondary signals provided by accessory receptors on the T cell. Among the most important are proteins that interact with members of the B7 family of proteins, particularly CD80 (B7-1) and CD86 (B7-2) that are expressed on the APC surface. Using BRET, a useful tool for analysing the quaternary structure of cell surface molecules, we studied the organizational properties of CD80 and CD86 and confirmed that the ability of CD80 to homodimerize in solution also manifests at the cell surface. CD80 monomers and dimers co-exist in a dynamic equilibrium, which can be perturbed by interaction with its receptors. The mouse homologue of CD80 exhibits similar behaviour, corroborating the importance of this property to its function. In addition, CD80 dimerization is mainly driven by extracellular interactions, as previously observed in the crystal structures. CD86, on the other hand, is monomeric at the cell surface and receptor engagement does not change its stoichiometry. Having confirmed the potential of this technique using members of the B7 family, we extended our study and investigated the overall organization of the T cell surface, by applying this approach to a range of different cell surface receptors. Interestingly, most of the representative molecules selected, all of which are involved in T cell signaling, tend to be monomeric entities. This suggests that dimerization is a relative rare property that may confer a special functional role to particular proteins. Our results also indicate that the cell surface comprises a crowded microenvironment with a significant fraction of the BRET signal arising from random interactions within the membrane. In addition, the recruitment of molecules from the cytoplasm to the cell surface is likely to be the rate-limiting step for activation.

Complementing this work on the interaction of cell surface receptors at the molecular level, we also examined the large-scale reorganization of a particular protein, CD6, in the context of the immunological synapse formation. CD6 is an accessory molecule that mediates T cell-APC contact and is considered to have a role in thymocyte selection and T cell activation. During the analysis of the expression pattern of CD6 mRNA in rat and human T cells, we surprisingly found a novel isoform that excluded the ligand-binding domain, CD6Δd3. This CD6 variant is present in all T lineage cells studied, and is up regulated upon activation. In contrast to full-length CD6, however, CD6Δd3 is not targeted to the immunological synapse during Ag presentation. This new finding constitutes a rare example of an alternatively splice-coded isoform with distinct physiological properties. Notably, accumulation at the contact site is not only dependent on the presence of the ligand-binding domain, but requires also the expression of CD6 ligand on the APC surface. We have additionally ascertained an important role for CD6 as a signaling attenuator. Remarkably, the inhibitory effect of CD6 does not depend on its

restricted accumulation at the synapse, but rather on its cytoplasmic domain. Since numerous CD6 cytoplasmic isoforms have been described, it is most likely that the modulatory effects of CD6 on T cell responses may be dependent on their expression at a certain stage of cellular activation or differentiation. Thus, CD6 displays an elegant mechanism to regulate its function and localization to the synapse: through differential expression of distinct segments of the cytoplasmic tail, it has the potential to induce divergent responses. Via expression in the absence of its ligand-binding domain, it can be excluded from the contact site and act in a broader manner. Overall, the stoichiometries and distributions of cell surface proteins are likely to have a major impact on their function.

A resposta fisiológica de uma célula T naive é iniciada através da ligação do seu receptor com o respectivo antigénio. Porém, ela depende não só de um primeiro sinal induzido por esse receptor mas também de sinais secondários, mediados por co-receptores, que resultam da associação destes com ligandos específicos. Entre os mais importantes co-receptores dos linfócitos T, encontram-se proteínas que interactuam com membros da família B7 de proteinas, de que são exemplo o CD80 (B7-1) e o CD86 (B7-2), ambos expressos à superfície da célula apresentadora do antigénio. Utilizando BRET, uma técnica com elevado potencial para analisar a estrutura quaternária de moléculas de superfície, estudaram-se as propriedades organizacionais do CD80 e do CD86 e confirmou-se que a capacidade do CD80 formar homodímeros em solução se mantém quando este se encontra na membrane celular. Monómeros e dímeros de CD80 co-existem num equilíbrio dinâmico que pode ser perturbado pela interacção com os seus receptores. A proteína homóloga de CD80 de ratinho exibe um comportamento semelhante, o que realça a importância desta propriedade para a função desta molécula. Verificou-se ainda que a dimerização do CD80 na membrana se deve maioritariamente a interacções extracelulares, tal como havia sido observado em estudos de cristalografia. O CD80, por sua vez, é um monómero à superfíce da célula, e a sua associação com o receptor não altera esta estequiometria. Após confirmação do potencial desta técnica em membros da família B7 de proteínas, o estudo foi alargado e a organização geral da superfície da célula T investigada. Para tal, aplicou-se o mesmo tipo de abordagem a uma série representativa de diferentes receptores de superfície. Foi interessante observar que a maioria das moléculas seleccionadas, todas elas envolvidas no processo de sinalização da célula T, tendem a ser entidades monoméricas. Tal facto sugere que a dimerização é uma propriedade relativamente rara que poderá conferir uma função especial a determinadas proteínas. Os resultados obtidos indicam igualmente que a superfície celular engloba um microambiente sobrelotado, em que uma parte significativa do sinal de BRET provém de interacções casuais, não específicas, na membrana. Além disso, o recrutamento de moléculas do citoplasma para a superfície da célula parece ser o passo limitante do processo de activação celular.

Para complementar o estudo das interacções de receptores de superfície a nível molecular, foi também examinada a reorganização em larga escala de uma proteína específica, o CD6, no contexto da formação da sinapse imunológica. O CD6 é uma molécula acessória que medeia a interacção da célula T com a célula apresentadora do antigénio, e que está envolvida em processos de selecção tímica e activação celular. Durante a análise do padrão de expressão do mRNA do CD6 em células T humanas e de rato, verificou-se a existência de uma isoforma que não possui o domínio de ligação ao ligando, que foi denominada CD6$\Delta$d3. Esta variante do CD6 encontra-se em toda a

linhagem de células T analisada, e a sua expressão aumenta após activação. Contrariamente à molécula completa de CD6, o CD6Δd3 não é recrutado para a sinapse imunológica durante a apresentação do antigénio. Este resultado constitui um raro exemplo de uma molécula resultante de "splicing" alternativo com propriedades fisiológicas distintas. É de salientar que a acumulação do CD6 na zona de contacto entre as células não é unicamente dependente da presença do domínio de ligação ao ligando, mas também necessita que esse mesmo ligando seja expresso à superfície da célula apresentadora do antigénio. Foi ainda possível demonstrar que o CD6 tem um papel importante como atenuador de vias de transdução do sinal. Notavelmente, o efeito inibitório do CD6 não é uma consequência da sua acumulação restrita na sinapse, mas deriva antes da presença da sua cauda citoplasmática. Visto que várias isoformas citoplasmáticas de CD6 já foram descritas, é bastante plausível que os efeitos modeladores desta molécula nas respostas da célula T sejam dependentes da expressão dessas variantes numa determinada fase da activação celular. Assim, o CD6 dispõe de um elegante mecanismo para regular a sua função e localização na sinapse imunológica: através de uma expressão diferencial de segmentos distintos da cauda citoplasmática, tem a capacidade de induzir respostas divergentes. Aquando da sua expressão sem domínio de ligação ao ligando, pode ser excluído da zona de contacto e actuar de uma forma mais disseminada. Em suma, as estequiometrias e distribuições das proteínas de superfície têm, provavelmente, um elevado impacto nas funções por si desempenhadas.

La réponse physiologique d'une cellule T naïve suite à la stimulation de son TCR clonotypique par un complexe peptide-CMH requiert, outre les signaux dépendants du TCR, des signaux secondaires délivrés par des récepteurs accessoires sur la cellule T. Parmi ceux-ci figurent les protéines interagissant avec les molécules de la famille B7 telles que CD80 (B7-1) et CD86 (B7-2) à la surface des cellules présentant l'antigène (CPA). En utilisant la technique de BRET, qui permet de determiner la structure quaternaire des molécules présentes à la surface cellulaire, nous avons analysé l'organisation spatiale des molécules CD80 et CD86. Nous avons d'une part confirmé que l'homodimérisation de CD80 observée en solution est également détectable au sein de la membrane cellulaire. Il existe un équilibre dynamique entre les états monomérique et dimérique de CD80 qui peut être altéré lors de son interaction avec ses récepteurs. L'homologue murin de CD80 présente le même comportement, soulignant l'importance fonctionnelle de ce phénomène. En outre, la dimérisation de CD80 est essentiellement gouvernée par les interactions engagées par son domaine extracellulaire, conformément aux données cristallographiques. D'autre part, nous avons montré que CD86 est monomérique à la surface cellulaire et que l'engagement du récepteur ne modifie pas sa stœchiométrie. Nous avons ensuite étendu cette approche méthodologique à un ensemble d'autres récepteurs impliqués dans la signalisation lymphocytaire T afin de préciser l'organisation structurale de la membrane du lymphocyte T. De façon intéressante, la plupart de ces molécules sont présentes à la membrane à l'état de monomères. Ceci suggère que la dimérisation est une propriété relativement rare qui pourrait conférer à certaines protéines un rôle fonctionnel particulier. Nos résultats suggèrent également l'existence à la surface cellulaire de microenvironnements présentant une forte densité de récepteurs membranaires dont les interactions aléatoires génèrent une fraction non négligeable du signal BRET mesuré. L'étape limitante de l'activation est vraisemblablement le recrutement des molécules depuis le cytoplasme vers la membrane.

En complément de ce travail à l'échelle moléculaire, nous avons également analysé la redistribution spatiale d'une protéine particulière, la molécule CD6, lors de la formation d'une synapse immunologique entre une cellule T et une CPA. CD6 est une molécule accessoire qui semble jouer un rôle dans la sélection des thymocytes et l'activation lymphocytaire T. L'analyse des transcrits de CD6 dans les cellules T humaines et murines nous a permis d'identifier un nouveau variant d'épissage codant une isoforme de CD6 dépourvue du domaine de liaison au ligand, notée CD6Δd3. Ce variant est présent dans toutes les cellules de la lignée T analysées et son expression augmente suite à l'activation. Toutefois, contrairement à la forme CD6 entière, CD6Δd3 n'est pas recruté à la synapse immunologique lors d'une stimulation antigénique. De façon

cohérente, nous avons montré que le recrutement synaptique de CD6 est dépendant de la présence de son ligand à la surface de la CPA. CD6 constitue donc un exemple original de molécule pour laquelle un mécanisme d'épissage alternatif permet de générer un variant ayant des propriétés physiologiques distinctes. En outre, nos données suggèrent que CD6 pourrait fonctionner comme un atténuateur du signal d'activation dans les lymphocytes T, cette fonction inhibitrice étant indépendante de sa relocalisation à la synapse mais requérant un domaine intracytoplasmique intact. Dans la mesure où différents variants du domaine intracytoplasmique ont été décrits, il est vraisemblable que les effets modulateurs de CD6 sur les réponses T dépendent de l'isoforme exprimée au cours des différentes étapes la différenciation et de l'activation des cellules T. L'expression différentielle de certains segments du domaine intracytoplasmique permettrait donc à CD6 d'induire des réponses physiologiques distinctes. En outre, lorsqu'il est exprimé sans son domaine de liaison au ligand, CD6 peut être exclu de la zone de contact et agir de manière non localisée dans toute la cellule T. L'ensemble de ces travaux démontre que la stœchiométrie et la distribution des protéines de la signalisation à la surface cellulaire sont deux paramètres critiques susceptibles d'affecter leurs propriétés fonctionnelles.

## Acknowledgments/ Agradecimentos

Em primeiro lugar, e como não podia deixar de ser, gostaria de agradecer ao Alexandre por todos os ensinamentos, pela atitude crítica mas sempre optimista e pelos incentivos constantes ao longo deste tempo. Obrigada também pela amizade e pela partilha de conhecimentos que se traduz num crescimento científico mas também pessoal.

À Prof. Maria de Sousa, por me ter recebido no Laboratório de Imunologia Molecular onde comecei a dar os primeiros passos deste percurso e por transmitir sempre elevados valores e padrões científicos.

À Alexandra pelo seu entusiasmo e alegria contagiantes e a todas as outras pessoas que fazem ou já fizeram parte do grupo de Cell Activation and Gene Expression, pelo companheirismo e bom ambiente de trabalho que sempre me proporcionaram. Em especial, à Mónica, à Raquel e à Carine pela amizade. Ao Pedro, pela infindável paciência nos meus dias menos bons. A todos aqueles que, dentro do IBMC, me ajudaram a realizar este trabalho disponibilizando-me condições, reagentes ou dando-me importantes opiniões e sugestões.

I would like to take this opportunity to acknowledge my co-supervisor, Prof. Simon Davis, for continuous encouragement and support. Also, thank you very much to everyone from the Davis' lab for receiving me so nicely and making my time there so enjoyable and valuable (which probably explains why I returned 3 times!). It was a great experience! In particular, muito obrigado to John James for his incessant enthusiasm and his friendship. It was lovely to work with you.

J'aimerais remercier à George pour m'accueillir dans son laboratoire, pour sa sympathie et sa disponibilité. Pour tout le monde de ce labo-là qui m'a soutenu et supporté durant ma visite. Merci beaucoup à vous tous pour votre aide et votre hospitalité. Je souhaite particulièrement remercier à Stephanie pour son temps et pour toutes les expériences qu'elle a répétées pendant mon absence. Agradeço também à Eliana por ter tornado a minha estadia em Paris ainda mais agradável e me ter feito sentir mais perto de casa.

Ao Pedro Tarroso e ao Nuno, que pacientemente fizeram as imagens incluídas nesta tese.

O meu obrigado também a várias outras pessoas que, de uma forma ou de outra, sempre me motivaram e me ajudaram a chegar até aqui. Em particular, à Mónica, pela sua força, e por ser um exemplo de que vale a pena acreditar e lutar por algo. Aos meus pais, incontornavelmente, o meu profundo e sentido Obrigado pelo apoio constante, incondicional, e por me terem ensinado a nunca desistir. Vocês são uma força da natureza cujos pilares tento manter e fazer prevalecer a cada dia que passa. E a ti, Nuno,

que estás sempre presente, por me ensinares a viver um dia de cada vez e me fazeres sorrir todos os dias.

Finalmente, à Fundação para a Ciência e a Tecnologia pelo apoio financeiro concedido através da bolsa de doutoramento.

## Abbreviations

| | |
|---|---|
| Ag | Antigen |
| APC | Ag presenting cell |
| AP-1 | Activator protein-1 |
| BRET | Bioluminescence resonance energy transfer |
| C | Constant |
| CDR | Complementarity determining region |
| cSMAC | Central supramolecular activation cluster |
| DAG | 1,2-diacylglycerol |
| dSMAC | Distal supramolecular activation cluster |
| FRET | Fluorescence resonance energy transfer |
| GFP | Green fluorescent protein |
| GPCR | G protein coupled receptor |
| Ig | Immunoglobulin |
| IL-2 | Interleukin-2 |
| $IP_3$ | Inositol-1,4,5-trisphosphate |
| IS | Immunological synapse |
| ITAM | Immunoreceptor tyrosine based activation motif |
| LAT | Linker for activation of T cells |
| Luc | Luciferase |
| MC | Microcluster |
| MHC | Major histocompatibility complex |
| NFAT | Nuclear factor for activated T cells |
| PH | Pleckstrin homology |
| PI3K | Phosphatidylinositol 3-kinase |
| PKC$\theta$ | Protein kinase C-$\theta$ |
| PLC$\gamma$1 | Phospholipase C-$\gamma$ |
| pMHC | peptide-MHC |
| pSMAC | Peripheral supramolecular activation cluster |
| PTK | Protein tyrosine kinase |
| PTKR | Protein tyrosine kinase receptor |
| PTP | Protein tyrosine phosphatase |
| RPTP | Receptor protein tyrosine phosphatase |
| SH2 | Src-homology 2 |
| SLP-76 | SH2-domain containing leukocyte protein of 76 KDa |

| | |
|---|---|
| SRCR | Scavenger receptor cysteine rich |
| TCR | T cell receptor |
| V | Variable |
| ZAP-70 | Zeta-chain-associated protein 70 |

## Publications

The following articles are of relevance for the work presented in this thesis:

1. Castro MAA, Nunes RJ, **Oliveira MI**, Tavares PA, Simões C, Parnes JR, Moreira A, Carmo AM (2003). OX52 is the rat homologue of CD6: evidence for an effector function in the regulation of CD5 phosphorylation. *J. Leukoc. Biol.* **73**:183-190.

2. James JR, **Oliveira MI**, Carmo AM, Iaboni A, Davis SJ (2006). A rigorous experimental framework for detecting protein oligomerization using bioluminescence resonance energy transfer. *Nat. Methods*, **3**: (12):1001-6.

3. Castro MAA*, **Oliveira MI***, Nunes RJ, Fabre S, Peixoto A, Brown MH, Parnes JR, Bismuth G, Moreira A, Rocha B, Carmo AM (2007). Extracellular isoforms of CD6 generated by alternative splicing regulate targeting of CD6 to the immunological synapse. *J. Immunol.*, **178**: (7): 4351–4361.
   * *Both authors contributed equally to this work*

4. **Oliveira MI,** Fabre S, Castro MAA, Nunes RJ, Bismuth G, Carmo AM (2006) CD6 attenuates calcium signals on the onset of T cell activation. Submitted to *Eur. J. Immunol.*

### Other publications:

5. Pinto PAB, **Oliveira MI**, Saraiva J, Thomas B, Akoulitchev A, Sunkel CE, Carmo AM, Moreira A. mRNA 3'-end formation in the *Drosophila melanogaster* cell cycle kinase *polo*. Submitted to *Mol.Cell.Biol.*

6. Castro MAA, Nunes RJ, Bamberger M, Maia AR, **Oliveira MI**, Carmo AM, Lck-dependent and independent mechanisms in the activation-induced translocation of T lymphocyte accessory molecules to lipid rafts. Submitted to *Eur. J. Immunol.*

# I - General Introduction

## Introductory notes

The mammalian immune system is extremely efficient in defending the host from a variety of pathogenic microorganisms. When an invader is detected, it is initially countered by the first line of defence, the innate immunity. However, if this response is somehow evaded or bypassed, the adaptive immune system is then activated. This second line of defence, in contrast to the innate immunity, has immunological memory and is able to specifically recognize an almost infinite diversity of antigens (Ags). On the basis of this capacity is a key feature, single specificity. Nowhere this is more evident than in T lymphocytes, which recognize their targets through a single clonotypic T cell receptor (TCR). Its ability to make fine distinctions between very similar Ags allows T cells to distinguish foreign from self-entities, thus preventing autoimmunity. Ags are detected in the form of short peptide fragments associated with major histocompatibility complex (MHC) molecules present on the membrane of Ag-presenting cells (APCs). When T cells encounter mature APCs loaded with their cognate Ag, they become activated. This can result in a number of different responses such as proliferation, differentiation and secretion of cytokines and growth factors. However, cells can also become unresponsive or apoptotic. Positive responses are in fact accompanied by later negative signals that help to maintain homeostasis [1, 2]. In addition to the signal delivered by the Ag, the ultimate T cell response will also be influenced by ligand binding of accessory cell surface molecules. They provide essential co-stimulatory signals while stabilizing and strengthening T cell-APC interactions. Moreover, the diversity of T cell surface receptors serves as the primary conduits for transmission of extracellular signals into the cell's signaling network. Yet, how the external message is initially decoded across the membrane is still poorly understood. Although we have already identified the players and even perceived their transient assembly and spatial reorganization upon Ag recognition, we are still not able to anticipate the actual sequence of events from the initial T cell/APC interaction to the final biological outcome. Therefore, at the present the characterization of the molecular mechanisms underlying T cell recognition and the complex orchestration of its components has become one of the most exciting challenges.

In the next chapter, an overall view of the T cell surface with its major constituents and their cognate ligands will initially be described. Following that, a description of what is currently known about the dynamics of these receptor-ligand interactions at the cell surface and the intracellular signaling cascades triggered by them, will be given. Finally, the general features of membrane interactions and the two pre-eminent methods used to characterize them will be discussed.

## 1. Elements of T cell recognition

The T cell surface is embedded with a variety of proteins that belong to diverse structural and functional classes that include immunoreceptors, cytokine and chemokine receptors, as well as adhesion molecules. Over 110 different molecules have been found at the surface of a single resting cytotoxic T cell, and it is believed that the list of T cell constituents is now close to being, if not yet, complete [3]. This multitude of proteins tends to be differentially expressed according to its functional importance, with key receptors in initiating adhesion and T cell activation among the most abundant [3]. Only the proteins thought to play a crucial role in the process of T cell recognition will be described in detail (Fig.1).

It is important to note that the T cell surface is not a restricted concept. T cells comprise diverse subsets that, at different activation stages, might display an altered profile due to lineage commitment or activation induced expression of additional molecules or isoforms. More than an exhaustive list of the proteins that are expressed, it is critical to understand their complex interactions in the unique membrane environment, how they can be functionally regulated and how their interactions contribute to T cell Ag recognition. These issues will be discussed in the next section.

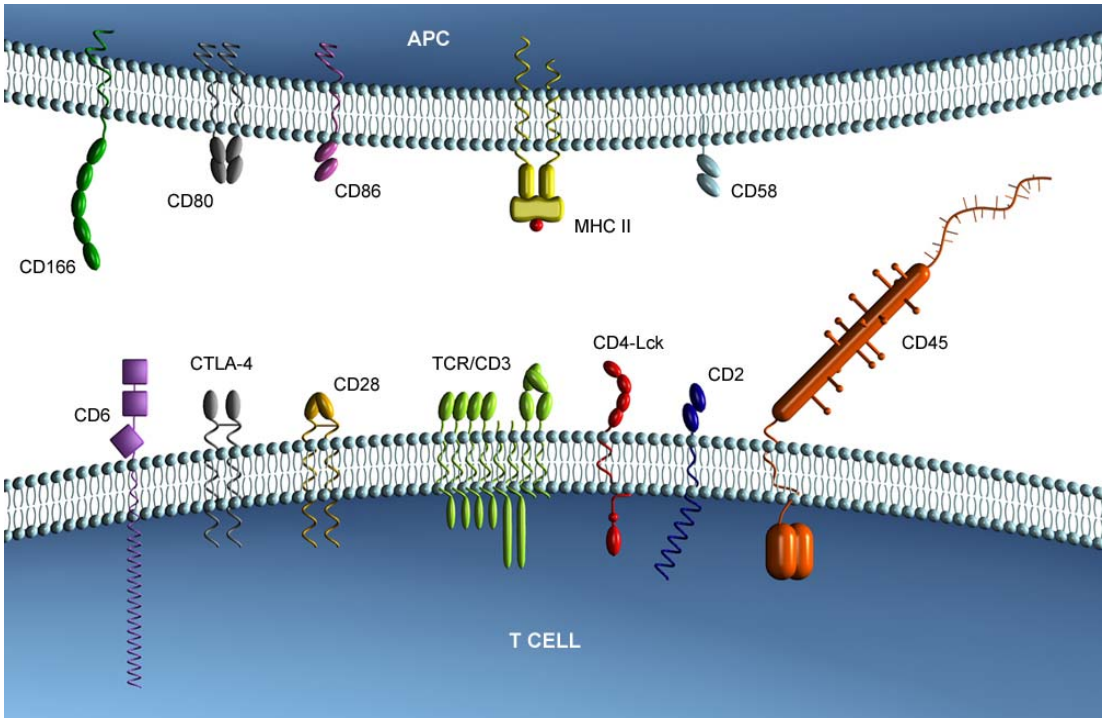



**Figure 1.** Cell surface molecules involved in T cell antigen recognition. A schematic view of the architecture and dimensions of important cell surface proteins involved in T cell antigen recognition.

## 1.1 Important T cell surface molecules and their ligands

### 1.1.1 The T cell receptor

The TCR is a multicomponent structure containing distinct Ag binding and signal transduction subunits. The Ag binding subunit comprises two transmembrane disulphide-linked chains, each chain having a variable (V) and a constant (C) immunoglobulin (Ig)-like domain [4]. The membrane-distal V domain is responsible for the Ag recognition and is encoded in separate segments that rearrange randomly in each T cell, giving rise to a vast repertoire of TCRs which ensures Ag specificity [5]. The ligand-binding subunit is a heterodimer of α and β chains [6, 7] in the majority of lymphocytes, whereas a small percentage of other T cells contains $\gamma$ and $\delta$ chains [8].

Each TCR is constitutively associated with at least six CD3 polypeptides, which include CD3εγ and CD3εδ heterodimers and a CD3ζζ homodimer [9, 10]. Their function is to couple the TCR to the intracellular signaling machinery of the cell, and for that reason constitute the signal transduction subunit.

The physiological ligand for the TCR is a foreign peptide bound to class I or class II MHC molecules [11]. However, how the TCR discriminates among the enormous diversity of highly similar peptide-MHC (pMHC) surfaces remains an open question. Some general principles have emerged though, namely a conserved docking mode of the TCR towards the pMHC, from the numerous expression and crystallization studies that have been performed so far.

In the TCR, the pMHC binding site is formed by six loops called complementarity determining regions (CDRs), with each Vα and Vβ chain contributing with three loops [12]. Two of these loops, CDR1 and 2 are germline-derived, that is constant for a given V$\alpha$ chain, while CDR3 loops are extremely variable. On the other hand, both MHC classes possess a binding platform formed by a β-sheet, with the presented Ag bound between two α helices that form the walls of the binding groove [13].

Different lines of evidence, which include structural and biochemical studies, have elucidated how the TCR is adapted for pMHC recognition [14, 15] and how MHC molecules bind and display antigenic peptides [16-21]. Yet, an important achievement was the determination of the structure of a complex between the TCR and the pMHC that has uncovered the atomic details of this interaction. In fact, a generalized diagonal orientation of the TCR on the pMHC surface [22, 23] has emerged from the current database of 24 TCR/pMHC complex structures solved so far [24]. In all of them, the similar binding mode places the CDR1 and CDR2 loops of the TCR mainly in contact with the conserved residues of the MHC, whereas CDR3 loops largely interact with the peptide. Furthermore,

the Vα domain is always closer to the N-terminal residues of the peptide and the Vβ to the C-terminal end [25, 26], with the TCR assuming a diagonal geometry relative to the long axis of the pMHC binding groove. Regardless of sharing an identical overall binding topology, the complexes show a substantial degree of structural variability in the twist, tilt or shift of the TCR over the pMHC surface [27]. This raises the question of what could then be controlling and/or constraining the docking topology.

One possibility is that sets of conserved contacts would dictate and serve as a rule for TCR/pMHC interactions. However, this is inconsistent with most structural studies, as no overall conserved contacts were found [26]. Very recently, similar anchor points were observed, but in just two TCR/pMHC complexes [28, 29].

Alternatively, the binding topology could be affected by the shape of the TCR and/or the pMHC. Whilst the TCR binding surface is relatively flat [30], the pMHCs surface has two high peaks near the N-termini of the two helical regions that form the sides of the peptide-binding groove [23]. In order to maximize the interaction between the two surfaces, a diagonal orientation seems to be imposed on binding. Recent crystallographic studies [31] and a new calculation of the crossing angles for all TCR/pMHC complexes [24], showed no distinct binding mode for the two MHC classes, in contrast to previous suggestions [32]. Yet, the shape of the MHC does not completely explain the binding topology observed in the crystal structures as it would be compatible with a rotation of 180º of the TCR, that would place the Vα (rather than the Vβ) domain over the C-terminal end of the peptide or vice-versa [33].

The TCR does not bind to pMHC individually, but as part of a multicomponent complex that additionally comprises the CD3 polypeptides and the coreceptors CD4 or CD8. Therefore, another possibility for the unique geometry of the interaction could be that it results from external forces imposed by the coreceptors. Both CD4 and CD8 are nonpolymorphic and thus most likely interact with the MHC and the TCR in a conserved manner. Consequently, the TCR and the pMHC are confined to the same docking topology in order to accommodate the identical positioning of the coreceptor. However, structures of CD4 and CD8 bound to MHC [34-36] have revealed the unlikelihood of a direct association between the coreceptor and the TCR while making contact with the same pMHC molecule.

Crystal structures provide a static picture of the dynamic Ag recognition process, though. For a complete understanding, additional approaches that complement and integrate the different findings are thus required. Some binding energetic studies of the TCR/pMHC interactions have been performed, but with contradictory results. Whereas some indicated that the TCR residues contacting essentially the MHC contributed most of the binding free energy [37, 38], others implied a larger role for the peptide [39]. Another

study showed that the MHC residues are important for the initial contact, while the stability of the interaction is assured by the peptide residues [40]**.** This finding, together with structural [41-44] and thermodynamic [45-47] analyses, which indicate that the Ag-binding surface of the TCR exhibits conformational plasticity, suggested a two-step mechanism for TCR recognition of the pMHC. The emerging picture is one in which the TCR may scan MHC molecules using a 'lock and key' type of binding with its CDR1 and CDR2 loops which are more rigid, followed by an induced fit of its highly flexible CDR3 loops over the peptide [40]. Because the CDR3 loops could adopt a variety of final conformations, this model would also explain the apparently high level of TCR crossreactivity [48], necessary for expanding its specificity [49-51]. Nevertheless, other studies are not consistent with this two-step model and raise objections against its feasibility [52-55]. Further investigations on TCR binding are necessary to fully understand the function of TCR mobility and conformational change in T cell activation. Specially, because recent data suggest that the TCR is much less degenerate, both structurally and functionally, than previously believed [28, 54]. At the moment, it is uncertain whether crossreactivity is a feature of T cell recognition, and if so, whether it is achieved by CDR3 flexibility and/or repositioning of the TCR/MHC binding orientation.

Despite the impressive amount of work, the structural basis of MHC recognition remains elusive. Interestingly, a highly unconventional TCR/pMHC docking orientation has been recently reported. Rather than being centred over the pMHC surface, this TCR only contacts the N-terminal peptide segment [53]. In the future, an important breakthrough would be the determination of a complete αβ TCR signaling complex, including CD4/CD8 and the CD3 polypeptides, for which only a model has been proposed [24]. This would reveal the global changes that dictate T cell Ag recognition and may also furnish an explanation for the fixed orientation of MHC-peptide/TCR complexes.

Compared with αβ TCRs, the structural basis for ligand recognition for γδ TCRs is much less well characterized. From the few defined γδ TCR ligands, it is apparent that, unlike αβ TCRs, γδ TCRs recognize these antigens directly, without requirement of antigen processing and presentation [56]. Recent determination of a bound γδ TCR structure has enabled comparisons of the modes of antigen recognition by αβ and γδ T cells. The most striking observation is the sideways orientation of the γδ TCR relative to its ligand [57]. Whereas all CDR loops of αβ TCRs are used in antigen recognition, γδ TCR contacts are primarily mediated in this instance by the δ chain, particularly by the germline-encoded residues of the CDR3 δ, with a minor contribution from CDR3 γ. There are two γδ TCR molecules in the crystallographic asymmetric unit forming a dimer, in contrast to the lack of crystallographic evidence supporting oligomerization for αβ TCRs [57]. Another important feature of γδ TCRs has to do with their co-receptor independent

activation [58]. This focuses attention on the possible influence of co-receptor recruitment in the conserved docking topology of the αβ TCR-pMHC interaction.

### 1.1.2 The coreceptors CD4 and CD8

The expression of either CD4 or CD8 defines two distinct types of T lymphocytes, the helper and the cytotoxic T cells, respectively. Their response to Ag is different, with the former proliferating and secreting cytokines that will activate other effector cells, and the latter directly killing the target cell. Regardless of its type, an effective response depends not only on the specific TCR/pMHC engagement but also on the interaction of this same pMHC with a CD4 or CD8 coreceptor. This enhances T cell stimulation by allowing the recruitment of a key protein tyrosine kinase expressed in T cells, Lck, to the vicinity of the TCR.

Although functionally very alike, CD4 and CD8 have structural dissimilarities. Both contain Ig-like extracellular domains, a single transmembrane region, and a short cytoplasmic tail [59-61]. However, unlike the covalently linked CD8 dimer, CD4 is traditionally accepted as a monomeric molecule on the cell surface, although new evidence has highlighted the possible role of dimeric and oligomeric forms of functional CD4 [62, 63]. Also, the extracellular region of CD4 consists of four Ig-like domains [60, 61] whereas each chain of its counterpart CD8 has a single Ig-like domain supported on a stalk that anchors it to the membrane [64]. CD8 is predominantly expressed as a heterodimer of an α and a β chain, but in some cells is present exclusively as a CD8αα homodimer [65]. The heterodimeric form of CD8 has been shown to be a more effective T cell activator than CD8αα [66], indicating that it is the primary coreceptor for the conventional MHC class I-restricted T cells. CD8αα, on the other hand, is the principal ligand of a non-classical MHC molecule [67]. Clearly, further studies are required to elucidate why CD8αα cannot functionally replace or complement CD8αβ. The most important of these, perhaps, would be the determination of the CD8αβ structure in complex with pMHC that has not yet been solved.

Both coreceptors recognize MHC molecules, but CD4 binds to class II MHCs while CD8 interacts with class I MHCs [68-70]. Peptides presented by MHC class I molecules are 8–10 peptide residues long [71], whereas MHC class II molecules display peptides with an average length of 14–25 residues [72]. Crystallographic studies have shown that both CD4 and CD8 bind to nonpolymorphic regions at the base of MHCs, but in a surprisingly distinct way. The two CD8 domains cooperate to bind class I MHC [35, 36], contrarily to CD4 where only the N-terminal domain makes contact with the MHC and the

second CD4 domain is distal to the interface [73]. By superimposing these independent structures on TCR/pMHC complex structures it was possible to obtain a complete trivalent model that excluded direct TCR/coreceptor interactions when binding to the same pMHC [74]. One possibility is that the TCR and the coreceptor are indirectly linked *via* other proteins such as CD3 and associated signaling molecules [75, 76]. Alternatively, the coreceptor binds not to the same MHC as the associated TCR, but to an adjacent one creating a TCR pseudodimer [77].

It was initially thought that the role of CD4 and CD8 was solely to increase the stability of the TCR/pMHC complex [78, 79]. However, this idea has been revised by the fact that the binding affinity of CD8/pMHC is lower than most other interactions involving cell surface proteins [64, 67, 80]. It is therefore likely that for an efficient binding to the MHC, the coreceptor needs also to interact with the TCR to form a stable complex. This occurs through the cytoplasmic association of CD4 and CD8 with the key protein tyrosine kinase of T cells, Lck [76, 81]. A recruitment model has been proposed for coreceptor function in which following TCR engagement, the coreceptor is recruited to the activated TCR/pMHC complex via CD4/CD8 bound-Lck and enhances TCR triggering by increasing the duration and/or the strength of the initial weak signal [82].

### 1.1.3 Co-stimulation and co-inhibition: the case of CD28 and CTLA-4

Co-stimulatory and co-inhibitory signals are essential for the regulation of the T cell response and maintenance of T cell homeostasis. The former are defined as those that combined with Ag-receptor signals, lead to productive cell activation. On the contrary, the latter attenuate Ag-receptor signals, resulting in decreased cell activation. The coreceptors CD28 and CTLA-4 and their shared, related ligands CD80 and CD86, represent a sequential co-stimulatory/co-inhibitory system that acts to control the magnitude and duration of an immune response. CD28 is the most important co-stimulatory protein and its inhibition may render T cells anergic or unresponsive [83]. In fact, CD28-deficient mice are unable to mount an effective immune response. On the other hand, CTLA-4-knockout mice die soon after birth from multiorgan destruction [84, 85], which also illustrates the critical role of this negative regulatory receptor.

Structurally, CD28 and CTLA-4 are closely related type I transmembrane proteins with a single variable Ig-like domain [86, 87] and highly conserved cytoplasmic domains. At the surface, they exist as disulphide-linked homodimers but their expression pattern is quite distinct. While CD28 is constitutively expressed in most T cells [88], CTLA-4 is only induced upon activation [89]. Likewise, CD86 is detected at low levels on resting APCs

and rapidly up-regulated, whereas CD80 is slowly induced after activation [90, 91]. The existence of two, sequentially expressed ligands constituted for a long time a puzzling issue, partially because they were thought to have similar structures and affinities for CD28 versus CTLA-4. However, recent studies have revealed important findings that suggest an entirely different view. Firstly, CD80 binds CD28 and CTLA-4 with much lower affinities than previously assumed and with very fast kinetics [92]. Secondly, CD28 binds CD86 more effectively than CD80 whereas the CTLA-4/CD80 interaction is of higher affinity than that of CTLA-4/CD86 [93]. Thirdly, that in contrast to CTLA-4 which is bivalent, CD28 is functionally monovalent [93]. Modeling based on the recently solved crystal structure of a soluble CD28-Fab complex supports this observation. The structure of the monomer shows similarities to that of CTLA-4 [94]. Nevertheless, in the CD28 homodimer the two domains form a U-like structure, which prevents the simultaneous binding of two CD80 molecules by a physical clash of their membrane proximal domains. CTLA-4/CD80 complexes show, however, that CTLA-4 is bivalent with the two domains arranged in a V-like structure that allows the formation of a cross-linked CD80-CTLA-4 lattice [95]. Such stoichiometric differences result in profound changes in the stability of the signaling complexes that these molecules form [93]. Lastly, CD80 and CD86 have different oligomeric states. CD80 tends to form homodimers as shown by solution [93], crystallographic [95, 96] and in FRET-based analyses [97]. CD86, on the contrary, is present as a monomer at the cell surface [97]. Unbound CD86 was also monomeric both in solution and in the crystal state [93, 98] but it was detected as a dimer when complexed with CTLA-4 [95, 99], probably due to crystal artifacts.

All these observations support a model where CD80 preferentially binds to CTLA-4 while CD86 is the favored CD28 ligand. The emerging picture is that of an initial interaction between CD86 and CD28 that will continue to be privileged even in the presence of CTLA-4. However, after CD80 expression, its interactions with CTLA-4 will be much favored over interaction with CD28, both due to its increased affinity and bivalent binding to CTLA-4 [93]. This preferential interaction of CD80 with CTLA-4 and CD86 with CD28 was recently demonstrated *ex vivo* [100]. As a consequence, inhibition or activation of T cell functions can be privileged. In fact, the differences in temporal regulation of the two ligands, led to the conclusion that CD86 is largely activating and CD80 inhibitory [93]. Thus, CD28 constitutively expressed on the T cell initially binds CD86 on the APC inducing early positive signals. After the T cell is activated, CTLA-4 is expressed on its surface but only when it finds it most effective ligand, CD80, T cell activation is turned off.

The distinct valencies of CD28 and CTLA-4 result in a 100-fold difference in the stability of their signaling complexes [93], with the former being much less stable than the latter. This suggests that the weak interactions involving CD28 and CD86 are necessary

to provide efficient physiological co-stimulation without inducing Ag-independent responses, whereas the much stronger and extremely stable CTLA-4/CD80 interactions are required for overwhelming the ongoing positive signals and stop activation. Indeed, monovalency of CD28 has been shown to maintain the Ag dependence of T cell co-stimulatory responses [101]. Thus, both the hierarchy and the characteristics of these interactions are crucial and provide an intrinsic mechanism for modulating the T cell response.

The relationship between the intrinsic properties of co-stimulatory protein interactions measured in solution and their likely effects at cellular interfaces had not been analyzed until recently. Jansson *et al*. [102] combined biophysical and expression data in an *in silico* simulation and confirmed the concept that CD86 and CD80 are the dominant ligands of CD28 and CTLA-4, respectively [102]. However, they also showed that affinity and stoichiometric differences are not the only factors influencing the accumulation of co-stimulatory receptors at intercellular junctions. In fact, expression levels and competition effects are also likely to profoundly influence complex formation. A 10-fold reduction in affinity and in the numbers of molecules per cell leads to a partial or complete elimination of complex formation by CD28, respectively, whereas CTLA-4 interaction is largely unaffected by affinity reduction, but is highly sensitive to expression levels [102]. The importance of stoichiometry is clearly demonstrated as the CTLA-4 bias is 18-fold higher for CD80 than for CD86, when both CD80 and CTLA-4 are made bivalent. Moreover, CD80 appears not to be absolutely required as a ligand for CD28 and CTLA-4, since in its absence CTLA-4 is fully engaged by CD86, raising the possibility that the inhibitory role of CD80 might not be its main function. Hence, co-stimulatory interactions seem to be influenced by a variety of factors previously not anticipated. Further studies are likely to help to integrate the effects of these factors.

### 1.1.4 The phosphatase CD45

The first recognized receptor protein tyrosine phosphatase (RPTP), CD45, is essential for the development and Ag-induced activation of T cells [103-106]. This type I transmembrane protein is found in all nucleated cells of haematopoietic origin and is expressed as multiple isoforms [107]. It is particularly abundant in T and B cells, where it comprises up to 10% of the cell surface area [108]. Like may other RPTPs, CD45 is composed of an extracellular receptor-like region, a single transmembrane segment, and a long cytoplasmic tail embracing tandem protein tyrosine phosphatase domains. Only the membrane-proximal domain is catalytically active [109], contrarily to the membrane-distal

domain that has been proposed to have a role in substrate recruitment [110]. The extracellular segment provides all the protein isoform variation, with essentially three exons being differently used [111]. Such diversity is generated by alternative splicing, an important regulatory mechanism of the immune system (see section 2). Although theoretically the number of possible isoforms is quite large, only a few are observed at reasonable levels, and show lineage and developmental-stage specific expression. Naïve T cells express high levels of the larger CD45 isoform that includes all exons (CD45RABC), whereas activated T cells express predominantly the smaller CD45 isoform (CD45RO) which lacks the alternative spliced exons [112] (Fig. 2). Many studies have been carried out to assess the role of the different CD45 variants, but with conflicting results. Even transgenic mice expressing single isoforms of CD45 on a null background showed no clear functional differences between them [104, 113, 114]. The alternatively used sections encompass many O-linked glycosylation sites and as a consequence, the multiple isoforms have significant dissimilarities both in structure and overall charge [108]. This suggested that they might have distinct ligand specificities, but despite intense investigation, no solid evidence for a specific external ligand has yet been found.

CD45 controls immune responses, both positively and negatively, by dephosphorylating a number of signaling molecules, including the protein tyrosine kinase Lck [111]. Dephosphorylation of a negative regulatory residue at the C-terminal end of the kinase by CD45 mantains Lck in a “primed” state capable of full activation upon antigen receptor stimulation. As dephosphorylation of Src-kinases is key step in T cell activation, CD45 plays a crutial role in this process. Nevertheless, how the phosphatase activity is regulated is still unknown. A proposed regulatory mechanism has been dimerization, based on the observation that experimentally induced self-association of CD45 resulted in inhibition of its phosphatase activity [115]. This was possibly due to blockage of the catalytic site of CD45 by an inhibitory wedge, upon dimer formation [116]. However, the long-awaited determination of the crystal structure of CD45 cytoplasmic domains has ruled out this wedge hypothesis, by showing that such dimeric interaction is impossible because of the orientation of two phosphatase domains [110]. This orientation was in fact very similar to that of another RPTP, LAR, for which no evidence of dimerization in the crystal could also be found, despite the presence of the wedge motif [117]. That the wedge region is conserved in other RPTPs, including CD45, suggests that it may be important for their activity. In agreement with this, a single point mutation in this region causes lymphoproliferation and autoimmunity *in vivo* [118].

Studies supporting the principle that CD45 can form dimers [118-120] in a cytoplasmic tail-, and thus wedge-independent manner [120] have been reported. However, others could not observe homodimerization for the intact extracellular structure

of rat CD45 [121]. Intracellular dimerization was also ruled out by the observation that the CD45 cytoplasmic region is a stable monomer both in solution [122] and in the crystal lattice [110]. Together these findings suggest an alternative regulatory mechanism for the phosphatase activity. Ligand binding has been shown to play an important role in regulating the function of other RPTPs, such as RPTPζ and LAR [123, 124], but whether this involved changes in the RPTP dimerization is not known. LAR, like many other RPTPs, displays features of cell-adhesion molecule and has been implicated in cell-cell and cell-matrix interactions [125]. The extended extracellular portions of all but RPTPα and RPTPε, comprising different types of domains, reflect the receptor-like fashion in which these proteins interact [126]. A further level of regulation seems to be conferred by oxidative stress. Treatment of cells with hydrogen peroxide resulted in the stabilization of inactive RPTPα dimers [127]. As for CD45, its regulation remains unclear, although changes in the protein distribution controlled by the ectodomain have been shown to modulate CD45 function [128]. It is therefore likely that the extracellular region of CD45 influences the role of the phosphatase, either by preventing its accumulation near the site of TCR engagement [129], altering its self-association state [120] or by regulating its interaction with components of the plasma membrane [128].

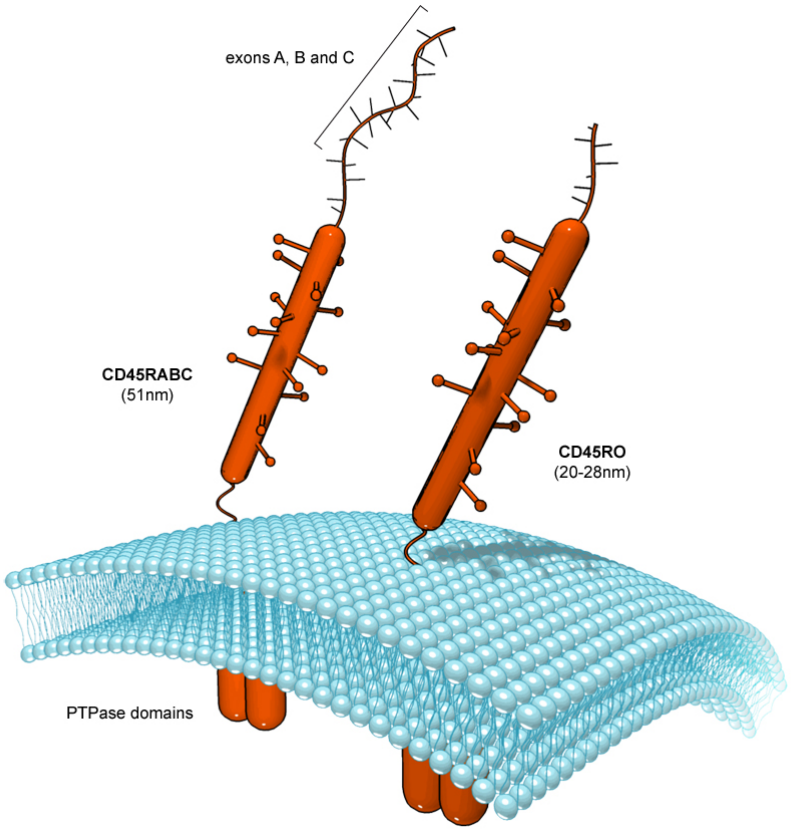



**Figure 2.** Structure of CD45. CD45 is expressed in multiple isoforms as a result of alternative splicing of variable exons. The high molecular weight containing exons A, B and C (CD45RABC) and the low molecular weight isoforms (CD45RO) are shown. These two variants significantly differ in size and glycosylation patterns, as the alternative spliced region comprises many O-glycosylation sites.

### 1.1.5 The accessory receptor CD2

CD2 was the first heterophilic cell-adhesion molecule to be discovered and has been established as one of the main receptors mediating T cell-APC interactions. Expressed on virtually all T cells, thymocytes, and natural killer cells [130], it binds different protein ligands, CD58 in humans [131] and CD48 in rodents [132]. All these three molecules have similar extracellular regions, composed of two Ig-like domains and a short stalk, with the N-terminal domain containing the ligand binding site [133-135]. The main characteristic of CD2-CD58/CD48 interactions is the very low affinity but, nevertheless, high specificity. In the case of rat CD2 with CD48, binding is particularly weak and barely sufficient to sustain adhesive interactions [136], which implies that CD2 is not a conventional cell adhesion molecule. Different lines of evidence have, nevertheless, elucidated the CD2 binding mechanism and provided insights into the structural basis of cell surface recognition.

Structural and mutational analyses have shown that although large, the interacting surfaces of CD2 and its ligands exhibit little shape complementarity [135, 137-139]. This complementarity is, even so, greater in the rat proteins but does not confer a high affinity to the interaction, contrarily to what would be expected [135]. In fact, the interaction in the rat is 4 to 5 fold weaker than that of human CD2/CD58. In both cases, however, the binding interfaces are dominated by a strikingly high number of charged residues [135]. Unexpectedly, substitution of almost half of the CD2 residues involved in electrostatic contacts did not greatly affect binding to CD58 [140]. Similarly, only modest changes in the CD48 binding affinity were observed upon mutation of more than half of the charged or polar residues of the CD2 binding site. Strikingly, it was the specificity of CD48 recognition that was severely compromised by the loss of the charged residues [141]. This suggests that electrostatic contacts are necessary to compensate for the poor surface shape complementarity and account for the high degree of specificity without increasing the affinity [141]. Therefore, this mode of recognition is well suited to mediating biological interactions that need to be weak and specific [141]. Another striking feature of CD2-ligand interactions is that despite the low solution affinity, they cooperate to precisely align adhering membranes leading to a high physiological affinity [136]. An overall paradigm emerges, however, from the analysis of other weak interactions such as that between CTLA-4 and its ligands. Contrarily to CD2-CD58/CD48, the binding interfaces exhibit a very high degree of shape complementarity with few electrostatic contacts [95, 99]. Binding is still weak due to the small interacting area of CTLA-4 and its ligands, and because the reaction is limited, as in the case of CD2/CD58 by a large, yet unexplained, entropic barrier [135]. Here again, human and rat CD2 interactions differ, as the latter has equivalent enthalpic and entropic components [135]. Thus, cell surface proteins appear to

have heterogeneous binding properties mediating weak, specific recognition at the membrane. CD2 is perhaps a rather extreme example of these weak interactions, based primarily on electrostatic contacts.

CD2 establishes contacts with its ligands in a head-to-head fashion, whose size is similar to that of TCR/pMHC interactions [142]. The observation that CD2 enhances T cell activation both *in vitro* and *in vivo* at low Ag densities [143], supports the prediction that it facilitates TCR scanning of pMHC complexes by bringing the two apposing membranes close together [139]. The formation of an effective T cell-APC junction requires CD2 clustering and cytoskeleton polarization. These processes are CD2 cytoplasmic tail-dependent and mediated through recruitment of cytosolic adaptor proteins that link the adhesion receptor to the cytoskeleton [144-146]. Likewise, cytoplasmic association with signaling molecules [147-149] couples CD2 to signaling events. These include augmented T cell cytokine production [150, 151] and IL-12 responsiveness [152, 153] as well as reversal of T cell anergic state [154]. Nevertheless, CD2-deficient mice could mount effective immune responses, even upon viral infections [155, 156]. Rather that promoting T cell activation by a co-stimulatory mechanism, CD2 has a critical role in setting quantitative thresholds for T cell activation [143].

### 1.1.6 The accessory receptor CD6

Among the molecules mediating T cell-APC contact is the type I glycoprotein CD6, a member of the Scavenger Receptor Cysteine Rich (SRCR) superfamily [157]. Expressed primarily by thymocytes and mature T cells, it can also be found in some B cells and in the brain [158]. Instead of the common Ig-like domains present in many cell surface molecules, the extracellular region of CD6 is composed of three SRCR domains, followed by a transmembrane segment and an unusually long cytoplasmic tail [157]. Numerous CD6 cytoplasmic isoforms generated by alternative splicing have been reported [159-161], but with no specific physiological function been attributed so far. The molecular basis of CD6/CD166 interaction has been extensively characterized [158]. CD166 is a widely expressed protein with five Ig-like domains, of which the N-terminal domain binds to the membrane proximal domain of CD6 [162, 163]. Hence, this binding mode is unusual in that it occurs laterally, rather than in the “head to head” manner commonly seen in most cell surface contacts. Thermodynamic studies have recently revealed that although of low affinity, CD6/CD166 interaction is one of the strongest ($K_d$ = 0.4-1.0 $\mu$M) involving adhesion molecules that participate in T cell recognition [164].

The ultimate function of CD6 has not been deciphered yet, but available data supports a role in T cell activation and differentiation. An involvement of CD6 in thymocyte maturation has also been suggested [165]. Antibody-mediated CD6 cross-linking enhances T cell proliferation, suggesting a co-stimulatory function for this accessory protein [166-168]. Accordingly, engagement of CD6 by CD166 results in increased interleukin 2 (IL-2) production [169]. Moreover, blocking studies with either soluble monomeric, recombinant CD6 or CD166 proteins, or antibodies against these molecules showed an inhibition of specific T cell responses [164, 169-171]. On the other hand, expression of CD6 in T cells has been shown to limit their responsiveness [169] and correlation of CD6 expression on thymocytes with resistance to apoptosis [172] implies some inhibitory signaling properties for the receptor cytoplasmic tail. These apparently opposing functions can be reconciled if possible inhibitory signals mediated by the intracellular region are necessary to reduce the activating ones triggered by the relatively strong CD6/CD166 interaction [164], thereby regulating the level of T cell activation. Recently, a physical association between CD6 and the closely related molecule CD5 at the surface of T cells has been reported [173, 174]. It is likely that these two receptors provide either similar or complementary signals to T cells. CD6 has actually an important role in the regulation of CD5 phosphorylation [174]. In addition to CD5, CD6 associates with the TCR/CD3 complex and, along with its ligand, is recruited to the T cell-APC contact area in an Ag-dependent manner [170, 171]. The interaction between CD6 and CD166 was shown to be important for stabilizing the interface and required during early and later phases of T cell activation [171]. The functional role of a second, recently reported, ligand for CD6 has not yet been described [175].

The signaling pathways used by CD6 to influence T cell activation are sill poorly understood. Its remarkably long cytoplasmic tail is devoid of intrinsic catalytic activity, but rich in potential signal transduction motifs. Upon CD3 stimulation, CD6 becomes tyrosine phosphorylated [176]. Indeed, the rat homologue of CD6 has the capacity of associating with tyrosine kinases of different families [174]. Recent studies identified further two intracellular binding partners of CD6, the adaptor proteins syntenin-1 and SLP-76 [169, 177]. Both interactions require the C-terminal region of CD6 and may be controlled by phosphorylation. To further understand role of CD6 in T cell activation, new molecular partners and the signaling pathways triggered by CD6 need to be further characterized. The development of CD6-deficient mice may complement the ongoing research and help to ultimately elucidate the function of this accessory receptor.

# 2. Alternative Splicing

Between a third and a half of all human genes appear to undergo alternative splicing, with a bias towards the immune and nervous system, particularly cell surface proteins [178-182]. This mechanism, in which individual exons are selectively included or excluded from the final mRNA, thus generates a high degree of protein diversity and it is more likely the rule than the exception. The Dscam gene, which encodes a cell surface protein in *Drosophila melanogaster*, exemplifies the extreme complexity that can be achieved, with more than 38,000 alternatively spliced isoforms [183]. This molecular variety of *Dscam* transcripts is highly conserved across major insect orders, suggesting that alternative splicing is a mechanism for creating immune receptor diversity in insects [184]. Nevertheless the mechanisms that regulate splicing are still poorly understood. In this section, recent advances on this field will be discussed, with particular emphasis on the role of alternative splicing in T cell activation and function.

## 2.1 Mechanisms

The term alternative splicing describes a variation of the splicing process in which the primary gene transcript can be cut and reconnected in different ways to yield various, distinct mRNAs [185, 186]. This includes selective inclusion or exclusion of exons, differential use of only one or an array of two or more exon variants, or competition between specific splice sites [187]. When the splicing machinery, known as the spliceosome, recognizes and binds appropriately to the splice sites that flank an exon, it is included in the final mRNA; otherwise the exon is omitted from the final transcript. In addition to the splice-site consensus sequences, a number of other auxiliary elements can influence alternative splicing. Sequences that recruit proteins which promote spliceosome recognition of an exon are known as exonic or intronic splicing enhancers (ESE or ISEs), while sequences that are necessary to inhibit exon recognition are known as exonic or intronic splicing silencers (ESS or ISSs). The balance of these competing activities determines exon inclusion or skipping, which in turn determines the ratio of the mRNA isoforms that are expressed.

## 2.2 Functional consequences

The possibility of creating numerous mRNA transcripts and proteins from a single gene illustrates the importance of this mechanism in influencing cellular function. A functional

role of alternative splicing may not always be found, but with regard to T-cell activation there are some examples of splice variants shown to be translated whose expression can be regulated, for example, in a tissue, temporal or stimuli-dependent manner to control the activity of the cell. Many protein tyrosine kinases, like Lck and Fyn, undergo alternative splicing in T cells [188]. Other important alternative spliced transcripts expressed during the early steps of T cell activation encode cell surface adhesion molecules. ICAM1, CD31 and CD44 have all been associated with in splicing events, and a link between cell signaling and CD44 splicing control has been established [189]. Also, an overlapping, but distinct signaling pathway seems to be involved in the regulation of CD45 splicing, whose transcripts are significantly altered in response to prolonged T cell activation [108]. Stimulated T cells express predominantly the smaller CD45 isoform which is reported to show the greatest tendency to dimerize [120]. Because it is claimed that multiple CD45 variants have different homodimerization efficiencies which appear to be inversely proportional to their ability to support TCR signaling, this isoform switch has been proposed to contribute to the termination of the primary T cell response [120].

Another mechanism by which T cells block T cell activation is through the regulated expression of CTLA-4. In resting cells, this protein is mainly present as a soluble form [190] and little, if any, CTLA-4 is expressed at the cell surface. However, upon stimulation almost all the final mRNA transcripts include the exon coding for the transmembrane region and the new protein in targeted to the membrane [191]. This ensures increased levels of CTLA-4 on the surface of activated T cells in order to prevent hyperstimulation [84, 85]. A further example of a gene that is alternatively spliced in T cells is that of the accessory receptor CD6. The majority of the isoforms described arise from alternative splicing of cytoplasmic exons [159-161], but so far, no physiological significance has been attributed to any of these variations.

There are additional indications that control of splicing contributes to the regulation of cytokine responses and apoptosis. The transcripts of many genes that encode cytokines, their receptors and apoptotic proteins, are subject to alternative splicing, which can substantially alter the behaviour of the T cell. These include IL-6, the IL-7 receptor and Fas [188].

Further evidence of the importance of the alternative splicing mechanism in the immune system is provided by diseases associated with alternative splicing mistakes. Altered expression of the adhesion molecule CD44 and CD45 isoforms has been correlated to increased susceptibility to cancer or multiple sclerosis, respectively [192-195]. Accordingly, increased serum levels of soluble CTLA-4 and soluble CD2 have been observed in several diseases [190, 196]. In the case of mouse CTLA-4, disease susceptibility is related to the alternative splicing-induced absence of the CD80/CD86 ligand-binding domain [197].

# 3. T cell activation

To become activated the T cell needs to efficiently recognize its cognate pMHC-expressing APC. To achieve efficient cell-cell interaction, the T cell arrests migration, scans the APC and in the presence of the specific antigen, the TCR engages it, inducing triggering. This, in turn, leads to the recruitment of cell surface receptors and signaling components to the contact area, known as the immunological synapse (IS). In this region, proteins are organized into distinct compartments, suggesting that their specific organization may be essential for modulating T cell activation. The external signals are then transduced intracellularly leading ultimately to the activation of nuclear factors and transcription of specific genes. In the following paragraphs, different models of TCR triggering will be analysed and recent findings regarding the formation of the IS, as well as the dynamic regulation of T cell activation signals will be highlighted.

## 3.1 The triggering question

TCR triggering refers to the mechanism by which TCR signaling is initiated upon antigen recognition. Despite extensive efforts, and the wide variety of proposed models, this issue is still relatively controversial [198, 199]. A major point of debate is whether, as in the case of other receptors, such as growth factor receptors, the TCR itself requires binding-induced oligomerization or aggregation for triggering. Various aggregation mechanisms have been proposed, ranging from simple dimerization to increasingly complex variants [200]. However, some data does not support the oligomerization model, in particular the observation that soluble monomeric [201], and a single [77] pMHC could induce a T cell calcium response, provided that a co-receptor was present. Although two following studies [202, 203] argued against the initial report, the results obtained by Irvine *et al*. [77] appeared to rule out conventional aggregation models. Thus, two distinct models have been proposed to interpret these findings, the heterodimerization [199] and the pseudo-dimerization [77] models. The former postulates that TCR signaling can be initiated by binding of the TCR and the co-receptor to the same pMHC, whereas the latter, recently modified [204], postulates that a specific engaged-TCR can be crosslinked by one CD4 molecule to a different and more abundant, self-pMHC. Although attractive, these models fail to account for residual T cell function in mice devoid of co-receptors [205, 206], and for TCR triggering in the absence of self-pMHC [207], respectively.

On the contrary, a third model, the kinetic segregation model [208], is compatible with all the different observations mentioned above. In the kinetic-segregation hypothesis,

triggering occurs as the local balance of phosphorylation and dephosphorylation events generally taking place on a resting T cell and that result from random protein interactions in the membrane, is altered by the formation of close-contact zones between the T cell and an APC. This process is "nucleated" by small proteins such as CD2 and results in the local, size-dependent exclusion of molecules with large ectodomains, such as the phosphatases CD45 or CD148. As a consequence, these areas became tyrosine phosphorylation rich, where bound TCRs are trapped for long periods, leading to TCR triggering followed by sequential recruitment and activation of adaptor and effector molecules. Given that bulky phosphatases are excluded, phosphorylated TCRs are less likely to be dephosphorylated and downstream signaling occurs. Several other observations also support this model. For instance, truncation of the extracellular region of both CD45 and CD148 abrogates TCR triggering [128, 209]. Conversely, increasing the dimensions of the TCR-pMHC complex, and therefore the intermembrane distance, abrogates TCR triggering without affecting its binding to the pMHC [129]. Moreover, triggering in an artificial TCR-ligand system exhibited a similar dependence on the ectodomain size [129]. Although this model seems to better explain all the available data, it cannot, however, account for the ability of triggering by soluble pMHC monomers [199]. Yet, this form of TCR triggering is observed only with adherent T cells *in vitro*, leaving open the possibility that this may be a result of this particular cellular system.

Finally, other proposed models invoke binding-induced conformational changes as mechanism for signal transduction [198]. These so-called conformational change models are not supported by the majority of crystal studies and are, therefore, very unlikely. Yet it is not possible to completely exclude them from the other suggested models and combinations of the different mechanisms may account for TCR triggering.

## 3.2 From the membrane to the nucleus

The multitude of interactions that take place at the cell surface upon activation starts a number of signaling cascades that lead to a specific T cell response. One of the earliest detectable events following activation is tyrosine phosphorylation, which requires the activation of Src-family protein tyrosine kinases. These are negatively regulated by another kinase, Csk, via phosphorylation of an inhibitory tyrosine residue sited near to their C-terminus [210-212]. Dephosphorylation of this negative regulatory residue by the phosphatase CD45 results in enhanced kinase activity [213]. According to the kinetic-segregation model [208], in a resting T cell constitutive phosphorylation/dephosphorylation events are balanced by the activity of Src-kinases and tyrosine phosphatases. The

formation of a close contact zone between a T cell and its interacting APC alters this equilibrium by excluding large receptors such as CD45 and allowing small signaling proteins to remain in the interface. This leads to increased phosphorylation, mediated by the Src kinases Lck and Fyn, of the immunoreceptor tyrosine-based activation motifs (ITAMs) located in the cytoplasmic tails of the CD3 and ζ chains of the TCR. In addition, because a portion of Lck is constitutively associated with the CD4 co-receptor, the peptide-MHC-induced recruitment of CD4 to the TCR/pMHC complex results in an augmented local concentration of Lck around the TCR, boosting ITAM phosphorylation. Once fully phosphorylated, these motifs serve as binding sites for proteins containing Src homology-2 (SH2) domains, such as the Syk-family kinase ZAP-70 [214]. After it is attached to the ITAM motifs, ZAP-70 is phosphorylated by Lck, and becomes activated [215]. In this state, ZAP-70 autophosphorylates at different tyrosine residues, which serve to recruit various signaling effectors to the TCR complex, ensuring sustained ITAM phosphorylation [214]. In addition to serving as a scaffold via self-phosphorylation, ZAP-70 also phosphorylates a restricted set of substrates, the most notable ones being the adaptor linker for activation of T cell (LAT) and the SH2 domain-containing leukocyte protein of 76 kDa (SLP-76). When phosphorylated, both LAT and SLP-76 act as anchor points for the recruitment of other soluble signaling molecules, forming multimolecular complexes that robustly signal to the interior of the cell leading to full activation and concomitant expression of biologically important genes. Three transcription factors in particular have been found to play a key role in TCR-stimulated changes in gene expression. These are NFAT (nuclear factor of activated transcription factors), NF-κB, and AP-1 (activator protein 1).

TCR engagement leads to the phosphorylation and activation of phospholipase C γ1 (PLC-γ1), a critical component of NFAT activation. Once catalytically active, PLC-γ1 is responsible for the production of diacylglycerol (DAG) and inositol trisphosphate (IP3), by cleaving phosphatidylinositol 4, 5-bisphosphate (PIP2). DAG is a second messenger in the PKCθ (protein kinase C θ) pathway, whereas IP3 releases calcium ($Ca^{2+}$) from its intracellular stores in the endoplasmic reticulum, increasing cytosolic $Ca^{2+}$ [216]. $Ca^{2+}$ binds to calmodulin that, in turn, activates calcineurin, a $Ca^{2+}$/calmodulin dependent protein phosphatase. Calcineurin dephosphorylates NFAT enabling it to migrate to the nucleus and activate the expression of cytokines, including that of IL-2 which promotes proliferation of T cells [217].

The activation of NF-κB is mediated by PKCθ-induced signals that ultimately lead to the migration of NF-κB to the nucleus, where it regulates the activity of its target genes [218]. PKCθ also contributes to AP-1 activation, although it can occur through PKCθ-independent pathways too, such as those involving Ras-family GTPases [219].

In addition to the different signaling cascades triggered by TCR engagement, further pathways are elicited by the CD28 co-stimulatory receptor through the activation of the phosphatidylinositol 3 kinase (PI3K). PI3K is involved in the formation of phosphatidylinositol 3,4,5-triphosphate, a lipid that serves as a selective binding site in the plasma membrane for proteins containing a PH (pleckstrin homology) domain [220]. Among the most important of these, is the kinase Atk that sends signals throughout the cell via interactions with other proteins to promote both proliferation and cellular survival [221]. Moreover, signals elicited by CD28 are implicated in cytoskeleton reorganization as well, particularly in actin polymerization and assembly of different cytoskeletal proteins at the TCR contact site [222].

Negative regulation of TCR signaling is also of significance, in order to prevent deregulation of the activation processes or adequately terminate an ongoing response. This is achieved through the intervention of several negative regulators that finely control T cell activation at different steps [223]. These include inhibitory kinases and adaptor molecules, phosphatases, as well as ubiquitin ligases. In the light of the central role played by protein tyrosine phosphorylation in T cell signaling, inhibition of this event provides an efficient means of interfering with cell activation. Consequently, protein tyrosine phosphatases (PTP) are crucial to balance and regulate the activity of protein tyrosine kinases (PTK). In fact, PTK and PTP are partners, and together ensure that appropriate signaling thresholds are achieved and maintained at the right time. This equilibrium can also be perceived from analysis of the human genome given that it encodes approximately the same number of PTK and PTP [126, 224]. Nevertheless, inhibition of PTKs can also be mediated by other kinases, as exemplified by the inhibitory kinase Csk. This protein has the capacity to phosphorylate the inhibitory tyrosine of Src kinases, thereby suppressing their activity [212]. Additionally, the kinase activity can be down-modulated by the phosphatase PEP, which is able to remove the phosphate from the positive-regulatory tyrosine [225]. Csk and PEP constitutively associate in T cells and thus are thought to synergize in inactivating Src family kinases and TCR signaling [226]. The adaptor protein PAG is responsible for recruiting Csk and Csk-associated PEP to the membrane where the activity of Src kinases can be controlled [227, 228]. This negative effect is counterbalanced by the activity of another phosphatase, CD45. CD45 keeps the inhibitory tyrosine dephosphorylated, rendering the enzyme in a primed state. However, CD45 can also have a negative effect on TCR-elicited signal transduction, given its ability to also dephosphorylate the activating tyrosine of Src kinases [111].

Other important PTP in negative signaling regulation include SHP1, which directly dephosphorylates ZAP-70, PEP-related PTPs, SHIP1, PTEN and CD148 [126]. Furthermore, immunoreceptor signaling may be negatively regulated by the Cbl family of

ubiquitin ligases, which act as adaptor proteins and are also able to promote ubiquitination of associated targets, inducing their degradation [229, 230]. The expression of inhibitory receptors is an additional means to influence the T cell response. CTLA-4, PD-1 and BTLA are three inhibitory receptors of the B7 family that profoundly down-regulate the immune activation after binding to their ligands [231]. CTLA-4 inhibits TCR- and CD28-mediated signal transduction [232, 233]. The strong inhibitory role of CTLA-4 is clearly illustrated by the phenotype of CTLA-4 negative mice, which develop a profound lymphoproliferative disorder [84, 85]. As for PD-1, binding to its ligands results in phosphorylation of specific intracellular tyrosines and subsequent generation of negative signals [234]. The recently identified BTLA contains two inhibitory motifs in its cytoplasmic tail that are responsible for the recruitment of soluble PTPs [235]. An additional transmembrane receptor implicated in fine tuning of T cell responses is the CD5. Although initially regarded as a co-stimulatory molecule, CD5-knockout mice indicated a negative role for this protein on TCR signaling [236]. This complex and organized apparatus aimed at restricting the duration or intensity of cell activation counterbalances the activating machinery. The nature of the response is thus determined by integrated positive and negative regulatory events.

## 3.3 The Immunological synapse: formation and importance

The engagement of cell surface receptors during interactions between T cells and APCs results in the formation of a contact zone named the immunological synapse, due to its similarities with neuronal cell–cell contacts [237]. When a IS exhibits a specific rearrangement of the membrane proteins, with separation of receptors into a particular pattern it is designated as a mature synapse. In this phase, the pMHC-engaged TCR and associated signaling molecules are enriched in the centre of the interface, known as the central supramolecular activation cluster (c-SMAC), whereas a peripheral region called peripheral SMAC (p-SMAC) contains adhesion molecules and integrin-associated cytoskeleton proteins [238]. Additionally, another more peripheral region than the p-SMAC can be defined, named the distal SMAC (d-SMAC) to where the large sialoprotein CD43 was shown to be localized upon TCR stimulation [239]. This large scale molecular segregation also occurs in $\gamma\delta$ T cells, but in contrast to αβ T lymphocytes, it can take place in the absence of exogenous TCR ligands, although under these conditions full activation is not achieved [240].

A question that arises is what are the driving forces for the reorganization of the cell surface upon TCR engagement? The simplest mechanism to explain changes in

receptor distribution and accumulation at the synapse is through ligand recruitment to the contact site. The co-stimulatory molecules CD28 and CTLA-4 are indeed selectively recruited to the IS by their ligands CD86 and CD80, respectively [100]. Nevertheless, cytoskeleton interactions also appear to contribute to the spatial localization of proteins at the IS, as shown by the requirement of CD80 cytoplasmic tail for segregation of its receptors and signaling molecules in that region [241]. In the case of the TCR, an intrinsic, cytoskeleton-independent, lateral mobility *per se* allows it to diffuse over the entire T cell surface and ensures TCR supply to the IS during sustained T cell activation [242]. In addition, translocation of endocytosed TCRs was recently demonstrated [243], suggesting that vesicular trafficking may be another process implicated in the accumulation of proteins, as well as in the targeting of cytokine secretion [244], into the IS.

Once receptors are recruited to the IS, they can be differentially segregated giving rise to the highly organized mature synapse. The formation of the c-SMAC can be driven by lateral diffusion of the proteins according to their size [129, 245], by actin cytoskeleton rearrangements [246] or even by the quality and quantity of the presented Ag [247, 248]. However, not all cell-cell contacts exhibit a well-defined c-SMACs as is the case of productive T cell-dendritic cell and thymocyte-ephithelial cell interactions [249, 250]. In fact, the morphology and molecular organization of the IS can be quite diverse [251]. It has been suggested that the inability to form an obvious c-SMAC correlates with T cell hyper-responsiveness [252]. Moreover, compelling evidence indicates that c-SMAC formation is required neither for activation of naïve $CD8^+$ T cells [253] nor for cytolytic killing by effector T cells [254-256]. Similarly, in $CD4^+$ T cells TCR engagement and signaling are independent of the assembly of a mature IS [257, 258]. Collectively, all these findings suggest that the c-SMAC in itself is not the primary signaling site within the IS nor is it required for full T-cell activation, in contrast to what was once believed [259, 260].

Unlike the c-SMAC, another type of structure designated microcluster (MC) has been observed in all types of synapses. MCs are generated prior to the formation of a mature IS [261] and have been proposed to be important for initiation of TCR signaling. Indeed, TCR-mediated tyrosine kinase signaling occurs primarily at the periphery of the IS [252, 258, 262], exactly in the same region where MCs are formed [263, 264]. Using a combined system of planar bilayers and total internal reflection fluorescence microscopy two recent studies [263, 264] analysed precisely and in real time the dynamic process of IS formation, particularly the movement of signaling molecules during T cell activation (Fig. 3). They identified MCs containing TCRs, kinases and adaptor molecules that appeared in the periphery of the contact site, migrated towards the centre of the interface and converged to form the c-SMAC. The generation of these MCs coincided with signaling and during translocation into c-SMAC they dissociate from phosphorylated kinases and

adaptors. Moreover, no increase in phosphotyrosine was detected upon formation of the c-SMAC [264], consistent with the indication that the majority of signaling events occurs in the p-SMAC. New MCs containing all necessary signaling molecules are continuously generated in the periphery even after the formation of the mature IS. The authors, therefore, suggest that MCs are important not only for initiating T cell activation but also to sustain it. In agreement with this, retention of MCs in the periphery of the IS augments signaling [265]. Recent evidence indicates that TCR signaling, indeed, terminates in the c-SMAC, as elimination of MCs, but not of the c-SMAC, abrogated calcium mobilization [266]. Unlike MCs, the c-SMAC appears not to exclude CD45 [266, 267], a key phosphatase in TCR signaling that has an essential role in priming of Lck for activation [106], but can also act as a negative regulator [268, 269]. Others have, however, gathered evidence of CD45 exclusion from the contact area upon synapse formation [262, 270]. The particular behaviour of CD45, absent from all peripheral MCs, being possibly recruited to the cSMAC at an early time point and later on moving to the d-SMAC [262], may allow increased phosphorylation in the MCs while stopping signaling at the c-SMAC [266]. The mechanisms by which the location of CD45 is controlled are unknown, but irregular membrane topology or vesicular trafficking could be responsible for its accumulation, without size-based exclusion, at the centre of the interface [266]. It has also been shown that the c-SMAC is rich in lysobisphosphatidic acid [266], a lipid abundantly present in multivesicular endosomes where TCR degradation takes place [271, 272]. Hence, this finding is consistent with the c-SMAC being a degradative compartment, as previously suggested [252, 258]. Significant ubiquitination, a process essential for targeting proteins to degradation [273] at the IS has, indeed, been recently reported [274]. Together, these emerging data support a picture of a compartmentalized IS that has signaling MCs and c-SMACs involved, among other functions [275], in TCR elimination. Although this model has been well characterized for the T cell-supported planar bilayer IS, further studies are required to determine its precise relationship to the different T cell-APC synapses.

Despite much work on this issue, the purpose of a mature IS remains an open question. Besides allowing cells to communicate with each other, the reason why molecules rearrange in a specific pattern is poorly understood. Initially, the large-scale segregation was thought to be required for TCR triggering [276]. However, the mature synapse forms several minutes after T cell-APC contact, whereas TCR triggering occurs within seconds, suggesting an alternative function for the IS [245, 277]. Later, the stability of the interface was proposed to enhance and/or sustain TCR signaling [277, 278], but Lee *et al.* [258] clearly showed that TCR triggering is maximal well before the formation of the mature IS and is weak at the centre of the mature IS [258]. So what can be the role of

the mature IS? A number of functions have been suggested [279]. One of them has to do with directed granule release and cytokine secretion [280]. The close membrane interdistance would help to retain the contents of secretory lysosomes and allow their release directly towards the target cell without affecting bystander cells. Consistent with this, CD8 T cells target their secretory granules to the centre of the IS [281]. In the light of their findings, Lee *et al*. [258] have, in contrast, argued that the synapse is involved in TCR down-regulation and degradation [258]. Together with others [252], they propose the synapse balances TCR signaling and degradation. It is also reasonable that the intimate contact of the IS may facilitate the engagement of small, weak positive or negative receptors. In fact, CD28 engagement is optimal at the centre of the mature IS, although on unstimulated T cells it binds very poorly to a lipid-anchored form of its ligand CD80 [282]. This indicates that the large-scale molecular rearrangement may additionally favour the coalescence of signaling pathways, reinforcing the signal transduction cascade and fine-tuning the quality and extent of the response [257]. Prolonged TCR signaling has, indeed, been shown to be required for full T cell activation, despite rapid internalization of the TCR in the first few minutes [283, 284]. Nevertheless,T cells can be activated even upon destruction and reformation of the IS by summation of interrupted signals gathered on APC surfaces [285]. The formation of multiple synapses allows T cells to communicate with different APCs and enables selective helper T cells polarization [286]. Conversely, cytotoxic T cells polarize their lytic granules towards different targets before large-scale segregation and with no discrimination of their antigenic potential [287].

The role of the mature IS is still elusive and may serve several, not mutually exclusive, functions. In the future, a combination of different approaches will be important to clarify these controversies and to gain a full understanding of the mechanisms and biological consequences of the formation of the IS, which has been referred to as a dynamic multitasking system [279].

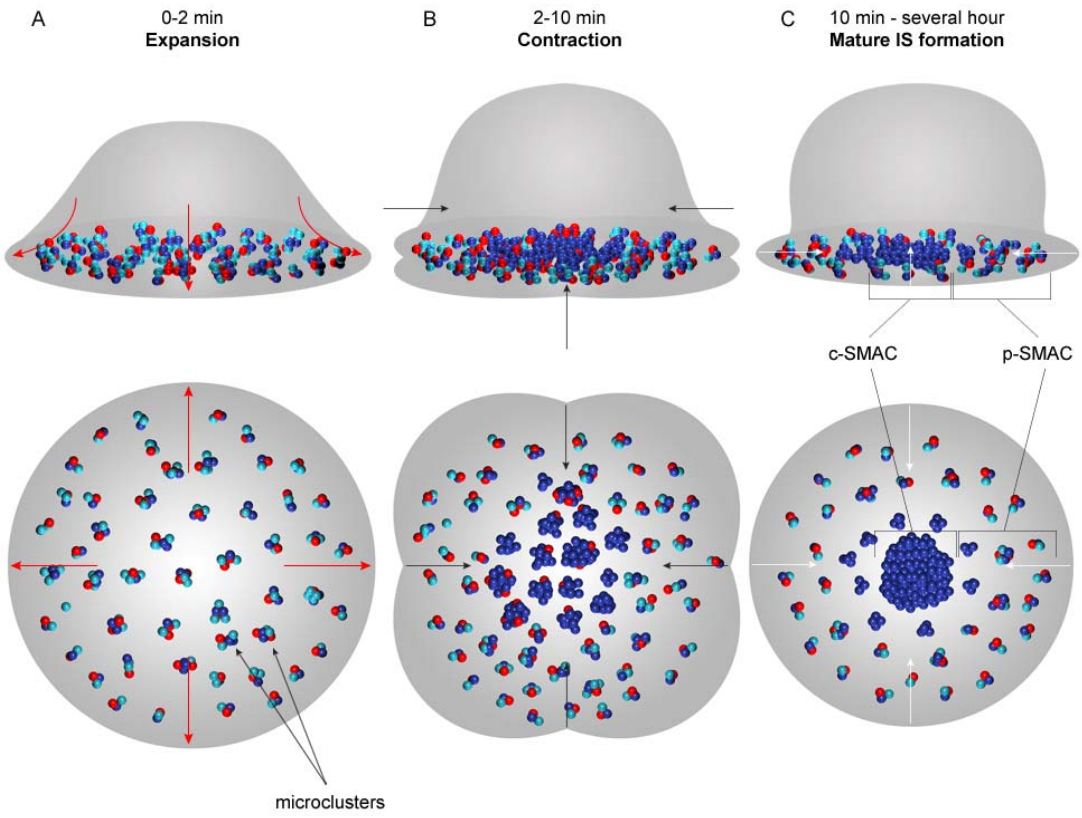



**Figure 3.** Dynamic process of immunological synapse formation. A) Upon T cell-pMHC-containing planar bilayer contact, functional microclusters (MCs) composed of the kinase (red), the receptor (dark blue) and the adaptor (light blue), are generated at the interface. Following the first attachment, the T cell continues to spread on the bilayer, with new MCs generated on the edge (red arrows). (B) After the full expansion, the T cell begins to contract (black arrows) and MCs accumulate at the central region of the interface. During this process, the MCs fuse each other to form larger MCs, whereas kinases and adaptors dissociate from TCR-MCs. (C) Ten minutes after T cell-bilayer conjugation, TCR-MCs finally accumulate at the center of the IS to form 'c-SMACs'. The c-SMACs contain minimal levels of kinases and adaptors. New functional MCs are continuously generated on the peripheral edge, which are translocated to the c-SMACs to sustain TCR signals, which last for hours (white arrows). Adapted from [275].

## 4. General features of interactions at the membrane

The plasma membrane is the theatre that accommodates a significant number of proteins with diverse structures and tasks necessary for the appropriate function of cells. The unique properties of this environment along with intrinsic characteristics of cell surface molecules have important functional implications for the process of cell-cell recognition. Furthermore, the strength of receptor-ligand binding and the mechanisms that may modulate the interactions between transmembrane proteins should also be considered. The following paragraphs will focus on these important aspects and examine the significance of oligomerization in protein function.

## 4.1 Consequences of membrane tethering

The dynamic interactions of cell surface proteins within the membrane are conditioned by two main aspects: intrinsic properties of the molecules and the membrane environment itself. For the cell-cell recognition process to take place, the apposing membranes need to come into proximity and the receptors to diffuse laterally in order to encounter and interact with their ligands at the intercellular junction. As a consequence, each individual binding event will be, in part, influenced by the initial adhesive contacts that ensure the alignment of the membranes. CD2 plays an important role in this early phase because the low affinity interactions with its ligand lead to a precise alignment of the membranes, enhancing other interactions [136, 288]. For example, CD2/CD48 binding has been shown to augment CD28-CD80 interactions [282]. Unlike CD2/CD48, the adhesive capacity of CD28/CD80 is very limited. This is not related to binding affinities, since they are actually higher than those of CD2/CD48. It is due, instead, to the low lateral mobility of CD28 [282]. On the contrary, the TCR [242] and CD2 [282, 289] exhibit an increased diffusion on the cell surface. Moreover, random collisions between molecules will slow down their diffusion process, thereby affecting the receptor-ligand encounter.

In addition to differences in mobility, proteins also have distinct physical dimensions. This is particularly important in the context of T cells, since T cell surface molecules vary enormously is size [245]. The TCR and accessory receptors are small, compared to some highly abundant proteins such as CD43 and CD45. During Ag recognition, the close proximity of the membranes limits the ability of large proteins to be accommodated within intermembrane region, or “contact zone”. Therefore, an efficient TCR/pMHC engagement may require a size-dependent segregation of the molecules into distinct zones, in which the larger ones are placed in the periphery of the interface [290]. Consistent with this, elongated forms of CD2/CD48 complexes inhibited TCR Ag recognition, whereas the wild-type CD2/CD48 interaction, that spans the same dimensions as the TCR/pMHC complex, significantly enhanced this process [291]. Similarly, increasing the dimensions of the TCR-pMHC interaction by elongating the pMHC ectodomain greatly reduces TCR triggering without affecting TCR-pMHC ligation [129] .

The membrane environment poses additional limitations to interacting proteins. The diffusion rate of receptors on the cell surface is, indeed, considerably slower than that of similarly sized soluble proteins [292, 293]. Molecules have to cross barriers imposed by cytoskeleton fences and/or by membrane “picket fences” formed by transmembrane proteins that are anchored to the cytoskeleton [294]. Moreover, the plasma membrane apparently contains distinct microdomains, designated lipid rafts [295] that can trap and

limit the free diffusion of rafts-associated proteins. Some T cell surface molecules important in TCR triggering preferentially accumulate there [296, 297]. Although attempts to directly observe these structures in live cells have failed, possibly because they are very small, the presence of these microdomains could contribute to the segregation of cell surface molecules at the T cell-APC contact area. As many signaling effectors seem to concentrate in lipid rafts, these membrane microdomains are thus considered signaling platforms where optimal conditions for cell activation are met [295]. However, this is still an extremely controversial issue since others did not observe accumulation of proteins normally associated with these microdomains in the TCR activation sites [298, 299]. As rafts and cytoskeleton “fences” disturbe the free diffusion of the molecules [300], they could be assumed to be the two main compartmentalizing forces at work in the plasma membrane. Nevertheless, a recent study by Douglass *et al.* [301] argues that rafts are not the primary factor in the clustering and immobilization of molecules in the T cell membrane. Although they do not exclude the existence of rafts, the authors rather suggest that other membrane subdomains, distinct from rafts and built by a network of protein-protein interactions, concentrate (e.g. Lck, LAT, CD2) or exclude (CD45) cell surface proteins to facilitate T cell signaling [301]. Finally, all interactions between transmembrane proteins are subject to mechanical stress that can be caused by, among other factors, thermal fluctuation in the membranes, repulsive forces between the membranes and cell movement [198].

## 4.2 Binding properties – an overview

Following the identification of interactions between cell surface molecules and their ligands, it then becomes important to understand the nature of the properties of these interactions. This includes the characterization of the thermodynamic properties of binding. Most studies have used surface plasmon resonance, in which solution affinities of soluble forms of the binding partners are measured [302]. In addition to this method, CD2-CD58/CD48 [136, 288] and CD28/CD80 [282] binding were also characterized in a model of cell-cell contact area which is directly related to the natural function of these proteins. From the large body of work produced so far, a general principle has emerged. Essentially all interactions involving membrane proteins are of very low affinity ($K_d$ 1-200 µM) (Fig. 4) and fast dissociation rate constants [303, 304]. Nevertheless, the coreceptors CD4 and CD8 (≥ 200 µM) and the CTLA-4/CD80 pair (0.2 µM) constitute two exceptions in that they lie well outside the typical $K_d$ range. Their unusual binding properties can be functionally explained, though. Whereas the extremely low affinity of the coreceptor for the MHC is

necessary to enhance the stability of the TCR/pMHC complex but not dominate the interaction [80], the much stronger CTLA-4/CD80 interaction is required to inhibit T cell activation [93].

Despite the overall low affinities and rapid dissociation rate constants, a very high level of specificity is achieved in these cell surface protein interactions. Affinities much greater than 10 μM can prevent disengagement [305], so having surface receptors with a higher affinity could hinder the ability of a T cell to detach from cells expressing the cognate Ag. The transient nature of cell surface interactions appears to be necessary for proper scanning and discrimination of the specific Ag, leading to productive signaling when it is present or to a rapid disengagement when it is not.

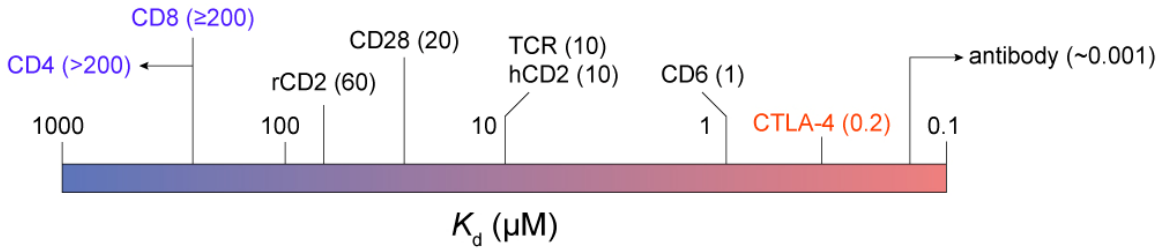



**Figure 4.** Binding affinities of some T cell surface molecules with their ligands. The solution affinities measured using surface plasmon resonance methods are shown on a logarithmic scale. After the name of each molecule is indicated the actual $K_d$ value. A typical antibody-protein antigen affinity is included for comparison. Adapted from [303].

## 4.3 Oligomerization

Oligomerization or dimerization events involve physical interactions between related proteins. The functional importance of this mechanism, in the context of cell surface receptors is that it increases the number of signaling outcomes, including productive signaling *per se* [306]. Some receptors are catalytically active, and upon ligand-binding are activated by ligand-induced dimerization or oligomerization. In the absence of intrinsic enzymatic activity, triggering occurs predominantly through recruitment of soluble proteins to the receptors' cytoplasmic tails that will activate intracellular signaling pathways. Furthermore, many components of intracellular signaling pathways are themselves able to dimerize. This intrinsic functional property thus appears to play an important role in the process of signal transduction. Bivalency has indeed been shown to stabilize signaling complex formation several-fold [93]. In addition to homodimerization, multiple proteins undergo hetererodimerization, which increases the magnitude of interactions mediated by this mechanism. The role of dimerization in single- and multipass transmembrane receptors triggering will be discussed below.

### 4.3.1 Role in triggering of single-pass (class I) membrane receptors

Many growth factors bind receptors with tyrosine kinase activity. The first protein-tyrosine kinase receptor (PTKR) shown to dimerize upon ligand binding was the epidermal growth factor (EGF) receptor [307]. Its ligand is monomeric but a number of other PTKR ligands can form dimers as well. After ligand-induced association of PTKRs, the following step is receptor autophosphorylation, which results from one receptor molecule phosphorylating the other in the dimer [308]. This enhances the receptor kinase activity and creates docking sites for down-stream signaling effectors. On the contrary, cytokine receptors lack intrinsic enzymatic activities but ligand engagement induces their dimerization or oligomerization, allowing activation of cytoplasmic PTKs that are associated with the receptor's intracellular tail.

Since the TCR is also enzymatically inactive, a controversial issue is whether the TCR itself requires binding-induced oligomerization or aggregation for triggering. Different aggregation models have been proposed but they can only partially explain what is known about TCR signaling [208]. The co-receptors CD4 and CD8 are two of the most significant contributors to this process. Although the former is assumed to be predominantly expressed as a monomer, oligomerization of CD4 has also been described at the surface of T cells and monocytes/macrophages [62, 63, 309]. Some reports have actually indicated that the functional form of CD4 is a dimer or oligomer [62, 63, 310-312] but the exact role and significance of CD4 dimerization remains unclear. Likewise, CD80 dimers and monomers coexist in dynamic equilibrium at the T cell surface [97]. Engagement with its bivalent ligand, which is expected to stabilize CD80 dimers [95], leads indeed to an increase in CD80 self-association that is important for delivering a strong inhibitory signal to T cells. Monomeric and dimeric forms of another relevant receptor for TCR-mediated signaling, the transmembrane phosphatase CD45, have been reported as well [119, 313]. Experimentally induced self-association of CD45 leads to inhibition of its phosphatase activity [115], suggesting that the dimerization could act as its regulatory mechanism [314]. However, other studies by Nam *et al*. do not support this hypothesis [110].

In addition to other types of membrane receptors, such as the TNF receptor family and proline-serine/threonine kinase receptors, several other soluble proteins involved in regulation of apoptosis and transcriptional activation undergo oligomerization [306].

### 4.3.2 GPCRs – too many dimers?

G-protein coupled receptors (GPCRs), also know as seven transmembrane receptors, are integral membrane proteins that possess seven membrane-spanning domains. They

represent the largest family of cell surface molecules involved in signal transduction, and can be grouped into 4 classes according to their structural homology and functional similarity. Recent studies led to the identification of a variety of proteins that, in addition to binding ligands and G-proteins, interact directly with the GPCRs [315]. Some examples are GPCR kinases, second-messenger-dependent kinases and arrestins. Furthermore, different lines of evidence suggest that these molecules can self-associate, existing and likely functioning as dimers or higher-structure oligomers [316]. The first experimental observations indicating GPCR homo- and heterodimerization were obtained by co-immunoprecipitation studies [317, 318]. However, as GPCRs are highly hydrophobic peptides they could form artifactual aggregates when removed from the lipid environment of the plasma membrane. Therefore, they were predominantly seen as monomeric entities. It was the finding that the functional GABAβ receptor is a dimer comprising two distinct receptor subtypes, GABAβ RI and GABAβ R2 [319-321], that changed the conventional view. When expressed alone GABAβ R1 was retained in the endoplasmatic reticulum, while GABAβ R2 was targeted to the membrane but could not bind the ligand. Co-expression of the two receptors resulted in a proper targeting to the cell surface, ligand binding and function of the complex. Moreover, the development and usage of RET-based methods seemed to confirm the existence of dimeric entities, thus fueling many subsequent studies. Since then an increasingly number of investigations has been carried out to monitor GPCR-GPCR complex formation, with the concept of GPCR dimerization changing from a hypothesis to being widely accepted [322].

One question that has attracted considerable attention is whether dimerization is constitutive or ligand-induced, as in the case of many other receptor families. Regardless of the technique used, evidence exists to support both situations [323]. In fact, transition from monomer to dimer upon ligand engagement and constitutive dimers that are, or not, affected by ligand binding could all be observed. The diversity of results obtained may be related to intrinsic characteristics of the different receptors studied or, perphaps, reflect interpretational difficulties associated with the various approaches employed.

Another significant issue was to understand the role of dimerization in receptor function. In the light of the results obtained with GABAβ R1, in which when expressed alone was retained in the endoplasmatic reticulum [319-321], it has been proposed that self-association would be involved in receptor trafficking. Indeed, the currently view is that dimerization seems to occur early after receptor biosynthesis [324], although this may not be the case for all GPCRs [325]. Other studies, mainly on the opioid receptors [326] indicate that heterodimers have distinct pharmacological properties compared to those of the individual GPCRs, whereas other observations indicate that receptor dimerization can be involved in internalization processes [327, 328] and/or required for activation [329-331].

However, dimerization was shown to have distinct effects on receptor function. Using a peptide that hinders dimerization, Herbert *et al*. [317] showed that receptor activation was also inhibited [317]. On the other hand, for another GPCR, a peptide that restrains receptor function does not affect the formation of dimers [332]. Although contradictory data has been gathered for different receptors regarding their function as dimeric signaling units, the work done with GABAβ and mentioned above, clearly demonstrated that this receptor, at least, functions as an obligatory constitutive dimer [319-321]. Further studies are required to investigate if GPCR dimerization is a general mechanism and if so, its physiological relevance.

## 5. Characterization of protein-protein interactions

Protein-protein interactions can be analysed from a variety of perspectives. In addition to the identification of protein partners and the necessary sequence determinants of the interactions, it is also essential to understand the mechanisms underlying the function of the proteins involved. A number of different approaches have been established for addressing these issues, both *in vivo* and *in vitro* [333]. The later include classical biochemical techniques like immunoprecipitation and pull-down assays, isothermal titration calorimetry and surface plasmon resonance. However, large amounts of purified stable protein are often required, in addition to well-characterized proteins in comparably high amounts and concentrations for control purposes. Moreover, a rigorous analysis of protein interactions must take into consideration the cellular environment, thus requiring *in vivo* methodologies to complement the *in vitro* observations. The yeast two-hybrid system and protein fragment complementation assays are frequently used for dissecting interaction networks *in vivo*, but generate rather high numbers of false positive results. On the other hand, biophysical techniques involving resonance energy transfer, namely FRET (fluorescence resonance energy transfer) and BRET (bioluminescence resonance energy transfer) enable the real-time monitoring of protein interactions in living cells. The main disadvantage of the bulk RET method is that the two fluorophores need to be close enough for energy transfer to occur (1-10 nm). A more general approach is to use single molecule detection. This includes the usage of atomic force microscopy and fluorescence techniques. Many variations of fluorescence analysis have been developed and successfully applied both *in vitro* and in living cells [334]. The major drawback of this type of imaging is the relatively fast photobleaching of organic fluorophores. A combination of these different techniques is likely to be required for fully understanding the proteins'

function and their intricate networks. Two distinct methodologies, surface plasmon resonance for which the Biacore is the major system provider and BRET will be here described in detail. The former has contributed considerably to the understanding of the nature of cell-cell interactions, whereas the latter is becoming the system of choice for studying the nature of lateral interactions within the membrane.

## 5.1 Interactions between cells: the Biacore

The Biacore system was introduced in the early 1990s and since then a wide variety of protein-protein interaction studies based on solid-phase detection has been performed [335, 336]. This system detects the interaction of a soluble ligand with a receptor immobilized on a solid surface. Purified samples containing the ligand are then injected through the flow cell, maintaining the sample concentration constant. If the injected ligand binds to the immobilized receptor, an increase in the refractive index near the sensor surface will occur; which will be detected in the Biacore by surface plasmon resonance. Since interactions are detected in real time, both the equilibrium and interaction kinetics can be gathered. Additional important advantages are that the interacting partners do not need to be labelled, and the reduced sample handling and consumption.

The interactions between cell adhesion molecules are often very weak [303, 304] which makes them hard to study. Due to its features the Biacore is a well-fitted system to characterize low-affinity interactions [302]. As wash steps can be avoided, even a very weak interaction can be detected because it will not be disturbed by washing steps as it would in conventional assays. The interaction between CD2 and CD48 was the first to be analysed with the Biacore and demonstrated its applicability [337]. In fact, similar results were recently obtained by isothermal titration calorimetry, confirming the reliability of surface plasmon resonance-derived affinity data [135]. The kinetic data on CD2 was later on expanded, this time measuring its binding affinity with the human ligand, CD58 [338]. It was shown that human CD2 interactions are stronger ($K_d$ of 10-20 μM) than those of rat proteins ($K_d$ of 60-90 μM), and have very fast dissociation rate constants (> 4 $s^{-1}$), which are still measurable on the Biacore [338]. Furthermore, studies using mutant proteins allowed the identification of CD2-binding site on CD48 [139].

The binding properties of many other lymphocyte cell-cell recognition molecules have been analysed. These include the TCR-pMHC, the coreceptors CD4 and CD8 with the MHC and the costimulatory molecules CD28 and CTLA-4 with their shared ligands, among others [304]. The use of the Biacore has indeed revealed a completely new

perspective on the interaction of the latter proteins, demonstrating that the ligands have different binding affinities relative to both CD28 and CTLA-4 [93].

There are, however, potential pitfalls associated with the technique [302]. As one of the partners has to be immobilized, in addition to appropriately tether the protein to the surface, one has to be sure that the binding properties are not modified by that procedure. In recent years, substantial progress has been made in this regard [336]. Likewise, enormous technological improvements were introduced in this system and now it is used in a wide range of applications that include food analysis and drug discovery [335]. As for proteomics, confirmation of binding specificity and identification of novel binding partners are currently also addressed [335].

## 5.2 Interactions within the membrane/ stoichiometry: BRET

Although the interactions mediated by cell surface proteins have been well characterized, less is known about the nature of lateral interactions within the membrane. Bioluminescence resonance energy transfer (BRET) [339] is emerging as the methodology of choice to directly monitor protein interactions in vivo. Also, it is a useful tool for characterizing the quaternary structures of cell surface molecules. The phenomenon results from the non-radiative energy transfer between luminescent donor and fluorescent acceptor molecules, as first described by Förster [340]. In the presence of oxygen, the bioluminescent protein Luciferase (Luc), isolated from the coral *Renilla reniformis*, oxidizes its substrate, coelenterazine, releasing photons with wavelengths peaking at ~ 475 nm. If a suitable acceptor (GFP – green fluorescent protein) is in close proximity, i.e. 10 to 100 Å, energy transfer can occur between Luc and GFP, which results in the emission of photons with longer wavelengths (~ 510 nm). The BRET$^2$ assay is an optimized version of this technology that uses DeepBlueC, a modified form of the natural substrate, which has maximal emission at 410 nm and GFP$^2$, a UV-GFP variant, which can be excited at this wavelength whilst emitting at 515 nm, providing a greater signal resolution [341]. The major distinction between BRET and its counterpart FRET (fluorescence resonance energy transfer) is that FRET involves energy transfer between two fluorophores, one of which requires external excitation by a suitable light source, whereas BRET occurs after oxidation of a substrate leading to light generation, obviating a need of extrinsic illumination. This greatly reduces the signal to noise ratio. Therefore, the superiority of BRET over FRET lies in its extremely low background. As it does not require an external source of excitation, BRET circumvents problems associated with autofluorescence, photobleaching and simultaneous excitation of both donor and acceptor

fluorophores, often formed with FRET. The exceptional sensitivity of BRET [342] allows the detection of weaker interactions at physiological levels of expression.

In the BRET methodology, proteins of interest are genetically fused to either Luc or GFP and expressed as “BRET pairs” in a suitable cell line. If the two partners do not interact at all, only luciferase signals are emitted. However, if they come into close proximity due to protein-protein interactions, energy transfer can occur between Luc and GFP and an additional signal emitted by the GFP can be detected (Fig. 5). This energy transfer depends critically on both the distance and the orientation of the BRET partners used. As will be seen, substantial energy transfer arises from random interactions.

An increasing number of studies have employed this technology to study a wide range of protein-protein interactions [343]. These include constitutive or agonist-promoted membrane receptor-receptor interactions, oligomerization of transcription factor complexes, specific protease activity and quantification of intracellular protein concentration [344]. In particular, BRET has been frequently used to investigate the regulation of GPCRs by different proteins and to characterize GPCR dimer and/or oligomer formation [322].

Despite having many advantages over other techniques, BRET does not provide information about the cellular location of the interaction. Single-cell BRET has been performed in an attempt to overcome this limitation, but the signal was detected from the entire cell rather than distinct subcellular locations [345]. Also, current BRET assay systems cannot detect endogenous protein interactions as the proteins of interest need to be tagged. Moreover, donor and acceptor must be in close molecular proximity for energy transfer to occur, preventing RET-based systems from being a general method, as dimensions of a given protein may not be known. Improvements in the methodology [346] and in detection systems are necessary to expand even more the wide range of biological applications of this technique.

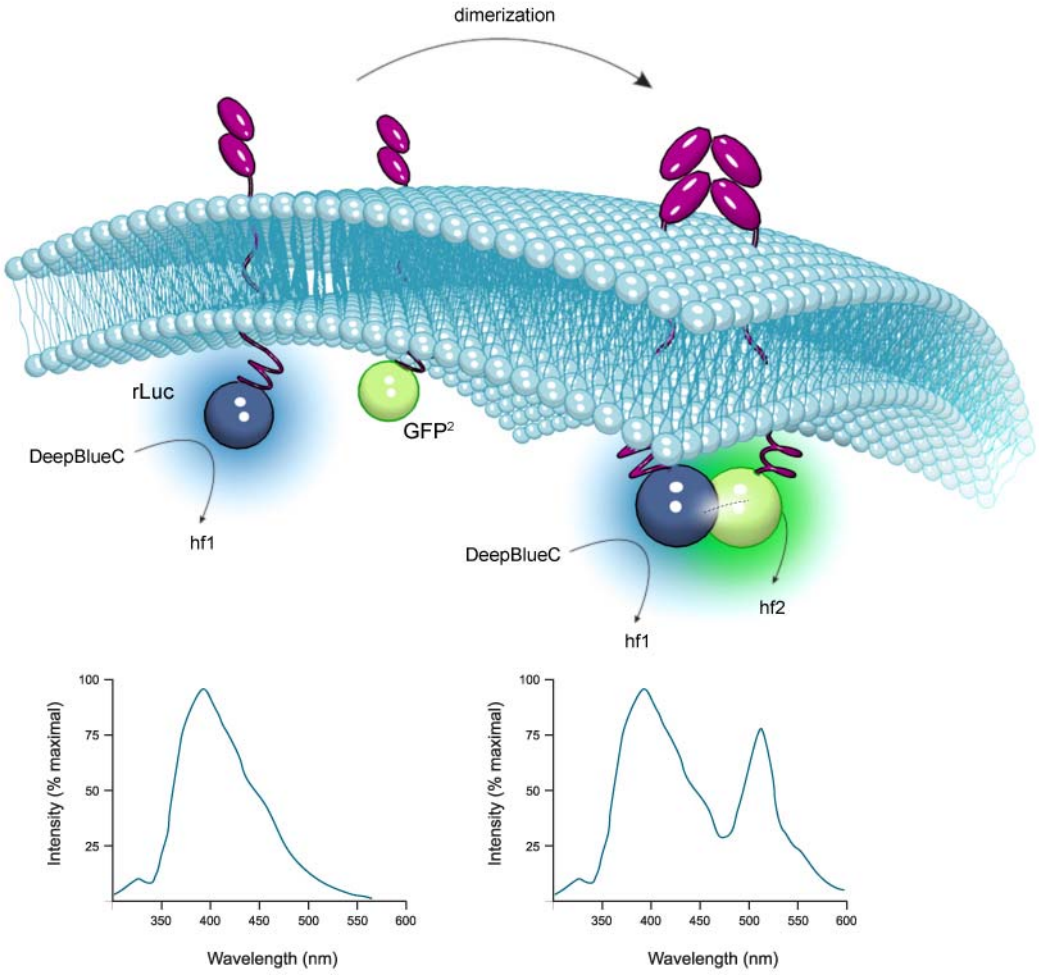



**Figure 5.** Bioluminescence resonance energy transfer and the BRET$^2$ assay. BRET relies on nonradiative energy transfer between donor and acceptor fluorophores and can be applied to study protein-protein interactions at the cell surface. Each molecule is genetically fused to either the donor (rLuc) or the acceptor (GFP$^2$) molecule and co-expressed in live cells. When all GFP molecules are further than 10nm from rLuc (left), BRET cannot occur so only the light emitted by rLuc, resultant from the degradation of its substrate, DeepBlueC, will be detected (left graph). When GFP is within 10nm, BRET can occur (dashed line on the right), which gives rise to additional light emission by GFP, and detection of a second, longer-wave length emission peak (right graph). BRET$^2$ is an optimized version of BRET that uses DeepBlueC and GFP$^2$, which allows a spectral separation of more than 100nm.

## 3. Aims of the thesis

An understanding of cell surface organization is instrumental to understanding how cellular pathways are skewed to drive specific functions. In this thesis we proposed to investigate the basal and synapse-dependent organization of the T cell surface, focusing on the functional analysis of a particular T lymphocyte antigen, CD6. In this context, the specific aims were:

I. To elucidate the general features of the molecular organization of the T cell surface.

II. To further characterize the functional and physiological role of the T lymphocyte specific antigen CD6.

III. To assess the cellular relevance of novel extracellular isoforms of CD6 upon T cell-APC interactions and T cell activation.

# II – Research work

# 1. A rigorous experimental framework for detecting protein oligomerization using bioluminescence resonance energy transfer

**John R. James, Marta I. Oliveira, Alexandre M. Carmo, Andrea Iaboni and Simon J. Davis**

*Nature Methods*, 3 (12): 1001-6 (2006)

## 1.1 Abstract

Bioluminescence resonance energy transfer (BRET), which relies on nonradiative energy transfer between luciferase-coupled donors and GFP-coupled acceptors, is emerging as a useful tool for analyzing the quaternary structures of cell-surface molecules. Conventional BRET analyses are generally done at maximal expression levels and single acceptor/donor ratios. We show that under these conditions substantial energy transfer arises from random interactions within the membrane. The dependence of BRET efficiency on acceptor/donor ratio at fixed surface density, or expression level at a defined acceptor/donor ratio, can nevertheless be used to correctly distinguish between well-characterized monomeric and oligomeric proteins, including a very weak dimer. The pitfalls associated with the nonrigorous treatment of BRET data are illustrated for the case of G protein– coupled receptors (GPCRs) proposed to form homophilic and/ or mixed oligomers on the basis of previous, conventional BRET experiments.

## 1.2 Introduction

BRET relies on nonradiative energy transfer between donor and acceptor fluorophores [1]. The bioluminescent protein, luciferase, oxidizes its substrate, coelenterazine, releasing photons. An appropriate fluorophore in close-enough physical proximity, typically **<** 100 Å, can be excited to a higher energetic state, before emitting photons with longer wavelengths. An optimized version of this technology, the $BRET^2$ assay, uses DeepBlueC, an analog of the natural substrate with maximal emission at 410 nm, and a UV-GFP variant ($GFP^2$) that is excited at this wavelength and emits at 515 nm, giving a spectral separation of >100 nm. The key advantage of BRET over other forms of resonance energy transfer technology, such as fluorescence resonance energy transfer (FRET), is the very high signal/noise ratio gained from luminescence detection, which is unaffected by photobleaching or other optical effects, and allows protein interactions to be detected at physiological expression levels. Proteins of interest are expressed as 'BRET pairs' after being genetically fused to either *Renilla* luciferase (Luc) or '$GFP^{2}$' (GFP). BRET efficiency ($BRET_{eff}$), that is, the ratio of GFP emission to that of Luc emission, is dependent on the inverse sixth-power of the mean separation of donor and acceptor. For donors and acceptors forming constitutive oligomeric structures, $BRET_{eff}$ will therefore usually be high. A potential complication of all RET experiments is that background signals may arise from random interactions if donor and acceptor levels are sufficiently high. $BRET_{eff}$ in this case will generally be lower than that for oligomers as a result of the larger average separation

of donors and acceptors. In principle, however, $BRET_{eff}$ maxima for *bona fide* oligomeric interactions may nevertheless be comparable to those arising from random interactions if the subunits are well separated and/or interact weakly, complicating discrimination between the two types of interactions. Theoretical considerations [2-5] predict that, in addition to differences in $BRET_{eff}$ maxima that may or may not be obvious, the dependence of $BRET_{eff}$ on fluorophore concentrations will differ systematically for proteins interacting randomly versus those that form oligomers, in two types of experiments. For the first, or 'type-1', experiment, wherein the combined number of donors and acceptors is held constant, $BRET_{eff}$ for random interactions will be independent of acceptor/donor ratios above a certain threshold [2, 3]. This is because, at acceptor/donor ratios high enough to prevent competition between donors for acceptors, each donor will 'experience' the same acceptor environment (Fig. 1a; a fuller explanation of the theoretical predictions is available in Supplementary Note at the end of this chapter). In contrast, $BRET_{eff}$ for oligomers is predicted [4] to be highly dependent on the relative donor concentration because donors self-associate, reducing the overall efficiency of energy transfer (Fig. 1b,c). In this case, the acceptor/donor ratio *(f)* should affect $BRET_{eff}$ in a hyperbolic fashion that is dependent on the stoichiometry of the oligomer (*n*); reducing the relative concentration of donors will increase $BRET_{eff}$ to saturation (equation (1) is derived in Supplementary Methods at the end on this chapter).

$$\frac{BRET_{eff}}{BRET_{max}} = 1 - \frac{1}{(1+f)^{n-1}} \qquad (1)$$

For the second, or 'type-2', experiment, wherein expression level is varied and acceptor/donor ratio kept constant, $BRET_{eff}$ for random or very weak interactions will be pseudo-linearly dependent on expression and may fall to zero at very low expression levels (Fig. 1d,e). Conversely, for oligomers $BRET_{eff}$ is expected to be expression level–independent because, generally, expression will itself be dependent on the correct assembly of the oligomer, making this type of experiment especially useful for identifying obligate oligomers (Fig. 1f). We test these predictions for a series of monomeric and oligomeric proteins of known stoichiometry and then consider the case of class-A GPCRs proposed to form oligomeric structures in previous BRET experiments [6].

## 1.3 Materials and Methods

### 1.3.1 BRET assay

We collected cells from wells 24 h post-transfection using phosphate-buffered saline, pelleted them at *600g* for 3 min and resuspended them at ~ 1.5 x $10^6$ cells/ml in minimal essential medium. For each transfection, we added 10 μM DeepBlueC (final concentration; PerkinElmer) to 100 *μ*l of cells in a 96-well OptiPlate (PerkinElmer) and collected light emission in the 410 ± 40 nm (BRET-A) and 515 ± 15 nm (BRET-B) wavelength ranges three times for each range, integrated over 1 s on a Fusion microplate analyzer (PerkinElmer). To determine GFP and Luc expression, we dispensed 100 μl of cells in a separate well, excited them at 420 nm and measured emission at 515 ± 15 nm three times over 1 s, to obtain the total fluorescence units (FU). We then incubated the cells in the same well with 10 μM coelenterazine-h for 2 min before reading total emission three times integrated over 1 s, to obtain the total luminescence units (LU). We calculated BRET values, after background subtraction, as BRET-B/BRET-A, corrected for luciferase expression alone (typically 7% of BRET-A luminescence). As the concentration of tagged molecules is proportional to the signal detected (Fig. 3a), the acceptor/donor ratio can be calculated as [GFP]/[Luc] = ($k_G$FU)/($k_L$LU) = K(FU/LU), where $k_G$ and $k_L$ are constants specific to GFP and Luc, respectively, and K = $k_G$ / $k_L$. The FU/LU value calculated for the sGFP-Luc expression in each experiment gives 1/K because the acceptor/donor ratio is fixed at one. We used this derived value of K to convert the measured acceptor/donor ratio (FU/LU) to one of concentrations ([GFP]/ [Luc]), before plotting against the $BRET_{eff}$ at that value.

For the type-2 BRET analysis, we transfected the cells with a particular acceptor/donor ratio (12:1), and then collected samples at regular intervals so that the expression level could be varied systematically, before being assessed as above for BRET. We determined the level of protein expression using total Luc expression as this gave the most reliable measure of low-level expression.

### 1.3.2 Statistical analysis

We used the two-tailed Student's *t*-test, where appropriate, to assess the difference between data sets. We used the nonlinear least-squares fitting function of Origin 7.5 (Originlab) to fit functions to data and estimate parameters, as described in Supplementary Methods at the end of this chapter.

### 1.3.3 Additional methods

Description of DNA constructs, cell culture and transfection, confocal microscopy and FACS analysis are available in Supplementary Methods.

## 1.4 Results

### 1.4.1 Conventional BRET experiments

The monomeric, noninteracting type-I membrane proteins CD2 and CD86 mediate cell adhesion and signaling in the immune system [7-9] (Fig. 2a). When we expressed CD2 and CD86 separately as BRET pairs (by cotransfecting genes encoding $CD2_{Luc}$ and $CD2_{GFP}$ or $CD86_{Luc}$ and $CD86_{GFP}$), or as a single BRET pair (by cotransfecting $CD2_{Luc}$ and $CD86_{GFP}$), in 'conventional' BRET experiments in HEK-293T cells, that is, involving maximal expression at a single ratio of donors and acceptors, $BRET_{eff}$ was approximately one-fifth that for a control protein consisting of a soluble, fused form of Luc and GFP (sGFP-Luc; Fig. 2b). Fluorescence-activated cell sorting (FACS) analysis and confocal microscopy confirmed that energy transfer resulted almost exclusively from interactions at the cell surface (Fig. 2c,d) rather than intracellular aggregation or other artifacts resulting from overexpression. This indicated that, for type-I membrane proteins, substantial energy transfer results solely from random, nonspecific protein interactions. $BRET_{eff}$ for a type-I membrane glycoprotein that dimerizes in crystal lattices and in solution, CD80 [10, 11], was almost twice that of the monomers ($P < 0.001$), but considerably less than that of sGFP-Luc (Fig. 2b).

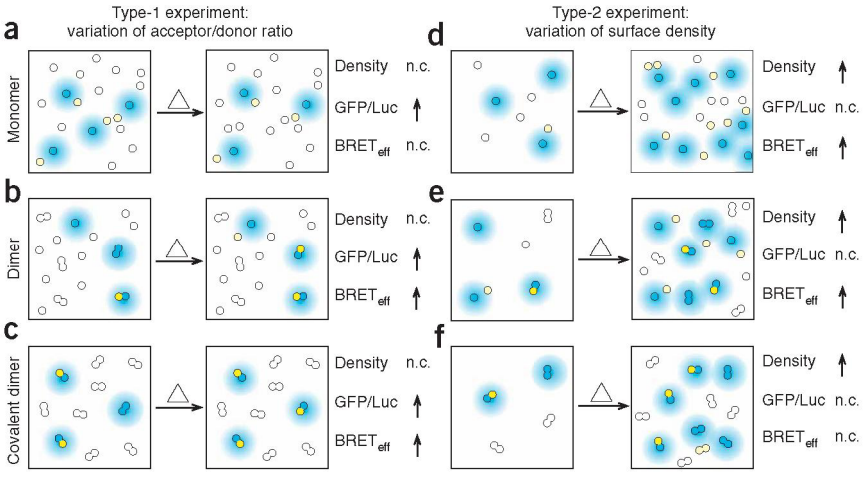


**Figure 1.** Effects of acceptor/donor ratio and surface density on $BRET_{eff}$. **(a)** $BRET_{eff}$ for random interactions is unaffected by donor concentration because as acceptor/donor ratio increases and total surface density remains essentially constant (n.c., no change), each donor continues to 'experience' a similar separation from the nearest acceptor. This independence breaks down if there are more donors than available acceptors, that is, when the acceptor concentration ceases to be effectively constant. **(b,c)** Molecules that can oligomerize are sensitive to changes in the acceptor/donor ratio because donors and acceptors compete to form multimeric complexes. Oligomerization reduces the effective surface density, reducing $BRET_{eff}$ from random interactions. **(d)** Increasing surface density at a given acceptor/donor ratio forces monomeric acceptor and donor molecules into closer proximity, increasing the likelihood of BRET owing to random interactions. At low surface densities, $BRET_{eff}$ will tend to zero. **(e)** Noncovalent oligomers are biased toward oligomer formation at higher surface densities but will also exhibit density-dependent BRET owing to random interactions. $BRET_{eff}$ should not decrease to zero at low densities, however, owing to the effect of affinity on complex formation. **(f)** Covalent or other constitutive oligomers are expected to produce $BRET_{eff}$ that is independent of surface density because folding and complex formation are generally density independent. However, at high surface densities the random interactions of oligomers will contribute to the overall signal. Fluorescing and nonfluorescing acceptor molecules are shown as yellow and open circles, respectively, and donors shown as blue circles. The BRET-permissible area surrounding donors is shown approximately to scale.

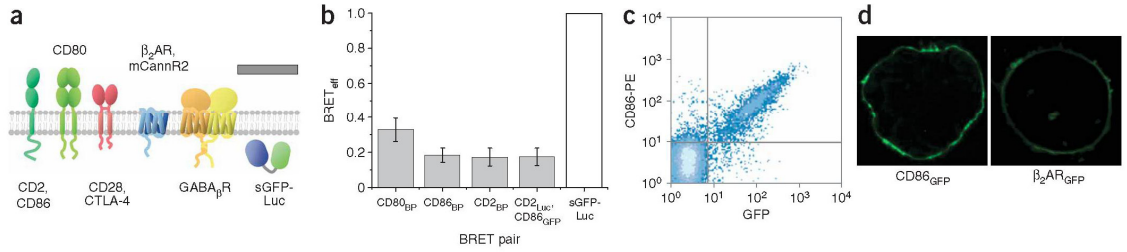



**Figure 2.** Monomeric proteins expressed at the cell surface give substantial resonance energy transfer in conventional BRET experiments. **(a)** Schematic of the architecture of proteins used in this study, approximately to scale. Scale bar, 10 nm. **(b)** $BRET_{eff}$ for the indicated proteins expressed as BRET pairs, normalized against the value obtained for sGFP-Luc. ''BP'' denotes single proteins coexpressed as both Luc and GFP fusions. Error bars represent mean ± s.d., n = 8. **(c)** FACS analysis of $CD86_{GFP}$-transfected HEK 293T cells after 24 h, stained with anti–CD86-PE (Serotec). **(d)** Confocal microscopy–based analysis of $CD86_{GFP}$ (left) and $\beta_2AR_{GFP}$ (right) expression, demonstrating GFP localization to the cell surface.

### 1.4.2 Type-1 experiments

We determined whether these $BRET_{eff}$ differences complied with the theoretical predictions for the two classes of interactions by examining the dependence of $BRET_{eff}$ on acceptor/donor ratio (the type-1 experiment). Twenty-four hours after transfection with equivalent amounts of total DNA comprised of various ratios of the GFP- or Luc-tagged fusion protein–expressing vectors, 293T cells expressed physiological levels of each of the cell surface proteins (that is, 50,000–500,000 copies/cell [12]; Fig. 3a). Comparison of light emission in the 370–450 nm and 500–530 nm ranges, measured for cells expressing the GFP- and Luc-tagged fusion proteins, with that obtained for cells expressing sGFP-Luc, allowed $BRET_{eff}$ to be plotted against the ratio of GFP and Luc concentrations ([GFP]/[Luc]). This was important as it permitted stoichiometric information to be derived, and rendered the method instrument-independent, facilitating interexperimental comparisons. Others have shown that fluorescence levels are largely unaffected by the precise structural context of the N- or C-terminal fusions [13], which we confirmed by showing that, for all constructs tested, equivalent levels of cell-surface expression gave exactly the same GFP fluorescence (Fig. 3a). We also failed to see any correlation between cytoplasmic tail length and $BRET_{eff}$ for cytoplasmic domains less than ~150 residues (data not shown). Others have reported construct-specific variation in fluorophore intensity [14] but this may have been due to differential protein expression levels not directly assayed in their experiments.

$BRET_{eff}$ values obtained for CD2 and for CD86 expressed as BRET pairs, and for the two proteins coexpressed as a single BRET pair, exhibited similar maxima (~0.2) and were independent of the [GFP]/[Luc] ratio beyond a value of 2 (Fig. 3b): fits of the data to a constant beyond this [GFP]/[Luc] ratio were better than hyperbolic fits (equation 1), fully in accord with the theoretical predictions (Fig. 3c; fits to all the data, along with the goodness of each fit represented numerically as the root mean square of the residuals, are available in Supplementary Fig.1 and Supplementary Table 1 at the end of this chapter, respectively). Other non-interacting proteins expressed as BRET pairs, that is ALCAM and PD-L1, gave equivalent data (Fig. 3b). Notably, all the monomers gave the same $BRET_{eff}$ maxima (~0.2), implying that this is the threshold above which all oligomeric type-I membrane proteins may be identifiable. Conversely, the covalent type-I homodimers CD28 and CTLA-4 (Fig. 2a) yielded data that gave very good fits to equation 1 ($n$ = 2), with $BRET_{eff}$ approaching the unitary value assigned to sGFP-Luc (Fig. 3b). As in the conventional experiment (Fig. 2b), $BRET_{eff}$ for CD80 expressed as a BRET pair (Fig. 3b) was higher than that for the monomers and gave a better fit to equation 1 than did $BRET_{eff}$ for CD86 (Fig. 3c). The asymptote is substantially smaller than that for CD28

or CTLA-4, however, consistent with the coexistence of CD80 dimers and monomers in dynamic equilibrium. The observation that $BRET_{eff}$ is enhanced by coincubation with soluble, bivalent ligand (CTLA-4Fc; Fig. 3d), which would be expected to stabilize CD80 dimers [11], supported this interpretation. A chimeric protein consisting of the CD80 extracellular domain and CD86 transmembrane and cytoplasmic domains yielded similar data, implying that, at the cell surface, CD80 dimerizes via its extracellular domain, presumably in the manner observed in crystals of soluble CD80 [10, 11] (and data not shown). The affinity of soluble CD80 self-association is very low (50 μM) [10], indicating that type-1 experiments readily identify very weak homophilic interactions. The weak self-association of CD80 has recently been confirmed in FRET-based analyses [15].

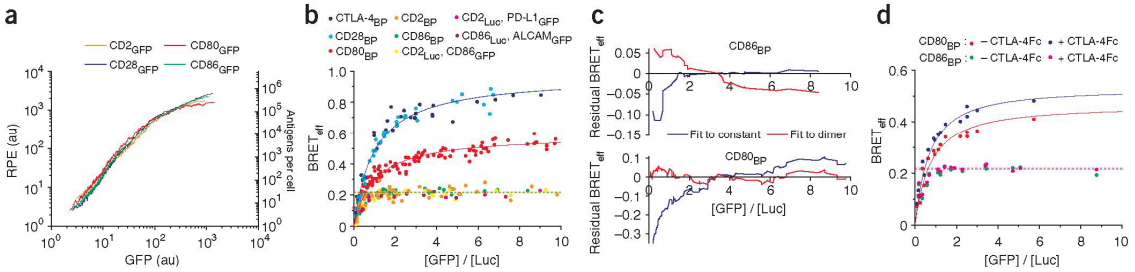



**Figure 3.** Type-1 experiments: varying the acceptor/donor ratio distinguishes between BRET arising from random versus oligomeric interactions. **(a)** FACS analysis using PE-conjugated antibodies to the specified antigens and QuantiBRITE beads, demonstrating that GFP expression correlates with equivalent cell-surface staining. **(b)** Solid lines show fits of data obtained for the indicated BRET pairs to equation (1), that is, for dimers, and the dotted lines show the fit (for [GFP]/[Luc] > 2) to a constant value, as predicted for random interactions. Only the model that gave the best fit is shown. **(c)** Residual $BRET_{eff}$ values after nonlinear least-squares fitting to the indicated model, plotted as a moving average of the data. A good fit reduces residuals to zero. **(d)** Cells expressing CD80 or CD86 as a BRET pair were incubated with phosphate-buffered saline (– CTLA-4Fc) or 50 μg/ml CTLA-4Fc (+ CTLA-4Fc) before assaying for BRET.

### 1.4.3 Type-2 experiments

It is not always feasible to vary the [GFP]/[Luc] ratio while keeping the combined number of donors and acceptors constant, in which case the expression level can be varied and the acceptor/donor ratio kept constant [5] (type-2 experiment). We transfected cells with constant ratios of donor- and acceptor-encoding vectors and measured $BRET_{eff}$ at successive time points, that is, at increasing expression levels. $BRET_{eff}$ levels for CD86 and CD2 exhibited a strict dependence on surface density, whereas for the covalent dimer, CTLA-4, it was largely expression-level independent (Fig. 4). The slight increase in

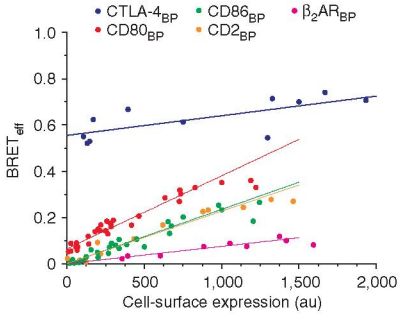



**Figure 4.** Type-2 experiments: BRET signals arising from random interactions of molecules are linearly related to surface density at a given acceptor/donor ratio. The expression level was calculated from Luc emission and fitted to linear equations for all molecules. Note that for the oligomers, CTLA-4 and CD80, the intercept of the ordinate is nonzero.

$BRET_{eff}$ observed in the case of CTLA-4 can be attributed to random interactions between homo-dimers and is further evidence that such interactions contribute substantially to $BRET_{eff}$, even though it is often assumed that transfer between oligomers can be neglected. For CD80, $BRET_{eff}$ was expression-level dependent, but did not fall to zero at low expression levels, as expected for nonconstitutive homodimers (Fig. 1e). The evidence that CD80 exhibited behavior distinct from that of randomly interacting proteins, although statistically significant ($P < 0.001$), was less compelling for this type of analysis than for the type-1 experiment (Fig. 3b, c).

### 1.4.4 Re-examination of class-A GPCR dimerization

Without exception, the authors of more than forty previous BRET-based studies of membrane protein oligomerization concluded that the proteins they were studying form dimers or higher-order structures [6]. The majority of studies addressed the quaternary structures of GPCRs, the largest family of cell-surface signaling proteins encoded by the mammalian genome. As the studies for the most part used conventional BRET experiments, that is assays in which donor- and acceptor-encoding plasmids were used at a single ratio [16, 17] we examined whether a more rigorous analysis of BRET data supported these conclusions.

We chose the class-A GPCR most studied in BRET experiments, human $\beta_2$-adrenergic receptor ($\beta_2$AR). We used a second class-A GPCR, mouse cannabinoid receptor 2 (mCannR2) and a hetero-dimerizing class-C GPCR, the neuronal γ-amino-*n*-butyric acid type β receptor ($GABA_{\beta}R$) for control purposes (Fig. 2a). In experiments in which we systematically varied the [GFP]/[Luc] ratio but kept the overall expression levels constant, $BRET_{eff}$ for $\beta_2$AR and mCannR2 expressed as BRET pairs were of the same low maximum values reported elsewhere (~0.1) [14, 16], and exhibited [GFP]/[Luc] ratio independence beyond a value of ~2 (Fig. 5a). When $\beta_2AR_{Luc}$ and $mCannR2_{GFP}$ were

coexpressed as a BRET pair, these two functionally unrelated proteins yielded the same low $BRET_{eff}$ values exhibiting [GFP]/[Luc] ratio independence (Fig. 5a).

The $BRET_{eff}$ maxima observed in these experiments were substantially lower than those obtained for CD2 or CD86. The likely explanation for this is that the larger hydrodynamic diameter of GPCR proteins (>50 Å versus 30 Å) [18] increases the distance of closest approach, reducing the maximum $BRET_{eff}$ obtainable via random, or any other, interaction. For type-I membrane proteins the limiting factor is very likely to be the dimensions of the Luc and GFP fluorophores. Supporting this possibility, coexpression of $\beta_2AR_{Luc}$ with $CD2_{GFP}$ as a BRET pair gave a $BRET_{eff}$ maximum slightly higher than that obtained for $\beta_2$AR expressed as a BRET pair (Fig. 5a). We tested the possibility that we had not expressed enough GPCR, that is, that we were sampling a point in the equilibrium dominated by monomers, by increasing expression. At GPCR levels as high as $2 \times 10^6$ molecules/cell, that is, double that used by others [14, 17], the same low $BRET_{eff}$ values and [GFP]/ [Luc] ratio independence seen at lower expression levels were obtained (Fig. 5b). In the type-2 experiment, in which the [GFP]/[Luc] ratio was held constant and overall expression level varied, $BRET_{eff}$ for $\beta_2$AR expressed as a BRET pair exhibited the same strict dependence on expression level, with $BRET_{eff}$ falling to zero at low surface densities *(*$P < 0.01$), as did $BRET_{eff}$ values obtained under the same conditions for CD2 and CD86 expressed as BRET pairs (Fig. 4).

### 1.4.5 Dimerization of a β 2AR/$GABA_{\beta}R$ chimera

We also sought confirmation that class-A GPCR dimerization, had it occurred, would have been detectable using the new approaches, by generating $\beta_2$AR and $GABA_{\beta}R$ chimeras. Heterodimerization of the $GABA_{\beta}R1$ and $GABA_{\beta}R2$ subunits is driven, at least in part, by the interactions of cytoplasmic sequences present in each subunit that together form 'coiled-coil' domains [19, 20] (Fig. 2a). Coexpression of $GABA_{\beta}R1_{Luc}$ and $GABA_{\beta}R2_{GFP}$ as a BRET pair yielded $BRET_{eff}$ data exhibiting the hyperbolic relationship expected for dimers in addition to a $BRET_{eff}$ maximum more than double those obtained for $\beta_2$AR or mCannR2 (Fig. 5c). Having established that $GABA_{\beta}R$ heterodimerization was readily detectable, we genetically fused the coiled-coil domains of $GABA_{\beta}R1$ (coil1) and $GABA_{\beta}R2$ (coil2), along with Luc and GFP, to the seven transmembrane domain-containing region of $\beta_2$AR, giving $\beta_2ARcoil1_{Luc}$ and $\beta_2ARcoil2_{GFP}$. $BRET_{eff}$ values obtained by coexpression of $\beta_2ARcoil1_{Luc}$ and $\beta_2ARcoil2_{GFP}$ as a BRET pair were almost indistinguishable from those obtained for coexpression of $GABA_{\beta}R1_{Luc}$ and $GABA_{\beta}R2_{GFP}$ (Fig. 5c). A second pair of constructs coexpressed as a BRET pair, $\beta_2ARcoil2A_{Luc}$ and $\beta_2ARcoil2A_{GFP}$, for which the coiled-coil domain of $GABA_{\beta}R2$ was truncated by 50% and

therefore likely to interact more weakly, gave $BRET_{eff}$ values intermediate between those obtained for the native forms of $\beta_2AR$ and $GABA_\beta R$ (Fig. 5c), consistent with $BRET_{eff}$ being sensitive to the affinity of oligomerization.

### 1.4.6 $GABA_\beta R2$ is a poor specificity control for GPCR interactions

In previous studies of GPCR interactions, coexpression with an 'irrelevant' GPCR [21-24] has been used as a control for nonspecific interactions. Notably, the same irrelevant GPCR, the $GABA_\beta R2$ subunit of $GABA_\beta R$, was used on each occasion. We replicated these experiments by coexpressing $\beta_2AR_{Luc}$ and $GABA_\beta R2_{GFP}$ as a BRET pair, and found substantial (50%) decreases in $BRET_{eff}$ compared to $\beta_2AR$ expressed alone as a BRET pair (Fig. 5d). Given that our irrelevant control for GPCR coexpression experiments, mCannR2, gave data indistinguishable from those obtained for $\beta_2AR$ alone, the question arose as to whether $GABA_\beta R2$ constituted an appropriate control for homodimerization. Expression of the $GABA_\beta R2$ subunit alone as a BRET pair gave $BRET_{eff}$ values that were substantially higher than those obtained for $\beta_2AR$ and exhibited a hyperbolic relationship with [GFP]/[Luc] ratio (Fig. 5d). This indicated that the $GABA_\beta R2$ subunit homodimerized as readily as it formed heterodimers with the $GABA_\beta R1$ subunit, as described elsewhere [25] (Fig. 5c). The significance of this is that $GABA_\beta R2$ homodimerization will halve the effective number of molecules available for energy transfer via random interactions with the test protein, reducing $BRET_{eff}$. Coexpression of $CD2_{Luc}$ and $CTLA\text{-}4_{GFP}$ as a BRET pair reproduced this effect (data not shown). These considerations suggest that $GABA_\beta R2$ is an inappropriate control for identifying GPCR dimers.

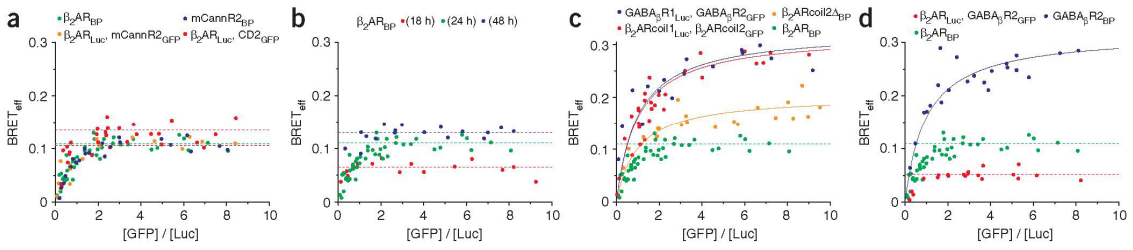



**Figure 5.** Two native class-A GPCRs are monomeric at the cell surface. **(a)** Both $\beta_2AR$ and mCannR2, expressed separately as BRET pairs or together as a BRET pair, and $\beta_2AR$ and CD2 expressed as a BRET pair, give similar low $BRET_{eff}$ values exhibiting [GFP]/[Luc] ratio independence beyond a [GFP]/[Luc] ratio of 2, with lines representing the best fit to the data, as described in the Figure 3 legend. **(b)** Variation of the acceptor/donor ratio for $\beta_2AR$ shows no evidence for oligomerization at three different levels of surface expression, with the highest level

being ~2 x $10^6$ molecules/cell. **(c)** $BRET_{eff}$ values for a heterodimerizing class-C GPCR, $GABA_{\beta}R$, consisting of $GABA_{\beta}R1$ and $GABA_{\beta}R2$ subunits, exhibit the hyperbolic relationship with acceptor/donor ratio expected for a dimer, as do $BRET_{eff}$ values obtained for a fusion protein consisting of $\beta_2AR$ and the heterodimerizing coiled-coil domains of the $GABA_{\beta}R$ complex ($\beta_2$ARcoil1 and $\beta_2$ARcoil2). $\beta_2$ARcoil2A is a truncated version of $\beta_2$ARcoil2 with only half the $GABA_{\beta}R2$ coiled-coil. **(d)** The decrease in interaction when $\beta_2AR$ is expressed as a BRET pair with $GABA_{\beta}R2$ is due to the homodimerization of $GABA_{\beta}R2$ at the cell surface, which decreases by half the effective density of molecules present.

## 1.5 Discussion

The use of BRET to discriminate between monomeric and oligomeric cell-surface proteins is not necessarily straightforward. This is because the interpretation of BRET data, as in the case of other resonance energy transfer experiments, is complicated by the dependence of energy transfer on several factors, including the distance of nearest approach (that is the cross-sectional area of donor and acceptor chimeras), expression level, subunit affinity and stoichiometry. An additional complication for analyses of cell-surface proteins is that random interactions contribute a larger fraction of the total energy transfer than seems previously to have been appreciated. Unless $BRET_{eff}$ is very high, the strategy implemented in conventional BRET experiments, that is, single estimates of energy transfer derived at maximum expression levels, is of limited use.

The prediction that the BRET 'signature' for randomly interacting proteins in type-1 experiments consists of the independence of $BRET_{eff}$ and acceptor/donor ratio, whereas, for type-2 experiments, it comprises the strict expression-level dependence of $BRET_{eff}$, greatly assists in the interpretation of the data. The independence of $BRET_{eff}$ and acceptor/donor ratio for randomly interacting proteins in type-1 experiments will only be apparent when the [GFP]/[Luc] ratio becomes sufficiently high that the donors are no longer competing for acceptors at the cell surface and acceptor concentration is essentially constant. The threshold for this effect appears to be an acceptor/donor ratio of ~2, as also determined empirically for FRET data [5]. For CD80, the case for dimerization was strengthened by control experiments with class-matched, *bona fide* monomers. The pitfalls associated with choosing inappropriate 'specificity' controls, however, was illustrated for $\beta_2AR$ and $GABA_{\beta}R2$ coexpression. In assigning a particular stoichiometry to a given protein, consideration should be given to (i) the $BRET_{eff}$ maximum, (ii) the relationship of $BRET_{eff}$ with acceptor/donor ratio and overall expression level in type-1 and type-2 experiments, respectively, (iii) comparisons with suitable controls and, ideally, (iv)

the effects of forced changes in native stoichiometry induced by, for example, mutagenesis.

According to these criteria, class-A GPCRs exemplified monomeric behavior, which challenges the notion [6] that these GPCRs are innately predisposed to forming homo- or hetero-oligomers. When this does occur, as in the case of the class-C $GABA_{\beta}R$ heterodimer, GPCR dimerization could be readily detected by varying acceptor/ donor ratio at constant expression. The possibility that random interactions of class-A GPCRs were responsible for the energy transfer observed previously has been addressed quantitatively only once, for $\beta_2$AR, and ruled out [14]. On that occasion, as in each of the more quantitative BRET analyses published, rather than increasing acceptor/donor ratio by decreasing the amount of donor, the acceptor concentration was varied and donor level kept constant. In such experiments the acceptor/donor ratio and total surface density vary simultaneously, making it very difficult to observe the type-1 or type-2 signatures of randomly interacting proteins. We were also unable to reproduce the type-2 observation [14] that $BRET_{eff}$ for $\beta_2$AR is independent of expression level at a constant acceptor/donor ratio, finding instead that it was entirely expression-level dependent. A second group [17] also obtained expression level-dependent $BRET_{eff}$ data for $\beta_2$AR and three other class-A GPCRs, but overlooked the possibility that this constituted clear-cut evidence for energy transfer resulting from random interactions only.

Our results indicate that nonradiative energy transfer between monomers can reach a level previously assigned only to the formation of oligomeric structures. Given that proteins occupy >25% of the cell surface by area [26], this degree of nonspecific energy transfer should probably not have been surprising. As there is no detectable energy transfer between GFP tethered to the membrane and luciferase expressed in the cytoplasm (J.R.J. and S.J.D.; unpublished data), it seems that the cell surface constitutes a microenvironment greatly favoring the *cis* interactions of proteins, such as those required for ‘signalosome’ formation [27]. Our results also imply that, over time, in addition to the assembly of nascent oligomeric complexes, resonance energy transfer will be sensitive to local changes in protein density. This offers new opportunities for following the reorganization of both interacting and noninteracting cell-surface molecules in the course of, for example, receptor triggering [28] and immunological synapse formation [29]. Rigorous quantitative analysis of the data will be required to tease out these effects.

## Acknowledgments

We thank A. Wise (GlaxoSmithKline) for the gift of the $GABA_{\beta}R2$ template, and E. Evans (Nuffield Dept. Clinical Medicine, Oxford University) and J. McIlhinney (MRC Anatomical Neuropharmacology Unit, Oxford University) for helpful discussion. This work was supported by the Wellcome Trust, the Rhodes Trust and the Programa Operacional Ciência e Inovação 2010, cofunded by the European Regional Development Fund.

## 1.6 References

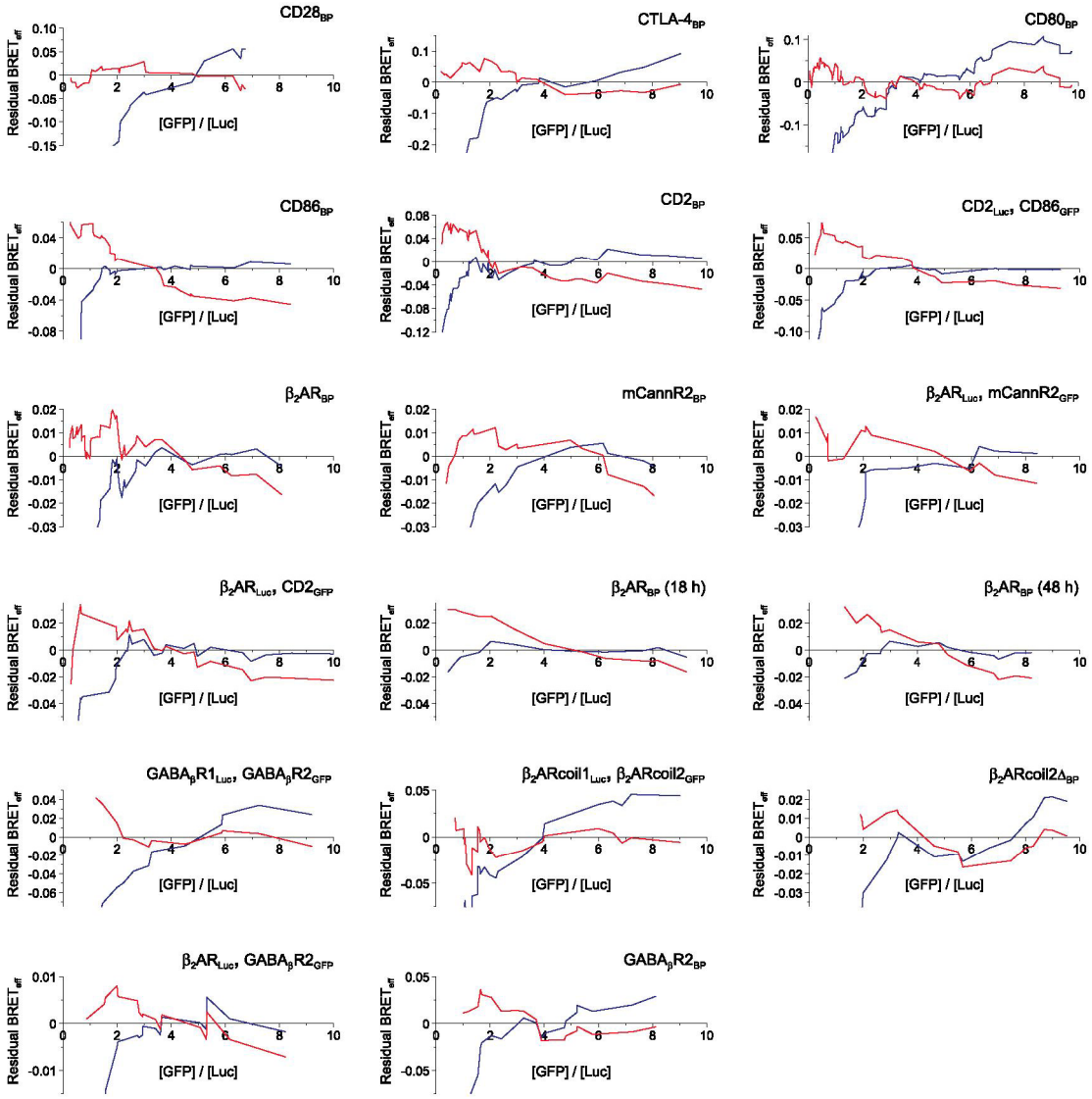
1. Xu, Y., et al., A bioluminescence resonance energy transfer (BRET) system: Application to interacting circadian clock proteins. *Proc. Natl. Acad. Sci. USA*, 1999. **96** p. 151-156.
2. Wolber, P.K. and B.S. Hudson, An analytical solution to the Forster energy transfer problem in two dimensions. *Biophys. J.*, 1979. **28**: p. 197-210.
3. Fung, B.K. and L. Stryer, Surface density determination im mebranes by fluorescence energy transfer. *Biochemistry*, 1978. **17**: p. 5241-5248.
4. Veatch, W. and L. Stryer, The dimeric nature of the gramicin A transmembrane channel: conductance and fluorescence energy transfer studies of hybrid channels. *J. Mol. Biol.*, 1977. **113**: p. 89-102.
5. Kenworthy, A.K. and M. Edidin, Distribution of a glycosylphosphatidylinositol-anchored protein at the apical surface of MDCK cells examined at a resolution of <100 Ä using imaging fluorescence resonance energy transfer. *J. Cell Biol.*, 1998. **142**: p. 69-84.
6. Pfleger, K.D.G. and K.A. Eidne, Monitoring the formation of dynamic G-protein-coupled receptor–protein complexes in living cells. *Biochem. J.*, 2005. **385** p. 625-637.
7. Jones, E.Y., et al., Crystal structure at 2.8 A resolution of a soluble form of the cell adhesion molecule CD2. *Nature*, 1992. **360**: p. 232-239.
8. Bodian, D.L., et al., Crystal structure of the extracellular region of the human cell adhesion molecule CD2 at 2.5 A resolution. *Structure*, 1994. **2**: p. 755-766.
9. Collins, A.V., et al., The interaction properties of costimulatory molecules revisited. *Immunity*, 2002. **17**: p. 201-210.
10. Ikemizu, S., et al., Structure and dimerization of a soluble form of B7-1. *Immunity*, 2000. **12**: p. 51-60.

11. Stamper, C.C., et al., Crystal structure of the B7-1/CTLA-4 complex that inhibits human immune responses. *Nature*, 2001. **410**: p. 608-611.
12. Barclay, A.N., et al., *The leucocyte antigen factsbook* 1997, San Diego: Academic Press.
13. Shaner, N.C., et al., Improved monomeric red, orange and yellow fluorescent proteins derived from Discosoma sp. red fluorescent protein. *Nat. Biotechnol.*, 2004. **22**: p. 1567-1572.
14. Mercier, J.F., et al., Quantitative assessment of β1 and β2-adrenergic receptor homo- and heterodimerization by bioluminescence resonance energy transfer. *J. Biol. Chem.*, 2002. **277**: p. 44925-44931.
15. Bhatia, S., et al., Different cell surface oligomeric states of B7-1 and B7-2: Implications for signalling. *Proc. Natl. Acad. Sci. USA*, 2005. **102** p. 15569-15574
16. Angers, S., et al., Detection of beta 2-adrenergic receptor dimerization in living cells using bioluminescence resonance energy transfer (BRET). *Proc. Natl. Acad. Sci. USA*, 2000. **97** p. 3684-3689.
17. Ramsay, D., et al., Homo- and hetero-oligomeric interactions between G-protein-coupled receptors in living cells monitored by two variants of bioluminescence resonance energy transfer (BRET): hetero-oligomers between receptor subtypes form more efficiently than between less closely related sequences. *Biochem. J.*, 2002. **365** p. 429-440.
18. Chen, Y., et al., Solubilization and molecular characterization of active galanin receptors from rat brain. *Biochemistry*, 1992. **31**: p. 2415-2422.
19. White, J.H., et al., Heterodimerization is required for the formation of a functional GABA(B) receptor. *Nature*, 1998. **396**: p. 679-682.
20. Jones, K.A., et al., GABA(B) receptors function as a heteromeric assembly of the subunits GABA(B)R1 and GABA(B)R2. *Nature*, 1998. **396**: p. 674-679.
21. Canals, M., et al., Homodimerization of adenosine A2A receptors: qualitative and quantitative assessment by fluorescence and bioluminescence energy transfer. *J. Neurochem.*, 2004. **88**: p. 726-734.
22. Canals, M., et al., Adenosine A2A-dopamine D2 receptor-receptor heteromerization: qualitative and quantitative assessment by fluorescence and bioluminescence energy transfer. *J. Biol. Chem.* , 2003. **278**: p. 46741-46749
23. Percherancier, Y., et al., Bioluminescence resonance energy transfer reveals ligand-induced conformational changes in CXCR4 homo- and heterodimers. *J. Biol. Chem.* , 2005. **280**: p. 9895-9903.

24. Breit, A., et al., Hetero-oligomerization between beta2- and beta3-adrenergic receptors generates a beta-adrenergic signaling unit with distinct functional properties. *J. Biol. Chem.*, 2004. **279**: p. 28756-28765.
25. Uezono, Y., et al., Coupling of GABAB receptor GABAB2 subunit to G proteins: evidence from Xenopus oocyte and baby hamster kidney cell expression system. *Am. J. Physiol. Cell Physiol.*, 2006. **290 C200-7**.
26. Saxton, M.J., Lateral diffusion in an archipelago. Distance dependence of the diffusion coefficient. *Biophys. J.*, 1989. **56**: p. 615-622.
27. Jun, J.E. and C.C. Goodnow, Scaffolding of antigen receptors for immunogenic versus tolerogenic signaling. *Nat. Immunol.*, 2003. **4**: p. 1057-1064
28. Davis, S.J. and P.A. van der Merwe, The structure and ligand interactions of CD2: implications for T-cell function. *Immunol. Today*, 1996. **17**: p. 177-187.
29. Davis, D.M. and M.L. Dustin, What is the importance of the immunological synapse? *Trends Immunol.*, 2004. **25**: p. 323-327.

# Supplementary Data

## Supplementary Figures




**Supplementary Figure 1.** Residual analysis of all constructs used in the study. The goodness-of-fit for the BRET data to models of monomeric or dimeric behaviour were used to assign the most plausible stoichiometry. The residual $BRET_{eff}$ values after fitting are given for the constant fit (blue) and for the fit to a dimer (red). A good fits reduces residuals to zero.

| | Constant Fit | Dimer Fit |
|---|---|---|
| $CD28_{BP}$ | 72.27 | 43.55 |
| $CTLA\text{-}4_{BP}$ | 64.31 | 41.33 |
| $CD2_{BP}$ | 31.91 | 42.90 |
| $CD2_{Luc}$, $CD86_{GFP}$ | 19.58 | 26.15 |
| $\beta_2AR_{BP}$ | 11.14 | 14.50 |
| $mCannR2_{BP}$ | 11.54 | 15.21 |
| $\beta_2AR_{Luc}$, $mCannR2_{Luc}$ | 10.49 | 14.14 |
| $\beta_2AR_{Luc}$, $CD2_{Luc}$ | 18.04 | 23.83 |
| $\beta_2AR_{BP}$ (18 h) | 13.68 | 19.40 |
| $\beta_2AR_{BP}$ (48 h) | 8.35 | 18.15 |
| $GABA_{\beta}R1_{Luc}$, $GABA_{\beta}R2_{GFP}$ | 30.98 | 20.50 |
| $\beta_2ARcoil1_{Luc}$, $\beta_2ARcoil2_{GFP}$ | 41.46 | 19.03 |
| $\beta_2ARcoil2\Delta_{BP}$ | 23.67 | 19.69 |
| $\beta_2AR_{Luc}$, $GABA_{\beta}R2_{GFP}$ | 8.22 | 9.52 |
| $GABA_{\beta}R2_{BP}$ | 25.02 | 21.28 |

**Supplementary Table 1.** Numerical representation of goodness-of-fits. The residual analysis of goodness-of-fit (Fig. 3c and Supplementary Fig. 1) can be represented numerically, as described in Supplementary Methods. The values have all been multiplied by 1000 for better clarity. The root mean square of the residuals is calculated from the monomer and dimer fits for $BRET_{eff}$ values at acceptor/donor ratio > 2. A lower value indicates a better fit to that model.

## Supplementary Methods

### Vector constructs

The full length sequences of all genes inclusive of their native signal peptide sequences, were amplified by PCR from cDNA or IMAGE sequences and cloned in-frame into either pGFP$^2$-N3 or prLuc-N3 (PerkinElmer), mutating the stop codon to an appropriate restriction site (see following table for all oligonucleotides used in this study and the corresponding protein sequences of each of the constructs). All constructs were sequenced to check reading frame and integrity. The sGFP-Luc expression vector was obtained from PerkinElmer. The $\beta_2$AR-GABA$_\beta$R1 ($\beta_2$ARcoil1) chimera was constructed by blunt-end ligating the serpentine domain of $\beta_2$AR (residues 1-343) to the coiled-coil domain of GABA$_\beta$R1 (residues 741-845) using a convenient *FspI* cleavage site in both sequences. For the $\beta_2$AR-GABA$_\beta$R2 ($\beta_2$ARcoil2) chimera, the coiled coil domain of GABA$_\beta$R2 (residues 764-946) from a published construct[1] was amplified by PCR incorporating an *FspI* site at the 5' end so that it could be ligated to $\beta_2$AR in the same manner as $\beta_2$ARcoil1. For $\beta_2$ARcoil2A, the $\beta_2$ARcoil2 sequence was used as a template to amplify a version of the coil2 sequence that was truncated at the hydrophilic midpoint of the coil and fused to the serpentine region of $\beta_2$AR as above.

[1]White, J. H. *et al.* Nature 396, 679-82 (1998)

| Molecule | Oligonucleotide sequence (5′→3′) | Translated Protein |
|---|---|---|
| CD2 | TAGTAGCTGCAGCCCCTAAGATGAGCTTTCC<br>ATCATCGGATCCTTAGAGGAAGGGGACAATGAG * | KEITN....SPSSK**DPPVAT[Luc/GFP]** |
| CD80 | TAGTAGGAATTCTTGGGTCCAAATTGTTGGCTTTCAC<br>CTACTAGGATCCACAGGGCGTACACTTTCCCTTCTC * | VIHVT....SVRPV**DPPVAT[Luc/GFP]** |
| CD86 | TAGTAGGATATCGACTCTCCCCATCCGCTCAAGC<br>CTACTACCGCGGAAAACATGTATCACTTTTGTCGCATGAAG * | APLKI....SDTCF**PRARDPPVAT[Luc/GFP]** |
| CTLA-4 | TAGTAGGAATTCGGTTTTGCTCTACTTCCTGAAGACCT<br>CTACTAGGTACCTTGATGGGAATAAAATAAGGCTGAAATTGC * | MHVAQ....FIPIK**VPRARDPPVAT[Luc/GFP]** |
| CD28 | TAGTAGAATTCGCCACCATGCTCAGGCTGCTCTTGGCTCTC<br>ATCATCGGATCCGAGCGATAGGCTGCGAAGTCGC * | NKILV....AAYRS**DPPVAT[Luc/GFP]** |
| $\beta_2$AR | TAGTAGCCGCGGCGCGCCATGGGGCAACCCGGG<br>CTACTAGGATCCAGCAGTGAGTCATTTGTACTAC * | MGQPG....NDSLL**DPPVAT[Luc/GFP]** |
| mCannR2 | TAGTAGCCGCGGCGCGCCATGGAGGGATGCCG<br>CTACTAGGATCCGTGGTTTTCACATCAGCCTCTG * | MEGCR....DVKTT**DPPVAT[Luc/GFP]** |
| $GABA_\beta R1$ | TAGTAGACGCGTGCCACCATGGGGCCCGGGGCCCCTTTTG<br>CTACTAGGTACCTTATAAAGCAAATGCACTCGACTCC * | SHSPH....HLLYK**VPRARDPPVAT[Luc/GFP]** |
| $GABA_\beta R2$ | TAGTGAAGCTTGCCACCATGGCCTTACCAGTGAC<br>CTACTAGGTACCAGGCCCGAGACCATGACTCGG * | DYASY....MVSGL**VPRARDPPVAT[Luc/GFP]** |
| $\beta_2$ARcoil1 | — | MGQPG....ELLCL\|RRLIT....HLLYK**VPRARDPPVAT[Luc/GFP]** |
| $\beta_2$ARcoil2 | TAGTAGTGCGCAGATTCCAGTTCACTCAGAATCAG | MGQPG....ELLCL\|RRFQF....MVSGL**VPRARDPPVAT[Luc/GFP]** |
| $\beta_2$ARcoil2Δ | CTACTAGGATCCATTCGCAGGCGATGGTTTTC * | MGQPG....ELLCL\|RRFQF....HRLRM**DPPVAT[Luc/GFP]** |

**Supplementary Table 2.** Oligonucleotides and derived protein sequences used in the study. All the oligonucleotides used to amplify genes from this study are shown, with reverse primers marked by an asterisk. No oligonucleotide was required to construct the $\beta_2$ARcoil1 chimera, as this was cloned directly from cDNA. The protein sequence of the N- and C-terminal regions of the expressed mature protein are given in the right hand column. Protein sequences derived from the vector are given in smaller type, leading into the GFP or Luc sequences. For the $\beta_2$ARcoil chimeras, the point of fusion is marked with a vertical bar.

## Cell culture and transfection

HEK-293T cells were grown in DMEM supplemented with 10% FCS, glutamine and antibiotics. Six-well plates were seeded with $6x10^5$ 293T cells to give 80% confluence on the day of transfection. Constructs were co-transfected in each well as “BRET pairs”, resulting in the expression of single proteins as both Luc and GFP fusions, or of two distinct proteins in the form of Luc and GFP fusions. For the “type 1” experiment, FuGene (Roche) was used according to manufacturers instructions to transfect 1µg total DNA, with the ratio of GFP/Luc constructs ranging from 1:2 to 66:1, since this gave the most usable data. This was done by keeping the volume and concentration of the DNA at 20µl and 0.05µg/ul, respectively. For the 19:1 ratio of the CD2 BRET pair, for example, 19µl of $CD2_{GFP}$ DNA at 0.05µg/µl and 1µl of $CD2_{LUC}$ DNA at 0.05µg/µl were co-transfected. In all experiments, the sGFP-Luc construct was also transfected in a separate well.

**Confocal microscopy and FACS analysis**

Transfected cells were attached to coverslips, excited with a 488-nm laser and examined using a Radiance 2000 (BioRad) confocal microscope under an oil immersed 60x objective with light filtered in the green channel from 515 ± 15nm. All constructs were assessed for GFP expression, and for cell surface staining using antibodies when these were available, by FACS analysis on a FACScalibur (Becton Dickinson).

To quantitate cell surface expression, QuantiBRITE-PE beads (Becton Dickinson) were used according to the manufacturer's instructions in conjunction with PE-labeled antibodies to label 293T cells expressing the GFP-tagged gene of interest. The relative fluorescence intensities could then be calibrated to known quantities of fluorophore, giving the number of molecules/cell assuming univalent antibody binding. FACS data (15,000 data points) were extracted using FlowJo software and corrected to give equivalent backgrounds between all samples. The moving average *(n* = 100) was then calculated and plotted in Origin 7.5 (Originlab).

**Statistical analysis**

Data were fitted to either Eqn. 1, or to a constant value (for points with [GFP]/[Luc] > 2). The residuals of the fits (observed - expected) were calculated and the moving average *(n* = 4) plotted to assess goodness of fit. Numerical representation of this is given for all constructs in Supplementary Table 1 as the root mean square of these residuals for each fit, calculated as $\sqrt{(\sum (y_i - \hat{y})^2)/n}$ for [GFP]/[Luc] > 2, where *n* is the number of points. Other goodness-of-fit tests are inappropriate for this type of analysis: Chi-squared testing is inappropriate as the data cannot be sufficiently binned to get reliable estimators and KS/Anderson-Darling tests are not possible on models without defined cumulative distribution functions.

**Derivation of the relationship between acceptor/donor ratio and $BRET_{eff}$ for oligomeric protein interactions**

$$a = \frac{[GFP]}{[GFP] + [Luc]} \qquad d = \frac{[Luc]}{[GFP] + [Luc]} \qquad a + d = 1 \tag{1}$$

$$\begin{aligned} \frac{Q}{Q_0} &= 1 - E + E(1-a)^{n-1} \\ &= 1 - E\left(1 - d^{n-1}\right) \end{aligned} \tag{2}$$

$$\begin{aligned} BRET_{eff} &= 1 - \frac{Q}{Q_0} \\ &= E\left(1 - d^{n-1}\right) \\ &= BRET_{max}\left(1 - d^{n-1}\right) \end{aligned} \tag{3}$$

$$\begin{aligned} f &= \frac{[GFP]}{[Luc]} \\ f &= \frac{a}{d} = \frac{1-d}{d} \\ d &= \frac{1}{1+f} \end{aligned} \tag{4}$$

$$BRET_{eff} = BRET_{max}\left(1 - \left(\frac{1}{1+f}\right)^{n-1}\right) \tag{5}$$

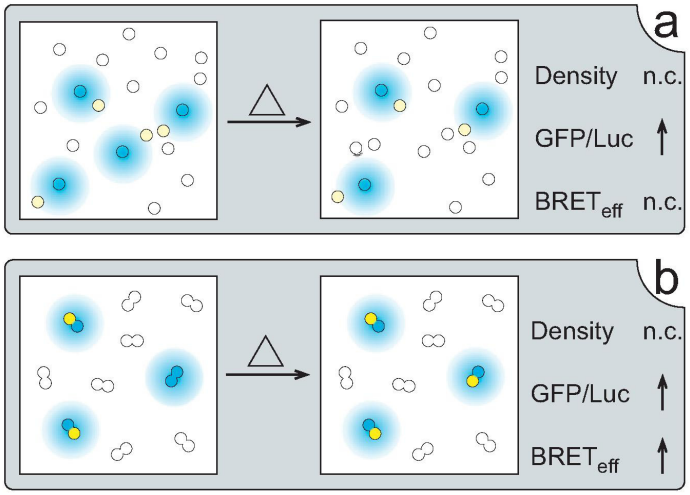
$$\frac{BRET_{eff}}{BRET_{max}} = 1 - \frac{1}{(1+f)^{n-1}} \tag{6}$$

The mole fraction of acceptors and donors are defined in (1). In the BRET assay, there are no competing unlabelled molecules, such that a + d = 1. From the theoretical considerations of Veatch and Stryer[1], the change in quantum yield can be expressed in terms of the energy transfer from a single donor to acceptor (E) and the mole fraction of a or d (2). $BRET_{eff}$ is defined as the apparent energy transfer for the ensemble of molecules, with E corresponding to the maximal BRET efficiency, $BRET_{max}$ (3). From the text, f is defined as the acceptor/donor ratio. The mole fraction of donors, d, can be expressed in terms of this ratio (4). Substitution of this into (3) gives (5), which can be simplified to the equation given in the text (6).

[1]Veatch, W. & Stryer, L. J Mol Biol 113, 89-102 (1977).

**Supplementary Note:** Why the dependence of transfer efficiency ($BRET_{eff}$) on acceptor/donor ratio is systematically different for randomly interacting proteins (a) versus oligomeric proteins (b), without recourse to theory

BRET relies on non-radiative energy transfer between luciferase (Luc)-coupled donors and green fluorescent protein (GFP)-coupled acceptors. In the illustration below, Luc-coupled donors are represented as blue circles and GFP-coupled acceptors are shown as white (i.e. non-fluorescing) and yellow (*i.e.* fluorescing) circles. BRET occurs when the acceptor and donor are within 100Å (*i.e.* a blue and yellow pair is formed). In the upper and lower panels, the yellow circles are pale and bright, respectively, reflecting the $BRET_{eff}$ level for each pair ($BRET_{eff}$ equals "*x*" for the monomer, and "*y*" for the oligomer; see below).




The two elements of BRET analysis are as follows. First, on a molecule for molecule basis, $BRET_{eff}$ for oligomers is higher than that for randomly interacting monomers because the donors and acceptors spend more time within 100Å of each other, and are generally much closer, making energy transfer more efficient (hence the pale and bright yellow circles in the illustration, *i.e., x* is less than *y*). Overall transfer efficiency will be affinity dependent in the case of oligomers. The cross-sectional area, *i.e.* the "excluded volume", of the proteins will also affect transfer efficiency. This differs according to protein class: *e.g.*, type I membrane proteins have a smaller cross-sectional area than multiple pass transmembrane proteins; the smaller the diameter, the closer donors and acceptors get, increasing energy transfer efficiency (for type I membrane proteins, the excluded volume is likely to be set by the diameters of GFP and luciferase, rather than their

transmembrane domains). For this reason it helps greatly to have carefully chosen, protein class-matched controls whose stoichiometry is known.

The second element relies on the prediction, discussed by Kenworthy and Edidin[1], that randomly interacting monomers and oligomers differ fundamentally in their dependence on acceptor/donor ratio ([GFP]/[Luc]). Illustrating this concept, for the examples shown above of a monomeric protein interacting randomly at the cell surface and another protein that forms a constitutive dimer, we start with a field of 20 molecules, with 16 acceptors and 4 donors. The acceptor/donor ratio is *increased* from 16:4 to 17:3 while keeping the overall density *constant* (*i.e.* 20), by removing one donor and replacing it with an acceptor, *i.e.* by "diluting out" the donor.

The question is: what happens to $BRET_{eff}$? A key point is that it is $BRET_{eff}$, and not the absolute level of energy transfer, that is important. In the case of the monomer, the initial BRET efficiency is 1*x*, *i.e.* each donor is close enough to one acceptor to transfer a fraction of its energy. When the acceptor/donor ratio is increased by replacing one of the donors with an acceptor, the remaining donors remain, on average, close to only one acceptor each, *i.e.* they continue to experience *the same acceptor environment*, so $BRET_{eff}$ remains at the level of 1*x*. This is only the case at relatively high acceptor/donor ratios, when the density of acceptors is *effectively* unchanged (in this case it actually changes slightly from 16/20 to 17/20. Empirically, it seems that this situation arises when the acceptor/donor ratio is increased anywhere beyond a threshold of ~2.

For the dimer, because the acceptor/donor ratio is already relatively high (4:1) the field consists mostly of acceptor dimers, but there will be a small number of donor dimers. Overall, the $BRET_{eff}$ is relatively low ($2y/4 = 0.5y$). When the acceptor/donor ratio is increased from 16:4 to 17:3 by replacing the donor with the acceptor, however, this doubles $BRET_{eff}$ (to $3y/3 = 1y$). Under conditions of essentially constant density and increasing acceptor/donor ratio, therefore, there is a non-linear (*i.e.* hyperbolic) increase in $BRET_{eff}$. The overall $BRET_{eff}$ level, and the dependence of $BRET_{eff}$ on acceptor/donor ratio at constant density or on expression level at constant acceptor/donor ratio (see the main text), allow these two types of interactions to be distinguished.

[1]Kenworthy, A. K. & Edidin, M. J Cell Biol 142, 69-84 (1998).

# 2. Analysis of cell surface organization using BRET

**Marta I. Oliveira, John R. James, Alexandre M. Carmo and Simon J. Davis**

## 2.1 Abstract

An important step in determining how lymphocytes respond to environmental cues is to understand how their cell surfaces are organized. Using Bioluminescence Resonance Energy Transfer (BRET), a powerful technology that monitors lateral protein-protein interactions in living cells, we analysed the stoichiometric arrangements of a number of representative type-I membrane receptors involved in T cell function. The majority of the cell surface proteins studied, including the phosphatase CD45, displayed a monomeric signature in 293T cells. Interestingly, however, the coreceptor CD4 and the accessory molecules CD5 and CD6 exhibited a tendency to self-associate although weakly and non-constitutively. Using chimeric and truncated forms of CD4, we show that CD4 dimerization appears to be dependent on the presence of its cytoplasmic domain. However, when complexed to Lck and in its active form, the protein assumes a monomeric configuration. In contrast, the association observed for the inhibitory receptor CD5 and the highly homologous molecule CD6 is mediated by extracellular interactions. Our results indicate that dimerization is likely to be relevant for the function of self-associating molecules but suggest a different regulatory mechanism for CD45. We also show that interactions within the microenvironment of the membrane are more prevalent, which suggests that the recruitment of molecules to the cell surface might be a crucial step for activation.

## 2.2 Introduction

Cellular responses triggered by an extracellular stimulus need to be relayed from the plasma membrane to specific intracellular targets. In large part, this communication relies on specific protein-protein interactions that can be either stable or dynamic. Membrane receptors play an important role in this process as they are the first to specifically engage in response to a particular signal. A common mode for a variety of membrane receptors to generate productive signaling is through dimerization upon ligand engagement [1]. Dimerization events bring two partners in close proximity and, if they are enzymatically active, they can act on one another. Ligand-induced pairing of cell surface receptors can also bring close together the proteins associated with these receptors that will activate intracellular signaling pathways. In addition, dimerization may accelerate biological reactions by placing substrates and active sites in favourable orientations. These types of self-association events can thus be, at some stage, a part of a decision point in a signaling process.

In the context of T cells, a controversial issue is whether, as with many other receptors, the T cell receptor (TCR) itself requires binding-induced oligomerization or

aggregation for triggering. Different multimerization moldels have been proposed that invoke binding-induced multimerization as the mechanism of signal transduction. However, although they can partially explain what is known about TCR triggering, they are not compatible with all available data [2].

Despite extensive studies it is still not clear how binding of a peptide-MHC complex to the TCR is initially communicated across the membrane. The T cell surface is embedded with a diversity of other molecules, most of them already identified [3], that contribute to the process of antigen recognition, but how they cooperate to mediate the different stages of recognition is still uncertain. The rate of protein interactions at the membrane is extremely high relative to intracellular interactions [4] and the behaviour of surface receptors would be expected to affect their signaling properties as bivalent binding stabilizes signaling complex formation several fold [5].

Two of the most significant contributors to the TCR triggering process are the co-receptors CD4 and CD8, which enhance TCR recognition. In the absence or blockade of CD4, much more peptide-MHC is required (10-100 fold) [6-9]. Although functionally very similar, CD4 and CD8 may have different structures, so whereas CD8 is indisputably a disulphide-linked monovalent dimer, its counterpart CD4 is assumed to be predominantly expressed as a monomer. Nevertheless, oligomerization of CD4 has also been reported at the surface of T cells and monocytes/macrophages [10-12]. Structural studies showed that CD4 is able to self-associate, although with a low dimer affinity [13]. Two residues present in the dimer interface have been postulated to be critical for dimer formation [12], however, different regions [14-16] have additionally been suggested to be responsible for CD4 self-association. Some reports have indicated that the functional form of CD4 is a dimer or oligomer [11, 12, 17-19], but the exact role and significance of CD4 dimerization remains unclear.

Monomeric and dimeric forms of another relevant receptor for the T cell signaling process, the transmembrane phosphatase CD45, have been detected as well [20, 21]. CD45 is expressed on all nucleated hematopoietic cells and exists as various isoforms due to alternative splicing of three exons coding for extracellular segments of the protein [22]. These alternatively used sections encompass many O-linked glycosylation sites so that the extracellular domain of the high molecular weight isoform (CD45RABC) differs in structure and overall charge from the low molecular weight isoform (CD45RO) whose transcripts lack all three exons [23]. It has been suggested that the multiple isoforms could differentially homodimerize, and that the extracellular and transmembrane domains were not only responsible but sufficient for the observed CD45 association [24]. Yet, others could not observe dimerization of the intact extracellular CD45 region [25]. The possibility that the self-association could be mediated by the cytoplasmic region was also not

supported by the recently determination of the crystal structures of the entire cytoplasmic fragment of human CD45 showing that it exists as a monomer [26].

Experimentally induced self-association of CD45 leads to inhibition of its phosphatase activity [27], suggesting that the dimerization could act as a regulatory mechanism [28]. The concept that protein associations could function as a means of regulation highlights the importance of identifying and characterizing these molecular interactions. The basal stoichiometric state of most molecules at the T cell surface is not currently known, thus a better characterization of the T cell surface organization is essential for the understanding of the heterogeneity of outcomes resulting from the stimulation of a single class of receptor.

Bioluminescence resonance energy transfer, BRET, is becoming the methodology of choice to monitoring protein-protein interactions in real- time, in living cells [29]. We have recently demonstrated that a large fraction of the BRET signal commonly reported to represent stable protein dimerization is in fact due to random collisions occurring at the cell surface, and that it is crucial to use appropriate controls to calibrate the BRET results in order to distinguish BRET signatures representing true dimers from non-residual background signals generated by casual interactions [30]. Taking advantage of the potential of this technique we have applied BRET to study the T cell surface and show that a significant number of the representative molecules selected, all of which are involved in T cell signaling, tend to be monomeric entities. This indicates that dimerization is a relative rare property that may confer a special functional role to particular proteins. By applying this approach to a range of different molecules it should be possible to infer the overall behaviour of the T cell surface proteins and to elucidate the general features of the molecular organization of the T cell surface.

## 2.3 Materials and Methods

### 2.3.1 cDNA cloning and plasmids

Standard molecular cloning techniques were used to produce fusion constructs of a representative selection of molecules involved in T cell activation. All genes not described in the next paragraph were amplified by a single-round PCR using the nucleotide primer pair shown in Table 1 and the stop codon mutated to an appropriated restriction site. CD2, CD4 and CD43 were amplified from the Jurkat cell line E6.1 and LICOS and mLICOS were amplified from dendritic cell cDNA. For the remaining genes, vector sequences were used as PCR templates. All sequences were cloned into both pGFP$^2$-N3 and prLuc-N3

(PerkinElmer), except for CD4-TM and CD166 which were cloned into the N2 and N1 variants of the vectors, respectively.

| Gene | Number | Primer Sequence | Restriction |
|---|---|---|---|
| CD2 | m-1 | TAGTAGCTGCAGCCCCTAAGATGAGCTTTCC | *Pst*I |
| | m-2 | ATCATCGGATCCTTAGAGGAAGGGGACAATGAG | *Bam*HI |
| CD2-Lck | 1094 | CTACTAGGTACCCCTTTTGGTGATATAGAAAACGAGCAG | *Kpn*I |
| CD4 | m-3 | TAGTAGCTGCAGGGCAAGGCCACAATGAACC | *Pst*I |
| | m-4 | CTACTAGGATCCATGGGGCTACATGTCTTCTG | *Bam*HI |
| CD4Ex | 1083 | TAGTAGAAGCTTGGCAAGGCCACAATGAACC | *Hin*dIII |
| | 1084 | CTACTAGGTACCGACACAGAAGAAGATGCCTAGCCC | *Kpn*I |
| CD4-Lck | 1081 | TAGTAGGGTACCATGGGCTGTGGATGCAGC | *Kpn*I |
| | 1082 | CTACTAGGTACCCAAGGCTGAGGCTGGTAC | *Kpn*I |
| $CD4^{K318E}$ | 1008 | CTAAGCTGATGCTGAGCTTGGAACTGGAGAACAAGGAGGC | — |
| | 1009 | GCCTCCTTGTTCTCCAGTTCCAAGCTCAGCATCAGCTTAG | — |
| $CD4^{Q344E}$ | 1006 | GGCGGGGATGTGGGAGTGTCTGCTGAGTGACTCGG | — |
| | 1007 | CCGAGTCACTCAGCAGACACTCCCACATCCCCGCC | — |
| $CD4^{\Delta Cys}$ | 1010 | GAGACTCCTCAGTGAGAAGAAGACCTCCCAGTCCCCTCACCGGTTTCAGAAGAC | — |
| | 1011 | GTCTTCTGAAACCGGTGAGGGGACTGGGAGGTCTTCTTCTCACTGAGGAGTCTC | — |
| CD5 | m-5 | TAGTAGGATATCGCCAGAAACCATGCCCATG | *Eco*RV |
| | m-6 | CTACTACCGCGGCAGCCTCTGAGCCCCATGC | *Sac*II |
| CD5Ex/CD2Int | m-7 | TCGTGTGCGGCCCCCTTGCCAAAAGGAAAAAACAGAGGAGTCG | — |
| | m-8 | CGACTCCTCTGTTTTTTCCTTTTGGCAAGGGGGCCGCACACGA | — |
| CD6Ex/CD2Int | m-9 | CGCGGATCCTCTAGATGTGGCTCTTCTTCGGGATCA | *Bam*HI |
| | m-10 | TCTTCATAGCCTTCATCCTCTTGAAAAGGAAAAAACAGAGGAGTCG | — |
| | m-11 | CGACTCCTCTGTTTTTTCCTTTTCAAGAGGATGAAGGCTATGAAGA | — |
| | m-12 | ATCATCGGATCCTTAGAGGAAGGGGACAATGAG | *Bam*HI |
| CD43 | m-13 | TAGTAGCTGCAGGCCTGGAAATGGCCACGCTTC | *Pst*I |
| | m-14 | CTACTAAAGCTTAGGGGCAGCCCCGTCTCCC | *Hin*dIII |
| CD45Ex | m-15 | TAGTAGACCGGTCACCACCATCACCATCACCACCATCAAAGCCCAACACCTTCCCCC | *Age*I |
| | m-16 | CATCTCCGTTTATCTCAGAGAG | (*Sac*II) |
| LICOS | 532 | TAGTAGGAATTCCTCCGCGGCCCGAGGTCTC | *Eco*RI |
| | 533 | CTACTAGGATCCACGTGGCCAGTGAGCTCTGTCTC | *Bam*HI |
| mLICOS | 538 | TAGTAGGAATTCAACTCTCCGCGTCCGAAATCCA | *Eco*RI |
| | 539 | CTACTAGGATCCGCGTGGTCTGTAAGTTCAAGCTG | *Bam*HI |
| PD-1 | 979 | TAGTAGCCGCGGCTCCAGGCATGCAGATCCC | *Sac*II |
| | 980 | CTACTAGGATCCAGGGGCCAAGAGCAGTGTCC | *Bam*HI |
| PD-L1 | 942 | TAGTAGAGATCTCCAGAAAGATGAGGATATTTGC | *Bgl*II |
| | 943 | CTACTAGGTACCGACGTCTCCTCCAAATGTGTATC | *Kpn*I |
| PD-L2 | 940 | TAGTAGAGATCTCAGAACATGATCTTCCTCCTGC | *Bgl*II |
| | 942 | CTACTAGGATCCCAGATAGCACTGTTCACTTCCC | *Bam*HI |

**Table 1.** Oligonucleotide primers used to construct vectors expressing proteins genetically fused to luciferase or GFP[2]

The CD2-Lck chimera was obtained by first amplifying CD2 using primers m-1 and 1094 from the wild type construct and cloning into pGFP[2]-N3 before amplifying the full length sequence of Lck of a pcDNA3 vector using primers 1083 and 1084. The *Kpn*I digest of Lck was cloned in-frame with CD2 into the vector before the complete CD2-Lck was subcloned into prLuc-N3. The CD4-Lck construct was prepared by inserting the *Kpn*I fragment of Lck directly in-frame into the CD4Ex vectors. For CD45Ex, the extracellular and transmembrane domains of human CD45RO were amplified with primers m-15 and m-16. The m-15 primer incorporated a $His_8$ affinity tag at the 5'-end of the mature CD45 protein. The m-16 primer complemented a region of the CD45 sequence downstream from a convenient *Sac*I natural site that truncated the sequence at the start of the

intracellular sequence. This PCR product was cloned into the pLEX vector using *Age*I and *Sac*II digestion that added an efficiently-cleaved signal peptide to the 5'-end of the product. The *Hind*III/*Sac*II fragment from this product was then cloned into the BRET vectors. For chimeric or point-mutated constructs, two rounds of PCR amplification were performed. The oligonucleotide pairs for the overlapping 5' and 3' products were:

| | 5′ Product | | 3′ Product | |
|---|---|---|---|---|
| | Primers | Template | Primers | Template |
| $CD4^{K318E}$ | m-3 & 1009 | $CD4_{GFP}$ | 1008 & m-4 | $CD4_{GFP}$ |
| $CD4^{Q344E}$ | m-3 & 1007 | $CD4_{GFP}$ | 1006 & m-4 | $CD4_{GFP}$ |
| $CD4^{\Delta Cys}$ | m-3 & 1011 | $CD4_{GFP}$ | 1010 & m-4 | $CD4_{GFP}$ |
| CD5Ex/CD2Int | m-5 & m-8 | $CD5_{GFP}$ | m-7 & m-6 | $CD2_{GFP}$ |
| CD6Ex/CD2Int | m-9 & m-11 | $CD6_{GFP}$ | m-10 & m-12 | $CD2_{GFP}$ |

The amplified products were then used as templates in a chimeric PCR reaction scheme. The resulting genes were gel purified, digested using the appropriate restriction sites and cloned into the BRET vectors. All constructs produced were sequenced to check reading frame and integrity.

### 2.3.2 BRET$^2$ assay

The BRET experiments were carried out as described previously [30], using the type-I assay. No modifications were made to the assay. For investigating the influence of ICOS binding on LICOS binding, 100µl cells transfected with constant amounts but varying ratios of GFP:Luc were incubated on ice for 30 minutes with either 100µl of 100µg/ml ICOS:Fc (a king gift from Dr Chao Yu) or 10µl PBS as a control. $BRET_{eff}$ values were assayed after this incubation by adding DeepBlueC substrate and measuring luminescence immediately.

## 2.4 Results

### 2.4.1 A survey of representative T cell surface molecules

Several receptors on T cells can potentiate the T cell response, and their engagement is often required for successful activation *in vivo*. We selected some of the most important T cell surface receptors (Fig. 1) and tested their oligomerization state at the cell membrane using BRET. All molecules were fused to either rLuc or GFP, expressed as BRET pairs at

the surface of 293T cells, and the BRET signal measured, as previously described [30]. The study included the adhesion molecule CD2, the co-receptor CD4, the accessory molecules CD5 and CD6, the ligand for CD6, CD166, the highly glycosylated surface protein CD43, the protein tyrosine phosphatase CD45, the B7 family members LICOS and PD-1, as well as PDL-1 and PDL-2, the two ligands of PD-1. The disulfide-linked homodimer CTLA-4 was used as a reference for constitutive dimerization. To correctly distinguish between BRET signals arising due to oligomeric versus random interactions [30], the acceptor:donor ratio was varied but the overall expression level was kept constant, throughout the experiments. Only under these conditions, is it possible to observe dependence (hyperbolic fit) or independence (fit to a constant) of the $BRET_{eff}$ values on the acceptor:donor ratio for oligomers or random interactions, respectively. Because, for dimers, the acceptor and donor pairs spend more time together than randomly interacting acceptors and donors, it is also necessary to consider the strength of the BRET signal.

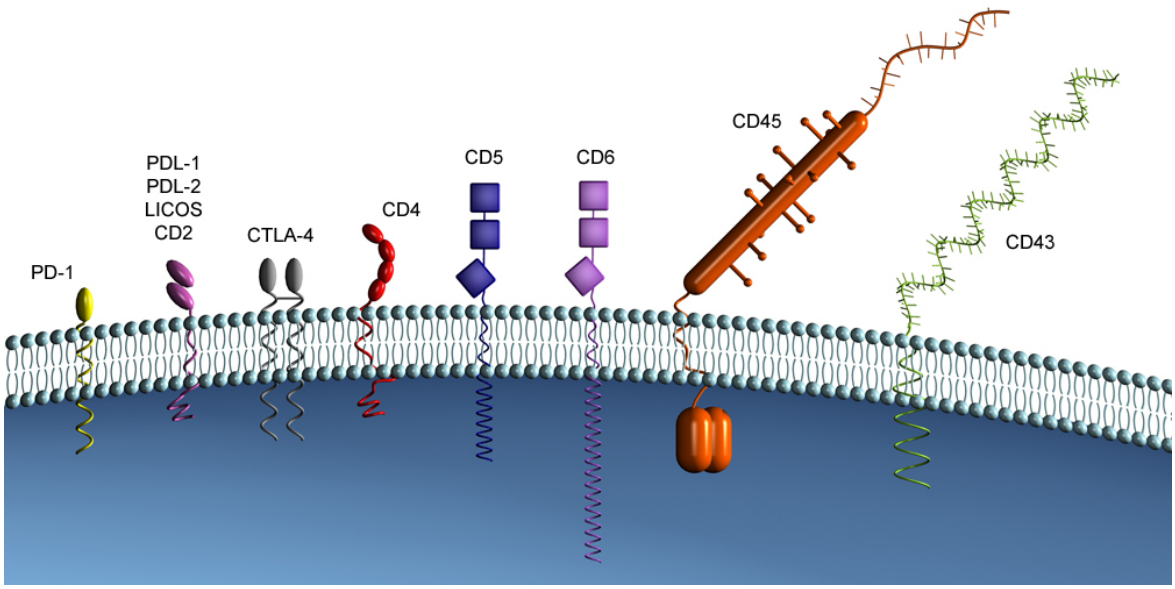



**Figure 1.** Cell surface molecules involved in T cell antigen recognition. A schematic view of the architecture and dimensions of the cell surface proteins used in this study.

### 2.4.2 CD45 and CD43 do not form dimers at the cell surface

The stoichiometric state of CD45 was investigated using BRET. Of the various isoforms, we selected and analyzed the smallest, CD45RO, since it has been claimed to be the one forming dimers more efficiently [24]. To avoid a possible interference of its large cytoplasmic domains on the association of the donor and the acceptor engineered forms of the protein, and since crystallographic studies indicated no self-association mediated by this part of the phosphatase [26], we truncated CD45 at the beginning of the intracellular domain and fused it directly to rLuc or GFP. By introducing a histidine tag at the N-terminal end of the mature protein, we were able to efficiently express it at the cell surface, at levels equivalent to those of native T cells (Fig. 2a). As shown in Figure 2b, the $BRET_{eff}$ levels observed for CD45 are low and independent of the acceptor:donor ratio, characteristic of a monomeric interaction. Because expression was very high, it is unlikely that we failed to see an interaction because we were sampling under the equilibrium for dimerization.

The ectodomain of full-length CD45 is as long and as heavily glycosylated as that of the surface protein CD43. Thus, we addressed the dimerization properties of CD43 to assess the effect of high glycosylation levels on $BRET_{eff}$ measurements. The BRET signals obtained for CD43 were similar to those exhibited by CD45, with both molecules displaying a BRET monomeric signature (Fig. 2b). Together, these results indicate that it is unlikely that the extracellular domain, and hence full length CD45 protein homodimerizes at the cell surface and point towards a different mechanism for the regulation of the phosphatase activity of this protein.

### 2.4.3 PD family proteins are monovalent

Programmed death-1 (PD-1) is an inhibitory receptor involved in cellular activation, which interacts with the ligands, PDL-1 and PDL-2 [31-33]. Using BRET we tested the association stoichiometry of the PD family using all three molecules in full-length forms. The results obtained indicate that PD-1 exists as a monomer at the cell surface, in agreement with previous reports [34]. Like PD-1, its two ligands give the same low $BRET_{eff}$ levels exhibiting independence of the acceptor:donor ratio (Fig. 3).

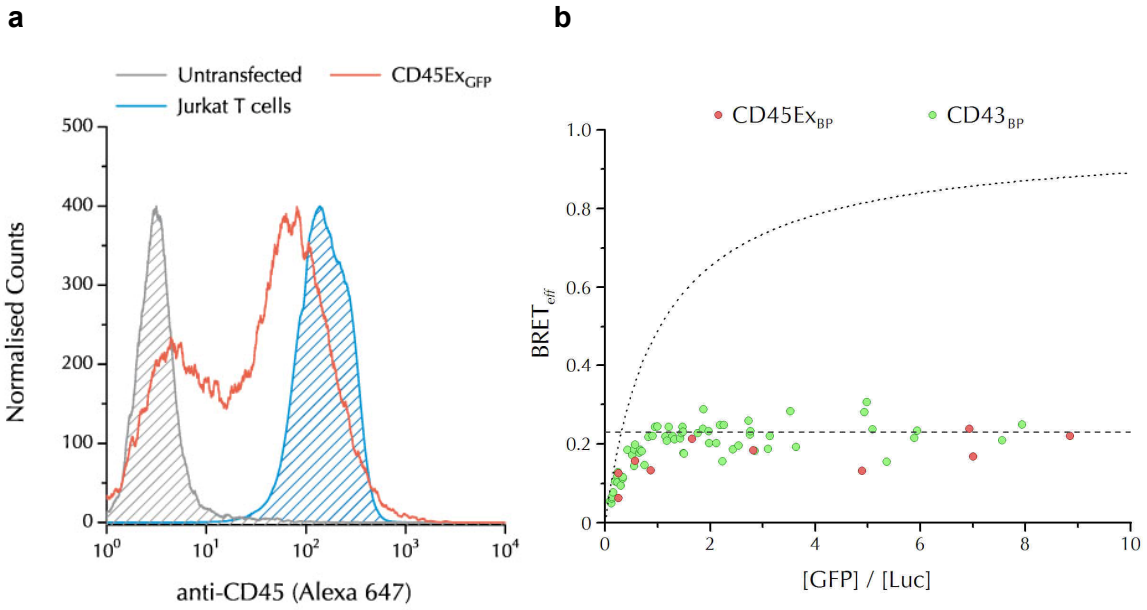



**Figure 2.** The extracellular domain of CD45RO showns no evidence of dimerization. **(a)** Comparison of CD45Ex$_{GFP}$ expression in 293T cells transiently transfected and wild type Jurkat T cells. CD45RO levels in the BRET assay are similar to that of native T cells. **(b)** CD45Ex$_{GFP}$ showed low BRET$_{eff}$ values independent of the acceptor:donor ratio. A similar large and glycosylated protein, CD43, gave values that were indistinguishable from those of CD45Ex. The dotted line corresponds to CTLA-4, used as a control for constitutive dimerization.

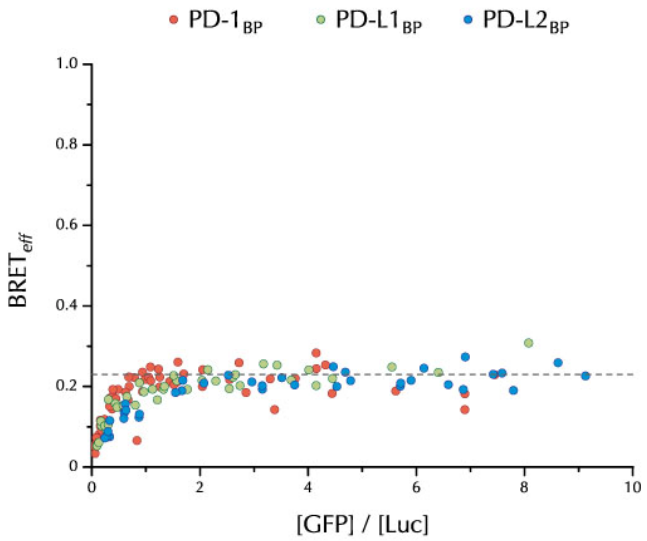



**Figure 3.** The B7 family member PD-1 and its two ligands are monomeric at the cell surface. Equivalent BRET$_{eff}$ data was observed for the PD family when expressed as BRET pairs.

### 2.4.4 LICOS has an evolutionary conserved stoichiometry

As in the case of PD-L1 and PD-L2, LICOS is a B7 family ligand [35]. However, contrarily to PD-1, the LICOS counter-receptor ICOS is co-stimulatory rather than inhibitory. To test whether LICOS is a monomer at the cell surface, as has been observed in solution [5], both human and mouse LICOS homologues were fused to Luc and GFP molecules and used in the $BRET^2$ assay. The predominant state of LICOS at the membrane is monomeric, giving $BRET_{eff}$ values that are comparable with those of known monomers, such as CD2 and CD86 (Fig. 4). The mouse homologue exhibits similar BRET signals that follow the same profile as the human protein, suggesting that the monovalency of LICOS has been conserved through evolution (Fig. 4). Importantly, both homologues showed independence from the acceptor:donor ratio, in accordance to monomeric behaviour. We next incubated soluble ICOS:Fc protein with cells expressing human LICOS, a disulphide-linked homodimer, as a BRET pair in order to evaluate any potential effect on LICOS stoichiometry caused by receptor binding. No significant changes were observed in the $BRET_{eff}$ values (Fig. 4), indicating that ICOS does not bind in a “lattice array”. It seems, instead, to bind its ligand monovalently.

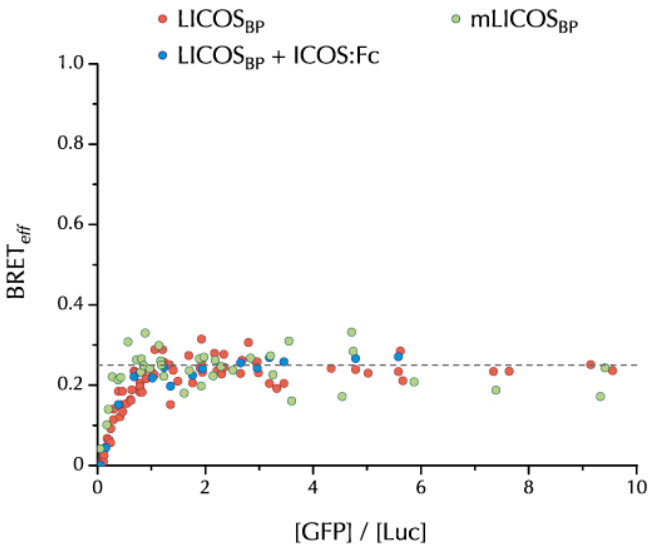



**Figure 4.** LICOS exists as an evolutionarily conserved monomer and remains so upon ligand binding. Low $BRET_{eff}$ values and independence on the acceptor:donor ratio, characteristics of monomers, were observed for both human and mouse LICOS that were unaffected by ligation with soluble ICOS:Fc.

### 2.4.5 CD5 and CD6 can dimerize weakly at the membrane

CD5 and CD6, two highly homologous representatives of the Scavenger Receptor Cysteine-Rich (SRCR) superfamily are among the molecules capable of mediating T cell-APC interactions. Expression of full-length CD5 as a BRET pair revealed that it is able to form weak dimers at the cell membrane, with the $BRET_{eff}$ values exhibiting a dependence on the acceptor: donor ratio (Fig. 5a). To assess the involvement of the extracellular domain of CD5 in dimerization, we generated a chimeric protein, CD5Ex/CD2Int, composed of the extracellular and transmembrane regions of CD5 fused to the cytoplasmic tail of the monomeric molecule CD2, already confirmed as a monomer in BRET assays [30]. The $BRET_{eff}$ levels obtained for the CD5Ex/CD2Int chimera were indistinguishable from those obtained for the wild-type molecule, implying a role for the extracellular domain of CD5 in its dimerization (Fig. 5a).

The possibility that the related protein CD6 could also display an analogous pattern of oligomerization mediated by its extracellular region was investigated using a similar approach. We thus constructed a CD6Ex/CD2Int chimera that gave $BRET_{eff}$ data that were suggestive of an extracellular association, although to a much smaller extent than CD5 (Fig. 5b). Due to the large cytoplasmic tail of native CD6, it was not feasible to evaluate the basal oligomerization state of the full-length CD6 molecule.

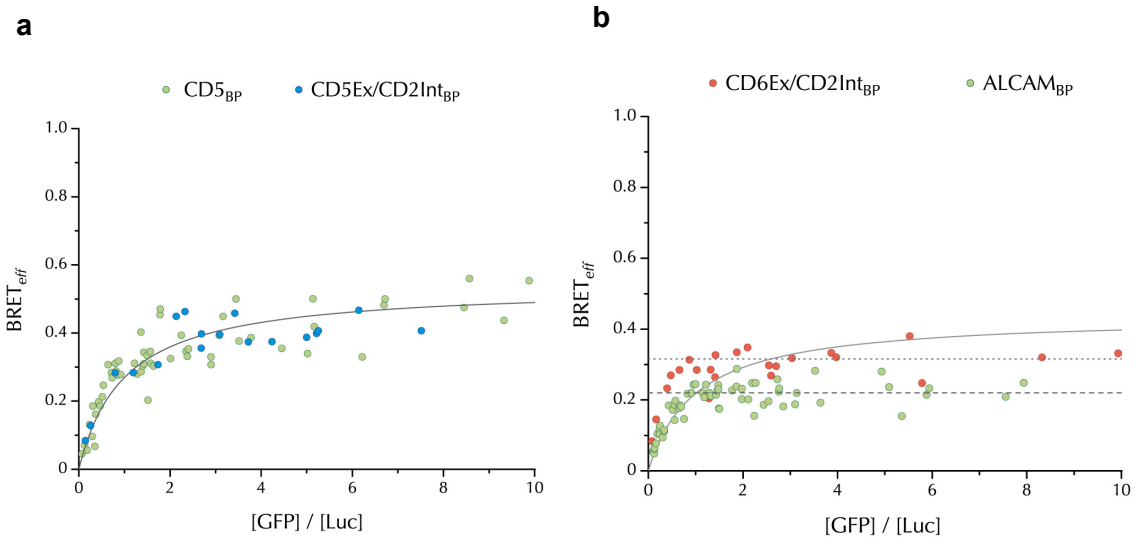



**Figure 5.** The close related molecules CD5 and CD6 are able to self-associate weakly at the cell surface through their extracellular domains. **(a)** The CD5Ex/CD2Int chimera shows $BRET_{eff}$ values that follow the same profile as seen for the CD5 wild type BRET pair, which can be readily fitted by a dimerization model. **(b)** The CD6Ex/CD2Int BRET pair shows some self-association, with significantly higher $BRET_{eff}$ values than its ligand, CD166, which is a monomer. However, CD6Ex/CD2Int is too weak to be convincingly fitted by a dimer model.

CD166, an Ig Superfamily member and the described ligand for CD6 [36], has been shown to establish homotypic interactions when expressed in interacting cells [37]. Expression of CD166 as a BRET pair, results in low $BRET_{eff}$ values that are independent of the acceptor:donor ratio, a feature of monomeric proteins (Fig 5b), thus indicating that CD166 tends be a monomer at the cell surface.

### 2.4.6 The co-receptor CD4 is able to forms dimers but is monomeric when complexed with Lck

BRET analysis of the CD4 interaction at the cell surface of 293T cells resulted in BRET signals consistent with the likely co-existence of CD4 monomers and dimers in a dynamic equilibrium (Fig. 6a), comparable to those observed for the B7 family member CD80 [28]. The $BRET_{eff}$ values obtained for CD4 are dependent on the acceptor:donor ratio, a characteristic of multimeric interactions. This basal level of CD4 dimerization has been previously reported [10-12]. The crystal structure of the soluble protein indicated that CD4 molecules can dimerize through the fourth domain (d4) in a crystal lattice [13]. More recently, the dimerization site was mapped at residues K318 and Q344 within domain 4 [12]. We therefore point mutated these residues to glutamate, recapitulating previous experiments [12] and evaluated the ability of the molecule to dimerize. Surprisingly, the oligomeric state of the protein was not affected by any of the point mutations (Fig. 6a), suggesting that other factors must be influencing this interaction. In order to evaluate the importance of the cytoplasmic tail in CD4 self-association, we generated a CD4/CD2 chimera, in which the intracellular region of CD4 was replaced by that of CD2. The decrease in the $BRET_{eff}$ levels indicated that this segment is likely to be relevant for CD4 dimerization (Fig. 6b). To confirm this, the protein sequence was truncated at the end of the transmembrane domain, and a new construct generated, CD4Ex that expressed only the extracellular domain of CD4. Its ability to dimerize was then determined and a large reduction in the $BRET_{eff}$ values was observed, to the levels of monomeric proteins (Fig. 6b).

The cytoplasmic tail of CD4 is relatively short, with a segment at the C-terminal end involved in the binding to the protein tyrosine kinase Lck. For that interaction to occur four conserved cysteine residues, two from CD4 and two from Lck are required [38, 39]. Given that Lck is not present in 293T cells, we reasoned that likely candidates for mediating CD4 self-association would be those pairs of cysteines, one from each CD4 molecule. To address this question, we point-mutated these residues to serine and tested the new construct (CD4$\Delta$cys) for its capacity to self-associate. The double substitution of the cysteines, did not completely abrogate CD4 ability to form dimers, but induced a slight

decrease in the $BRET_{eff}$ levels (Fig. 6b). This result indicates that these residues may, at least to some extent, be involved in CD4 dimerization.

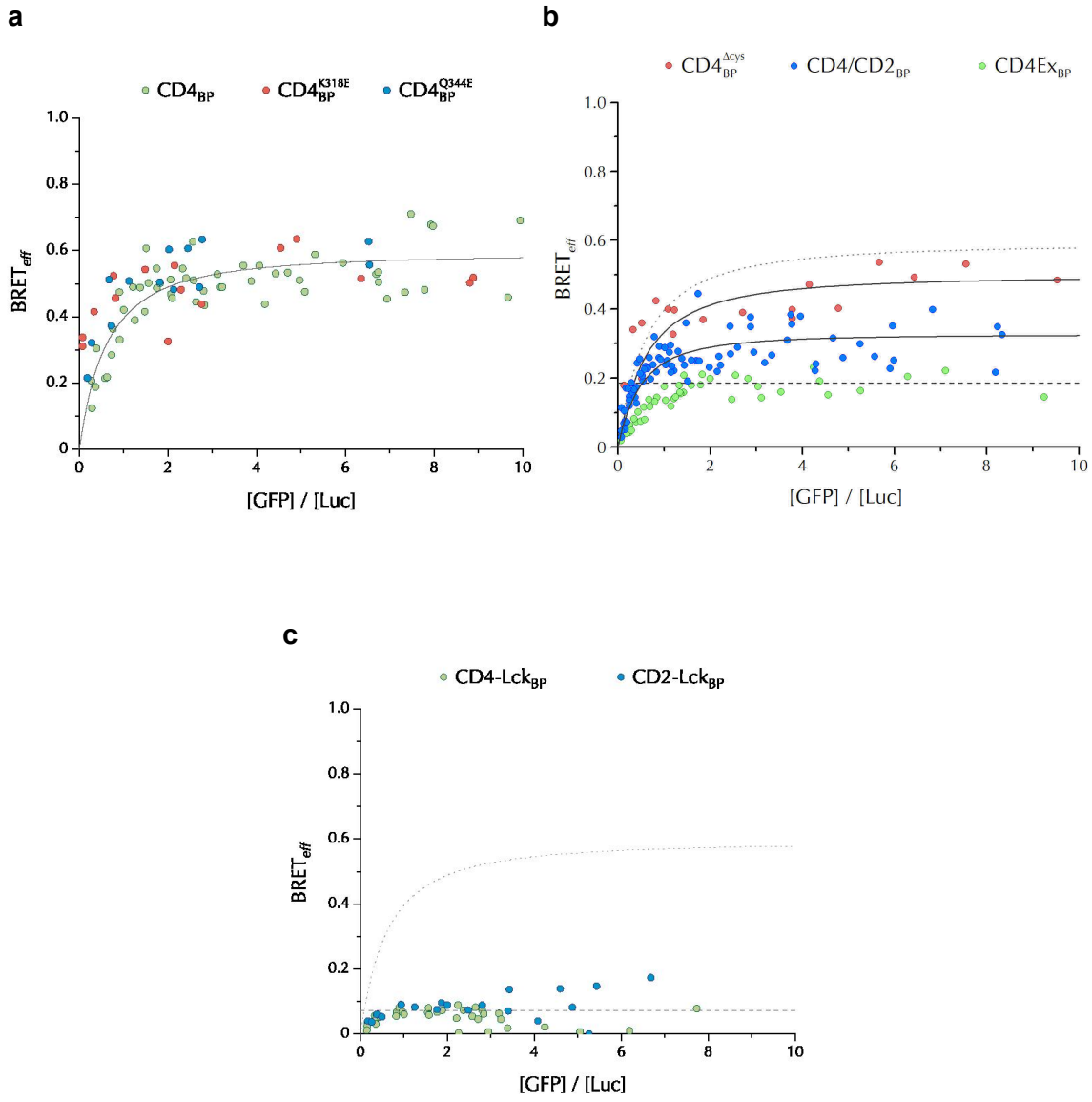



**Figure 6.** The active form of the CD4 coreceptor is a monomer. **(a)** Expression of full length CD4 as a BRET pair gives $BRET_{eff}$ values that are high and are a better fit to an oligomeric interaction. Mutation of residues supposedly mediating dimerisation through the membrane-proximal D4 domain (K318E and Q344E) does not affect the observed BRET profile. **(b)** Both replacement of the entire citoplasmic tail by that of CD2 (CD4/CD2) and mutation of the intracellular cysteine residues of the zinc "clasp" (ΔCys) lower CD4 association but complete removal of the intracellular region (CD4Ex) causes a large decrease in $BRET_{eff}$ values to levels observed only for monomeric proteins and shows independence from the acceptor:donor ratio. **(c)** Fusing the extracellular domain of CD4 to Lck (CD4-Lck), a construct that is known to function *in vivo* shows no self-association and gives $BRET_{eff}$ values that are identical to an equivalent construct using the CD2 extracellular domain (CD2-Lck).

The interaction between the cytoplasmic tail of CD4 and Lck was shown to be absolutely required for the activation of T cells *in vivo* [40]. The CD4/Lck hybrid molecule used in that study was able to replace wild-type CD4 as a co-receptor. We therefore reproduced that chimera, by fusing the extracellular and transmembrane domains of CD4 directly to the full-length Lck sequence, and assessed its oligomerization. Since this construct lacks the entire CD4 intracellular region, it was not expected to dimerize. Consistent with this, the $BRET_{eff}$ levels are severely reduced in comparison to the wild-type protein and show an independence of the acceptor:donor ratio (Fig 6c). That they were lower than those normally associated with monomeric interactions can be explained by the large cytoplasmatic domains of the constructs. Identical results were, indeed, obtained for an equivalent construct that was generated using the CD2 extracellular domain (CD2/Lck) (Fig 6c), and used for length-control purposes. This finding indicates that the functional moiety of CD4 at the cell surface is likely to be a monomer.

### 2.4.7 Interactions at the membrane are more prevalent and independent of the length of the intracellular regions of the proteins

In this study, the stoichiometry of a variety of type-I membrane proteins was assessed. Notably, almost all were found to have the same low $BRET_{eff}$ values that were invariant to changes in acceptor:donor ratio. Importantly, however, a significant BRET signal could be readily detected even for monomeric proteins. To confirm that the values observed were not due to the length of the cytoplasmic tails affecting the response, this length was plotted against the maximal $BRET_{eff}$ values obtained for each protein (Fig. 7). Clearly, there is no correlation between the two, indicating that the intracellular regions of most of the proteins have no particular structural variation that would lead to bias in their $BRET_{eff}$ values.

Approximately 25% of the membrane total area consists of protein [41] which suggests that the molecules are in a crowded microenvironment. Therefore, a high level of non-specific protein-proteins interactions and clustering effects within the lipid bilayer would be expected to occur. In order to have a better perception of the concentrating effect of the membrane environment, we compared the BRET signal between $CD2_{Luc}$ and $CD2_{GFP}$ to that seen between $CD2_{Luc}$ and soluble GFP (Fig.8). No energy transfer could be detected between membrane-bound Luc and GFP expressed in the cytoplasm in contrast to the robust BRET observed within the membrane.

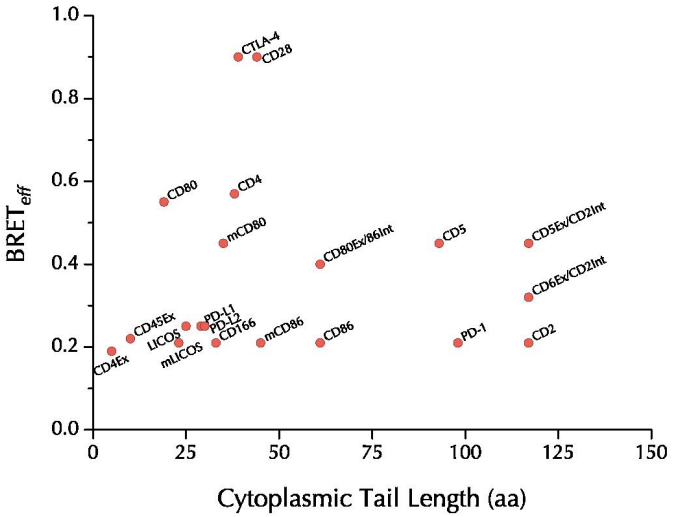



**Figure 7.** Length of membrane protein cytoplasmic tail does not correlate with BRET signal. The calculated length of the intracellular regions of the proteins used in this study was plotted against the maximal $BRET_{eff}$ values determined for them. There is no correlation between cytoplasmic length and strength of BRET, confirming that significant interactions determined by BRET reflect specific association within the membrane.

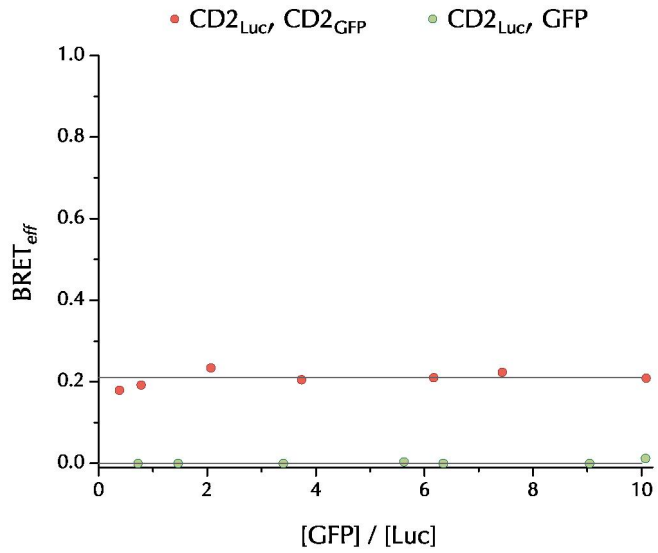



**Figure 8.** Interactions within the cell membrane are very common. Comparison of $BRET_{eff}$ values for the monomeric protein CD2 expressed at physiological levels with itself or with cytoplasmic GFP, demonstrated that molecules confined to the membrane inevitably interact non-specifically.

## 2.5 Discussion

The aim of this investigation was to elucidate the general features of the molecular organization of the T cell surface. For that, we selected a range of representative membrane proteins and assessed their basal stoichiometric state using BRET. As bivalency has been shown to stabilize signaling complex formation several-fold [5], the valency of the molecules studied, all involved in T cell signaling, would be expected to profoundly affect their function. In addition, most surface proteins are part of a cognate receptor-ligand interaction, which reinforces the importance of identifying their oligomerization tendency and understanding how that could be affected by receptor/ligand binding. Interestingly, almost all molecules exhibited a monomeric profile at the cell surface, with low $BRET_{eff}$ values and independence of the acceptor:donor ratio. This was also the case of CD45, a key phosphatase in the T cell signaling process, whose activity has been proposed to be regulated by dimerization [24]. CD45 is expressed at the surface as various alternative spliced isoforms that differ in structure and overall charge [42]. The smaller isoform, CD45RO, has been proposed to preferentially homodimerize due to its reduced negative charge and O-glycosylation, thus being more subject to negative regulation [24]. Furthermore, the observed association was shown to be independent of the intracellular region of the molecule [24]. Our BRET analysis on this variant indicates, however, that CD45RO is monomeric at the cell surface. The BRET results are not affected by high levels of glycosylation as the glycoprotein CD43 that mimics the basic physicochemical properties of full-length CD45 gave similar $BRET_{eff}$ values to those of CD45. The recently solved crystal structure of the entire cytoplasmic tail of CD45 clearly showed that no dimerization of the intracellular region occurs [26], which together with our data suggests an alternative regulatory mechanism for CD45 activity. One possibility has to do with CD45 localization as changes in the protein distribution controlled by the ectodomain have been shown to modulate CD45 function [43].

Unlike CD45, the co-receptor CD4 exhibited an ability to dimerize. Initial crystallographic studies of CD4 extracelullar fragments [44-46] showed no indication of dimerization in the crystal lattice. Recombinant soluble rat CD4 also did not dimerize in solution [47]. However, the crystal structure of intact soluble CD4 has provided evidence of a dimeric association of the receptor through its membrane-proximal domain, although with a low dimer affinity ($K_d$ >1mM) [13]. More precisely, two residues present in the dimer interface, K318 and Q344, were reported to be critical for dimer formation [12]. Mutation of these two residues did not significantly affect the initial $BRET_{eff}$ values, that were similar to those observed for CD80 homodimerization [30], and indicated an oligomeric association. On the contrary, removal of the cytoplasmic tail abrogated CD4 dimerization,

suggesting that CD4 dimerization is dependent on the presence of specific cytoplasmic elements. These results are not consistent with findings reported by others, which suggest a major contribution of D4 for CD4 dimerization and a minor, stabilizing role for the cytoplasmic tail [12, 13]. However, Wang *et al*. showed that alanine substitutions of residues K318 and Q344 are without effect on CD4-pMHC binding, arguing against this CD4 dimerization mode [48]. Other regions have been implicated in dimerization as well [14-16].

In the light of our results, one cytoplasmic element involved in CD4 self-association seems to be the pair of cysteines responsible for its interaction with Lck [38, 39], as substitution of these residues led to a decrease in the $BRET_{eff}$ values. Nevertheless, additional factors are likely to be affecting the co-receptor association. An alpha-helix structure has been predicted in the membrane-proximal region of CD4 [49], that can interact with Lck [50] and contributes to CD4 sensitivity to two HIV proteins, Vpu [51] and Nef [52]. Mutational analysis showed that CD4 endocytosis and degradation induced by the viral proteins requires the co-receptor α-helix structure, whereas the cysteines were dispensable for binding to both Nef and Vpu [51, 52]. Interestingly, this CD4 region is highly homologous to the corresponding one of the epidermal growth factor (EGF) receptor [49], which has been suggested to be involved in the receptor homo- and heterodimerization [53, 54]. Such a scenario could thus be applied to CD4, with the α-helix serving as the binding site for another CD4 molecule. In fact, it is only when the amphipathic α-helix is not present, i.e., in the CD4 Ex construct, and not solely in the absence of the cysteines that we observe a complete abrogation of CD4 dimerization. Hence, it seems reasonable that, at least in 293T cells, this structural element is largely implicated in CD4 self-association. Importantly, when complexed with Lck and in its active form, the protein assumes a monomeric configuration, as demonstrated by the monomeric BRET signature obtained with the CD4-Lck chimera, previously shown to be functional *in vivo*.

The overall organization of the T cell surface was herein investigated by BRET. In this study, we showed that the majority of the molecules have a monomeric profile. Those that possess the unusual ability to dimerize are likely to have a specific function favoured by this property. Accordingly, through dimerization CD4 appears to modulate the threshold of T cell activation [11] and the efficiency of HIV-entry [55]. Likewise, the formation of weak dimers through the extracellular domain might be important for the accessory molecule CD5, as no extracellular ligand engagement appears to be necessary for its negative regulation of TCR signaling [56]. Furthermore, our data indicate that surface receptors are confined to a highly packed environment where non-specific associations are inevitable. Interactions at the membrane are much more frequent than in solution, or

between membrane and soluble proteins. Therefore, it is plausible that the recruitment of proteins from the cytoplasm to the surface may be a key, rate-determining step for T cell activation (James *et al*. unpublished results). Further studies will help to integrate and reconcile these first insights into the arrangement, at the T cell surface, of receptors with important roles in T cell activation.

## Acknowledgments

We thank Dr. Denis Alexander (The Babraham Institute, Cambridge) for the gift of CD45 template. This work was supported by the Wellcome Trust, the Rhodes Trust and the Programa Operacional Ciência e Inovação 2010, cofunded by the European Regional Development Fund.

## 2.6 References

1. Heldin, C.H., Dimerization of cell surface receptors in signal transduction. *Cell*, 1995. **80**(2): p. 213-223.
2. Davis, S.J. and P.A. van der Merwe, The kinetic-segregation model: TCR triggering and beyond. *Nat. Immunol.*, 2006. **7**(8): p. 803-809.
3. Evans, E.J., et al., The T cell surface - how well do we know it? *Immunity*, 2003. **19**: p. 213-223.
4. Batada, N.N., et al., Spatial regulation and the rate of signal transduction activation. *PLoS Comput. Biol.*, 2006. **2**: p. 343-349.
5. Collins, A.V., et al., The interaction properties of costimulatory molecules revisited. *Immunity*, 2002. **17**: p. 201-210.
6. Hampl, J., et al., CD4 augments the response of a T cell to agonist but not to antagonist ligands. *Immunity*, 1997. **7**: p. 379-385.
7. Irvine, D.J., et al., Direct observation of ligand recognition by T cells. *Nature*, 2002. **419**: p. 845-849.
8. Madrenas, J., et al., The efficiency of CD4 recruitment to ligand-engaged TCR controls agonist/partial agonist properties of peptide-MHC molecule ligands. *J. Exp. Med.*, 1997. **185**: p. 219-229.
9. Marrack, P., et al., The major histocompatibility complex-restricted antigen receptor on T cells. II. Role of the L3T4 product. *J. Exp. Med.*, 1983. **158**: p. 1077-1091.

10. Lynch, G.W., et al., Direct evidence for native CD4 oligomers in lymphoid and monocytoid cells. *Eur. J. Immunol.*, 1999. **29**: p. 2590-2602.
11. Moldovan, M.C., et al., Triggering of T cell activation via CD4 dimers. *J. Immunol.*, 2006. **176**: p. 5438-5445.
12. Moldovan, M.C., et al., CD4 dimers constitute the functional component required for T cell activation. *J. Immunol.*, 2002. **169**: p. 6261-6268.
13. Wu, H., et al., Dimeric association and segmental variability in the structure of CD4. *Nature*, 1997. **387**: p. 527-530.
14. Briant, L., et al., Transduction of activation signal that follows HIV-1 binding to CD4 and CD4 dimerization involves the immunoglobulin CDR3-like region in domain 1 of CD4. *J. Biol. Chem.*, 1997. **272**: p. 19441–19450.
15. Langedijk, J.P.M., et al., Location of CD4 dimerization site explains critical role of CDR3-like region in HIV-1 infection and T-cell activation and implies a model for complex of coreceptor-MHC. *J. Biol. Chem.*, 1993. **268**: p. 16875-16878.
16. Matthias, L.J., et al., Disulfide exchange in domain 2 of CD4 is required for entry of HIV-1. *Nat. Immunol.*, 2002. **3**: p. pp727 - 732.
17. Konig, R., et al., Involvement of both major histocompatibility complex class II alpha and beta chains in CD4 function indicates a role for ordered oligomerization in T cell activation. *J. Exp. Med.*, 1995. **182**: p. 779-787.
18. Sakihama, T.A.S. and E.L. Reinherz, Oligomerization of CD4 is required for stable binding to class II major histocompatibility complex proteins but not for interaction with human immunodeficiency virus gp120. *Proc. Natl. Acad. Sci. USA*, 1995. **92**: p. 6444-6448.
19. Weber, S. and K. Karjalainen, CD4 binds MHC class II with extremely low affinity. *Int. Immunol.*, 1993. **5**: p. 695-698.
20. Dornan, S., et al., Differential association of CD45 with CD4 and CD8 regulates the actions of specific pools of p56Lck tyrosine kinase in T cell antigen receptor signal transduction. *J. Biol. Chem.*, 2002. **277**: p. 1912-1918.
21. Takeda, A., et al., Evidence for monomeric and dimeric forms of CD45 associated with a 30-KDa phosphorylated protein. *J. Biol. Chem.*, 1992. **267**(23): p. 16651-16659.
22. Streuli, M., et al., Differential usage of three exons generates at least five different mRNAs encoding human leukocyte common antigens *J. Exp. Med.*, 1987. **166**: p. 1548-1566.
23. McCall, M.N., et al., Expression of soluble isoforms of rat CD45. Analysis by electron microscopy and use in epitope mapping of anti-CD45R monoclonal antibodies. *Immunology*, 1992. **76**: p. 310-317.

24. Xu, Z. and A. Weiss, Negative regulation of CD45 by differential homodimerization of the alternative spliced isoforms *Nat. Immunol.*, 2002. **3**: p. 764-771.
25. Symons, A., et al., Domain organization of the extracellular region of CD45. *Protein Eng.*, 1999. **12**: p. 885-892.
26. Nam, H.-J., et al., Structural basis for the function and regulation of the receptor protein tyrosine phosphatase CD45. *J. Exp. Med.*, 2005. **201**: p. 441-452.
27. Desai, D.M., et al., Ligand-mediated negative regulation of a chimeric transmembrane receptor tyrosine phosphatase. *Cell*, 1993. **73**: p. 541-554.
28. Bilwes, A., et al., Structural basis for inhibition of receptor protein-tyrosine phosphatase-α by dimerization. *Nature*, 1996. **382**: p. 555-559.
29. Eidne, K.A., et al., Applications of novel resonance energy transfer techniques to study dynamic hormone receptor interactions in living cells. *Trends Endocrinol. Metab.*, 2002. **13**: p. 415-421.
30. James, J.R., et al., A rigorous experimental framework for detecting protein oligomerization using bioluminescence energy transfer. *Nat. Methods*, 2006. **3**: p. 1001-1006.
31. Freeman, G.J., et al., Engagement of the PD-1 immunoinhibitory receptor by a novel B7 family member leads to negative regulation of lymphocyte activation. *J. Exp. Med.*, 2000. **192**: p. 1027-34.
32. Ishida, Y., et al., Induced expression of PD-1, a novel member of the immunoglobulin gene superfamily, upon programmed cell death. *EMBO J.*, 1992. **11**: p. 3887-3895.
33. Latchman, Y., et al., PD-L2 is a second ligand for PD-1 and inhibits T cell activation. *Nat. Immunol.*, 2001. **2**: p. 261 - 268.
34. Zhang, X., et al., Structural and functional analysis of the costimulatory receptor programmed death-1. *Immunity*, 2004. **20**: p. 337-347.
35. Carreno, B.M. and M. Collins, The B7 family of ligands and its receptors: new pathways for costimulation and inhibition of immune responses. *Annu. Rev. Immunol.*, 2002. **20**: p. 29-53.
36. Bowen, M.A., et al., Cloning, mapping and characterization of activated leukocyte-cell adhesion molecule (ALCAM), a CD6 ligand. *J. Exp. Med.*, 1995. **181**: p. 2213-2220.
37. Bowen, M.A., et al., The amino-terminal immunoglobulin-like domain of activated leukocyte cell adhesion molecule binds specifically to the membrane-proximal scavenger receptor cysteine-rich domain of CD6 with a 1:1 stoichiometry. *J. Biol. Chem.*, 1996. **29**: p. 17390-17396.

38. Shaw, A.S., et al., The Lck tyrosine protein kinase interacts with the cytoplasmic tail of the CD4 glycoprotein through its unique amino-terminal domain. *Cell*, 1989. **59**: p. 627-636
39. Turner, J.M., et al., Interaction of the unique N-terminal region of tyrosine kinase $p56^{lck}$ with cytoplasmic domains of CD4 and CD8 is mediated by cysteine motifs *Cell*, 1990. **60**(5): p. 755-765
40. Xu, H. and D.R. Littman, A kinase-independent function of Lck in potentiating antigen-specific T cell activation. *Cell*, 1993. **74**: p. 633-643.
41. Saxton, M.J., Lateral diffusion in an archipelago. Distance dependence of the diffusion coefficient. *Biophys. J.*, 1989. **56**: p. 615-622.
42. Trowbridge, I.S. and T.M. L., CD45: an emerging role as a protein tyrosine phosphatase required for lymphocyte activation and development. *Annu. Rev. Immunol.*, 1994. **12**: p. 85-116.
43. Irles, C., et al., CD45 ectodomain controls interaction with GEMs and Lck activity for optimal TCR signaling. *Nat. Immunol.*, 2002. **4**: p. 189-197.
44. Ryu, S.-E., et al., Crystal structure of an HIV-binding recombinant fragment of human CD4. *Nature*, 1990. **348**: p. 419-425.
45. Wang, J., et al., Anatomic structure of a fragment of human CD4 containing two immunoglobulin-like domains. *Nature*, 1990. **348**: p. 411-418.
46. Brady, R.L., et al., Crystal structure of domains 3 and 4 of rat CD4: relation to the N-terminal domains. *Science*, 1993. **260**: p. 979-983.
47. Davis, S.J., et al., High level expression in chinese hamster ovary cells of soluble forms of CD4 T lymphocyte glycoprotein including glycosylation variants. *J. Biol. Chem.*, 1990. **265**: p. 10410-10418.
48. Wang, J.H., et al., Crystal structure of the human CD4 N-terminal two-domain fragment complexed to a class II MHC molecule. *Proc. Natl. Acad. Sci. USA*, 2001. **98**: p. 10799-10804.
49. Shin, J., et al., Phosphorylation-dependent down-modulation of CD4 requires a specific structure within the cytoplasmic domain of CD4. *J. Biol. Chem.*, 1991. **266**: p. 10658-10665.
50. Kim, P.W., et al., A zinc clasp structure tethers lck to T cell coreceptors CD4 and CD8. *Science*, 2003. **301**: p. 1725-1728.
51. Yao, X.-J., et al., Degradation of CD4 induced by human immunodeficiency virus type I Vpu protein: a predicted alpha-helix structure in the proximal cytoplasmic region of CD4 contributes to Vpu sensitivity. *Virology*, 1995. **209**: p. 615-623.

52. Aiken, C., et al., Nef induces CD4 endocytosis: requirement for a critical dileucine motif in the membrane-proximal CD4 cytoplasmic domain. *Cell*, 1994. **76**: p. 653-664.
53. Carlin, C.R., et al., Epidermal growth factor receptor is down-regulated by a 10,400 MW protein encoded by the E3 region of adenovirus. *Cell*, 1989. **57**: p. 135-144
54. Stern, D.F. and M.P. Kamps, EGF-stimulated tyrosine phosphorylation of p185neu: a potential model for receptor interactions. *EMBO J.*, 1988. **7**: p. 995-1001.
55. Bourgeois, R., et al., Association between disruption of CD4 receptor dimerization and increased human immunodeficiency virus type 1 entry. *Retrovirology*, 2006. **3**: p. 31-38.
56. Bhandoola, A., et al., CD5-mediated inhibition of TCR signaling during intrathymic selection and development does not require the CD5 extracellular domain. *Eur. J. Immunol.*, 2002. **32**: p. 1811-1817.

## 3. Extracellular isoforms of CD6 generated by alternative splicing regulate targeting of CD6 to the immunological synapse

***Mónica A. A. Castro, *Marta I. Oliveira, Raquel J. Nunes, Stéphanie Fabre, Rita Barbosa, António Peixoto, Marion H. Brown, Jane R. Parnes, Georges Bismuth, Alexandra Moreira, Benedita Rocha and Alexandre M. Carmo**

* Both authors contributed equally to this work

*The Journal of Immunology,* 178 (7):4351-61 (2007)

## 3.1 Abstract

The great majority of mammalian genes yield multiple transcripts arising from differential mRNA processing, but in very few instances have alternative forms been assigned distinct functional properties. We have cloned and characterized a new isoform of the accessory molecule CD6 that lacks the CD166 binding domain and is expressed in rat and human primary cells. The novel isoform, CD6Δd3, results from exon 5 skipping and consequently lacks the third scavenger receptor cysteine-rich (SRCR) domain of CD6. Differential expression of the SRCR domain 3 resulted in a remarkable functional difference: whereas full-length CD6 targeted to the immunological synapse, CD6Δd3 was unable to localize at the T cell:APC interface during Ag presentation. Analysis of expression of CD6 variants showed that, while being more frequent in coexpression with full-length CD6, the CD6 Δd3 isoform constituted the sole species in a small percentage of T cells. In the rat thymus, CD6Δd3 is less represented in double-positive thymocytes but is detectable in nearly 50% of single-positive CD4 or CD8 thymocytes, suggesting that CD6 switching between full-length and Δd3 isoforms may be involved in thymic selection. Strikingly, CD6Δd3 is markedly up-regulated upon activation of T lymphocytes, partially substituting full-length CD6, as evaluated by RT-PCR analysis at the single-cell level, by immunoblotting, and by flow cytometry using Abs recognizing SRCR domains 1 and 3 of human CD6. This elegant mechanism controlling the expression of the CD166 binding domain may help regulate signaling delivered by CD6, through different types of extracellular engagement.

## 3.2 Introduction

The TCR recognition of peptide-MHC complexes expressed on APCs involves the formation of a tight cell-cell contact area, the immunological synapse (IS), where individual proteins are selectively partitioned [1, 2]. The model of synapse formation predicts an initial stabilization of the contact by engaged integrins, which anchor the region of the contact and allow the TCRs to scan MHC-peptide complexes [3]. With time, stably engaged TCR complexes coalesce into a central area (cSMAC; central supramolecular activation clusters), surrounded by a ring (pSMAC; peripheral supramolecular activation clusters) enriched in the integrin LFA-1 [2, 4]. In the mature synapse, cSMAC are also enriched in the costimulatory molecule CD28 and the CD4 or CD8 coreceptors [3, 5]. It has been suggested that the formation of the synapse is favored by receptor-ligand interactions of small auxiliary molecules such as CD2-CD58 and CD28-CD80 that stabilize the cell contact by the formation of low-affinity interactions, in a size dependent-manner. According to this

model, the small adhesion pairs cluster at a tight membrane region, thus segregating larger glycoproteins such as CD43 or CD45 [1, 6].

CD6 is a 100- to 130-kDa surface glycoprotein expressed primarily on medullary thymocytes and mature T lymphocytes [7]. CD6 has been regarded as a costimulatory molecule as Ab-mediated CD6 cross-linking can potentiate proliferative T cell responses [8-10]. Moreover, a subpopulation of CD6-negative T cells displayed lower alloreactivity in MLRs compared with normal $CD6^+$ T cell populations [11]. CD6 could additionally play a role in thymocyte maturation, because CD6 Abs have been shown to partially block the adhesion of thymocytes to thymic epithelial cells [12]. This observation also provided the first evidence that CD6 had a cell surface ligand. A requirement for ligand engagement for costimulatory effects of CD6 was shown by inhibition of Ag-specific and CD3 mAb-induced T cell responses by soluble CD6 [13, 14]. Recently, CD6 has been reported to accumulate at the IS, mediating early and late T cell-APC interactions required for IS maturation and cell proliferation [13, 15].

Upon CD3 engagement CD6 becomes phosphorylated on tyrosine residues, suggesting that interactions with Src homology (SH)2 domain-containing intracellular effectors may occur [16]. An interaction with the SH2 domain of SLP-76 has been shown to be critical for the costimulatory effects of CD6 [17]. The cytoplasmic domain of CD6 is unusually long and also contains two well-conserved proline-rich sequences, which are potential binding sites for SH3 domain-containing proteins well suited for signal transduction [16, 18]. Indeed, the rat homolog of CD6 has been shown to associate with protein tyrosine kinases of different families, namely Src-family kinases Lck and Fyn, Zap70 of the Syk family, and the Tec-family kinase Itk [19]. CD6 has additionally been shown to associate at the surface of T cells with CD3 (13) and with the structurally related receptor CD5 [19, 20]. However, there are still no data proposing a functional role for these interactions.

By contrast, the molecular basis of the interaction between CD6 and the extracellular physiological ligand, CD166, has been comprehensively investigated in human and murine models [21]. CD166 is a widely expressed glycoprotein containing five Ig superfamily domains, of which the N-terminal domain has been shown to bind to the third scavenger receptor cysteine-rich (SRCR)-type domain of CD6, the membrane-proximal domain [22, 23]. The residues of CD6 involved in the contact with CD166 are located in the E-F loop, a region that, in the particular case of the third domain of CD6, is most divergent from all known SRCR domains [24]. The resulting interaction between CD6 and CD166 is therefore unusual, because most other T cell surface proteins mediating cell-cell interactions bind through their N-terminal domains. However, affinity and kinetic measurements revealed that, in solution, binding occurs with a $K_d$ of 0.4-1.0

μM [14], relatively strong compared with most other leukocyte adhesion pairs, albeit in the range of low-affinity interactions characteristic of cell surface receptors [25-27].

The human, rat, and mouse *Cd6* genes contain 13 exons, of which the last 6 code for the cytoplasmic tail. Numerous CD6 isoforms have been reported that result from alternative splicing of the exons coding for the cytoplasmic domain [18, 28-30], but no specific physiological function has been attributed to any of these isoforms. Exon 7 contains the sequence coding for the transmembrane domain, and the first 6 exons code for most of the extracellular domain. Alignment of the CD6 extracellular sequence with that of the scavenger receptor domain of Mac-2 binding protein, for which a crystal structure has been obtained [24], predicts that each scavenger-type domain of CD6 is encoded by a single exon, and that removal of each of these exons would result in a protein only devoid of the correspondent domain. We have obtained from rat thymocytes and peripheral rat and human T cells, cDNAs of CD6 omitting exon 5, whose corresponding translated polypeptides lack the SRCR domain 3. This CD6 isoform, CD6Δd3, is present in all T lineage cells studied and is up-regulated upon activation, paralleling a decline in the expression of full-length CD6. The failure of CD6Δd3 binding to CD166 highlights the role of domain 3 in addressing CD6 to the IS, and the down-modulation of domain 3 induced upon T cell activation reveals a rare mode of positional control of cell surface receptors dependent on alternative mRNA splicing.

## 3.3 Materials and Methods

### 3.3.1 Cells and cell lines

Rat thymocytes, splenocytes, and cervical lymph node cells were from 9-to 12-wk-old Lewis male rats (Charles River Laboratories). Human primary T cells were isolated from peripheral blood by centrifugation on a Ficoll gradient followed by negative depletion on magnetic beads (T cell-negative isolation kit; Dynal Biotech), or using the RosetteSep human T cell enrichment mixture (StemCell Technologies), where indicated. Cell lines COS7 [31] and Raji [32] were maintained in RPMI 1640 supple mented with 10% FCS, 1 mM sodium pyruvate, 2 mM L-glutamine, penicillin G (50 U/ml), and streptomycin (50 μg/ml).

### 3.3.2 Abs and reagents

Rat mAbs used were CD6-OX52 [33] (a gift from N. Barclay, University of Oxford, U.K.), TCR-R73 [34], and CD28-JJ319 [35] (gifts from T. Hünig, University of Würzburg, Germany). Conjugated mAbs used for cell sorting were as follows: biotinylated CD4-W3/25 (obtained from Serotec); CD6-OX52 FITC-labeled, CD3-1F4, and CD45RC-OX22, conjugated with PE, biotinylated CD8/3-341 and CD134-OX40, and CD4-OX35 conjugated with allophycocyanin (obtained from BD Biosciences). Biotinylated Abs were detected with streptavidin conjugated with PE, PE-Cy7, or allophycocyanin. Human mAbs were as follows: OX126 [17], specific for human CD6 domain 3, FITC-labeled UMCD6 [9], anti-domain 1 of CD6 (obtained from Ancell); MEM-98 [36] (anti-CD6 domain 1; a gift from V. Hořejší, Academy of Sciences, Prague, Czech Republic), CD166-3A6 [37] (BD Pharmingen); and CD71 (DakoCytomation). Goat anti-mouse peroxidase conjugated was obtained from Molecular Probes Europe and rabbit anti-mouse FITC-labeled from DakoCytomation. Biotinylated proteins were detected in Western blotting with ExtrAvidin peroxidase (Sigma-Aldrich).

### 3.3.3 cDNA cloning and plasmids

Rat CD6 cDNAs were cloned as described previously [19]. Full-length rat CD6 (CD6FL) cDNA [19] was extracted from pCR2.1-TOPO vector (In-vitrogen Life Technologies) using *Spe*I and *Apa*I and blunt-end cloned into the expression vector pEF-BOS [38]. rCD6Δd3/pEF-BOS was obtained by digestion with *Sma*I of a sequence flanking the alternatively spliced exon 5 from the rCD6Δd3/pCR2.1-TOPO template. The vector encoding rat CD6FL-YFP was produced as follows: rat CD6 cDNA was amplified from the original clone rCD6/pCR2.1-TOPO [19] by PCR using as the reverse primer 5'-GCAGAATTCGAAGCTTGGCTGCTCCAATGTCATCG-3'. The PCR product was then cloned into the pEYFP-N1 vector (Clontech Laboratories) in frame with the N-terminal sequence of the yellow fluorescent protein (YFP), in the *Hind*III restriction sites included in the primers. The rCD6Δd3/pEYFP-N1 construct was obtained by digestion as described above and cloned in frame with pEYFP-N1. A cytoplasmic deletion mutant of rat CD6 fused to YFP was produced by PCR from rCD6/pCR2.1-TOPO using as reverse primer 5'-CTACTAAAGCTTTTGTCCTTTGGC TTTCAAGAG-3', terminating just after the codon of the fifth amino acid of the cytoplasmic domain. The PCR product was cloned into the *Hind*III restriction site of the pEYFP-N1 vector to produce rCD6CY5/pEYFP-N1.

Total RNA was isolated from human PBMC and E6.1 Jurkat cells using the RNA extraction kit (Qiagen). cDNA was obtained using the ThermoScript RT-PCR system (Invitrogen Life Technologies) from total RNA primed with oligo(dT). Human *Cd6* was amplified with primer design based on the reported sequence (GenBank accession no. U34625). The following primers were used in the cloning of the isoforms: forward primer spanning the initiation codon (shown in bold) 5'-CGCGGATCCTCTAG**ATG**TGGCTCT TCTTCGGGATCACTGGATTG-3' and reverse primer in the exon 7 (TM-coding sequence) of human *Cd6* 5'-GGAGCATTAGCTCCCGAGATTCCTTG-3'. The PCR fragments were cloned into pCR2.1-TOPO vector. The sequences were confirmed by dedeoxy sequencing.

Human CD6FL/pEGFP-N1 was produced by amplifying a full-length sequence from the clone CD6/pBJ-neo [18] by PCR, using as the forward primer 5'-CGCGGATCCTCTAG**ATG**TGGCTCTTCTTCGGGATCACTGGATTG-3' and the reverse primer 5'-CTACTAGAATCCGCTGCGCTGATGTCATCG-3'. The PCR product was then cloned into the *Bam*HI restriction site of the pEGFP-N1 vector (Clontech Laboratories) producing CD6FL/pEGFP-N1. The isoform CD6Δd3 was amplified from the vector pCR2.1-TOPO using the primer M13-R from the vector as the forward primer, and a reverse primer in the exon 7 of human CD6 including a naturally occurring *Eco*RI restriction site 5'-CTACTAGAATTCCCAGAACGATGGAGGGGATGAGGAGCATTAGCTCCCGAGATTCCT TG-3'. The PCR product was inserted in the CD6FL/pEGFP-N1 producing CD6Δd3/pEGFP-N1. A cytoplasmic deletion mutant of human CD6 fused to GFP was produced by PCR from CD6/pBJ-neo with the forward primer 5'-CTCCAGAC**ATG**TGGCTCTTCTTCGG-3**'** and the reverse primer 5'-GCCTTCAT CCTCTTGAGAATTAAAGGAAAA-3', terminating just before the first tyrosine residue codon of the cytoplasmic domain. The PCR product was cloned into the TOPO cloning site of pcDNA3.1/CT-GFP-TOPO, using GFP Fusion TOPO TA Expression Kits (Invitrogen Life Technologies; version I), to produce CD6CY5/pcDNA3.1/CT-GFP-TOPO.

Rat CD166 cDNA was obtained from total RNA isolated from Lewis rat lungs and reverse transcribed using a gene-specific primer 5'-CCAGGACAGCTTAGTA GGAT-3'. Amplification of the full-length molecule was performed using as forward primer 5'-TAGTAGAAGCTTCTAGGAGGAGGAATATGGC-3' and reverse primer 5'-CTACTACTCGAGACTCCTCTCTTAGGCTTCTG-3'. Cloning the resulting PCR product into the *Hind*III-*Pst*I restriction site of the pECFP-N2 vector handled rCD166/pECFP-N2.

### 3.3.4 Cell transfections

Rat CD6FL and CD6Δd3 in pEF-BOS, or the empty vector, were transiently transfected in COS7 cells following the procedures described previously [39].

Transient transfections of primary T lymphocytes (5 X $10^6$ cells) were performed with 5 μg of rat CD6FL/pEYFP-N1, CD6Δd3/pEYFP-N1 or CD6CY5/pEYFP-N1 or human CD6FL/pEGFP-N1, CD6Δd3/pEGFP-N1 or CD6CY5/pcDNA3.1/CT-GFP-TOPO plasmids using the Human T cell Nucleofector kit (Amaxa), and T cells were used 24 h posttransfection. Transfection of Raji B cells was performed as follows: $10^7$ cells were centrifuged, resuspended in 900 μl of prewarmed complete medium, mixed with 20 μg of rat CD166/pECFP-N2 plasmid, and transferred into a Gene-Pulse cuvette (Bio-Rad). Electroporation was performed in a Bio-Rad Gene Pulser II electroporator at 950 μF and 260 V. Cells were maintained in complete medium at 37°C and used 48 h after transfection.

### 3.3.5 Cell surface biotinylation, immunoprecipitations, and western blotting

Cell surface biotinylation, immunoprecipitations and detection of biotinylated Ags, and immunoblotting were performed as described previously [40].

### 3.3.6 Single-cell RT-PCR analysis

RT-PCR were performed on single cells purified on the basis of their expression of selected markers after two rounds of cell sorting using a FACSVantage equipped with an automatic deposition unit (BD Bio-sciences). The characteristics and sensitivity of the RT-PCR method have been previously described in detail [41]. Briefly, cells were lysed and the RNA reverse transcribed using a *Cd6*-specific 3**'** primer, 5'-GAGTCCTT ATCCTTCACGCT-3', and the resulting cDNAs amplified in a two-step nested PCR. The 5**'** primers used were as follows: 5'-ATCCACCGTGACCAAGTGAA-3' and 5'-AGACCAGTACTGCGGTCACA-3' (nested), and the same reverse primer was used for the reverse transcription reaction. None of the primer combinations amplifies genomic DNA.

### 3.3.7 Flow cytometry

Flow cytometry was performed as described previously [40].

### 3.3.8 Cellular activation

A cell suspension was obtained from rat spleen, and 2 X $10^6$ cells/ml were activated for 72 h in vitro by incubation with anti-TCR (R73) plus anti-CD28 (JJ319) mAbs used at 2-10 µg/ml, or left untreated. Cells were incubated at 37°C with 5% $CO_2$ and, after the indicated period, collected, labeled for OX40, sorted or lysed, and analyzed by immunoblotting.

Human primary T cells were activated by incubating 3 X $10^6$ cells/ml with PHA-p at 5 µg/ml in RPMI 1640, at 37°C with 5% $CO_2$, or left untreated. After 72 h, cells were collected and analyzed by flow cytometry or immunoblotting.

### 3.3.9 Conjugate formation and fluorescence analysis

Raji B cells were incubated with a mix of superantigens (staphylococcal enterotoxin A (SEA), SEB, and SEC3, 200 ng/ml each; Toxin Technologies) and plated on poly-D-lysine-coated glass coverslips for 30 min at 37°C. T cells were added to APCs and then incubated at 37°C for 45 min. Cells were fixed with 4% paraformaldehyde in PBS for 10 min and washed several times with PBS before analysis. Where indicated, T cells were preincubated, for 30 min at 4°C, with the mAbs OX126 or UMCD6-FITC, and Raji B cells preincubated with 3A6 (CD166), all at 10 µg/ml, or left untreated. Immunofluorescence and transmission light images were acquired on an Eclipse TE300 inverted microscope (Nikon) equipped with a cooled CCD camera (CoolSNAPFx; Roper Scientific). Images were acquired and analyzed using the Metamorph software (Roper Scientific). Conjugate formation and synapse localization of CD6 or CD166 were quantified with blind scoring, counting a minimum of 50 productive conjugates in each of two or more experiments, and each experiment was observed by two to three examiners.

## 3.4 Results

### 3.4.1 A novel isoform of rat CD6 devoid of the CD166 binding domain arises from alternative splicing

Human and mouse CD6 possess several isoforms characterized by cytoplasmic tails of variable lengths, resulting from alternative splicing of exons coding for the intracellular domain [18, 28-30]. Subsequent to our recent cloning of a cDNA of rat CD6 [19] containing all 13 exons homologous to the mouse and human sequences, we proceeded to a systematic search for novel rat CD6 isoforms. Using total RNA isolated from Lewis male

rat spleens, cDNAs were obtained by reverse transcription followed by PCR using primers complementary to sequences immediately before and after the coding sequence. We obtained five cDNA species displaying distinct mobility on agarose gels (Fig. 1*A*). Sequencing confirmed the longest product as full-length CD6. Interestingly, sequencing of the third largest product (indicated by an arrow) revealed a novel isoform lacking not a cytoplasmic-coding exon, but missing instead the sequence corresponding to exon 5 (GenBank accession no. AY683561). Alignment of the corresponding amino acid sequence with that of wild-type rat CD6 shows that this cDNA codes for a novel isoform lacking the third SRCR domain, which contains the binding site for the ligand, CD166 (Fig. 1, *B-D).*

### 3.4.2 CD6Δd3 is expressed at the cell surface

To verify whether the novel isoform, CD6Δd3, could be correctly folded, transported, and expressed at the cell surface, we cloned the corresponding cDNA into the expression vector pEF-BOS and used it for transfecting COS7 cells. In parallel, COS7 cells were transfected with rCD6FL/pEF-BOS, encoding full-length rat CD6, and also with an empty vector. Forty-eight hours after transfection, cells were analyzed for membrane expression of CD6 by immunoprecipitation, using the CD6-specific mAb OX52, and streptavidin-peroxidase detection from lysates of surface biotinylated cells. As shown in Fig. 2, detection of CD6Δd3 confirmed its correct folding and expression at the cell surface. The apparent molecular mass of this isoform is 112 kDa, compared with 126 kDa of full-length CD6. No product was detected in the lane corresponding to empty vector.

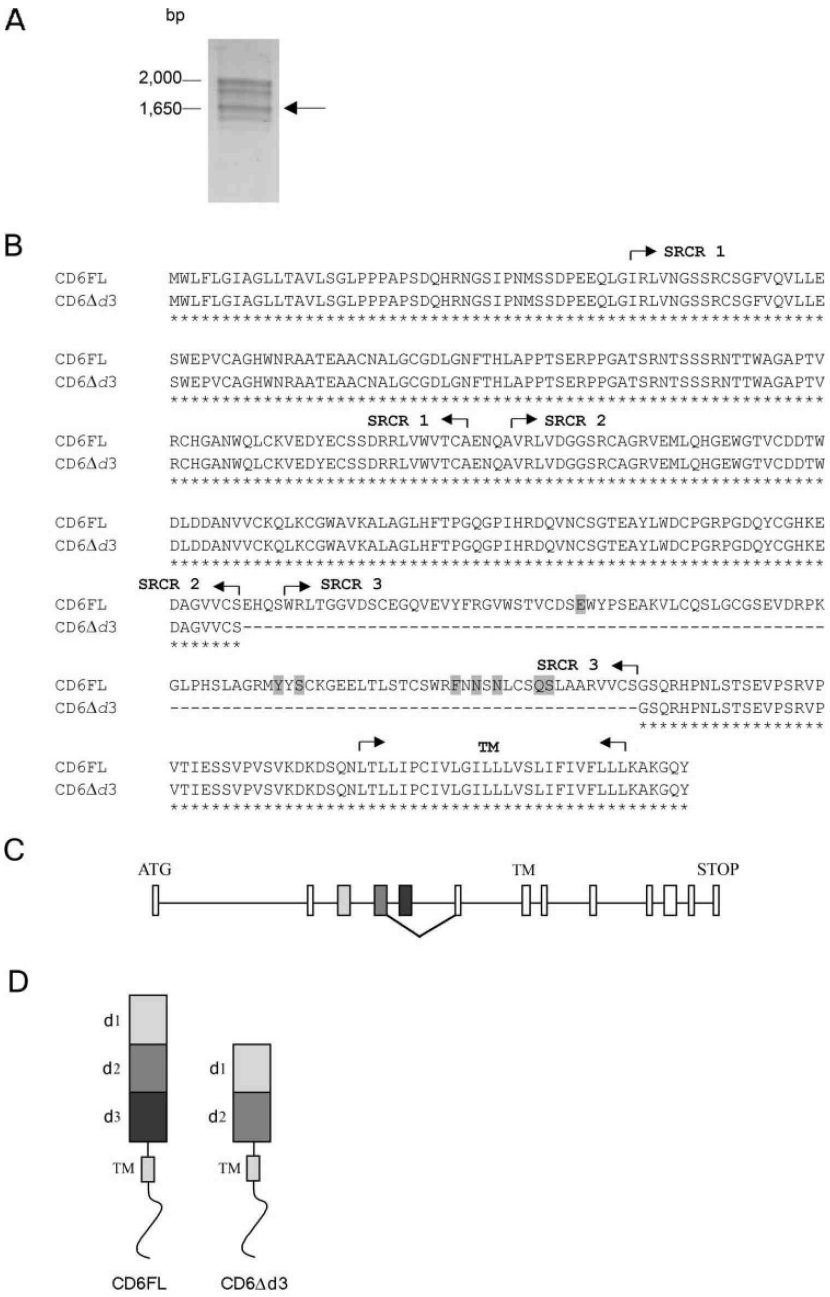



**Figure 1**. A novel CD6 isoform lacks the CD166 binding domain. *A,* Total RNA from Lewis rat spleens was used for RT-PCR. The cDNA products were analyzed on gels, isolated, and sequenced. One mRNA species, indicated by an arrow, corresponded to an isoform lacking the coding sequence of the SRCR domain 3. *B,* Alignment of CD6FL and CD6Δd3 peptide sequences from the N terminus up to the transmembrane domain. The boundaries of the SRCR domains are indicated by arrows, according to Hohenester et al. [24]. Residues involved on binding to CD166 are gray shaded [42] and are missing in the sequence CD6Δd3 (dashed lines). Asterisks denote identical residues. *C*, Organization of the rat *Cd6* locus. Introns are shown as thin lines connecting exons, represented by white boxes *D*, Grey boxes indicate the exons coding for the three SRCR domains. Alternative splicing across exon 5 is indicated by solid lines. *D,* Scheme of the structure obtained for the two CD6 protein isoforms.

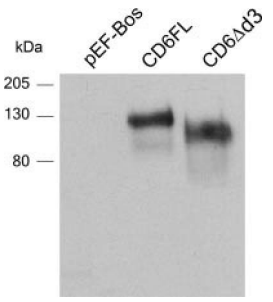



**Figure 2.** CD6Δd3 is expressed at the surface of COS7 cells. CD6FL and CD6Δd3 coding cDNAs were cloned in pEF-BOS and transfected in COS7 cells. Forty-eight hours post-transfection, cells were surface biotinylated, lysed, and CD6 was immunoprecipitated using OX52. Cells transfected with the empty vector were used as a negative control. Both isoforms were efficiently expressed at the cell surface.

### 3.4.3 Full-length CD6, but not CD6Δd3, targets to the IS upon T cell-APC conjugate formation

An accumulation of human CD6 at the IS has been recently reported in Jurkat-Raji cell conjugates [20]. We thus tested the dependence on CD166-binding interactions for CD6 recruitment to the synapse, by using both CD6FL and CD6Δd3 isoforms. T cells were transfected with constructs coding for either CD6FL-YFP or CD6Δd3-YFP fusion proteins. In isolated T cells, the distribution of both isoforms is homogenous at the plasma membrane (Fig. 3*A*), a result which additionally confirms that CD6Δd3 can be efficiently expressed at the plasma membrane. Incubation of T cells with Raji B cells primed with superantigen, but not expressing rat CD166, did not change the pattern of CD6FL or CD6Δd3 distribution at the cell surface (Fig. *3B).* However, when Ag-primed Raji expressed rat CD166 (shown in green) and T cells expressed CD6FL, both molecules were able to concentrate at the Raji-T cell contact zone (Fig. 3*C*, *left panels,* and *E).* Interestingly, the CD6Δd3 isoform did not efficiently relocalize to the synapse, and, moreover, did not induce colocalization of CD166 as well (Fig. 3*C*, *right panels,* and *E).* This result indisputably proves that the effective CD166-dependent CD6 recruitment to the synapse relies on the presence of the third SRCR domain of CD6. Conversely, rat CD166 targets to the synapse when its T cell ligand rat CD6, expressing the SRCR domain 3, is expressed at the T cell surface. To verify whether intracellular interactions with other signaling intermediates or with the cytoskeleton could also be involved in the translocation of CD6 to the IS, T cells were induced to express CD6CY5, a truncated form of the protein retaining only 5 aas of the cytoplasmic domain, fused to YFP. These cells were incubated with Ag-primed Raji cells, expressing rat CD166 (Fig. 3*D*). The truncated form of CD6 was found to localize in the IS as efficiently as the full-length form (Fig. 3, *D* and *E*), excluding an exclusive role for cytoplasmic domain interactions on CD6 targeting to the contact zone.

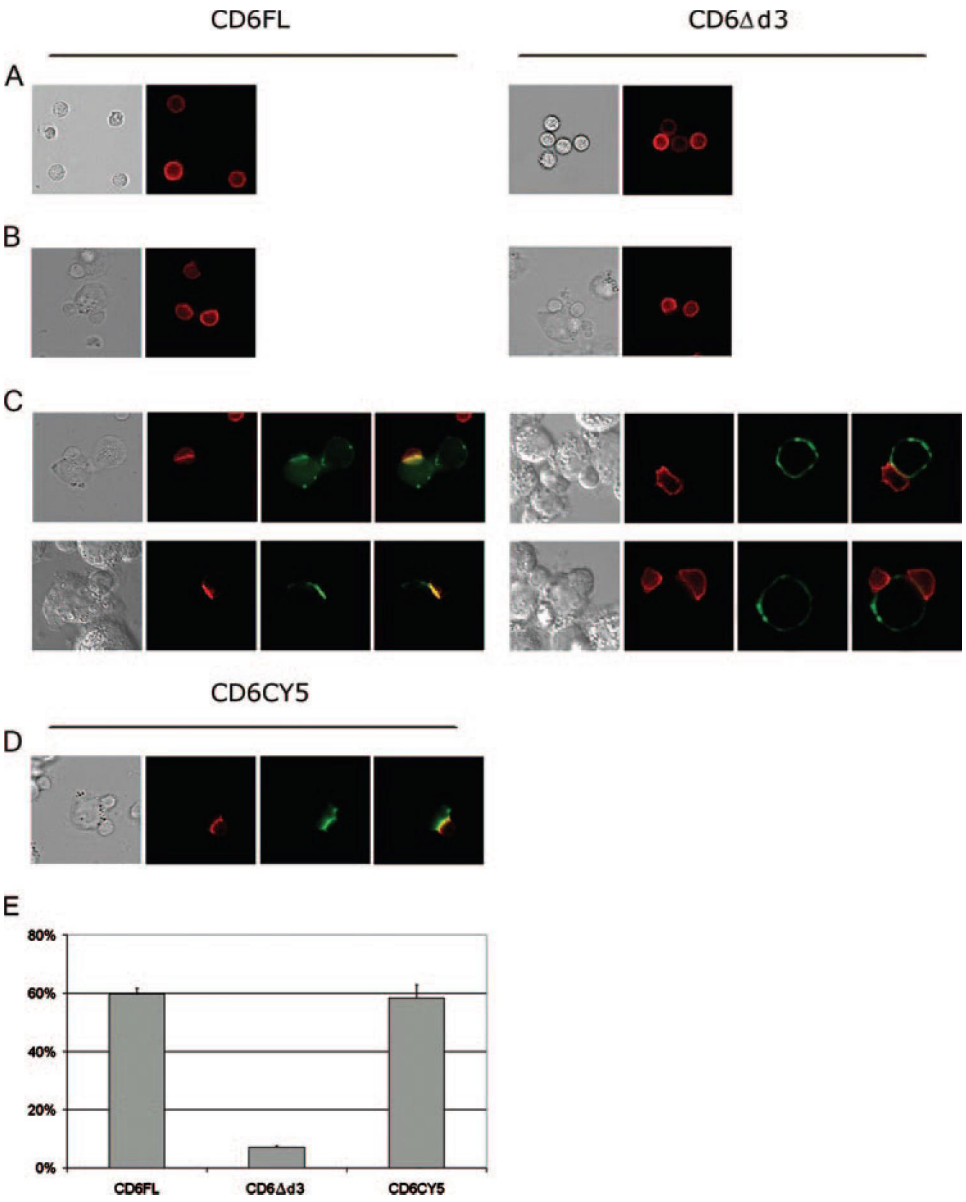



**Figure 3.** Localization of CD6 to the IS is dependent on the SRCR domain 3 of CD6 and its interaction with CD166, but not on intracellular interactions. *A,* Differential interferential contrast and fluorescence images of unstimulated primary T cells transfected with CD6FL-YFP *(left panels)* or CD6Δd3-YFP *(right panels).* Labeled CD6 is shown in red. *B,* IS formed between superantigen-pulsed Raji B cells and CD6FL-YFP or CD6Δd3-YFP-transfected primary T cells. Cells were fixed after 45 min of interaction. *C*, Raji B cells were transfected with CD166-CFP (detected as green) and pulsed with 1 μg/ml superantigen mix before incubation with transfected T cells. Localization of CD6FL-YFP or CD6Δd3-YFP and CD166-CFP as well as fluorescence overlays are shown. Two examples of each experiment are represented. *D,* Interaction of T cells expressing CD6CY5-YFP with CD166-CFP expressing Raji show colo-calization of CD6 and CD166. *E,* Frequency of cells translocating rat isoforms CD6FL, CD6Δd3, and CD6CY5 to the IS in T cells forming conjugates with rat CD166-expressing Raji. Positive translocation was only considered in conjugates with

synaptic CD6 accumulation coinciding with a clear CD166 patch in Raji. Results are from three independent experiments, with a minimum of 50 productive conjugates considered per experiment. All counts were performed with blind scoring.

### 3.4.4 Cd6 expression in different lymphoid tissues and individual cells

Given a potential distinct role of the two isoforms, we conducted a detailed analysis on the profiling of expression of *Cd6* in different lymphoid organs, specifically addressing the frequency of *Cd6*Δ*d3.* We performed PCR from mRNA from thymus, spleen, and lymph nodes amplifying only the sequences corresponding to the extracellular and transmembrane domains, thus excluding cytoplasmic domain isoforms. Two major isoforms were obtained in all three organs, and at similar proportions (Fig. 4*A*). The heaviest and most abundant product matched the entire sequence, whereas the smallest product, 300 nt shorter, matched the isoform lacking exon 5. This experiment was reproducible and PCR products from several trials were extensively sequenced and confirmed the expression of only these two isoforms but not of others, for example excluding exons 3 or 4.

The pattern of expression of the CD6 gene in bulk cellular preparations suggested that both isoforms could be found in all tissues analyzed. However, it did not clarify whether each isoform was the sole species in a given cell, or whether both isoforms could be coexpressed in the same cell. We sorted different cell populations and addressed *Cd6* expression at the single-cell level. The target populations for this study were developing thymocytes at different maturation stages as well as diverse subsets of T lymphocytes (Fig. *4B).* Cells were sorted based on the protein expression of specific markers, and expression of each isoform was assayed by single cell RT-PCR. All sorted populations were gated on $CD6^{high}$-expressing cells, and thus *Cd6* amplification directly attested for plating efficiency, with no need for parallel amplification of an internal control. PCR amplification was performed using primers flanking the spliced exon, rendering products of 452 bp for full-length *Cd6* and 148 bp for *Cd6*Δ*d3.* Fig. *4C* shows an analysis of PCR products obtained from $CD3^{+}CD4^{+}CD8^{-}$ individual thymocytes. All possible CD6 phenotypes were present in this population, with many cells expressing only full-length CD6, a few expressing exclusively the Δd3 isoform, whereas others coexpressed both. In mature T cells, the frequency of *Cd6*Δ*d3* expression was remarkably consistent, regardless of the cell type studied.

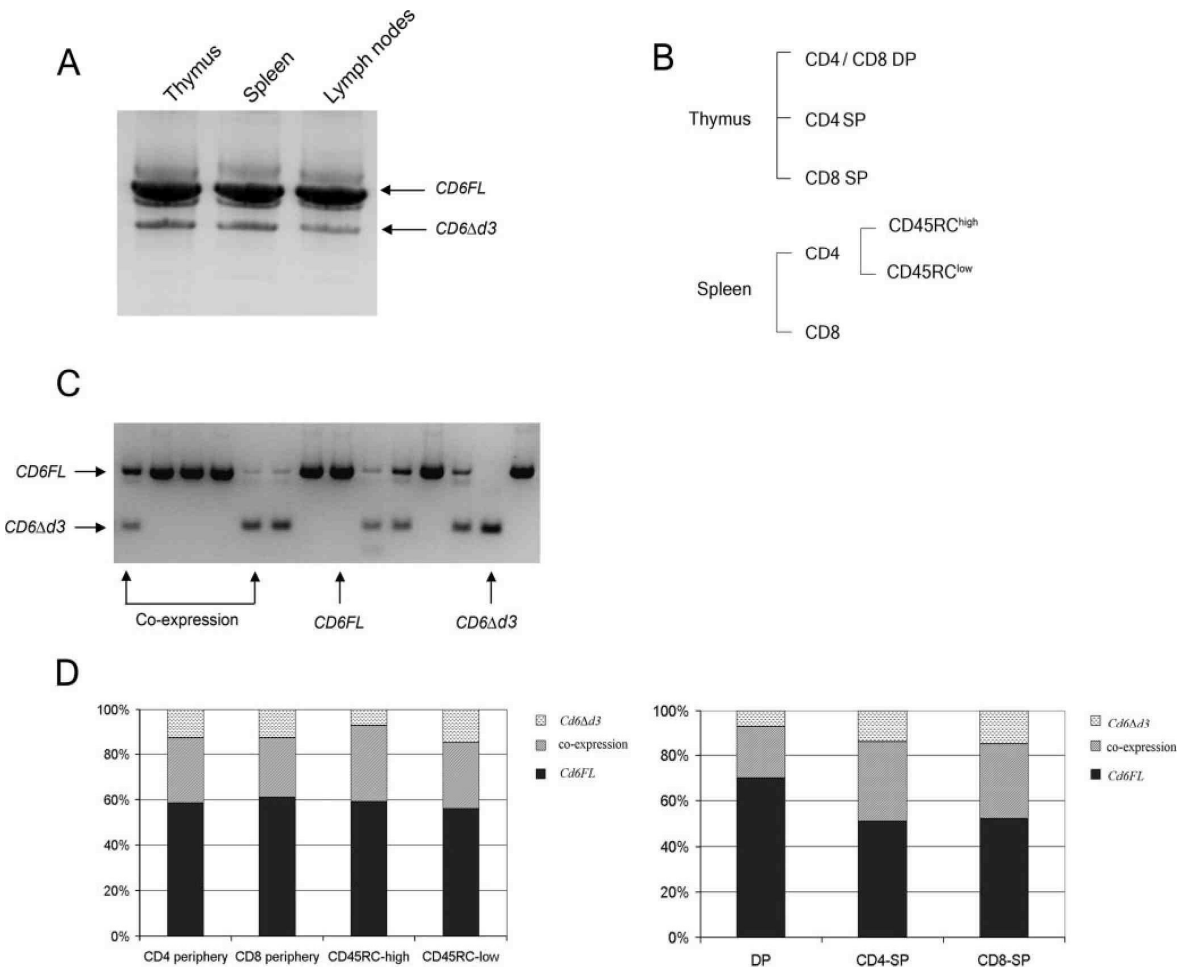



**Figure 4.** Expression of *Cd6* mRNA isoforms. *A,* RT-PCR analysis of the expression of *Cd6* mRNA in lymphoid organs. Total RNA was isolated from thymocytes, lymph nodes, and splenocytes, and reverse transcribed. PCR was performed amplifying the sequence between exons 1 and 7. Expression of *Cd6FL (upper band)* and *Cd6Δd3 (lower band)* was detected in all lymphoid tissues. *B.* Individual cells from the population indicated were sorted: CD4/CD8 DP, CD4 SP, and CD8 SP thymocytes; and CD4 and CD8 mature T cells from spleen. CD4 T cells were further separated into $CD45RC^{high}$ and $CD45RC^{low}$ subpopulations, associated with a naive and memory phenotype, respectively. *C,* Example of expression of the two different CD6 isoforms, *Cd6FL* and *Cd6Δd3,* by individual cells. Results shown are of $CD4^{+}CD8^{-}CD3^{+}$ thymocytes. Coexpression was considered in individual cells where both isoforms could be detected, as illustrated. *D,* Frequency of *Cd6* mRNA expression in sorted populations from the periphery *(left panel)* and thymus *(right panel).* Over 40 individual cells were considered for each population. All sorted populations were gated on $CD6^{high}$-expressing cells.

Nearly 40% of total CD4 or CD8 T cells expressed *Cd6Δd3* at detectable levels (Fig. *4D, left panel).* In addition, $CD4^{+}CD45RC^{high}$ and $CD4^{+}CD45RC^{low}$ splenocytes, which have been associated with a naive and memory phenotype, respectively, showed no significant variation in the percentage of cells expressing *Cd6Δd3* (Fig. *4D, left panel),* although the

ratio between the number of cells expressing only *Cd6*Δ*d3* and cells where coexpression was observed was the highest overall in memory cells and the lowest in naive cells. As distinct from mature T cells, levels of *Cd6*Δ*d3* expression fluctuated noticeably between different thymocyte populations. *Cd6*Δ*d3* was least abundant in double-positive (DP) thymocytes, being expressed in just 30% of the cells (Fig. *4D, right panel).* By contrast, nearly 50% of single-positive (SP) CD4 or CD8 thymocytes expressed *Cd6*Δ*d3,* and no differences were registered between these two subpopulations.

### 3.4.5 Cell activation increases rat CD6Δd3 expression

We next analyzed the pattern of expression of rat CD6 isoforms upon cell activation. Activated T cells were generated by incubating rat splenocytes with anti-TCR plus anti-CD28 mAb over 3 days. The percentage of $CD4^+$ T cells with an activated phenotype, as determined by OX40 expression [43], increased from 20 to 91% (Fig. 5*A*). $CD4^+OX40^+$ cells were sorted as individual cells and compared with the nonactivated phenotype. RT-PCR analysis of individual cells revealed a clear modification in the pattern of expression of *Cd6* isoforms following activation, with an increase in the number of cells coexpressing both isoforms (Fig. *5B).* The relative levels of CD4 T cells expressing the *Cd6*Δ*d3* mRNA increased significantly from 42 to 86% upon stimulation (Fig. 5*C*). Analysis of CD6 expression at the protein level was also performed by immunoblotting. Two isoforms of CD6 with molecular masses of ~130 and 122 kDa (indicated by dashed arrows) were clearly detected in resting splenocytes. These two isoforms should be products of alternative splicing, but still retain domain 3, given that the size is very close to that displayed by full-length rat CD6 in COS7 cells (126 kDa), whereas the CD6Δd3 mutant expressed in COS7 cells had a molecular mass of 112 kDa (see Fig. 2). Splenocytes were stimulated with TCR and CD28 mAb, and after 72 h cells were collected, lysed with detergent, and CD6 was immunoprecipitated and detected by immunoblotting. Interestingly, after 72 h of activation two smaller isoforms of 106 and 99 kDa were expressed (Fig. *5D,* solid arrows). It is plausible that these new isoforms correspond to protein products missing domain 3.

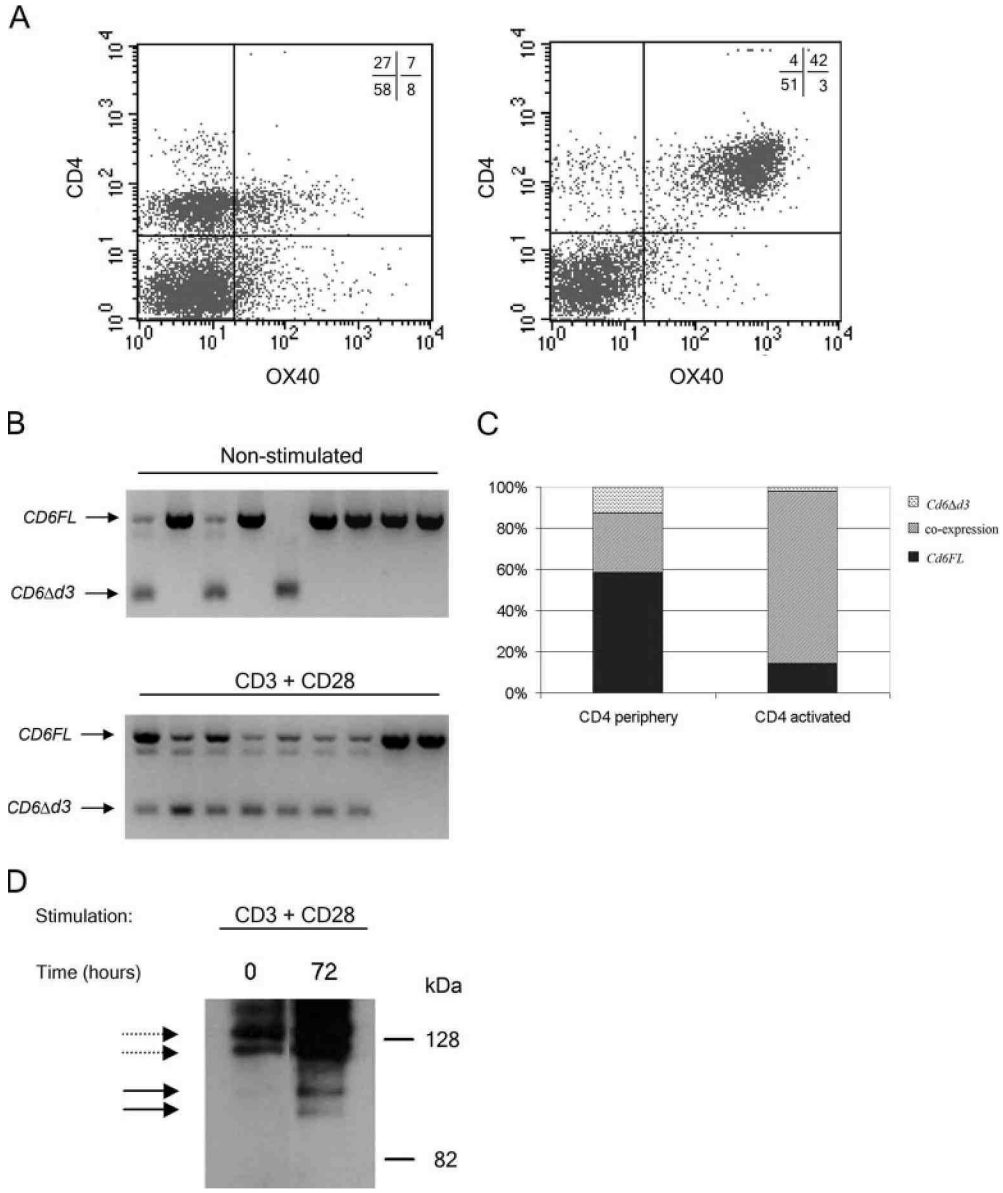



**Figure 5.** CD6Δd3 expression is up-regulated upon activation. *A,* Rat spleen cells were activated in vitro via TCRα/β and CD28 for 72 h or left untreated. OX40 expression was analyzed by flow cytometry in $CD4^+$-resting cells *(left panel)* and at day 3 of activation *(right plot).* Individual $CD4^+OX40^+$-activated cells were sorted from the gated $CD6^{high}$ population *(upper right quadrant).* The percentage of cells in each quadrant is indicated in the *upper right. B,* RT-PCR performed on activated vs nonactivated individual cells sorted. Gel is only illustrative; over 40 cells were always considered for calculations. *C*, Percentage of activated $CD4^+OX40^+$ T cells vs nonactivated T cells expressing *Cd6FL, Cd6Δd3,* or showing coexpression. *D,* Rat splenocytes were activated by TCRα/β and CD28 mAb for 72 h or left untreated. After that time, cells were collected, lysed, and immunoprecipitated with OX52. CD6 was detected by Western blotting. Dashed arrows indicate high molecular mass CD6 isoforms, presumably containing domain 3 of CD6, and thick arrows indicate low molecular mass isoforms, suggestive of CD6 isoforms lacking domain 3.

### 3.4.6 T cell activation controls expression of the human SRCR domain 3 of CD6

We obtained from human PBMC, as well as from the Jurkat cell line E6.1 (data not shown), cDNAs coding for the full-length molecule and also several PCR products with sizes ranging from 2,000 down to 1,600 bp (Fig. 6*A*, *middle lane)*. We then tested for the existence of the CD6Δd3 isoform in human cells, and following the same strategy as for the rat CD6 gene, performed RT-PCR amplifying just the extracellular domain-coding sequences. A prominent band of 1,200 bp and also a 300 nt shorter product were clearly detected (Fig. 6A, right lane, compare with Fig. 4A).

Next, we gel-purified the cDNA fragments, subcloned them, and sequenced multiple clones. We could confirm that the message coding for the extracellular domain isoform CD6Δd3 (GenBank accession no. DQ786329), lacking exon 5, was present in both PBMC and E6.1 Jurkat cells. An additional mRNA species (GenBank accession no. DQ786330) was detected in the cells analyzed, lacking not only exon 5 but also exon 6, which codes for a linker between the membrane proximal SRCR domain and the transmembrane stretch (Fig. 6B).

The previous results suggested that, as in the rat, multiple CD6 isoforms coexist in human T cells. We compared the expression of the putative CD6 extracellular isoforms between resting and PHA-activated T cells. For detection of CD6, we used mAbs specific for CD6 domain 3, OX126, or CD6 domain 1, UMCD6 [22]. In purified resting T lymphocytes, both SRCR domains 1 and 3 of CD6 are expressed at similar levels, a result consistent with resting T cells expressing mostly CD6FL (Fig. 6*C*, *left panel*). In contrast, 3 days following stimulation with PHA, the expression of domain 3 was significantly down-modulated, compared with the relatively unchanged labeling of domain 1 (Fig. 6*C*, *right panel*). We have also analyzed the changes on CD6 isoform expression upon cell activation by immunoblotting. Nonactivated human T cells expressed a major CD6 species of 130 kDa. However, 3 days postactivation with PHA, an additional CD6 isoform with a molecular mass of 97 kDa was clearly detected by immunoblotting, whereas the expression of the larger CD6 species was decreased to a level equivalent to that of the smaller isoform (Fig. 6*D*). Together, the cytometry and Western blotting analysis suggest that, following activation of human T lymphocytes, the expression of full-length CD6 is partially down-regulated with the concomitant appearance of the CD6Δd3 isoform.

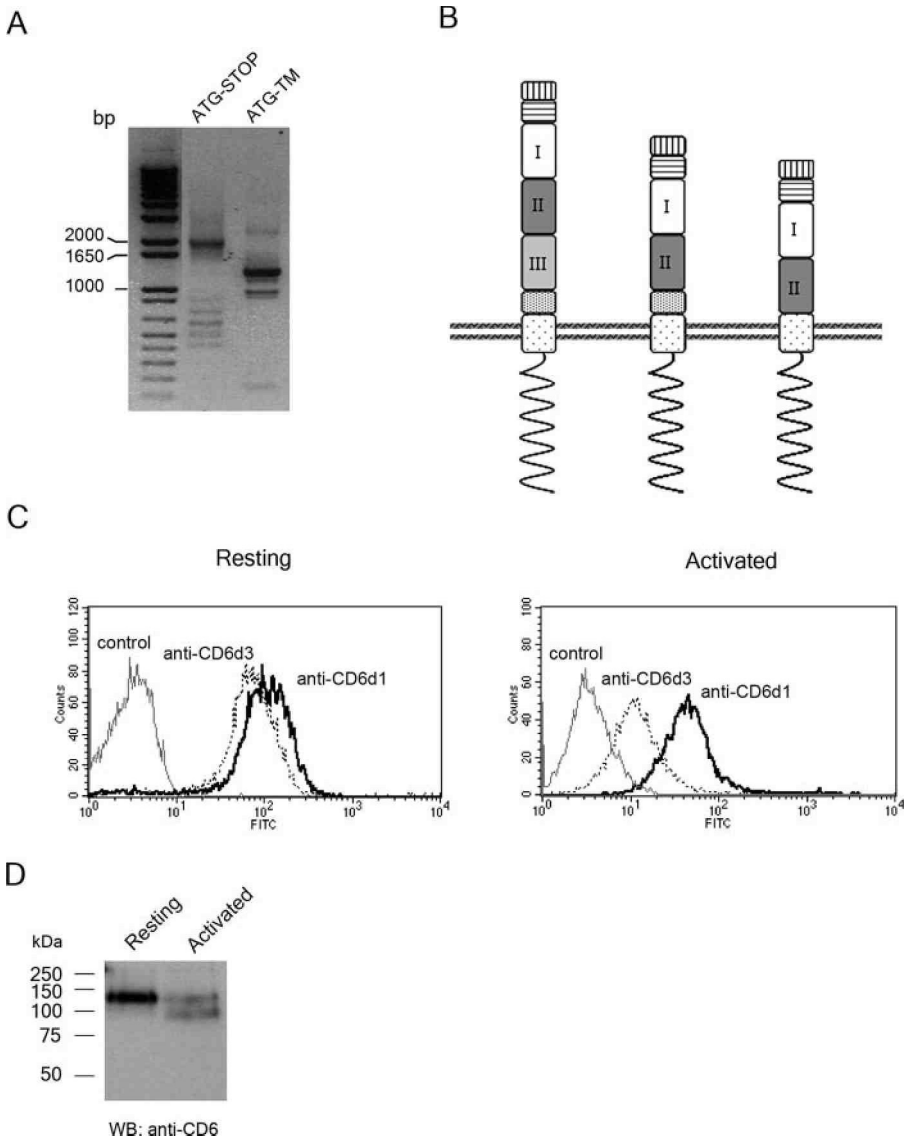



**Figure 6.** Increased expression of CD6Δd3 in human cells, upon activation. *A,* Total RNA from human PBMC was used for RT-PCR and amplified from the ATG up to the transmembrane region (TM) or the STOP codon. The cDNA products were analyzed on gels, isolated, and sequenced. The *middle lane* shows the amplification of the full-length cDNA, clearly visible at 2,071 bp, and additional shorter products between 2,000 and 1,600 bp. As can be seen on the *right lane,* products of amplification of the extracellular region were obtained, including the full-length isoform of 1,200 bp and a smaller band of 900 bp. *B,* Schematic representation of the extracellular isoforms of human CD6 protein deduced from sequencing of the RT-PCR products obtained from human PBMC and E6.1 Jurkat cells. The full-length transcript was the most abundant in both PBMC and Jurkat E6.1 cells. The CD6Δd3 isoform excluding only exon 5 and also a similar isoform excluding additionally exon 6 were also recurrent, as evaluated by the frequency in the number of clones sequenced. *C*, Human primary T cells isolated from peripheral blood, using the RosetteSep human T cell enrichment mixture, were analyzed by flow cytometry for the expression of CD6 extracellular isoforms by using specific Abs recognizing either domain 1, UMCD6, or domain 3, OX126. The

expression is compared with the fluorescence of the control secondary Ab FITC conjugated *(left panel).* After 3 days of stimulation with PHA, a significant decrease in the level of expression of the isoform lacking domain 3 could be detected, as can be seen by using the same Abs *(right panel).* PHA-activated cells were gated based on the expression of the activation marker CD71 (data not shown). *D,* The expression of CD6 in resting cells, and in cells 3 days postactivation with PHA, was analyzed by Western blotting with anti-CD6 MEM-98 mAb. A decrease in the level of the higher molecular mass isoform and the appearance of a lower molecular mass species can be seen after activation.

### 3.4.7 Human CD6 targeting to the IS: analysis of binding to CD166

We proceeded to confirm that human CD6 isoforms behaved similarly to those analyzed in rat, regarding translocation to the IS upon Ag recognition. Human T lymphocytes were induced to express full-length human CD6 (CD6FL), the CD6Δd3 isoform, or the CD6CY5 mutant, all fused to GFP. Following incubation of T cells with superantigen-loaded Raji cells, which expressed endogenous CD166 at high levels on the surface (data not shown), conjugate formation and CD6 translocation to the synapse was evaluated in all conditions. Both CD6FL and CD6CY5 localized very efficiently to the IS in ~80% of total conjugates, whereas CD6Δd3 was typically dispersed throughout the cell surface (Fig. 7, A and B).

To test whether nonengineered endogenous CD6 expressed in T lymphocytes was still capable of targeting to the synapse, and that this effect was due to the binding to endogenous Raji-expressed CD166, we evaluated, through immunofluorescence, the localization of CD6 in T:Raji interfaces using blocking, as well as non-blocking Abs. Characteristically, CD6 confined to the synapse in 75% of unblocked T cell:Raji conjugates, a figure that did not significantly change when T cells had been previously incubated with UMCD6, an Ab recognizing domain 1 of CD6, and not able to block CD6-CD166 interactions (Fig. 7, *C* and *D).* However, when T cells had been incubated with the blocking, anti-CD6 domain 3, mAb OX126, CD6 localization at the synapse dropped dramatically to residual levels (Fig. 7, *C* and *D).* Similarly, previous incubation of Raji with the CD166 mAb, described to obstruct the interaction with CD6 [37], resulted in the noticeable reduction of the translocation of CD6 to the synapse (Fig. 7, *C* and *D),* in agreement with a previous study using blocking CD166 Abs in T cell-dendritic cell conjugates [15]. Taken together, the results demonstrate that the direct interaction between CD166 and the SRCR domain 3 of CD6 is the driving force for the translocation of CD6 to the IS.

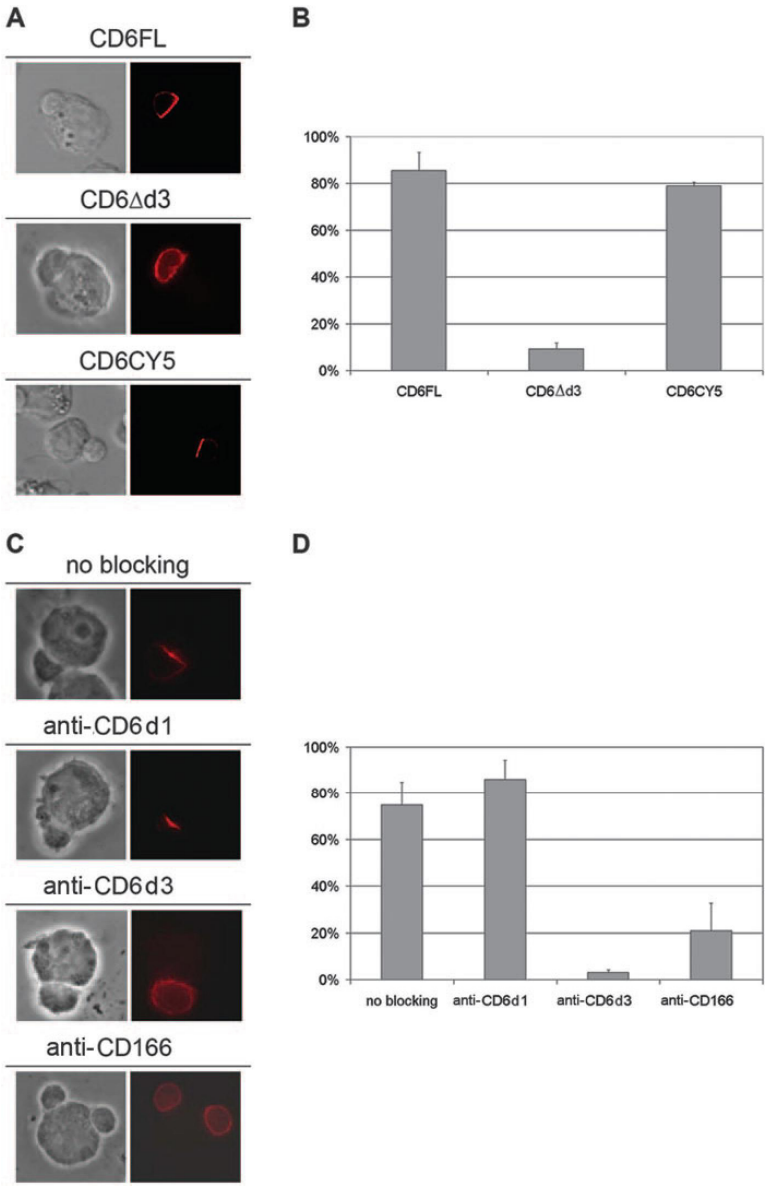



**Figure 7**. Human CD6 colocalizes at the synapse depending on the binding of the CD6 SRCR domain 3 to endogenous CD166 expressed at the surface of Raji cells. *A,* T cells expressing CD6FL-GFP, CD6Δd3-GFP, or CD6CY5-GFP (shown in red) were incubated with Raji B cells prepulsed with 1 μg/ml superantigen mix and analyzed for localization at the IS. *B,* Bar chart representing CD6 accumulation at the IS in T cells expressing the different CD6 isoforms. Results are from three independent experiments. *C,* Ab-blocking interference of CD6-ligand interaction on the localization of CD6 at the IS. Before incubation with superantigen-pulsed Raji B cells, T lymphocytes were incubated with the mAbs UMCD6, recognizing CD6 domain 1 (anti-CD6d1), or OX126, recognizing CD6 domain 3 (anti-CD6d3), or left untreated. Alternatively, Raji B cells were treated with anti-CD166 mAb (anti-CD166). The localization of CD6 was performed by immunolabeling with UMCD6-FITC, or with RAM-FITC in the case of blocking with anti-CD6d3. *D,* Quantification of the number of cell conjugates displaying CD6 at the IS.

### 3.5 Discussion

The great majority of mammalian genes yield multiple mRNA transcripts arising from diverse promoter selection, alternative splicing, and/or differential polyadenylation [44]. Despite the frequency and potential impact of this phenomenon, particularly relevant in the immune system, the cases in which distinct functional properties have been assigned to different isoforms of the same molecule are scarce. In T lymphocytes, just a few examples of naturally occurring alternatively spliced-encoded isoforms of transmembrane proteins have been reported, and only in three cases with clear distinct functional consequences: CTLA4 and CD95 can become transmembrane molecules instead of being secreted [45, 46], as a consequence of the inclusion of membrane-spanning domains following cell stimulation; and CD45, upon T cell differentiation, is produced with a shorter N-terminal extracellular domain, which increases the dimerization capacity of the molecule [47]. Alongside this general trend, multiple isoforms resulting from alternative splicing of cytoplasmic domain-coding exons have been described for CD6, but with no distinct functions assigned [18, 28-30]. In this study, we describe a rare example of a functional consequence resulting from alternative splicing in molecules of the immune system: the localization of CD6 with respect to the IS depends on the regulated expression of the CD166 binding domain by means of alternative mRNA splicing.

Targeting of CD6 to the synapse can be driven by simple lateral diffusion and does not require cytoskeletal reorganization, because deletion of the cytoplasmic tail did not affect the ability of CD6 to localize to the synapse. Therefore, the positioning of CD6 within the synapse must be largely determined by molecular interactions established with the contacting cell. Both human and rat CD6 molecules targeted very efficiently to the IS when expressing the CD166 binding domain, provided that the APCs were equally expressing CD166. However, when using T cells expressing CD6Δd3, synaptic localization of that isoform could still be attained in a small percentage of conjugates. A putative role for domain 2 of CD6, now substituting the positioning of domain 3 in CD6Δd3, or even for the membrane-juxtaposed stalk region, could be considered, given the fact that previous studies had suggested a minor participation of these domains in the binding to CD166 [22, 23]. Nevertheless, it is the presence of domain 3 that largely determines CD6 synaptic localization, and thus regulation of its expression is the key event establishing the positioning of CD6 upon conjugate formation and T cell activation.

The mode of action of CD6 appears to be significantly different from that of other accessory molecules that influence signaling at or near the IS. CD2 binding to its ligand CD58 (CD48 in rodents) contributes to enhanced signaling, because it associates with intracellular-positive mediators [48]. CD28 and CTLA-4 have devised a scheme whereby

sequential expression of each molecule, combined with binding to one of the alternative ligands, CD80 and CD86 (themselves also sequentially expressed during T cell-APC interactions), drives responses from costimulation to inhibition [49]. Differences in the affinity and avidity of binding determine the selective recruitment of CD28 or CTLA-4 to the IS upon recognition of CD86 or CD80 [50].

Meanwhile CD6, which was reported to deliver costimulatory signals as strongly as CD28 [15], mimics CD28 distribution with respect to synaptic localization, in that it is recruited to the IS at the onset of activation, and, according to the present study, is excluded from the cellular interface at later stages. However, it may display this same pattern of localization through a completely different mechanism: expressing the SRCR domain 3, CD6 is directed to the synapse where it can control signaling; choosing not to express the SRCR domain 3, it is no longer restricted to the cellular interface and its regulatory function may be diluted.

The reason why CD6 does not simply switch off its expression is not immediately evident. However, the existence of an alternative ligand for CD6 raises new perspectives for its overall function [51]. If the new ligand can interact with a different part of CD6, switching from full-length to Δd3 may allow CD6 to shift from the synapse established with the APC to either an interaction with a second adjacent cell or again to the initial interface, provided that the second ligand is present. Differential molecular interactions could then modulate the behavior of CD6.

The apparent steadiness in expression of the alternative CD6 mRNAs in different mature subpopulations may suggest that CD6Δd3 can define small subsets of thymocytes and mature T cells; however, the switch to the expression of the shorter isoform observed upon stimulation of T cells is undoubtedly a consequence or a product of activation. In the resting state, the majority of the cells express mainly the full-length CD6 form; upon productive T cell stimulation, there is a partial substitution of the full-length isoform by a substantial number of CD6 molecules per cell that no longer express the CD166 binding domain and thus are not restricted to the IS. This type of regulation of splicing is not unique, because it has long been known to control the expression of CD45 isoforms [52, 53]. The novel CD6 isoform reported in this study seems to have a more obvious function because it disables the interaction of the protein with its ligand. Productive TCR recognition of Ag may signal for the shorter CD6 isoform to be produced, and this response may reduce the activity of CD6 at the synapse, possibly inducing a different behavior.

The expression of the CD6FL isoform seems to be highly favored in the DP stage in the thymus. Previous observations suggest that CD6 can be involved in positive selection, where it correlates with the expression of CD69 in DP thymocytes [54]. Moreover, an inverse correlation between thymocyte CD6 expression and the rate of

apoptosis has been demonstrated. Our results may be indicative of a mechanism of regulation where the expression of CD6FL capable of interacting with the ligand CD166, expressed by thymic epithelial cells, is favored at the DP stage and bypassed later on during thymic selection

## Acknowledgments

We thank Simon Davis (Weatherall Institute of Molecular Medicine, University of Oxford, U.K.) and Neil Barclay (Sir William Dunn School of Pathology, University of Oxford, U.K.) for helpful discussions and critical reading of the manuscript.

## 3.6 References

1. Shaw, A.S. and M.L. Dustin, Making the T cell receptor go the distance: a topological view of T cell activation. *Immunity*, 1997. **6**: p. 361-369.
2. Monks, C.R., et al., Three-dimensional segregation of supramolecular activation clusters in T cells. *Nature*, 1998. **395**: p. 82-86.
3. Grakoui, A., et al., The immunological synapse: a molecular machine controlling T cell activation. *Science*, 1999. **285**: p. 221-227.
4. Bromley, S.K., et al., The immunological synapse. *Annu. Rev. Immunol.*, 2001. **19**: p. 375-396.
5. Bromley, S.K., et al., The immunological synapse and CD28-CD80 interactions. *Nat. Immunol.*, 2001. **2**: p. 1159-1166.
6. Davis, S.J. and P.A. van der Merwe, The structure and ligand interactions of CD2: implications for T-cell function. *Immunol. Today*, 1996. **17**: p. 177-187.
7. Aruffo, A., et al., The lymphocyte glycoprotein CD6 contains a repeated domain structure characteristic of a new family of cell surface and secreted proteins *J. Exp. Med.*, 1991. **174**: p. 949-952.
8. Gangemi, R.M., et al., Anti-T12, an anti-CD6 monoclonal antibody, can activate human T lymphocytes. *J. Immunol.*, 1989. **143**(8): p. 2439-2447.
9. Bott, C.M., et al., Activation of human T cells through CD6: functional effects of a novel anti-CD6 monoclonal antibody and definition of four epitopes of the CD6 glycoprotein. *Int. Immunol.*, 1993. **5**(7): p. 783-792.

10. Osorio, L.M., et al., The anti-CD6 mAb, IOR-T1, defined a new epitope on the human CD6 molecule that induces greater responsiveness in T cell receptor/CD3-mediated T cell proliferation. *Cell. Immunol.*, 1994 **154**: p. 123-133.
11. Rasmussen, R.A., et al., Isolation and characterization of CD6- T cells from peripheral blood. *J. Immunol.*, 1994. **152**(2): p. 527-536.
12. Patel, D.D., et al., Identification and characterization of a 100-kD ligand for CD6 on human thymic epithelial cells. *J. Exp. Med.*, 1995. **181**(4): p. 1563-1568.
13. Gimferrer, I., et al., Relevance of CD6-mediated interactions in T cell activation and proliferation. *J. Immunol.*, 2004. **173**: p. 2262-2270
14. Hassan, N.J., et al., Optimal T cell activation requires the engagement of CD6 and CD166. *Eur. J. Immunol.*, 2004. **34**: p. 930-940
15. Zimmerman, A.W., et al., Long-term engagement of CD6 and ALCAM is essential for T-cell proliferation induced by dendritic cells. *Blood*, 2006. **107**(8): p. 3212-3220.
16. Wee, S., et al., Tyrosine phosphorylation of CD6 by stimulation of CD3: augmentation by the CD4 and CD2 coreceptors. *J. Exp. Med.*, 1993. **177**(1): p. 219-223.
17. Hassan, N.J., et al., CD6 regulates T-cell responses through activation-dependent recruitment of the positive regulator SLP-76. *Mol. Cell. Biol.*, 2006. **26**: p. 6727-6738.
18. Robinson, W.H., et al., Human CD6 possesses a large, alternatively spliced cytoplasmic domain. *Eur. J. Immunol.*, 1995. **25**: p. 2765-2769.
19. Castro, M.A.A., et al., OX52 is the rat homologue of CD6: evidence for an effector function in the regulation of CD5 phosphorylation. *J. Leukocyte Biol.*, 2003. **73**: p. 183-190.
20. Gimferrer, I., et al., The accessory molecules CD5 and CD6 associate on the membrane of lymphoid T cells. *J. Biol. Chem.*, 2003. **278**: p. 8564–8571.
21. Aruffo, A., et al., CD6-ligand interactions: a paradigm for SRCR domain function? *Immunol. Today*, 1997. **18**: p. 498-504
22. Bowen, M.A., et al., The amino-terminal immunoglobulin-like domain of activated leukocyte cell adhesion molecule binds specifically to the membrane-proximal scavenger receptor cysteine-rich domain of CD6 with a 1:1 stoichiometry. *J. Biol. Chem.*, 1996. **29**: p. 17390-17396.
23. Whitney, G.S., et al., The membrane-proximal scavenger receptor cysteine-rich domain of CD6 contains the activated leukocyte cell adhesion molecule binding site. *J. Biol. Chem.*, 1995. **270**: p. 18187-18190.

24. Hohenester, E., et al., Crystal structure of a scavenger receptor cysteine-rich domain sheds light on an ancient superfamily *Nat. Struct. Biol.*, 1999. **6**: p. 228-232.
25. Davis, S.J., et al., The nature of molecular recognition by T cells. *Nat. Immunol.*, 2003. **4**(3): p. 217-224.
26. Dustin, M.L., et al., Low affinity interaction of human or rat T cell adhesion molecule CD2 with its ligand aligns adhering membranes to achieve high physiological affinity. *J. Biol. Chem.*, 1997. **272**: p. 30889-30898.
27. Evans, E.J., et al., Crystal structure and binding properties of the CD2 and CD244 (2B4)-binding protein, CD48. *J. Biol. Chem.*, 2006. **281**: p. 29309-29320.
28. Robinson, W.H., et al., Identification of a mouse protein homologous to the human CD6 T cell surface protein and sequence of the corresponding cDNA. *J. Immunol.*, 1995. **155**: p. 4739-4748.
29. Whitney, G., et al., Cloning and characterization of murine CD6. *Mol. Immunol*, 1995. **32**: p. 89-92.
30. Bowen, M.A., et al., Structure and chromosomal location of the human CD6 gene: detection of five human CD6 isoforms. *J. Immunol.*, 1997. **158**( 3 ): p. 1149-1156.
31. Gluzman, T., SV40-transformed simian cells support the replication of early SV40 mutants. *Cell*, 1981. **23**: p. 175-182.
32. Epstein, M.A., et al., Morphological and virological investigations on cultured Burkitt tumor lymphoblasts (strain Raji). *J. Natl. Cancer Inst.*, 1966. **37**: p. 547-559.
33. Robinson, A.P., et al., MRC OX-52: a rat T-cell antigen. *Immunology*, 1986. **57**: p. 527-531.
34. Hünig, T., et al., A monoclonal antibody to a constant determinant of the rat T cell antigen receptor that induces T cell activation. Differential reactivity with subsets of immature and mature T lymphocytes. *J. Exp. Med.*, 1989. **169**: p. 73-86.
35. Tacke, M., et al., Cellular distribution and costimulatory function of rat CD28. Regulated expression during thymocyte maturation and induction of cyclosporin A sensitivity of costimulated T cell responses by phorbol ester. *J. Immunol.*, 1995. **154**: p. 5121-5127.
36. Bazil, V., et al., Monoclonal antibodies against human leucocyte antigens. III. Antibodies against CD45R, CD6, CD44 and two newly described broadly expressed glycoproteins MEM-53 and MEM-102. *Folia Biol*, 1989. **35**: p. 289-297.
37. mKishimoto, T., et al., Leukocyte Typing VI: White cell differentiation antigens. *Garland Publishing, London*, 1997.
38. Mizushima, S. and S. Nagata, pEF-BOS, a powerful mammalian expression vector. *Nucleic Acids Res.*, 1990. **18**: p. 5322.

39. Castro, M.A.A., et al., CD2 physically associates with CD5 in rat T lymphocytes with the involvement of both extracellular and intracellular domains. *Eur. J. Immunol.*, 2002. **32**: p. 1509-1518.
40. Carmo, A.M., et al., CD2 and CD3 associate independently with CD5 and differentially regulate signaling through CD5 in Jurkat T cells. *J. Immunol.*, 1999. **163**: p. 4238-4245.
41. Peixoto, A., et al., Quantification of multiple gene expression in individual cells. *Genome Res.*, 2004. **14**: p. 1938-1947.
42. Bowen, M.A., et al., Cell surface receptors and their ligands: in vitro analysis of CD6-CD166 interactions. *Proteins*, 2000. **40**: p. 420-428.
43. Paterson, D.J., et al., Antigens of activated rat T lymphocytes including a molecule of 50,000 Mr detected only on CD4 positive T blasts. *Mol. Immunol.*, 1987. **24**: p. 1281-1290.
44. Johnson, J.M., et al., Genome-wide survey of Human alternative pre-mRNA splicing with exon junction microarrays. *Science*, 2003. **302**: p. 2141-2144.
45. Cheng, J., et al., Protection from Fas-mediated apoptosis by a soluble form of the Fas molecule. *Science*, 1994. **263**: p. 1759-1762.
46. Magistrelli, G., et al., A soluble form of CTLA-4 generated by alternative splicing is expressed by nonstimulated human T cells. *Eur. J. Immunol.*, 1999. **29**: p. 3596-3602.
47. Xu, Z. and A. Weiss, Negative regulation of CD45 by differential homodimerization of the alternative spliced isoforms *Nat. Immunol.*, 2002. **3**: p. 764-771.
48. Carmo, A.M., et al., Physical association of the cytoplasmic domain of CD2 with the tyrosine kinases p56lck and p59fyn. *Eur. J. Immunol.*, 1993. **23**: p. 2196-2201.
49. van der Merwe, P.A. and S.J. Davis, Molecular interactions mediating T cell antigen recognition. *Annu. Rev. Immunol.*, 2003. **21**: p. 659–684.
50. Pentcheva-Hoang, T., et al., B7-1 and B7-2 selectively recruit CTLA-4 and CD28 to the immunological synapse. *Immunity*, 2004. **21**: p. 401-413.
51. Saifullah, M.K., et al., Expression and characterization of a novel CD6 ligand in cells derived from joint and epithelial tissues. *J. Immunol.*, 2004. **173**(10): p. 6125-6133.
52. Ralph, S.J., et al., Structural variants of human T200 glycoprotein (leukocyte-common antigen). *EMBO J.*, 1987. **6**: p. 1251-1257.
53. Streuli, M., et al., Differential usage of three exons generates at least five different mRNAs encoding human leukocyte common antigens *J. Exp. Med.*, 1987. **166**: p. 1548-1566.

54. Singer, N.G., et al., CD6: expression during development, apoptosis and selection of human and mouse thymocytes. *Int. Immunol.*, 2002. **14**(6): p. 585-597.

# 4. CD6 attenuates calcium signals on the onset of T cell activation

**Marta I. Oliveira, Stéphanie Fabre, Mónica A. A. Castro, Raquel J. Nunes, Georges Bismuth and Alexandre M. Carmo**

## 4.1 Abstract

The early T lineage glycoprotein CD6 is considered to have a role in thymocyte selection and T cell activation. Here we demonstrate that CD6 can restrain the activation of T cells interacting with APC. Measuring calcium mobilization in single cells responding to Ag, we found that T cells expressing rat CD6 reacted significantly less to APC challenge than cells not expressing exogenous CD6. When CD6 was expressed as a cytoplasmic deletion mutant, calcium down modulation was abrogated, clearly assigning the inhibitory properties to the cytoplasmic domain. However, membrane localization of CD6 did not influence signaling, no differences being recorded whether CD6 was dispersed at the plasma membrane or targeted to the immunological synapse and contacting its natural ligand CD166 on APC. Thus, CD6 can be a signaling attenuator, whose function may depend on levels of expression, but not of restricted accumulation within the immunological synapse.

## 4.2 Introduction

CD6 is a 100-130-kDa integral membrane protein that is expressed on peripheral T lymphocytes and medullary thymocytes [1]. CD6 has been regarded as a co-stimulatory molecule since antibody-mediated CD6 cross-linking can potentiate proliferative T cell responses [2-4]. Moreover, a minor population of CD6 negative T cells displayed lower alloreactivity in mixed leukocyte reactions than normal $CD6^+$ T cell populations [5], and also soluble monomeric CD6 present in Ag-primed MLR inhibited specific T cell responses [6, 7]. CD6 could additionally play a role in thymocyte maturation, as CD6 antibodies have been shown to partially block the adhesion of thymocytes to thymic epithelial cells [8]. The expression of CD6 on immature thymocytes correlates nevertheless with resistance to apoptosis, implying some inhibitory signaling properties for CD6 during selection [9].

Upon TCR/CD3 engagement CD6 becomes phosphorylated on tyrosine residues suggesting that interactions with SH2 domain-containing intracellular mediators may occur [10]. The unusual long cytoplasmic domain of CD6 additionally contains multiple potential binding sites for SH3 domain-containing signaling effectors [11]. The rat homologue of CD6, also known as OX52, has indeed the capacity of associating with protein tyrosine kinases of different families, such as the Src-family kinases Lck and Fyn, ZAP-70 of the Syk family, and the Tec-family kinase Itk [12]. However, the signaling pathways triggered by CD6 stimulation are still poorly understood and await further clarification.

CD6 has additionally been shown to associate at the surface of T cells with CD3 [6] and with the structurally related receptor CD5 [12], an inhibitor of T cell responses [13, 14]. CD5 and CD6 share the pattern of expression during ontogeny, and a possibility of overlapping functions on repertoire selection has been previously suggested [15]. Stimulation of rat T cells with CD6 antibodies enhanced the tyrosine phosphorylation of CD5 [12], thus hinting that CD6 triggering could increase the inhibitory function of CD5, similarly to the effect exerted on CD5 by CD2 [16, 17]. However, it is possible that the divergent cytoplasmic domains of CD6 and CD5 and the quite distinct molecular associations with activating versus inhibitory effector enzymes are indicative of separate roles of the two molecules in T cell physiology.

The molecular basis of the interaction between CD6 and the extracellular physiological ligand, CD166, has been comprehensively investigated [18]. CD166 is expressed on cortical and medullary thymic epithelial cells, monocytes and also transiently on other activated leukocytes, indicating that the contact between CD6 and CD166 may be particularly relevant at certain stages of cellular maturation, activation and immune responses [7, 19]. Recently, CD6 has been reported to accumulate at the immunological synapse in T cell-APC conjugates [6]. Using a model of human T lymphocytes expressing exogenous wild-type and mutant rat CD6, we have ascertained herein that CD6 can have a modulatory role on T cell responses, dependently of its cytoplasmic domain but not of its interaction with its ligand.

## 4.3 Materials and Methods

### 4.3.1 Plasmid constructs

Rat CD6 cDNA was amplified from the original clone rCD6/pCR2.1-TOPO [12] by PCR using 5'-GCACTAAGCTTGGGCAGGCGTGAGTAGCAGT-3' as forward primer, and 5'-GCAGAATTCGAAGCTTGGCTGCTCCAATGTCATCG-3' as the reverse primer. The PCR product was then cloned into pEYFP-N1 vector (Clontech Laboratories, Palo Alto, CA) in frame with the N-terminal sequence of the yellow fluorescent protein (YFP), in the *Hind*III restriction sites included in the primers. The sequence of the construct rCD6/pEYFP-N1 was confirmed by de-deoxy sequencing. A cytoplasmic deletion mutant of rat CD6 fused to YFP was produced by PCR from rCD6/pCR2.1-TOPO using as forward primer 5'-GCACTAAGCTTGGGCAGGCGTGAGTAGCAGT-3' and as reverse primer 5'-CTACTAAAGCTTTTGTCCTTTGGCTTTCAAGAG-3', terminating just after the fifth amino

acid of the cytoplasmic domain. The PCR product was cloned into the *Hind*III restriction site of the pEYFP-N1 vector to produce rCD6CY5/pEYFP-N1.

Rat CD166 cDNA was obtained from total RNA isolated from Lewis male rat lungs and reverse transcribed using the gene specific primer 5'-CCAGGACAGCTTAGTAGGAT-3'. Amplification of the full-length molecule using as forward primer 5'-TAGTAGAAGCTTCTAGGAGGAGGAATATGGC-3' and reverse primer 5'- CTACTAGAATTCGGCTTCTGTTTTGTGATTGT-3' followed by cloning into the *Hind*III - *Pst*I restriction site of the pECFP-N2 vector handled rCD166/pECFP-N2.

### 4.3.2 Cells and transfections

Human primary T cells were isolated from peripheral blood by centrifugation on a Ficoll gradient followed by negative depletion on magnetic beads (T-cell negative isolation kit, Dynal Biotech, Compiègne, France). The cell line Raji [20] was maintained in RPMI 1640 supplemented with 10% FCS, 1 mM sodium pyruvate, 2 mM L-glutamine, penicillin G (50 U/ml) and streptomycin (50 μg/ml).

Transient transfections of primary T lymphocytes ($5 \times 10^6$ cells) were performed with 10 μg of rCD6/pEYFP-N1 or rCD6CY5/pEYFP-N1 plasmids using the Human T cell Nucleofector kit (Amaxa), according to the manufacturer's instructions, and T cells were used 24 h post-transfection. Transfection efficiency varied between 30 to 50%, allowing for the analysis in the same field of negative and positive cells for a given molecule. Transfection of Raji B cells was performed as follows: $10 \times 10^6$ cells in RMPI supplemented with 10% FCS were centrifuged, resuspended in 900 μl of pre-warm complete medium, mixed with 20 μg of rCD166/pECFP-N2 plasmid and transferred into a Gene-Pulse cuvette (Bio-Rad, Hercules, CA). Electroporation was performed in a Bio-Rad Gene Pulser II electroporator (Hercules, CA) at 950 μF and 260 V. Cells were maintained in complete medium at 37ºC and used 48 h after transfection.

### 4.3.3 Flow cytometry

Flow cytometry was performed as described previously [16]. Monoclonal antibodies used were MEM-98 [21], recognizing human CD6, and UCHT1 [22], recognizing human CD3.

### 4.3.4 Conjugate formation and fluorescence analysis

Raji B cells were incubated with a mix of superAgs (rSEE, SEA, SEB and SEC3, 200 ng/ml each) and plated onto poly-D-lysine-coated glass coverslips for 30 min at 37ºC. T cells were added to APCs, and then incubated at 37ºC for 45 min. Cells were then fixed with 4% paraformaldehyde in PBS for 10 min and after several washes, incubated in PBS. Fluorescence and transmission light images were acquired on an Eclipse TE300 inverted microscope (Nikon, Badhoevedorp, The Netherlands) equipped with a cooled CCD camera (CoolSNAPFx, Roper Scientific, Evry, France).

### 4.3.5 Calcium measurements

Raji cells were plated on glass coverslips mounted on 30 mm-Petri dishes and incubated for 30 min at 37°C with a mixture of superAgs. T cells were loaded for 20 min at 37°C with 1 mM Fura-2AM in 1 ml of Hepes buffer 10 mM, pH 7.5 containing 140 nM NaCl, 5 mM KCl, 1 mM $CaCl_2$, 0.5 mM $MgCl_2$, 1 mM $Na_2HPO_4$ and 1 mg/ml glucose. Cells were then washed and added to the APCs in a final volume of 200 µl. Transmitted light, YFP and intracellular calcium measurement images were acquired sequentially on an inverted microscope.

## 4.4 Results

### 4.4.1 Rat CD6 can down-modulate calcium signals in T cells interacting with APC

The use of primary T lymphocytes interacting with superantigen-loaded APC, and its transient genetic manipulation have proven to be useful tools in the determination of critical parameters for T cell activation [23]. To evaluate the role of the rat homologue of CD6 in T cell signaling, we transfected primary human T cells with a cDNA coding for rat CD6 fused to YFP (Fig. 1). Endogenous human CD6 was highly expressed, at comparable levels to CD3, and its expression was not affected by cell transfection procedures (Fig. 1a and b). The efficiency of transfection can be evaluated in Fig. 1c, where it is evident that a significant proportion of T lymphocytes expressed rat CD6. Following transfections with rat CD6 cDNA, intracellular calcium mobilization was measured in individual cells that interacted with antigen-loaded Raji cells. Strikingly, T cells that expressed exogenous CD6 were much less responsive to APC than were

untransfected T cells, as exemplified in Fig. 2a. Sixty percent of cells expressing CD6 did not respond to APC challenge, as compared to only thirty six percent of non-responding $CD6^-$ cells (Fig. 2b). Moreover, calcium increases registered in individual $CD6^+$ cells were lower than in untransfected cells, and much more transient with a strong reduction of the sustained phase of the response (Fig. 2c).

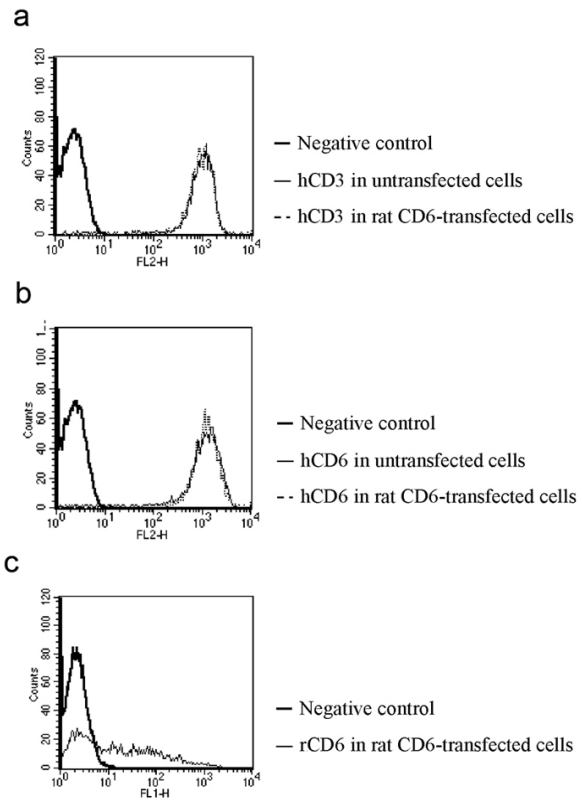



**Figure 1.** Expression of endogenous and exogenous CD6 in human T lymphocytes. Flow cytometric analysis of human CD3 **(a)**, and human CD6 **(b)** in purified T lymphocytes, before (thin line) and after transfection (dashed line) of rat CD6 cDNA. The negative control is shown as a thick line. **(c)** Expression of rat CD6 following cell transfection with a rat CD6 cDNA. Rat CD6 is detected as a CD6-YFP fusion protein (thin line).

### 4.4.2 The inhibitory role of CD6 does not depend on engagement to its ligand

An accumulation of CD6 at the immunological synapse (IS) has been recently reported in Jurkat cells [6], and as Raji cells express endogenous CD166 (data not shown), human CD6:CD166 interactions are likely to occur in T cell:Raji conjugates. However, in conjugates of rat $CD6^+$ cells interacting with Raji, rat CD6 was homogeneously distributed throughout the entire plasma membrane (Fig. 3a) indicating that probably rat CD6 does not interact with human CD166 and does not interfere with the binding of endogenous CD6 to human CD166 expressed in Raji cells. Given that in our system the T:APC cellular pairs were always kept constant and CD6:CD166 interactions were left undisturbed, any reduction in signaling should be attributed to a functional role of rat CD6 rather than to the disruption of the human CD6:CD166 ligation. Nevertheless, we raised the possibility that

rat CD6 could compete out the endogenous molecule for associations with intracellular molecules, and that the inhibitory effect of CD6 could be due to the sequestering of important signaling effectors from the immunological synapse, retained by rat CD6 at the cell periphery. We thus transfected Raji cells with a cDNA coding for rat CD166, and allowed for conjugate formation with $CD6^+$ T cells. Rat CD6 targeted very effectively to the immunological synapse only when T cells formed conjugates with CD166-expressing Raji cells (Fig. 3b). We then measured calcium mobilization in rat $CD6^+$ cells establishing contacts with Raji cells, expressing or not rat CD166. No differences in the registered profiles were observed, though, clearly indicating that the localization at the IS is not crucial for CD6 to down-modulate signalling (Fig. 4). This also excluded the possibility that rat CD6 inhibits T cell activation through the retention of signalling mediators away from the synapse.

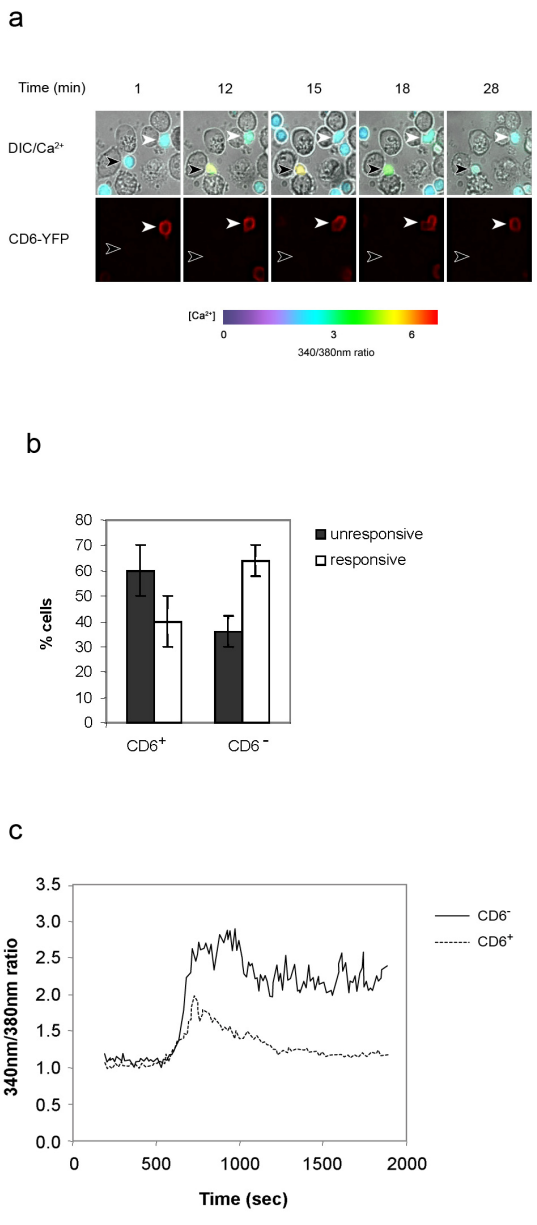



**Figure 2.** CD6 decreases the amplitude of $Ca^{2+}$ responses. **(a)** Raji cells incubated with superAg were allowed to interact with Fura-2 loaded T lymphocytes trans-fected with a cDNA construct encoding CD6-YFP. Time-lapse video imaging showing super-imposed DIC and calcium signals (upper panel) and CD6 expression (lower panel) on one CD6 negative T cell (black arrow) and one positive T cell (white arrow), interacting with APCs in the same field. **(b)** Percentage of CD6 negative or CD6 positive T cells that increase (ratio>1.5) or not their calcium after conjugate formation with superAg-pulsed Raji cells. Mean of 3 separate experiments with at least 30 individual cells analyzed in each. **(c)** Intracellular calcium was measured sequentially every 10s in T cells inter-acting with superAg-pulsed Raji cells. Calcium mobilization was measured for T cells expressing or not CD6-YFP. Averaged responses were determined from at least 10 individual cells.

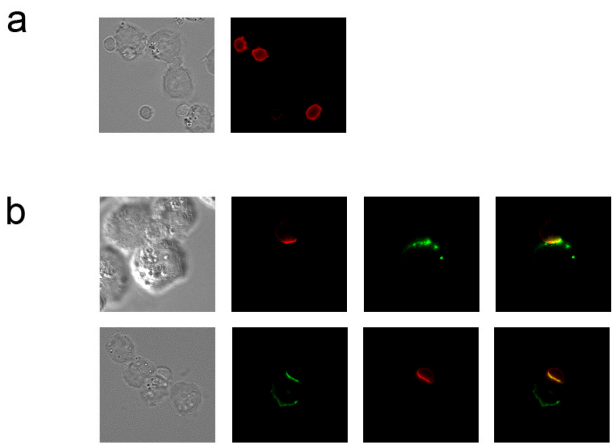



**Figure 3.** Accumulation of CD6 in the immunological synapse correlates with binding to CD166. **(a)** Conjugates formed between superAgs-pulsed Raji cells and CD6-YFP (visualized in red) transfected T cells. Cells were fixed after 45 min of interaction. In the absence of the ligand on the surface of Raji cells, rat CD6 does not accumulate at the immunological synapse. **(b)** Raji cells were transfected with CD166-CFP (detected as green) and pulsed with a mix of superAgs prior to incubation with CD6-YFP transfected T cells. Localization of CD6-YFP, and CD166-CFP as well as fluorescence overlays (yellow) are shown.

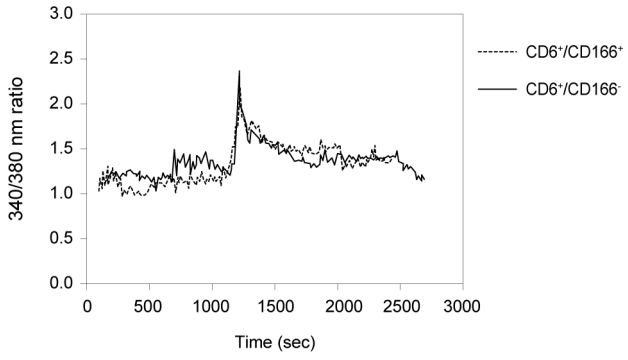



**Figure 4.** CD6 attenuates calcium responses independently of ligand-binding interactions. Intracellular calcium was measured in CD6 positive T cells (expressing CD6-YFP) interacting in the same field with CD166 negative or CD166 positive (expressing CD166-CFP) superAg-pulsed Raji cells. Averaged responses of at least 10 individual cells are shown.

### 4.4.3 The inhibitory role of CD6 depends on the cytoplasmic domain

The cytoplasmic domain of CD6 contains multiple potential binding sites for intracellular signaling effectors although no clear function has been assigned to these interactions. Hence, we addressed the role of the cytoplasmic domain of CD6 using an engineered isoform of rat CD6 devoid of the cytoplasmic domain, CD6CY5. Calcium signals were again measured during T cell-APC interactions followed by video imaging. We found that the percentage of T cells expressing CD6CY5 that increased calcium levels after conjugate formation matched that of $CD6^-$ cells (Fig. 5a, compare to Fig. 2b).

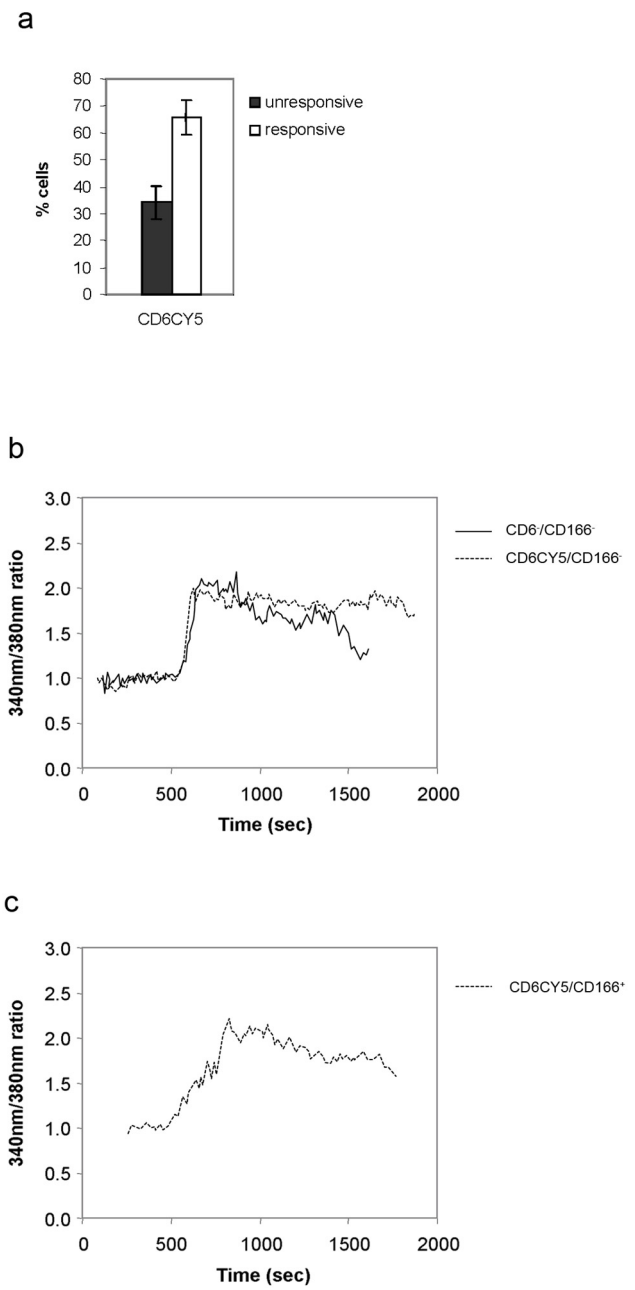



**Figure 5.** The inhibitory role of CD6 is dependent of its cytoplasmic domain. **(a)** Percentage of calcium responsive or unresponsive CD6CY5 T cells, after conjugate formation with superAg-pulsed Raji cells. Mean of 3 separate experiments with at least 30 individual cells in each. **(b)** Calcium signals were acquired sequentially every 10s, from CD6CY5-YFP expressing vs CD6 negative T cells interacting with superAg-pulsed Raji cells. Averaged responses were determined from at least 10 individual cells. **(c)** Calcium signals were measured from CD6CY5-YFP T cells interacting with CD166 positive superAg-pulsed Raji cells.

Also, the measured calcium signals of responding cells were nearly identical to those of untransfected cells (Fig. 5b), showing that in the absence of the cytoplasmic tail the inhibitory effect was removed.

We additionally evaluated the possible role of the cytoplasmic deletion form of CD6 at the immunological synapse. Similarly to the wild-type molecule, CD6CY5 only addressed to the synapse when rat CD166 was expressed on Raji cells (data not shown). The measured calcium signals of T cells expressing CD6CY5 localizing at the synapse interacting with CD166-expressing Raji cells were not significantly different from those obtained with untransfected Raji (Fig. 5c, compare to Fig. 5b).

We thus concluded that the cytoplasmic tail of rat CD6 is held responsible for the down-modulation of calcium signals, and that localization at the synapse is not essential for its function.

## 4.5 Discussion

In this report we show evidence that CD6 can down-modulate calcium signals initiated upon T cell interaction with superantigen-primed Raji cells. Intriguingly, most reports attribute to CD6 a positive or co-stimulatory function [2-7]. A possible explanation for some inconsistencies is that the majority of these studies have used human CD6, whereas we addressed the function of the rat homologue. However, given the very high homology between rat and human CD6, with 72% amino acid identity and the conservation of most putative signaling motifs [12], a complete reversal of function would be mostly unlikely, unless the cellular environment was significantly different. Nevertheless, it cannot be formally excluded that the use of diverse cellular systems may result in some discrepancy of results and disagreement over the conclusions drawn.

Some of the early reports on the co-stimulatory properties of CD6 relied on the use of monoclonal antibodies as the source of external stimuli [2-4]. Also, in our initial experiments crosslinking rat CD6 together with the TCR with the use of monoclonal antibodies we observed a very strong phosphorylation of LAT, an important mediator of T cell signalling. However, such type of stimulation can very likely induce the indiscriminate aggregation of protein tyrosine kinases that associate non-covalently with CD6 [12], possibly originating effects very dissimilar from those obtained through physiological stimulation. CD5, a highly homologous molecule also expressed in T lymphocytes, was originally accepted as a co-stimulatory molecule for analogous reasons [24-26]. It turned out to be a clear inhibitor of T-cell activation and thymocyte selection [14].

More recent work has demonstrated that blocking the human CD6-CD166 interaction with soluble CD6 or CD166 recombinant proteins diminished the levels of human T cell activation and proliferation upon T cell-APC engagement [6, 7]. It is possible, however, that the suppression of activation signals is due to the overall interference that the soluble reagents cause on the cell-to-cell contact, rather than to a very specific effect blocking just the CD6-CD166 ligation. Indeed, using as a blocking reagent an antibody against human CD6, OX126 (M. H. Brown, S. Simmonds and M. Puklavec, unpublished data), we observed that it resulted in the reduction of the number of T cell-APC conjugates formed, compared to the conditions where no blocking was produced (R. Nunes, S. Fabre, G. Bismuth and A. Carmo, unpublished results). This interpretation can nevertheless make the case that CD6 assists in T cell activation as well: given that, as we suggest, the CD6-associated enzymatic activity is kept constant regardless of the cellular localization of CD6, if CD6 localizes to the immunological synapse and binds to CD166, these interactions are likely to increase cellular adhesion and thus support a stimulatory role for CD6, albeit indirect.

An inhibitory role for CD6 on thymocyte development has been previously suggested [9, 27]. Here we provide biochemical evidence that CD6 can indeed modulate signals triggered upon antigen recognition. Whether this role is intrinsic, or dependent on regulated interactions with other surface molecules, is still to be determined. For example, the IgSF surface glycoprotein CD2 can transduce mitogenic signals due to its association with the tyrosine kinases Lck and Fyn [28], however, through its interaction with the inhibitory molecule CD5 it can also induce or amplify a negative response [16, 17]. Regarding CD6, it shares with CD5 the attribute to inhibit signaling upon T cell-APC interactions, not requiring ligand binding to do so [29]. Since CD5 and CD6 also associate at the surface of T cells and one major effect of CD6 stimulation is the phosphorylation of CD5 [12], it is feasible that CD5 can integrate or transform the signals triggered through CD6.

CD6 has been shown previously to localize to the immunological synapse during T cell-APC interactions [6]. Here we show for the first time that this localization depends on the expression on the APC of the CD6 ligand, CD166. Nevertheless, the inhibitory effect of CD6 does not fully depend on the localization of CD6 with respect to the immunological synapse, where antigen recognition takes place. Rather, the difference lies on whether or not the molecule is expressed, suggesting that CD6 can be a general attenuator of activation mechanisms. The physiological mode of regulation exerted by CD6 on cellular behaviour could therefore depend on the levels of expression, or most likely and given that very few T cells do not express CD6, on the isoforms of CD6 produced at a certain stage of cellular activation or differentiation.

A number of different isoforms resulting from alternative splicing of the exons coding for the intracellular domain have been reported [11, 30-32]. As we show that the cytoplasmic domain is crucial for the inhibitory role of CD6, variation on the composition of the cytoplasmic tail may translate into different associations with effector molecules that drive signaling events. Nevertheless, the full-length isoform seems to be the most abundant, so at least at some stages of immune responses, CD6 will display a capacity of down-modulating activation signals. As the cytoplasmic part of CD6 is highly tyrosine phosphorylated after T cell activation, the example made with CD5 should be followed [13], and a systematic and careful analysis of the various tyrosine residues present within this domain will be required. Also, further genetic approaches will be necessary to understand the regulation of CD6 expression, in order to establish the involvement of different CD6 isoforms and the corresponding cytoplasmic features in the inhibitory characteristics of CD6.

## Acknowledgments

We would like to thank Dr. Simon Davis for helpful discussions and the critical reading of the manuscript, and Dr Marion Brown for the kind gift of the anti-CD6 antibody OX126, and for useful comments and suggestions. We also thank Dr Vaclav Horejsi for providing anti-CD6 antibody MEM-98.

## 4.6 References

1. Aruffo, A., et al., The lymphocyte glycoprotein CD6 contains a repeated domain structure characteristic of a new family of cell surface and secreted proteins. *J. Exp. Med.*, 1991. **174**(4): p. 949-952.
2. Gangemi, R.M., et al., Anti-T12, an anti-CD6 monoclonal antibody, can activate human T lymphocytes. *J. Immunol.*, 1989. **143**(8): p. 2439-2447.
3. Bott, C.M., et al., Activation of human T cells through CD6: functional effects of a novel anti-CD6 monoclonal antibody and definition of four epitopes of the CD6 glycoprotein. *Int. Immunol.*, 1993. **5**(7): p. 783-792.
4. Osorio, L.M., et al., The anti-CD6 mAb, IOR-T1, defined a new epitope on the human CD6 molecule that induces greater responsiveness in T cell receptor/CD3-mediated T cell proliferation. *Cell. Immunol.*, 1994. **154**(1): p. 123-133.

5. Rasmussen, R.A., et al., Isolation and characterization of CD6- T cells from peripheral blood. *J. Immunol.*, 1994. **152**(2): p. 527-536.
6. Gimferrer, I., et al., Relevance of CD6-mediated interactions in T cell activation and proliferation. *J. Immunol.*, 2004. **173**(4): p. 2262-2270.
7. Hassan, N.J., et al., Optimal T cell activation requires the engagement of CD6 and CD166. *Eur. J. Immunol.*, 2004. **34**(4): p. 930-940.
8. Patel, D.D., et al., Identification and characterization of a 100-kD ligand for CD6 on human thymic epithelial cells. *J. Exp. Med.*, 1995. **181**(4): p. 1563-1568.
9. Singer, N.G., et al., CD6: expression during development, apoptosis and selection of human and mouse thymocytes. *Int. Immunol.*, 2002. **14**(6): p. 585-597.
10. Wee, S., et al., Tyrosine phosphorylation of CD6 by stimulation of CD3: augmentation by the CD4 and CD2 coreceptors. *J. Exp. Med.*, 1993. **177**(1): p. 219-223.
11. Robinson, W.H., et al., Human CD6 possesses a large, alternatively spliced cytoplasmic domain. *Eur. J. Immunol.*, 1995. **25**(10): p. 2765-2769.
12. Castro, M.A.A., et al., OX52 is the rat homologue of CD6: evidence for an effector function in the regulation of CD5 phosphorylation. *J. Leukoc. Biol.*, 2003. **73**(1): p. 183-190.
13. Gary-Gouy, H., et al., CD5-negative regulation of B cell receptor signaling pathways originates from tyrosine residue Y429 outside an immunoreceptor tyrosine-based inhibitory motif. *J. Immunol.*, 2002. **168**(1): p. 232-239.
14. Tarakhovsky, A., et al., A role for CD5 in TCR-mediated signal transduction and thymocyte selection. *Science*, 1995. **269**(5223): p. 535-537.
15. Pena-Rossi, C., et al., Negative regulation of CD4 lineage development and responses by CD5. *J. Immunol.*, 1999. **163**(12): p. 6494-6501.
16. Carmo, A.M., et al., CD2 and CD3 associate independently with CD5 and differentially regulate signaling through CD5 in Jurkat T cells. *J. Immunol.*, 1999. **163**(8): p. 4238-4245.
17. Teh, S.J., et al., CD2 regulates the positive selection and function of antigen-specific CD4- CD8+ T cells. *Blood*, 1997. **89**(4): p. 1308-1318.
18. Aruffo, A., et al., CD6-ligand interactions: a paradigm for SRCR domain function? *Immunol. Today*, 1997. **18**(10): p. 498-504.
19. Bowen, M.A., et al., Cloning, mapping, and characterization of activated leukocyte-cell adhesion molecule (ALCAM), a CD6 ligand. *J. Exp. Med.*, 1995. **181**(6): p. 2213-2220.

20. Epstein, M.A., et al., Morphological and virological investigations on cultured Burkitt tumor lymphoblasts (strain Raji). *J. Natl. Cancer Inst.*, 1966. **37**(4): p. 547-559.
21. Bazil, V., et al., Monoclonal antibodies against human leukocyte antigens. III. Antibodies against CD45R. CD6, CDw44 and two newly described broadly expressed glycoproteins MEM-53 and MEM-102. *Folia Biol. Praha*, 1989. **35**: p. 289-297.
22. McMichael, A.J., et al., eds. *Leukocyte Typing III. White Cell Differentiation Antigens*. 1987, Oxford University: Oxford.
23. Harriague, J. and G. Bismuth, Imaging antigen-induced PI3K activation in T cells. *Nat. Immunol.*, 2002. **3**(11): p. 1090-1096.
24. Ceuppens, J.L. and M.L. Baroja, Monoclonal antibodies to the CD5 antigen can provide the necessary second signal for activation of isolated resting T cells by solid-phase- bound OKT3. *J. Immunol.*, 1986. **137**(6): p. 1816-1821.
25. Imboden, J.B., et al., Stimulation of CD5 enhances signal transduction by the T cell antigen receptor. *J. Clin. Invest.*, 1990. **85**(1): p. 130-134.
26. June, C.H., et al., CD5 antibodies increase intracellular ionized calcium concentration in T cells. *J. Immunol.*, 1987. **138**(9): p. 2782-2792.
27. Sarrias, M.R., et al., The Scavenger Receptor Cysteine-Rich (SRCR) domain: an ancient and highly conserved protein module of the innate immune system. *Crit. Rev. Immunol.*, 2004. **24**(1): p. 1-37.
28. Carmo, A.M., et al., Physical association of the cytoplasmic domain of CD2 with the tyrosine kinases $p56^{lck}$ and $p59^{fyn}$. *Eur. J. Immunol.*, 1993. **23**(9): p. 2196-2201.
29. Brossard, C., et al., CD5 inhibits signaling at the immunological synapse without impairing its formation. *J. Immunol.*, 2003. **170**(9): p. 4623-4629.
30. Robinson, W.H., et al., Identification of a mouse protein homologous to the human CD6 T cell surface protein and sequence of the corresponding cDNA. *J. Immunol.*, 1995. **155**(10): p. 4739-4748.
31. Whitney, G., et al., Cloning and characterization of murine CD6. *Mol. Immunol.*, 1995. **32**(1): p. 89-92.
32. Bowen, M.A., et al., Structure and chromosomal location of the human CD6 gene: detection of five human CD6 isoforms. *J. Immunol.*, 1997. **158**(3): p. 1149-1156.

# III – Concluding Remarks

Although the completion of the Human Genome Project has now given us the human genome sequence, the exact number of genes encoded by the genome is still unknown. Nevertheless, the estimates have been sharply downgraded from the approximately 100,000 protein-coding genes initially predicted. Contrarily to what could be immediately thought, this relative poverty of our genetic patrimony does not constitute an evolutionary limitation. Rather than just gene count, the human genetic complexity most likely derives from other features, such as co- and post-transcription and translational mechanisms that can generate an overwhelming number of different proteins at a given stage in a single cell. Taking the leucocyte cell surface as an example, which remains the best-characterized of all mammalian cells, at least 347 distinct cell surface molecules have been identified [347], with over 110 found at the T cell surface alone [3]. Given such multitude and diversity, the surface receptors that are responsible for conveying outside driven signals to the cell core must act in concert as an ensemble in order to integrate and respond to both inter- and extracellular signals, thereby dictating the cell's fate. Following the identification of the protein constituents of the T cell surface, virtually all of them already discovered [3], the present challenge is focused towards a better understanding of the cell surface protein function. Included in this objective is the requirement to comprehend how these molecules are organized within the membrane, their ensemble behaviour and its consequences for signal transduction.

Bioluminescence Resonance Energy Transfer (BRET) is a powerful technology that has the distinct advantage of monitoring lateral protein-protein interactions *in situ* at the living cell surface with high efficiency and less background than similar techniques. Although BRET is experimentally simple, the interpretation of the data, however, is not necessarily so straightforward. Several factors, including distance, orientation and expression levels of the proteins of interest, affect the efficiency of the energy transfer and can make the analysis of the results potentially problematic. In addition, work described in this thesis showed that a large fraction of the BRET signal is derived from random collisions, further complicating the study of interactions between cell surface molecules. In fact, these non-specific contacts have been commonly reported to reflect stable protein dimerization in previous, conventional BRET experiments [322]. Using a series of monomeric and dimeric proteins of known stoichiometry, we tested theoretical considerations according to which the two types of interactions can, in principle, be distinguished, establishing in the process, a new experimental framework for detecting membrane protein self-association. Instead of using only single acceptor/donor ratios and maximal expression levels, in the new approach two types of analysis were performed: varing the relative acceptor/donor ratio at a constant expression level and varying the expression level at a constant acceptor/donor ratio. We also demonstrated the crucial

importance of using appropriate controls to calibrate the BRET results in order to distinguish BRET signatures representing true dimers from non-residual background signals generated by casual collisions. This aspect was clearly illustrated for the case of G-protein coupled receptors (GPCRs), whose association has been extensively investigated using BRET. Most of the studies focusing on these molecules, have suggested that these proteins typically form homo- and hetero-oligomers [322]. By applying the new quantitative method to several GPCRs, we were unable to reproduce earlier observations on GPCRs dimerization [348], except for a well-known dimeric GPCR [319, 320]. The remaining GPCRs tested, exhibited only the signals characteristic of monomers. These findings indicate that the extent of GPCR self-association may have been overestimated and fail to support the concept that all GPCRs dimerize. There is, however, significant early experimental evidence consistent with such a notion, but mainly derived from biochemical studies. Caution should be taken, however, in the interpretation of those results, as highly hydrophobic proteins like GPCRs exhibit a tendency to aggregate when removed from the lipid environment of the plasma membrane. Undoubtedly, RET techniques provide the best current means to examine the natural behaviour of these proteins, since they are performed with intact cells. Further studies are necessary to determine which GPCRs do function as dimers and to evaluate the physiological significance of such behaviour, but will require a rigorous treatment of the data to be indubitable. It will also be important to determine whether the “monomers” are also monomeric in their normal cellular environment, rather than only following expression as GFP and rLuc chimeras in 293T cells. Single-molecule spectroscopy, based on the detection of coincident fluorescence from single molecules labelled with two different fluorophores, is an alternative method to address this question and overcome this limitation of the existing BRET experiments.

Having established the advantages of the new BRET approach, we next broadened our study and applied it to a number of representative T cell surface molecules in order to elucidate the general features of the T cell surface molecular organization. This knowledge is essencial to the understanding on how membrane protein arrangements and interactions affect their function and are linked to specific intracellular signalling pathways. We have interestingly observed that almost all of the membrane proteins analysed displayed monomeric behaviour at the cell surface, even CD45RO, previously suggested as the most likely CD45 isoform to homodimerize [120]. The exceptions were the co-receptor CD4 and the accessory molecules CD5 and CD6, which associate weakly and non-constitutively. The former exhibits, even so, higher tendency to dimerize and requires the presence of its cytoplasmic tail to do so. On the other hand, extracellular interactions are responsible for CD5 and CD6 self-association. These findings suggest that

dimerization is a rare property that might favour a specific function of a particular protein. In the case of CD4, dimerization has been associated with fine-tuning of T cell activation thresholds. Dimeric forms of CD4, if they exist at all, are likely to bind MHC class II with stronger avidity, and have been suggested as the preferential MHC-interacting form [63, 310, 311, 349]. However, according to the data herein presented CD4 does not require dimerization to be functional since an active form of CD4 exhibits a monomeric signature. Nonetheless dimeric events might have other, perhaps indirect, consequences that are currently unclear. In fact, it was recently been reported that coreceptor dimerization reduces the efficiency of HIV-type I entry, suggesting that this mechanism might be important to modulate viral infection [350]. Regarding CD5, self-association may mimic the engagement effect of an external, yet unidentified ligand, and help the molecule to negatively regulate T cell signaling without requiring ligand binding. Consistent with this, we observe that CD5 dependent phosphorylation of a specific tyrosine kinase does not require crosslinking of the primary CD5 antibody (Bamberger *et al.*, unpublished results). In addition, we have gathered evidence that interactions at the membrane are more prevalent, with molecules confined to the cell surface being ~50 times more likely to interact than those in solution. It is therefore conceivable that the relatively paucity in interaction between the cell surface and the cytoplasm could make the recruitment of molecules to the cell surface the rate-limiting step for T cell activation. These first and important insights on the stoichiometric arrangement of membrane proteins provide a glimpse of the overall organization of the T cell surface that will help, as more work is carried out, to further understand the role of different receptors in the process of T cell activation.

Having examined the stoichiometric properties of the scavenger receptor proteins CD5 and CD6, the behaviour of CD6 in the context of synapse formation and signaling was investigated. This type-I cell surface glycoprotein is primarily expressed by thymocytes and mature T cells, and has been recognized as an important mediator of T cell interactions [157]. However, despite being proposed to have a crucial role on T cell development and activation, functional data are still scarce. Previous work has shown that antibody-mediated CD6 cross-linking can potentiate proliferative T cell responses [351-353], and these observations have supported the notion that CD6 had a stimulatory or signaling-enhancing effect. However, such type of stimulation can very likely induce potential cross-linking events, thereby influencing the outcome of CD6 stimulation. Hence, we have addressed the signaling role of CD6 upon T cell productive interaction with antigen presenting cells. Our results point, however, towards an inhibitory effect of CD6, with the crucial factor being whether or not the molecule is expressed, rather than its cell location. Others have used soluble or recombinant, non-cross-linking CD6 or CD166

proteins to block CD6-CD166 interaction and observed a decrease in the levels of T cell activation and proliferation upon T cell-APC engagement [354, 355]. Nevertheless, the reduced activation of T cells due to the interference on the CD6-CD166 interaction could be attributed to the lower adhesion between the cells rather than to the suppression of CD6-specific activation signals. We and others have, indeed, observed a reduction in the number of T cell-APC conjugates when using soluble reagents [170] (Nunes *et al*., unpublished results), compared to the conditions where no blocking was produced. Evidence suggesting an inhibitory role for CD6 in thymocyte development has been reported as well [172, 356]. It is much too early to judge whether the modulatory role of CD6 is intrinsic or dependent on interactions with other surface molecules. CD6 associates with both CD5 and TCR/CD3 at the cell membrane of lymphocytes and at the IS [170, 173]. Moreover, it has been shown to play an important role in the modulation of CD5 phosphorylation [174]. We, therefore, envisage a physical linkage between these two molecules, with CD5 co-engaging signals delivered through the associated CD6 molecules. Such a scenario would be reminiscent of that reported previously for CD2 and CD5 [357, 358]. In the future, the availability of double CD5/CD6-deficient mice will help to clarify whether both proteins share a common signaling pathway. The phenotype of single CD6-knockout mice which is currently unknown may, in addition, unveil the relevance of this receptor, whose role is yet to be fully explored.

Interestingly, we found that the negative signals induced by CD6 are not dependent on its localization with respect to the IS, where it accumulates upon T cell activation [170, 171]. Moreover, we found no absolute requirement for ligand engagement for the inhibition of signaling, a characteristic shared with CD5 [359]. Instead, the crucial feature is the presence of the molecule itself, as CD6-positive T cells are significantly less responsive to APC challenge than those not expressing the protein. Furthermore, we ascertained a key role for the cytoplasmic tail of CD6 for its inhibitory function, with removal of this region reversing this effect. Several CD6 cytoplasmic isoforms arising from alternative splicing have been described [159-161, 360]. This regulatory mechanism is of considerable importance for generating protein diversity and regulating protein expression, as it can largely multiply the number of gene products possible from the basic gene complement. In humans, alternative splicing is ubiquitous, being observed in 40-60% of human genes [178-182], and it affects particularly the immune and the nervous systems, with a bias towards cell surface receptors [182]. For the majority of these proteins, the role of alternative splicing in regulating their function, although intriguing, is still theoretical. This is also the case for the different CD6 cytoplasmic isoforms, for which a clear physiological role is yet to be established. The intracellular segment of CD6 is unusually long and contains several consensus sequences related to signal transduction

[159]. This fact, together with the data herein reported assigning the inhibitory properties of CD6 to its cytoplasmic tail, allows us to speculate that the modulatory role exerted by CD6 may rely on the expression of specific cytoplasmic isoforms and their different association with signaling effectors.

In addition to the CD6 variants lacking sequences encoding intracellular regions, we have determined that a significant fraction of CD6 transcripts is also expressed as novel isoforms devoid of exons coding for the extracellular domains. In fact, one of these naturally occurring mutant forms, CD6Δd3, excluded precisely the ligand-binding domain. We have cloned the cDNA coding for CD6Δd3 and found that CD6Δd3 is expressed in both rat and human primary lymphoid cells. These findings persuaded us to try to further understand the functional and physiological significance of CD6Δd3 upon T cell-APC interactions and T cell activation. Importantly, we showed for the first time that the recruitment of CD6 to the contact area is CD166-dependent, thus requiring the alternative splicing regulated-expression of domain 3 of CD6. This ability of CD6Δd3 to control the interaction with the ligand, and thereby failing to accumulate at the IS, represents a singular example of a functional role of an alternative spliced variant. Analysis of the expression profile of the two isoforms at different maturation stages and upon stimulation revealed that, whereas full-length CD6 is highly favored in early developmental stages in the thymus, CD6Δd3 expression remarkably increases following activation, indicating that CD6Δd3 is a product of activation. Moreover, we observed that the two variants are both capable of attenuating T cell signaling. In view of all these findings, it seems reasonable to consider that this type of regulatory mechanism effectively broadens the range of action of CD6. Full-length CD6 focusing at the synapse may negatively influence delimited and localised signaling, and at the same time signal back to the APC, whereas a form expressed without ligand-binding ability may result in a broader, albeit more diluted, inhibitory activity. By signalling for the shorter CD6 isoform, productive TCR antigen recognition may reduce the focal inhibition of CD6 at the IS, thus allowing a different pattern of inhibition in the interacting cells. Due to technical limitations, it was not possible to evaluate the responses of T cells co-expressing both isoforms throughout T cell-APC interactions. The development of new, more advanced, imaging methodologies will help to bridge the gap between the cellular and functional observations made thus far.

A series of important questions emerging from this work are currently being considered, such as the basis of the negative role exerted by CD6, the signaling consequences of targeting this molecule to the IS and the possible outcomes induced by CD6 variants in the APCs. Other aspects of the biology of CD6 also remain unclear, such as the role of the different cytoplasmic isoforms, the diversity of responses they can potentially originate within and outside the interface, and the factors regulating their

expression. With these uncertainties in mind it will be of great interest to characterize in detail the molecular associations of the cytoplasmic tail of CD6, as relatively few intracellular partners are currently known [169, 174, 177]. Also, it is tempting to examine the relation between the triggering properties of CD6 and the negative modulatory role of CD5, as well as to evaluate the possible linkage between CD6Δd3 and a second, already described, CD6 ligand [175], or other potential new ligands. The accomplishment of these different goals will contribute substantially to elucidating the physiological role of CD6 in lymphocyte biology.

# IV – References

1. Heissmeyer, V., et al., Calcineurin imposes T cell unresponsiveness through targeted proteolysis of signaling proteins. *Nat. Immunol.*, 2004. **5**: p. 255-265.
2. Riley, J.L. and C.H. June, The CD28 family: a T-cell rheostat for therapeutic control of T-cell activation. *Blood*, 2005. **105**: p. 13-21.
3. Evans, E.J., et al., The T cell surface - how well do we know it? *Immunity*, 2003. **19**: p. 213-223.
4. Weiss, A., Molecular and genetic insights into T cell antigen receptor structure and function. *Annu. Rev. Genet.*, 1991. **25**: p. 487-510.
5. Davis, M.M. and P.J. Bjorkman, T-cell antigen receptor genes and T-cell recognition. *Nature*, 1988. **334**: p. 395-402.
6. Meuer, S.C., et al., Evidence for the T3-associated 90K heterodimer as the T-cell antigen receptor. *Nature*, 1983. **303**(5920): p. 808-810.
7. Samelson, L.E., et al., Monoclonal antibodies against the antigen receptor on a cloned T-cell hybrid. *Proc. Natl. Acad. Sci. USA*, 1983. **80**(22): p. 6972-6976.
8. Brenner, M.B., et al., Identification of a putative second T-cell receptor. *Nature*, 1986. **322**(6075): p. 145-149.
9. Ashwell, J.D. and R.D. Klusner, Genetic and mutational analysis of the T-cell antigen receptor. *Annu. Rev. Immunol.*, 1990. **8**: p. 139-167.
10. Clevers, H., et al., The T cell receptor/CD3 complex: a dynamic protein ensemble. *Annu. Rev. Immunol.*, 1988. **6**: p. 629-662.
11. Germain, R.N., MHC-dependent antigen processing and peptide presentation: providing ligands for T lymphocyte activation. *Cell*, 1994. **76**: p. 287-299.
12. Amzel, L.M. and R.J. Poljak, Three-dimensional structure of immunoglobulins. *Annu. Rev. Biochem.*, 1979. **48**: p. 961-997.
13. Brown, J.H., et al., Three-dimensional structure of the human class II histocompatibility antigen HLA-DR1. *Nature*, 1993. **364**: p. 33-39.
14. Bjorkman, P.J., MHC restriction in three dimensions: a view of T cell receptor/ligand interactions. *Cell*, 1997. **89**: p. 167-170.
15. Padlan, E.A. and D.H. Margulies, Feeling out the complex. *Curr. Biol.*, 1997. **7**: p. 17-20.
16. Madden, D., The three-dimensional structure of peptide-MHC complexes. *Annu. Rev. Immunol.*, 1995. **13**: p. 587-622.
17. Bjorkman, P.J., et al., The foreign antigen binding site and T cell recognition regions of class I histocompatibility antigens. *Nature*, 1987. **329**: p. 512-518.
18. Matsumura, M., et al., Emerging principles for the recognition of peptide antigens by MHC class I molecules. *Science*, 1992. **257**: p. 927-934.

19. Stern, L.J. and D.C. Wiley, Antigenic peptide binding by class I and class II histocompatibility proteins. *Structure*, 1994. **2**: p. 245-251.
20. Wilson, I.A. and D.H. Fremont, Structural analysis of MHC class I molecules with bound peptide antigens. *Semin. Immunol.*, 1993. **5**: p. 75-80.
21. Jones, E.Y., MHC class I and class II structures. *Curr. Opin. Immunol.*, 1997. **9**: p. 75-79.
22. Garcia, K.C., et al., An αβ T cell receptor structure at 2.5 Å and its orientation in the TCR-MHC complex. *Science*, 1996. **274**: p. 209-219.
23. Garboczi, D.N., et al., Structure of the complex between human T-cell receptor, viral peptide and HLA-A2. *Nature*, 1996. **384**: p. 134-141.
24. Rudolph, M.G., et al., How TCRs bind MHCs, peptides, and coreceptors. *Annu. Rev. Immunol.*, 2006. **24**: p. 419-466.
25. Hennecke, J. and D.C. Wiley, T cell receptor-MHC interactions up close. *Cell*, 2001. **104**: p. 1-4.
26. Rudolph, M.G. and I.A. Wilson, The specificity of TCR:pMHC interaction. *Curr. Opin. Immunol.*, 2002. **14**: p. 52-65.
27. Teng, M.K., et al., Identification of a common docking topology with substantial variation among different TCR-peptide-MHC complexes. *Curr. Biol.*, 1998. **8**: p. 409-412.
28. Maynard, J., et al., Structure of an autoimmune T cell receptor complexed with class II peptide-MHC: insights into MHC bias and antigen specificity. *Immunity*, 2005. **22**: p. 81-92.
29. Reinherz, E.L., et al., The crystal structure of a T cell receptor in complex with peptide and MHC class II. *Science*, 1999. **286**: p. 1913-1921.
30. Wilson, I.A. and K.C. Garcia, T-cell receptor structure and TCR complexes. *Curr. Opin. Struct. Biol.*, 1997. **7**: p. 839-848.
31. Buslepp, J., et al., A correlation between TCR Vα docking on MHC and CD8 dependence: implications for T cell selection. *Immunity*, 2003. **19**: p. 595-606.
32. Wang, J.-H. and E.L. Reinherz, Structural basis of T cell recognition of peptides bound to MHC molecules. *Mol. Immunol.*, 2002. **38**: p. 1039-1049.
33. Sim, B.C., et al., V alpha 3.2 selection in MHC class I mutant mice: evidence for an alternate orientation of TCR-MHC class I interaction. *J. Immunol.*, 1997. **159**(7): p. 3322-3329.
34. Wang, J., et al., Anatomic structure of a fragment of human CD4 containing two immunoglobulin-like domains. *Nature*, 1990. **348**: p. 411-418.

35. Kern, P.S., et al., Structural basis of CD8 coreceptor function revealed by crystallographic analysis of a murine CD8 αα ectodomain fragment in complex with H-2Kb. *Immunity*, 1998. **9**: p. 519-530.
36. Gao, G.F., et al., Crystal structure of the complex between human CD8 αα and HLA-A2. *Nature*, 1997. **387**: p. 630-634.
37. Lee, P.U.Y., et al., Role of 2C T Cell Receptor Residues in the Binding of Self- and Allo-Major Histocompatibility Complexes. *J. Exp. Med.*, 2000. **191**(8): p. 1355-1364.
38. Manning, T.C., et al., Alanine scanning mutagenesis of an αβ T cell receptor: mapping the energy of antigen recognition. *Immunity*, 1998. **8**(4): p. 413-425.
39. Baker, B.M., et al., Identification of a crucial energetic footprint on the α 1 helix of human histocompatibility leukocyte antigen (HLA)-A2 that provides functional interactions for recognition by tax peptide/HLA-A2-specific T cell rseceptors. *J. Exp. Med.*, 2001. **193**(5): p. 551-562.
40. Wu, L.C., et al., A two-step binding mechanism for T cell receptor recognition of peptide-MHC. *Nature*, 2002. **418**: p. 552-556.
41. Garcia, K.C., et al., Structural basis of plasticity in T cell receptor recognition of a self peptide-MHC antigen. *Science*, 1998. **279**: p. 1166-1172.
42. Ding, Y.-H., et al., Four A6-TCR:peptide/HLA-A2 structures that generate very different T cell signals are nearly identical. *Immunity*, 1999. **11**: p. 45-56.
43. Hare, B.J., et al., Structure, specificity and CDR mobility of a class II restricted single-chain T-cell receptor. *Nat. Struct. Biol.*, 1999. **6**: p. 574-581.
44. Reiser, J.B., et al., A T cell receptor CDR3 β loop undergoes conformational changes of unprecedented magnitude upon binding to a peptide/ MHC class I complex. *Immunity*, 2002. **16**: p. 345-354.
45. Willcox, B.E., et al., TCR binding to peptide-MHC stabilizes a flexible recognition interface. *Immunity*, 1999. **10**: p. 357-65.
46. Boniface, J.J., et al., Thermodynamics of T cell receptor binding to peptide-MHC: evidence for a general mechanism of molecular scanning. *Proc. Natl. Acad. Sci. USA*, 1999. **96**: p. 11446-11451.
47. Garcia, K.C., et al., Kinetics and thermodynamics of T cell receptor-autoantigen interactions in murine experimental autoimmune encephalomyelitis. *Proc. Natl. Acad. Sci. USA*, 2001. **98**: p. 6818-6823.
48. Mason, D., A very high level of crossreactivity is an essential feature of the T-cell receptor. *Immunol. Today*, 1998. **19**: p. 395-404.
49. Kuzushima, K., et al., The role of self peptides in the allogeneic crossreactivity of CTLs. *J. Immunol.*, 1995. **155**: p. 594-601.

50. Ausubel, L.J., et al., Complementary mutations in an antigenic peptide allow for crossreactivity of autoreactive Tcell clones. *Proc. Natl. Acad. Sci. USA*, 1996. **93**: p. 15317-15322.
51. Nanda, N.K., et al., Recognition of multiple peptide cores by a single T cell receptor. *J. Exp. Med.*, 1995. **182**: p. 531-539.
52. Borg, N.A., et al., The CDR3 regions of an immunodominant T cell receptor dictate the 'energetic landscape' of peptide-MHC recognition. *Nat. Immunol.*, 2005. **6**: p. 171-180.
53. Hahn, M., et al., Unconventional topology of self peptide-major histocompatibility complex binding by a human autoimmune T cell receptor. *Nat. Immunol.*, 2005. **6**: p. 490-496.
54. Reiser, J.B., et al., CDR3 loop flexibility contributes to the degeneracy of TCR recognition. *Nat. Immunol.*, 2003. **4**: p. 241-247.
55. Housset, D. and B. Malissen, What do TCR–pMHC crystal structures teach us about MHC restriction and alloreactivity? *Trends Immunol.*, 2003. **24**(429-437).
56. Chien, Y.-h., et al., Recognition by γ/δ T cells. *Annu. Rev. Immunol.*, 1996. **14**(1): p. 511-532.
57. Adams, E.J., et al., Structure of a γδ T Cell Receptor in Complex with the Nonclassical MHC T22. *Science*, 2005. **308**: p. 227-231.
58. Crowley, M.P., et al., A Population of Murine γδ T Cells That Recognize an Inducible MHC Class Ib Molecule. *Science*, 2000. **287**: p. 314-316.
59. Littman, D.R., The structure of the CD4 and CD8 genes. *Annu. Rev. Immunol.*, 1987. **5**: p. 561-584.
60. Maddon, P.J., et al., The isolation and nucleotide sequence of a cDNA encoding the T cell surface protein T4: a new member of the immunoglobulin gene family *Cell*, 1985. **42**: p. 93-104
61. Wu, H., et al., Dimeric association and segmental variability in the structure of CD4. *Nature*, 1997. **387**: p. 527-530.
62. Moldovan, M.C., et al., CD4 dimers constitute the functional component required for T cell activation. *J. Immunol.*, 2002. **169**: p. 6261-6268.
63. Moldovan, M.C., et al., Triggering of T cell activation via CD4 dimers. *J. Immunol.*, 2006. **176**: p. 5438-5445.
64. Kern, P., et al., Expression, purification, and functional analysis of murine ectodomain fragments of CD8αα and CD8αβ dimers. *Biol. Chem.*, 1999. **274**: p. 27237-27243.
65. Moebius, U., et al., Expression of different CD8 isoforms on distinct human lymphocyte subpopulations. *Eur. J. Immunol.*, 1991. **21**: p. 1793-1800.

66. Renard, V., et al., CD8β increases CD8 coreceptor function and participation in TCR-ligand binding. *J. Exp. Med.*, 1996. **184**: p. 2439-2444.
67. Leishman, A.J., et al., T cell responses modulated through interaction between CD8αα and the nonclassical MHC class I molecule. *Science*, 2001. **294**: p. 1936-1939.
68. Salter, R.D., et al., A binding site for the T-cell co-receptor CD8 on the α 3 domain of HLA-A2. *Nature*, 1990. **345**: p. 41-46.
69. Konig, R., et al., MHC class II interaction with CD4 mediated by a region analogous to the MHC class I binding site for CD8. *Nature*, 1992. **356**: p. 796-798.
70. Cammarota, G., et al., Identification of a CD4 binding site on the β 2 domain of HLA-DR molecules. *Nat. Immunol.*, 1992. **356**: p. 799-801.
71. Cresswell, P., Assembly and transport of class I MHC-peptide complexes. *Annu. Rev. Immunol.*, 1994. **12**: p. 259-291.
72. Wolf, P.R. and H.L. Ploegh, How MHC class II molecules acquire peptide cargo: biosynthesis and trafficking through the endocytic pathway. *Annu. Rev. Cell Dev. Biol.*, 1995. **11**: p. 267-306.
73. Wang, J.H., et al., Crystal structure of the human CD4 N-terminal two-domain fragment complexed to a class II MHC molecule. *Proc. Natl. Acad. Sci. USA*, 2001. **98**: p. 10799-10804.
74. Gao, G.F., et al., Molecular coordination of αβ T-cell receptors and coreceptors CD8 and CD4 in their recognition of peptide-MHC ligands. *Trends Immunol.*, 2002. **23**: p. 408-413.
75. Thome, M., et al., Syk and ZAP-70 mediate recruitment of p56lck/CD4 to the activated T cell receptor/CD3/ζ complex. *J. Exp. Med.*, 1995. **181**: p. 1997-2006.
76. Thome, M., et al., The p56lck SH2 domain mediates recruitment of CD8/p56lck to the activated T cell receptor/CD3/ζ complex. *Eur. J. Immunol.*, 1996. **26**: p. 2093-2100.
77. Irvine, D.J., et al., Direct observation of ligand recognition by T cells. *Nature*, 2002. **419**: p. 845-849.
78. Ratnofsky, S.E., et al., Expression and function of CD8 in a murine T cell hybridoma. *J. Exp. Med.*, 1987. **166**: p. 1747-1757.
79. MacDonald, H.R., et al., Inhibition of Tcell-mediated cytolysis by monoclonal antibodies directed against Lyt-2: heterogeneity of inhibition at the clonal level. *J. Immunol.*, 1981. **126**: p. 1671-1675.
80. Wyer, J.R., et al., T cell receptor and coreceptor CD8 αα bind peptide-MHC independently and with distinct kinetics. *Immunity*, 1999. **10**: p. 219-225.

81. Veillette, A., et al., The CD4 and CD8 T cell surface antigens are associated with the internal membrane tyrosine-protein kinase $p56^{Lck}$. *Cell*, 1988. **55**: p. 301-308.
82. Xu, H. and D.R. Littman, A kinase-independent function of Lck in potentiating antigen-specific T cell activation. *Cell*, 1993. **74**: p. 633-643.
83. Schwartz, R.H., T cell anergy. *Annu. Rev. Immunol.*, 2003. **21**: p. 305-334.
84. Tivol , E.A., et al., Loss of CTLA-4 leads to massive lymphoproliferation and fatal multiorgan tissue destruction, revealing a critical negative regulatory role of CTLA-4. *Immunity*, 1995. **3**: p. 541-547.
85. Waterhouse, P., et al., Lymphoproliferative disorders with early lethality in mice deficient in CTLA-4. *Science*, 1995. **270**: p. 985-988.
86. Greene, J.L., et al., Covalent dimerization of CD28/CTLA-4 and oligomerization of CD80/CD86 regulate T cell costimulatory interactions. *J. Biol. Chem.*, 1996. **271**: p. 26762-26771.
87. Peach, R.J., et al., Complementarity determining region 1 (CDR1)- and CDR3-analogous regions in CTLA-4 and CD28 determine the binding to B7-1. *J. Exp. Med.*, 1994. **180**: p. 2049-2058.
88. Gross, J., et al., Identification and distribution of the costimulatory receptor CD28 in the mouse. *J. Immunol.*, 1992. **149**: p. 380-388.
89. Perkins, D., et al., Regulation of CTLA-4 expression during T cell activation. *J. Immunol.*, 1996. **156**: p. 4154-4159.
90. Hathcock, K.S., et al., Comparative analysis of B7-1 and B7-2 costimulatory ligands: expression and function. *J. Exp. Med.*, 1994. **180**: p. 631-640.
91. Lenschow, D.J., et al., Expression and functional significance of an additional ligand for CTLA-4. *Proc. Natl. Acad. Sci. USA*, 1993. **90**: p. 11054-11058.
92. van der Merwe, P.A., et al., CD80 (B7-1) binds both CD28 and CTLA-4 with a low affinity and very fast kinetics. *J. Exp. Med.*, 1997. **185**: p. 393-403.
93. Collins, A.V., et al., The interaction properties of costimulatory molecules revisited. *Immunity*, 2002. **17**: p. 201-210.
94. Evans, E.J., et al., Crystal structure of a soluble CD28-Fab complex. *Nat. Immunol.*, 2005: p. 271 - 279.
95. Stamper, C.C., et al., Crystal structure of the B7-1/CTLA-4 complex that inhibits human immune responses. *Nature*, 2001. **410**: p. 608-611.
96. Ikemizu, S., et al., Structure and dimerization of a soluble form of B7-1. *Immunity*, 2000. **12**: p. 51-60.
97. Bhatia, S., et al., Different cell surface oligomeric states of B7-1 and B7-2: Implications for signalling. *Proc. Natl. Acad. Sci. USA*, 2005. **102** p. 15569-15574

98. Zhang, X., et al., Crystal structure of the receptor-binding domain of human B7-2: insights into organization and signalling. *Proc. Natl. Acad. Sci. USA*, 2003. **100**: p. 2586-2591.
99. Schwartz, J.C., et al., Structural basis for co-stimulation by the human CTLA-4/B7-2 complex. *Nat. Immunol.*, 2001. **410**: p. 604-608.
100. Pentcheva-Hoang, T., et al., B7-1 and B7-2 selectively recruit CTLA-4 and CD28 to the immunological synapse. *Immunity*, 2004. **21**: p. 401-413.
101. Dennehy, K.M., et al., Cutting edge: monovalency of CD28 maintains the antigen dependence of T cell costimulatory responses. *J. Immunol.*, 2006. **176**: p. 5725-5729.
102. Jansson, A., et al., A theoretical framework for quantitative analysis of the molecular basis of costimulation. *J. Immunol.*, 2005. **175**(3): p. 1575-1585.
103. Kishihara, K., et al., Normal B lymphocyte development but impaired T cell maturation in CD45-exon 6 protein tyrosine phosphatase-deficient mice. *Cell*, 1993. **74**: p. 143-156.
104. Kozieradzki, I., et al., T cell development in mice expressing splice variants of the protein tyrosine phosphatase CD45. *J. Immunol.*, 1997. **158**(7): p. 3130-3139.
105. Byth, K.F., et al., CD45-null transgenic mice reveal a positive regulatory role for CD45 in early thymocyte development, in the selection of CD4+CD8+ thymocytes, and B cell maturation. *J. Exp. Med.*, 1996. **183**(4): p. 1707-1718.
106. Koretzky, G.A., et al., Tyrosine phosphatase CD45 is essential for coupling T-cell antigen receptor to the phosphatidyl inositol pathway. *Nature*, 1990. **346**(6279): p. 66-68.
107. Thomas, M.L., The leukocyte common antigen family. *Annu. Rev. Immunol.*, 1989. **7**: p. 339-369.
108. Trowbridge, I.S. and T.M. L., CD45: an emerging role as a protein tyrosine phosphatase required for lymphocyte activation and development. *Annu. Rev. Immunol.*, 1994. **12**: p. 85-116.
109. Streuli, M., et al., Distinct functional roles of the two intracellular phosphatase like domains of the receptor-linked protein tyrosine phosphatases LCA and LAR. *EMBO J.*, 1990. **9**: p. 2399-2407.
110. Nam, H.-J., et al., Structural basis for the function and regulation of the receptor protein tyrosine phosphatase CD45. *J. Exp. Med.*, 2005. **201**: p. 441-452.
111. Holmes, N., CD45: all is not yet crystal clear. *Immunology*, 2006. **117**(2): p. 145-155.

112. Birkeland, M.L., et al., Changes in CD45 isoform expression accompany antigen-induced murine T-cell activation. *Proc. Natl. Acad. Sci. USA*, 1989. **86**(17): p. 6734-6738.
113. Ogilvy, S., et al., Either of the CD45RB and CD45RO isoforms are effective in restoring T cell, but not B cell, development and function in CD45-null mice. *J. Immunol.*, 2003. **171**(4): p. 1792-1800.
114. Tchilian, E.Z., et al., Altered CD45 isoform expression affects lymphocyte function in CD45 Tg mice. *Int. Immunol.*, 2004. **16**: p. 1323-1332.
115. Desai, D.M., et al., Ligand-mediated negative regulation of a chimeric transmembrane receptor tyrosine phosphatase. *Cell*, 1993. **73**: p. 541-554.
116. Majeti, R., et al., Dimerization-induced inhibition of receptor protein tyrosine phosphatase function through an inhibitory wedge. *Science*, 1998. **279**: p. 88-91.
117. Nam, H.-J., et al., Crystal structure of the tandem phosphatase domains of RPTP LAR. *Cell*, 1999. **97**: p. 449-457.
118. Majeti, R., et al., An inactive point mutation in the inhibitory wedge of CD45 causes lymphoproliferation and autoimmunity. *Cell*, 2000. **103**: p. 1059-1070.
119. Dornan, S., et al., Differential association of CD45 with CD4 and CD8 regulates the actions of specific pools of p56Lck tyrosine kinase in T cell antigen receptor signal transduction. *J. Biol. Chem.*, 2002. **277**: p. 1912-1918.
120. Xu, Z. and A. Weiss, Negative regulation of CD45 by differential homodimerization of the alternative spliced isoforms *Nat. Immunol.*, 2002. **3**: p. 764-771.
121. Symons, A., et al., Domain organization of the extracellular region of CD45. *Protein Eng.*, 1999. **12**: p. 885-892.
122. Felberg, J. and P. Johnson, Characterization of recombinant CD45 cytoplasmic domain proteins. Evidence for intramolecular and intermolecular interactions. *J. Biol. Chem.*, 1998. **273**: p. 17839-17845.
123. Meng, K., et al., Pleiotrophin signals increased tyrosine phosphorylation of β -catenin through inactivation of the intrinsic catalytic activity of the receptor-type protein tyrosine phosphatase β/ζ. *Proc. Natl. Acad. Sci. USA*, 2000. **97**(6): p. 2603-2608.
124. Johnson, K.G., et al., The HSPGs syndecan and dallylike bind the receptor phosphatase LAR and exert distinct effects on synaptic development. *Neuron*, 2006. **49**(4): p. 517-531.
125. Chagnon, M.J., et al., Functional significance of the LAR receptor protein tyrosine phosphatase family in development and diseases. *Biochem. Cell Biol.*, 2004. **82**: p. 664-675.

126. Alonso, A., et al., Protein tyrosine phosphatases in the human genome. *Cell*, 2004. **117**: p. 699-711.
127. Blanchetot, C., et al., Regulation of receptor protein-tyrosine phosphatase alpha by oxidative stress. *EMBO J.*, 2002. **21**: p. 493-503.
128. Irles, C., et al., CD45 ectodomain controls interaction with GEMs and Lck activity for optimal TCR signaling. *Nat. Immunol.*, 2002. **4**: p. 189-197.
129. Choudhuri, K., et al., T-cell receptor triggering is critically dependent on the dimensions of its peptide-MHC ligand. *Nature*, 2005. **436**: p. 578-582.
130. Moingeon, P., et al., The structural biology of CD2. *Immunol. Rev.*, 1989. **111**: p. 111-44.
131. Dustin, M.L., et al., Purified lymphocyte function-associated antigen 3 binds to CD2 and mediates T lymphocyte adhesion. *J. Exp. Med.*, 1987. **165**: p. 677-692.
132. Kato, K., et al., CD48 is a counter-receptor for mouse CD2 and is involved in T cell activation. *J. Exp. Med.*, 1992. **176**: p. 1241-1249.
133. Arulanandam, A.R., et al., Interaction between human CD2 and CD58 involves the major β sheet surface of each of their respective adhesion domains. *J. Exp. Med.*, 1994. **180**: p. 1861-1871.
134. Bodian, D.L., et al., Crystal structure of the extracellular region of the human cell adhesion molecule CD2 at 2.5 A resolution. *Structure*, 1994. **2**: p. 755-766.
135. Evans, E.J., et al., Crystal structure and binding properties of the CD2 and CD244 (2B4)-binding protein, CD48. *J. Biol. Chem.*, 2006. **281**: p. 29309-29320.
136. Dustin, M.L., et al., Low affinity interaction of human or rat T cell adhesion molecule CD2 with its ligand aligns adhering membranes to achieve high physiological affinity. *J. Biol. Chem.*, 1997. **272**: p. 30889-30898.
137. Ikemizu, S., et al., Crystal structure of the CD2-binding domain of CD58 (lymphocyte function-associated antigen 3) at 1.8-A resolution. *Proc. Natl. Acad. Sci. USA*, 1999. **96**(8): p. 4289-4294.
138. Wang, J.-h., et al., Structure of a heterophilic adhesion complex between the human CD2 and CD58 (LFA-3) counterreceptors. *Cell*, 1999. **97**(6): p. 791-803.
139. van der Merwe, P.A., et al., Topology of the CD2-CD48 cell-adhesion molecule complex: implications for antigen recognition by T cells. *Curr. Biol.*, 1995. **5**: p. 74-84.
140. Kim, M., et al., Molecular dissection of the CD2-CD58 counter-receptor interface identifies CD2 Tyr86 and CD58 Lys34 residues as the functional "hot spot". *J. Mol. Biol.*, 2001. **312**: p. 711-720.

141. Davis, S.J., et al., The role of charged residues mediating low affinity protein-protein recognition at the cell surface by CD2. *Proc. Natl. Acad. Sci. USA*, 1998. **95**: p. 5490-5494.
142. Zhu, B., et al., Direct measurements of heterotypic adhesion between the cell surface proteins CD2 and CD48. *Biochemistry*, 2002. **41**: p. 12163-12170.
143. Bachmann, M.F., et al., CD2 sets quantitative thresholds in T cell activation. *J. Exp. Med.*, 1999. **190**: p. 1383-1392.
144. Dustin, M.L., et al., A novel adaptor protein orchestrates receptor patterning and cytoskeletal polarity in T-cell contacts. *Cell*, 1998. **94**: p. 667-677.
145. Li, J., et al., A cdc15-like adaptor protein (CD2BP1) interacts with the CD2 cytoplasmic domain and regulates CD2-triggered adhesion. *EMBO J.*, 1998. **24**: p. 7320-7336.
146. Nishizawa, K., et al., Identification of a proline-binding motif regulating CD2-triggered T lymphocyte activation. *Proc. Natl. Acad. Sci. USA*, 1998. **95**(25): p. 14897-14902.
147. Carmo, A.M., et al., Physical association of the cytoplasmic domain of CD2 with the tyrosine kinases p56lck and p59fyn. *Eur. J. Immunol.*, 1993. **23**: p. 2196-2201.
148. Bell, G.M., et al., The SH3 domain of p56lck binds to proline-rich sequences in the cytoplasmic domain of CD2. *J. Exp. Med.*, 1996. **183**: p. 169-178.
149. Lin, H., et al., Association of p59fyn with the T lymphocyte costimulatory receptor CD2. Binding of the Fyn Src homology (SH) 3 domain is regulated by the Fyn SH2 domain. *J. Biol. Chem.*, 1998. **273**(31): p. 19914-19921.
150. Meuer, S.C., et al., An alternative pathway of T-cell activation: a functional role for the 50 kd T11 sheep erythrocyte receptor protein. *Cell*, 1984. **36**: p. 897-906.
151. Bierer, B.E., et al., Synergistic T cell activation via the physiological ligands for CD2 and the T cell receptor. *J. Exp. Med.*, 1988. **168**: p. 1145-56.
152. Gollob, J.A., et al., CD2 regulates responsiveness of activated T cells to interleukin 12. *J. Exp. Med.*, 1995. **182**: p. 721-31.
153. Gollob, J.A., et al., Molecular interaction between CD58 and CD2 counter-receptors mediates the ability of monocytes to augment T cell activation by IL-12. *J. Immunol.*, 1996. **157**: p. 1886-1893.
154. Boussiotis, V.A., et al., CD2 is involved in maintenance and reversal of human alloantigen-specific clonal anergy. *J. Exp. Med.*, 1994. **180**: p. 1665-1673.
155. Killeen, N., et al., Development and function of T cells in mice with a disrupted CD2 gene. *EMBO J.*, 1992. **11**: p. 4329-4336.

156. Evans, C.F., et al., CD2-deficient mice generate virus-specific cytotoxic T lymphocytes upon infection with lymphocytic choriomeningitis virus. *J. Immunol.*, 1993. **151**: p. 6259-6264.
157. Aruffo, A., et al., The lymphocyte glycoprotein CD6 contains a repeated domain structure characteristic of a new family of cell surface and secreted proteins *J. Exp. Med.*, 1991. **174**: p. 949-952.
158. Aruffo, A., et al., CD6-ligand interactions: a paradigm for SRCR domain function? *Immunol. Today*, 1997. **18**: p. 498-504
159. Robinson, W.H., et al., Human CD6 possesses a large, alternatively spliced cytoplasmic domain. *Eur. J. Immunol.*, 1995. **25**: p. 2765-2769.
160. Robinson, W.H., et al., Identification of a mouse protein homologous to the human CD6 T cell surface protein and sequence of the corresponding cDNA. *J. Immunol.*, 1995. **155**: p. 4739-4748.
161. Whitney, G., et al., Cloning and characterization of murine CD6. *Mol. Immunol*, 1995. **32**: p. 89-92.
162. Bowen, M.A., et al., The amino-terminal immunoglobulin-like domain of activated leukocyte cell adhesion molecule binds specifically to the membrane-proximal scavenger receptor cysteine-rich domain of CD6 with a 1:1 stoichiometry. *J. Biol. Chem.*, 1996. **29**: p. 17390-17396.
163. Whitney, G.S., et al., The membrane-proximal scavenger receptor cysteine-rich domain of CD6 contains the activated leukocyte cell adhesion molecule binding site. *J. Biol. Chem.*, 1995. **270**: p. 18187-18190.
164. Hassan, N.J., et al., Optimal T cell activation requires the engagement of CD6 and CD166. *Eur. J. Immunol.*, 2004. **34**: p. 930-940
165. Patel, D.D., et al., Identification and characterization of a 100-kD ligand for CD6 on human thymic epithelial cells. *J. Exp. Med.*, 1995. **181**(4): p. 1563-1568.
166. Gangemi, R.M., et al., Anti-T12, an anti-CD6 monoclonal antibody, can activate human T lymphocytes. *J. Immunol.*, 1989. **143**(8): p. 2439-2447.
167. Bott, C.M., et al., Activation of human T cells through CD6: functional effects of a novel anti-CD6 monoclonal antibody and definition of four epitopes of the CD6 glycoprotein. *Int. Immunol.*, 1993. **5**(7): p. 783-792.
168. Osorio, L.M., et al., The anti-CD6 mAb, IOR-T1, defined a new epitope on the human CD6 molecule that induces greater responsiveness in T cell receptor/CD3-mediated T cell proliferation. *Cell. Immunol.*, 1994 **154**: p. 123-133.
169. Hassan, N.J., et al., CD6 regulates T-cell responses through activation-dependent recruitment of the positive regulator SLP-76. *Mol. Cell. Biol.*, 2006. **26**: p. 6727-6738.

170. Gimferrer, I., et al., Relevance of CD6-mediated interactions in T cell activation and proliferation. *J. Immunol.*, 2004. **173**: p. 2262-2270
171. Zimmerman, A.W., et al., Long-term engagement of CD6 and ALCAM is essential for T-cell proliferation induced by dendritic cells. *Blood*, 2006. **107**(8): p. 3212-3220.
172. Singer, N.G., et al., CD6: expression during development, apoptosis and selection of human and mouse thymocytes. *Int. Immunol.*, 2002. **14**(6): p. 585-597.
173. Gimferrer, I., et al., The accessory molecules CD5 and CD6 associate on the membrane of lymphoid T cells. *J. Biol. Chem.*, 2003. **278**: p. 8564–8571.
174. Castro, M.A.A., et al., OX52 is the rat homologue of CD6: evidence for an effector function in the regulation of CD5 phosphorylation. *J. Leukocyte Biol.*, 2003. **73**: p. 183-190.
175. Saifullah, M.K., et al., Expression and characterization of a novel CD6 ligand in cells derived from joint and epithelial tissues. *J. Immunol.*, 2004. **173**(10): p. 6125-6133.
176. Wee, S., et al., Tyrosine phosphorylation of CD6 by stimulation of CD3: augmentation by the CD4 and CD2 coreceptors. *J. Exp. Med.*, 1993. **177**(1): p. 219-223.
177. Gimferrer, I., et al., The lymphocyte receptor CD6 interacts with syntenin-1, a scaffolding protein containing PDZ domains. *J. Immunol.*, 2005. **175**: p. 1406-1414.
178. Brett, D., et al., EST comparison indicates 38% of human mRNAs contain possible alternative splice forms. *FEBS Lett.*, 2000. **474**: p. 83-86.
179. Croft, L., et al., ISIS, the intron information system, reveals the high frequency of alternative splicing in the human genome. *Nat. Genet.*, 2000. **24**: p. 340-341.
180. Kan, Z., et al., Gene structure prediction and alternative splicing analysis using genomically aligned ESTs. *Genome Res.*, 2001. **11**: p. 889-900.
181. Mironov, A.A., et al., Frequent alternative splicing of human genes. *Genome Res.*, 1999. **9**: p. 1288-1293
182. Modrek, B., et al., Genome-wide detection of alternative splicing in expressed sequences of human genes. *Nucleic Acids Res.*, 2001. **29**(13): p. 2850-2859.
183. Schmucker, D. and J.G. Flanagan, Generation of recognition diversity in the nervous system. *Neuron*, 2004. **44**: p. 219-222.
184. Watson, F.L., et al., Extensive diversity of Ig-superfamily proteins in the immune system of insects. *Science*, 2005. **309**: p. 1874-1878.
185. Black, D.L., Protein diversity from alternative splicing: a challenge for bioinformatics and post-genome biology. *Cell. Immunol.*, 2000. **103**: p. 367-370.

186. Graveley, B.R., Alternative splicing: increasing diversity in the proteomic world. *Trends Genet.*, 2001. **17**: p. 100-107.
187. Matlin, A.J., et al., Understanding alternative splicing: towards a cellular code. *Nat. Rev. Mol. Cell Biol.*, 2005. **6**: p. 386-398.
188. Lynch, K.W., Consequences of regulated pre-mRNA splicing in the immune system. *Nature*, 2004. **4**: p. 931-940.
189. Shin, C. and J.L. Manley, Cell signalling and the control of pre-mRNA splicing. *Nat. Rev. Mol. Cell Biol.*, 2004. **5**: p. 727-738.
190. Pawlak, E., et al., The soluble CTLA-4 receptor: a new marker in autoimmune diseases. *Arch. Immunol. Ther. Exp.*, 2005. **53**: p. 336-341.
191. Teft, W.A., et al., A molecular perspective of CTLA-4 function. *Annu. Rev. Immunol.*, 2006. **24**(1): p. 65-97.
192. Gunthert, U., et al., A new variant of glycoprotein CD44 confers metastatic potential to rat carcinoma cells. *Cell*, 1991. **65**: p. 13-24.
193. Eisterer, W., et al., CD44 isoforms are differentially regulated in plasma cell dyscrasias and CD44v9 represents a new independent prognostic parameter in multiple myeloma. *Leukemia Res.*, 2001. **25**: p. 1051-1057.
194. Bartolazzi, A., et al., Regulation of growth and dissemination of a human lymphoma by CD44 splice variants. *J. Cell Sci.*, 1995. **108**(4): p. 1723-1733.
195. Jacobsen, M., et al., A point mutation in PTPRC is associated with the development of multiple sclerosis. *Nat. Genet.*, 2000 **26**: p. 495-499.
196. Furukawa, S., et al., Soluble CD2 levels in serum during acute Kawasaki disease and infectious mononucleosis. *J. Infect Dis.*, 1993 **167**: p. 778-779.
197. Ueda, H., et al., Association of the T-cell regulatory gene CTLA4 with susceptibility to autoimmune disease. *Nature*, 2003. **423**: p. 506-11.
198. van der Merwe, P.A., The TCR Triggering Puzzle. *Immunity*, 2001. **14**: p. 665-668.
199. Trautmann, A. and C. Randriamampita, Initiation of TCR signalling revisited. *Trends Immunol.*, 2003. **24**(8): p. 425-428.
200. Krogsgaard, M. and M.M. Davis, How T cells 'see' antigen. *Nat. Immunol.*, 2005. **6**: p. 239-245.
201. Delon, J., et al., CD8 expression allows T cell signaling by monomeric peptide-MHC complexes. *Immunity*, 1998. **9**: p. 467-473.
202. Ge, Q., et al., Soluble peptide-MHC monomers cause activation of CD8+ T cells through transfer of the peptide to T cell MHC molecules. *Proc. Natl. Acad. Sci. USA*, 2002. **99**(21): p. 13729-13734.

203. Schott, E., et al., Class I negative CD8 T cells reveal the confounding role of peptide-transfer onto CD8 T cells stimulated with soluble H2-Kb molecules. *Proc. Natl. Acad. Sci. USA*, 2002. **99**(21): p. 13735-13740.
204. Krogsgaard, M., et al., Agonist/endogenous peptide-MHC heterodimers drive T cell activation and sensitivity. *Nature*, 2005. **434**: p. 238-243.
205. Locksley, R.M., et al., Helper T cells without CD4: control of leishmaniasis in CD4-deficient mice. *Science*, 1993. **261**(5127): p. 1448-1451.
206. Schilham, M.W., et al., Alloreactive cytotoxic T cells can develop and function in mice lacking both CD4 and CD8. *Eur. J. Immunol.*, 1993. **23**: p. 1299-1304.
207. Sporri, R. and C. Reis e Sousa, Self peptide/MHC class I complexes have a negligible effect on the response of some CD8+ T cells to foreign antigen. *Eur. J. Immunol.*, 2002. **32**.
208. Davis, S.J. and P.A. van der Merwe, The kinetic-segregation model: TCR triggering and beyond. *Nat. Immunol.*, 2006. **7**(8): p. 803-809.
209. Lin, J. and A. Weiss, The tyrosine phosphatase CD148 is excluded from the immunologic synapse and down-regulates prolonged T cell signaling. *J. Cell Biol.*, 2003. **162**(4): p. 673-682.
210. Bergman, M., et al., The human p50csk tyrosine kinase phosphorylates p56lck at Tyr-505 and down regulates its catalytic activity. *EMBO J.*, 1992. **11**: p. 2919-2924.
211. Nada, S., et al., Cloning of a complementary DNA for a protein-tyrosine kinase that specifically phosphorylates a negative regulatory site of p60c-src. *Nature*, 1991. **351**: p. 69-72.
212. Okada, M., et al., CSK: a protein-tyrosine kinase involved in regulation of src family kinases. *J. Biol. Chem.*, 1991. **266**: p. 24249-24252.
213. Mustelin, T. and A. Altman, Dephosphorylation and activation of the T cell tyrosine kinase pp56lck by the leukocyte common antigen (CD45). *Oncogene*, 1990. **5**: p. 809-13.
214. Wange, R.L. and L.E. Samelson, Complex complexes: signaling at the TCR. *Immunity*, 1996. **5**: p. 197-205.
215. Iwashima, M., et al., Sequential interactions of the TCR with two distinct cytoplasmic tyrosine kinases. *Science*, 1994. **263**: p. 1136-1139.
216. Berridge, M.J., et al., Calcium - a life and death signal. *Nature*, 1998. **395**(6703): p. 645-648.
217. Hogan, P.G., et al., Transcriptional regulation by calcium, calcineurin, and NFAT. *Gene Dev.*, 2003. **17**(18): p. 2205-2232.

218. Ghosh, S., et al., NF-κB and Rel proteins: evolutionarily conserved mediators of immune responses. *Annu. Rev. Immunol.*, 1998. **16**: p. 225-260.
219. Blanchard, J.M., Small GTPases, adhesion, cell cycle control and proliferation. *Pathol. Biol.*, 2000. **48**: p. 318-327.
220. Blomberg, N., et al., The PH superfold: a structural scaffold for multiple functions. *Trends Biochem. Sci.*, 1999. **24**: p. 441-445.
221. Alessi, D.R. and P. Cohen, Mechanism of activation and function of protein kinase B. *Curr. Opin. Genet. Dev.*, 1998. **8**: p. 55-62.
222. Billadeau, D.D., et al., Regulation of T-cell activation by the cytoskeleton. *Nat. Rev. Immunol.*, 2007. **7**: p. 131-143.
223. Leibson, P.J., The regulation of lymphocyte activation by inhibitory receptors. *Curr. Opin. Immunol.*, 2004. **16**: p. 328-336.
224. Manning, G., et al., The Protein Kinase Complement of the Human Genome. *Science*, 2002. **298**(5600): p. 1912-1934.
225. Gjorloff-Wingren, A., et al., Characterization of TCR-induced receptor-proximal signaling events negatively regulated by the protein tyrosine phosphatase PEP. *Eur. J. Immunol.*, 1999. **29**: p. 3845-3854.
226. Cloutier, J.-F. and A. Veillette, Cooperative Inhibition of T-Cell Antigen Receptor Signaling by a Complex between a Kinase and a Phosphatase. *J. Exp. Med.*, 1999. **189**(1): p. 111-121.
227. Brdika, T., et al., Phosphoprotein associated with glycosphingolipid-enriched microdomains (PAG), a novel ubiquitously expressed transmembrane adaptor protein, binds the protein tyrosine kinase Csk and is involved in regulation of T cell activation. *J. Exp. Med.*, 2000. **191**(9): p. 1591-1604.
228. Kawabuchi, M., et al., Transmembrane phosphoprotein Cbp regulates the activities of Src-family tyrosine kinases. *Nat. Genet.*, 2000. **404**: p. 999-1003.
229. Andoniou, C.E., et al., The Cbl proto-oncogene product negatively regulates the Src-family tyrosine kinase Fyn by enhancing its degradation. *Mol. Cell. Biol.*, 2000. **20**(3): p. 851-867.
230. Rao, N., et al., Negative regulation of Lck by Cbl ubiquitin ligase. *Proc. Natl. Acad. Sci. USA*, 2002. **99**(6): p. 3794-3799.
231. Greenwald, R.J., et al., The B7 family revisited *Annu. Rev. Immunol.*, 2005. **23**(1): p. 515-548.
232. Brunner, M.C., et al., CTLA-4-mediated inhibition of early events of T cell proliferation. *J. Immunol.*, 1999. **162**(10): p. 5813-5820.
233. Walunas, T.L., et al., CTLA-4 ligation blocks CD28-dependent T cell activation. *J. Exp. Med.*, 1996. **183**(6): p. 2541-2550.

234. Chemnitz, J.M., et al., SHP-1 and SHP-2 associate with immunoreceptor tyrosine-based switch motif of programmed death 1 upon primary human T cell stimulation, but only receptor ligation prevents T cell activation. *J. Immunol*, 2004. **173**: p. 945-954.
235. Watanabe, N., et al., BTLA is a lymphocyte inhibitory receptor with similarities to CTLA-4 and PD-1. *Nat. Immunol.*, 2003. **4**: p. 670-679.
236. Tarakhovsky, A., et al., A role for CD5 in TCR-mediated signal transduction and thymocyte selection. *Science*, 1995. **269**: p. 535-537.
237. Jacobelli, J., et al., New views of the immunological synapse: variations in assembly and function. *Curr. Opin. Immunol.*, 2004. **16**(3): p. 345-352.
238. Bromley, S.K., et al., The immunological synapse. *Annu. Rev. Immunol.*, 2001. **19**: p. 375-396.
239. Allenspach, E.J., et al., ERM-dependent movement of CD43 defines a novel protein complex distal to the immunological synapse. *Immunity*, 2001. **15**: p. 739-750.
240. Favier, B., et al., Uncoupling between immunological synapse formation and functional outcome in human γδ T lymphocytes. *J. Immunol.*, 2003. **171**(10): p. 5027-5033.
241. Tseng, S.-Y., et al., CD80 cytoplasmic domain controls localization of CD28, CTLA-4, and protein kinase Cθ in the immunological synapse. *J. Immunol.*, 2005. **175**(12): p. 7829-7836.
242. Favier, B., et al., TCR dynamics on the surface of living T cells. *Int. Immunol.*, 2001. **13**(12): p. 1525-1532.
243. Das, V., et al., Activation-induced polarized recycling targets T cell antigen receptors to the immunological synapse; involvement of SNARE complexes. *Immunity*, 2004. **20**: p. 577-588.
244. Huse, M., et al., T cells use two directionally distinct pathways for cytokine secretion. *Nat. Immunol.*, 2006. **7**: p. 247-255.
245. van der Merwe, P.A., et al., Cytoskeletal polarization and redistribution of cell surface molecules during T cell antigen recognition. *Semin. Immunol.*, 2000. **12**: p. 5-21.
246. Dustin, M.L. and J.A. Cooper, The immunological synapse and the actin cytoskeleton: molecular hardware for T cell signaling. *Nat. Immunol.*, 2000. **1**: p. 23-29.
247. Grakoui, A., et al., The immunological synapse: a molecular machine controlling T cell activation. *Science*, 1999. **285**: p. 221-227.

248. Sumen, C., et al., T cell receptor antagonism interferes with MHC clustering and integrin patterning during immunological synapse formation. *J. Cell Biol.*, 2004. **166**: p. 579-590.
249. Brossard, C., et al., Multifocal structure of the T cell-dendritic cell synapse. *Eur. J. Immunol.*, 2005. **35**: p. 1741-1753.
250. Richie, L.I., et al., Imaging synapse formation during thymocyte selection: Inability of CD3ζ to form a stable central accumulation during negative selection. *Immunity*, 2002. **16**: p. 595-606.
251. Friedl, P., et al., Tuning immune responses: diversity and adaptation of the immunological synapse. *Nat. Rev. Immunol.*, 2005. **5**: p. 532-545.
252. Lee, K.H., et al., The immunological synapse balances T cell receptor signaling and degradation. *Science*, 2003. **302**: p. 1218-1222.
253. O'Keefe, J.P., et al., Formation of a central supramolecular activation cluster is not required for activation of naive CD8+ T cells. *Proc. Natl. Acad. Sci. USA*, 2004. **101**(25): p. 9351-9356.
254. Purbhoo, M.A., et al., T cell killing does not require the formation of a stable mature immunological synapse. *Nat. Immunol.*, 2004. **5**: p. 524-530.
255. O'Keefe, J.P. and T.F. Gajewski, Cutting edge: cytotoxic granule polarization and cytolysis can occur without central supramolecular activation cluster formation in CD8+ effector T cells. *J. Immunol.*, 2005. **175**: p. 5581-5585.
256. Faroudi, M., et al., From the cover: lytic versus stimulatory synapse in cytotoxic T lymphocyte/target cell interaction: manifestation of a dual activation threshold. *Proc. Natl. Acad. Sci. USA*, 2003. **100**(24): p. 14145-14150.
257. Zaru, R., et al., Cutting edge: TCR engagement and triggering in the absence of large-scale molecular segregation at the T cell-APC contact site. *J. Immunol.*, 2002. **168**(9): p. 4287-4291.
258. Lee, K.H., et al., T cell receptor signaling precedes immunological synapse formation. *Science*, 2002. **295**: p. 1539-1542.
259. Monks, C.R., et al., Three-dimensional segregation of supramolecular activation clusters in T cells. *Nature*, 1998. **395**: p. 82-86.
260. Dustin, M.L. and A.S. Shaw, Costimulation: building an immunological synapse. *Science*, 1999. **283**: p. 649-650.
261. Krummel, M.F., et al., Differential clustering of CD4 and CD3ζ during T Cell recognition. *Science*, 2000. **289**: p. 1349-1352.
262. Freiberg, B.A., et al., Staging and resetting T cell activation in SMACs. *Nat. Immunol.*, 2002. **3**: p. 911-917.

263. Campi, G., et al., Actin and agonist MHC-peptide complex-dependent T cell receptor microclusters as scaffolds for signaling. *J. Exp. Med.*, 2005. **202**(8): p. 1031-1036.
264. Yokosuka, T., et al., Newly generated T cell receptor microclusters initiate and sustain T cell activation by recruitment of Zap70 and SLP-76. *Nat. Immunol.*, 2005. **6**: p. 1253-1262.
265. Mossman, K.D., et al., Altered TCR signaling from geometrically repatterned immunological synapses. *Science*, 2005. **310**: p. 1191-1193.
266. Varma, R., et al., T cell receptor proximal signals are sustained in peripheral microclusters and terminated in the central supramolecular activation cluster. *Immunity*, 2006. **25**: p. 117-127.
267. Johnson, K.G., et al., A supramolecular basis for CD45 tyrosine phosphatase regulation in sustained T cell activation. *Proc. Natl. Acad. Sci. USA*, 2000. **97**: p. 10138-10143.
268. D'Oro, U. and J.D. Ashwell, Cutting edge: the CD45 tyrosine phosphatase is an inhibitor of Lck activity in thymocytes. *J. Immunol.*, 1999. **162**: p. 1879-1883.
269. Mustelin, T., et al., Regulation of the p70zap tyrosine protein kinase in T cells by the CD45 phosphotyrosine phosphatase. *Eur. J. Immunol.*, 1995. **25**: p. 942-946.
270. Leupin, O., et al., Exclusion of CD45 from the T-cell receptor signaling area in antigen-stimulated T lymphocytes. *Curr. Biol.*, 2000. **10**: p. 277-280.
271. Liu, H., et al., On the dynamics of TCR:CD3 complex cell surface expression and downmodulation. *Immunity*, 2000. **13**: p. 665-675.
272. Matsuo, H., et al., Role of LBPA and Alix in multivesicular liposome formation and endosome organization. *Science*, 2004. **303**: p. 531-534.
273. Weissman, A.M., Themes and variations on ubiquitylation. *Nat. Rev. Mol. Cell Biol.*, 2001. **2**: p. 169-178.
274. Wiedemann, A., et al., T-cell activation is accompanied by an ubiquitination process occurring at the immunological synapse. *Immunol Lett.*, 2005. **98**: p. 57-61.
275. Saito, T. and T. Yokosuka, Immunological synapse and microclusters: the site for recognition and activation of T cells. *Curr. Opin. Immunol.*, 2006. **18**(3): p. 305-313.
276. Shaw, A.S. and M.L. Dustin, Making the T cell receptor go the distance: a topological view of T cell activation. *Immunity*, 1997. **6**: p. 361-369.
277. Delon, J. and R.N. Germain, Information transfer at the immunological synapse. *Curr. Biol.*, 2000. **10**: p. 923-933.

278. Dustin, et al., Signaling takes shape in the immune system. *Cell*, 2000. **103**: p. 283-294.
279. van der Merwe, P.A. and S.J. Davis, The immunological synapse - A multitasking system. *Science*, 2002. **295**(5559): p. 1479-1480.
280. Davis, S.J. and P.A. van der Merwe, The immunological synapse: required for T cell receptor signalling or directing T cell effector function? *Curr. Biol.*, 2001. **11**: p. 289-289.
281. Stinchcombe, J.C., et al., The immunological synapse of CTL contains a secretory domain and membrane bridges. *Immunity*, 2001. **15**: p. 751-761.
282. Bromley, S.K., et al., The immunological synapse and CD28-CD80 interactions. *Nat. Immunol.*, 2001. **2**: p. 1159-1166.
283. Huppa, J.B., et al., Continuous T cell receptor signaling required for synapse maintenance and full effector potential. *Nat. Immunol.*, 2003. **4**(8): p. 749-755.
284. Utzny, C., et al., Analysis of peptide/MHC-induced TCR downregulation: deciphering the triggering kinetics. *Cell Biochem. Biophys.*, 2006. **46**: p. 101-11.
285. Faroudi, M., et al., Cutting edge: T lymphocyte activation by repeated immunological synapse formation and intermittent signaling. *J. Immunol.*, 2003. **171**(3): p. 1128-1132.
286. Depoil, D., et al., Immunological synapses are versatile structures enabling selective T cell polarization. *Immunity*, 2005. **22**: p. 185-194.
287. Wiedemann, A., et al., Cytotoxic T lymphocytes kill multiple targets simultaneously via spatiotemporal uncoupling of lytic and stimulatory synapses. *Proc. Natl. Acad. Sci. USA*, 2006. **103**(29): p. 10985-10990.
288. Dustin, M.L., et al., Visualization of the CD2 interaction with LFA-3 and determination of the two-dimensional dissociation constant for adhesion receptors in a contact area. *J. Cell Biol.*, 1996. **132**: p. 465-474.
289. Liu, S.J., et al., Intracellular mediators regulate CD2 lateral diffusion and cytoplasmic Ca2+ mobilization upon CD2-mediated T cell activation. *Biophys. J.*, 1995. **68**(2): p. 459-470.
290. Davis, S.J. and P.A. van der Merwe, The structure and ligand interactions of CD2: implications for T-cell function. *Immunol. Today*, 1996. **17**: p. 177-187.
291. Wild, M.K., et al., Dependence of T cell antigen recognition on the dimensions of an accessory receptor–ligand complex. *J. Exp. Med.*, 1999. **190**(1): p. 31-42.
292. Reits, E.A. and J.J. Neefjes, From fixed to FRAP: measuring protein mobility and activity in living cells. *Nat. Cell Biol.*, 2001 **3**: p. E145-E147.
293. Jacobson, K., et al., Lateral diffusion of proteins in membranes. *Annu. Rev. Physiol.*, 1987. **49**: p. 163-175.

294. Kusumi, A., et al., Paradigm shift of the plasma membrane concept from the two-dimensional continuum fluid to the partitioned fluid: high-speed single-molecule tracking of membrane molecules. *Annu. Rev. Biophys. Biomolec. Struct.*, 2005. **34**: p. 351-78.
295. Simons, K. and E. Ikonen, Functional rafts in cell membranes *Nature*, 1997. **387**(6633): p. 569-572.
296. Xavier, R., et al., Membrane compartmentation is required for efficient T cell activation. *Immunity*, 1998. **8**: p. 723-732.
297. Montixi, C., et al., Engagement of T cell receptor triggers its recruitment to low density detergent-insoluble membrane domains. *EMBO J.*, 1998. **17**: p. 5334-5348.
298. Harder, T. and M. Kuhn, Selective accumulation of raft-associated membrane protein LAT in T cell receptor signaling assemblies. *J. Cell Biol.*, 2000. **151**: p. 199-207.
299. Glebov, O.O. and B.J. Nichols, Lipid raft proteins have a random distribution during localized activation of the T-cell receptor. *Nat. Cell Biol.*, 2004. **6**(238-243).
300. Lenne, P.F., et al., Dynamic molecular confinement in the plasma membrane by microdomains and the cytoskeleton meshwork. *EMBO J.*, 2006.
301. Douglass, A.D. and R.D. Vale, Single-molecule microscopy reveals plasma membrane microdomains created by protein-protein networks that exclude or trap signaling molecules in T cells. *Cell. Immunol.*, 2005. **121**: p. 937-950.
302. van der Merwe, P.A. and A.N. Barclay, Analysis of cell-adhesion molecule interactions using surface plasmon resonance. *Curr. Opin. Immunol.*, 1996. **8**: p. 257-61.
303. Davis, S.J., et al., The nature of molecular recognition by T cells. *Nat. Immunol.*, 2003. **4**(3): p. 217-224.
304. van der Merwe, P.A. and S.J. Davis, Molecular interactions mediating T cell antigen recognition. *Annu. Rev. Immunol.*, 2003. **21**: p. 659–684.
305. Leckband, D., et al., Molecular mechanisms determining the strength of receptor-mediated intermembrane adhesion. *Biophys. J.*, 1995. **69**: p. 1162-1169.
306. Klemm, J.D., et al., Dimerization as a regulatory mechanism in signal transduction. *Annu. Rev. Immunol.*, 1998. **16**: p. 569-592.
307. Yarden, Y. and J. Schlessinger, Epidermal growth factor induces rapid, reversible aggregation of the purified epidermal growth factor receptor. *Biochemistry*, 1987. **26**: p. 1443-1451.
308. Ullrich, A. and J. Schlessinger, Signal transduction by receptors with tyrosine kinase activity. *Cell. Immunol.*, 1990. **61**: p. 203-212.

309. Lynch, G.W., et al., Direct evidence for native CD4 oligomers in lymphoid and monocytoid cells. *Eur. J. Immunol.*, 1999. **29**: p. 2590-2602.
310. Konig, R., et al., Involvement of both major histocompatibility complex class II alpha and beta chains in CD4 function indicates a role for ordered oligomerization in T cell activation. *J. Exp. Med.*, 1995. **182**: p. 779-787.
311. Sakihama, T.A.S. and E.L. Reinherz, Oligomerization of CD4 is required for stable binding to class II major histocompatibility complex proteins but not for interaction with human immunodeficiency virus gp120. *Proc. Natl. Acad. Sci. USA*, 1995. **92**: p. 6444-6448.
312. Weber, S. and K. Karjalainen, CD4 binds MHC class II with extremely low affinity. *Int. Immunol.*, 1993. **5**: p. 695-698.
313. Takeda, A., et al., Evidence for monomeric and dimeric forms of CD45 associated with a 30-KDa phosphorylated protein. *J. Biol. Chem.*, 1992. **267**(23): p. 16651-16659.
314. Bilwes, A., et al., Structural basis for inhibition of receptor protein-tyrosine phosphatase-α by dimerization. *Nature*, 1996. **382**: p. 555-559.
315. Brady, A.E. and L.E. Limbird, G protein-coupled receptor interacting proteins: emerging roles in localization and signal transduction. *Cell. Signal.*, 2002. **14**: p. 297-309.
316. Salahpour, A., et al., Functional significance of oligomerization of G-protein-coupled receptors. *Trends Endocrinol. Metab.*, 2000. **11**: p. 163-168.
317. Hebert, T.E., et al., A peptide derived from a β2-adrenergic receptor transmembrane domain inhibits both receptor dimerization and activation. *J. Biol. Chem.*, 1996. **271**(27): p. 16384-16392.
318. Cvejic, S. and L.A. Devi, Dimerization of the δ opioid receptor: implication for a role in receptor internalization *J. Biol. Chem.*, 1997. **272**(43): p. 26959-26964.
319. White, J.H., et al., Heterodimerization is required for the formation of a functional GABA(B) receptor. *Nature*, 1998. **396**: p. 679-682.
320. Jones, K.A., et al., GABA(B) receptors function as a heteromeric assembly of the subunits GABA(B)R1 and GABA(B)R2. *Nature*, 1998. **396**: p. 674-679.
321. Kaupmann, K., et al., GABAB-receptor subtypes assemble into functional heteromeric complexes. *Nature*, 1998. **396**(6712): p. 683-687.
322. Pfleger, K.D.G. and K.A. Eidne, Monitoring the formation of dynamic G-protein-coupled receptor–protein complexes in living cells. *Biochem. J.*, 2005. **385** p. 625-637.

323. Angers, S., et al., Dimerization: an emerging concept for G protein: coupled receptor ontogeny and function. *Annu. Rev. Pharmacol. Toxicol.*, 2002. **42**(1): p. 409-435.
324. Terrillon, S., et al., Oxytocin and vasopressin V1a, and V2 receptors form constitutive homo- and hetero-dimers during biosynthesis. *Mol. Endocrinol.*, 2002: p. 2002-0222.
325. Dinger, M.C., et al., Homodimerization of neuropeptide Y receptors investigated by fluorescence resonance energy transfer in living cells. *J. Biol. Chem.*, 2003: p. 10562-10571.
326. Jordan, B.A. and L.A. Devi, G-protein-coupled receptor heterodimerization modulates receptor function. *Nature*, 1999. **399**(6737): p. 697-700.
327. George, S.R., et al., Oligomerization of μ and δ opioid receptors: generation of novel functional properties. *J. Biol. Chem.*, 2000: p. 26128-26135.
328. Jordan, B.A., et al., Oligomerization of opioid receptors with beta 2-adrenergic receptors: A role in trafficking and mitogen-activated protein kinase activation. *Proc. Natl. Acad. Sci. USA*, 2001. **98**(1): p. 343-348.
329. Conn, P.M., et al., Conversion of a gonadotropin-releasing hormone antagonist to an agonist. *Nature*, 1982. **296**(5858): p. 653-655.
330. Carrithers, M.D. and M.R. Lerner, Synthesis and characterization of bivalent peptide ligands targeted to G-protein-coupled receptors. *Chem. Biol.*, 1996. **3**: p. 537-542.
331. Gregory, H., et al., Luteinizing hormone release from dissociated pituitary cells by dimerization of occupied LHRH receptors. *Nature*, 1982. **300**(5889): p. 269-271.
332. George, S.R., et al., A transmembrane domain-derived peptide inhibits D1 dopamine receptor function without affecting receptor oligomerization. *J. Biol. Chem.*, 1998. **273**(46): p. 30244-30248.
333. Piehler, J., New methodologies for measuring protein interactions in vivo and in vitro. *Curr. Opin. Struct. Biol.*, 2005. **15**: p. 4-14.
334. Haustein, E. and P. Schwille, Single-molecule spectroscopic methods. *Curr. Opin. Struct. Biol.*, 2004. **14**: p. 531-540.
335. Karlsson, R., SPR for molecular interaction analysis: a review of emerging application areas. *J. Mol. Recognit.*, 2004. **17**: p. 151-61.
336. Cooper, M.A., Label-free screening of bio-molecular interactions. *Anal. Bioanal. Chem.*, 2003. **377**: p. 834-842.
337. van der Merwe, P.A., et al., Affinity and kinetic analysis of the interaction of the cell adhesion molecules rat CD2 and CD48. *EMBO J*, 1993. **12**: p. 4945-4954.

338. van der Merwe, P.A., et al., Human cell-adhesion molecule CD2 binds CD58 (LFA-3) with a very low affinity and an extremely fast dissociation rate but does not bind CD48 or CD59*. Biochemistry*, 1994. **33**: p. 10149-10160.

339. Xu, Y., et al., A bioluminescence resonance energy transfer (BRET) system: Application to interacting circadian clock proteins*. Proc. Natl. Acad. Sci. USA*, 1999. **96** p. 151-156.

340. Förster, V.T., Zwischenmolekulare energiewanderung und fluoreszenz*. Ann. Physic.*, 1948. **6**: p. 54-75.

341. Ramsay, D., et al., Homo- and hetero-oligomeric interactions between G-protein-coupled receptors in living cells monitored by two variants of bioluminescence resonance energy transfer (BRET): hetero-oligomers between receptor subtypes form more efficiently than between less closely related sequences*. Biochem. J.*, 2002. **365** p. 429-440.

342. Arai, R., et al., Demonstration of a homogeneous noncompetitive immunoassay based on bioluminescence resonance energy transfer*. Anal. Biochem.*, 2001. **289**: p. 77-81.

343. Eidne, K.A., et al., Applications of novel resonance energy transfer techniques to study dynamic hormone receptor interactions in living cells*. Trends Endocrinol. Metab.*, 2002. **13**: p. 415-421.

344. Prinz, A., et al., Application of bioluminescence resonance energy transfer (BRET) for biomolecular interaction studies *ChemBioChem*, 2006. **7**(7): p. 1007-1012.

345. Ayoub, M.A., et al., Monitoring of ligand-independent dimerization and ligand-induced conformational changes of melatonin receptors in living cells by bioluminescence resonance energy transfer*. J. Biol. Chem.*, 2002. **277**: p. 21522-21528.

346. Pfleger, K.D., et al., Extended bioluminescence resonance energy transfer (eBRET) for monitoring prolonged protein-protein interactions in live cells*. Cell. Signal.*, 2006. **18**: p. 1664-1670.

347. Zola, H., et al., CD molecules 2006--human cell differentiation molecules*. J. Immunol. Methods*, 2007. **319**: p. 1-5.

348. Mercier, J.F., et al., Quantitative assessment of β1 and β2-adrenergic receptor homo- and heterodimerization by bioluminescence resonance energy transfer*. J. Biol. Chem.*, 2002. **277**: p. 44925-44931.

349. Maekawa, A., et al., Evidence for a domain-swapped CD4 dimer as the coreceptor for binding to class II MHC*. J. Immunol.*, 2006. **176**: p. 6873-6878.

350. Bourgeois, R., et al., Association between disruption of CD4 receptor dimerization and increased human immunodeficiency virus type 1 entry. *Retrovirology*, 2006. **3**: p. 31-38.
351. Gangemi, R.M., et al., Anti-T12, an anti-CD6 monoclonal antibody, can activate human T lymphocytes. *J. Immunol.*, 1989. **143**(8): p. 2439-2447.
352. Bott, C.M., et al., Activation of human T cells through CD6: functional effects of a novel anti-CD6 monoclonal antibody and definition of four epitopes of the CD6 glycoprotein. *Int. Immunol.*, 1993. **5**(7): p. 783-792.
353. Osorio, L.M., et al., The anti-CD6 mAb, IOR-T1, defined a new epitope on the human CD6 molecule that induces greater responsiveness in T cell receptor/CD3-mediated T cell proliferation. *Cell. Immunol.*, 1994. **154**(1): p. 123-133.
354. Gimferrer, I., et al., Relevance of CD6-mediated interactions in T cell activation and proliferation. *J. Immunol.*, 2004. **173**(4): p. 2262-2270.
355. Hassan, N.J., et al., Optimal T cell activation requires the engagement of CD6 and CD166. *Eur. J. Immunol.*, 2004. **34**(4): p. 930-940.
356. Sarrias, M.R., et al., The Scavenger Receptor Cysteine-Rich (SRCR) domain: an ancient and highly conserved protein module of the innate immune system. *Crit. Rev. Immunol.*, 2004. **24**: p. 1-37.
357. Teh, S.J., et al., CD2 regulates the positive selection and function of antigen-specific CD4- CD8+ T cells. *Blood*, 1997. **89**: p. 1308-1318.
358. Carmo, A.M., et al., CD2 and CD3 associate independently with CD5 and differentially regulate signaling through CD5 in Jurkat T cells. *J. Immunol.*, 1999. **163**: p. 4238-4245.
359. Bhandoola, A., et al., CD5-mediated inhibition of TCR signaling during intrathymic selection and development does not require the CD5 extracellular domain. *Eur. J. Immunol.*, 2002. **32**: p. 1811-1817.
360. Bowen, M.A., et al., Structure and chromosomal location of the human CD6 gene: detection of five human CD6 isoforms. *J. Immunol.*, 1997. **158**( 3 ): p. 1149-1156.